Diabetes and the cardiac dysfunction caused by experimental sepsis

A thesis presented by

Sura Yahia Yosef Al Zoubi

Registered at

Barts and the London School of Medicine and Dentistry

Queen Mary University of London

For the degree of

Doctor of Philosophy

Centre of Translational Medicine & Therapeutics

The William Harvey Research Institute

John Vane Science Centre

Charterhouse Square

London, EC1M 6BQ

DECLARATION

I, Sura Yahia Yosef Al Zoubi, confirm that the research included within this thesis is my own work or that where it has been carried out in collaboration with, or supported by others, that this is duly acknowledged below and my contribution indicated.

I attest that I have exercised reasonable care to ensure that the work is original, and does not to the best of my knowledge break any UK law, infringe any third party's copyright or other Intellectual Property Right, or contain any confidential material.

I accept that the College has the right to use plagiarism detection software to check the electronic version of the thesis.

I confirm that this thesis has not been previously submitted for the award of a degree by this or any other university.

The copyright of this thesis rests with the author and no quotation from it or information derived from it may be published without the prior written consent of the author.

Signature: 

Date: 8/5/2018

Details of collaboration: Collaboration with Professor Massimo Collino's lab (Turin University) for kindly assisting me in performing the western blots and measuring the lung inflammation markers for samples I have generated.

ABSTRACT

Sepsis is the leading cause of death in ICU patients. Patients with sepsis may develop sepsis-related cardiac dysfunction. The presence of this cardiac dysfunction can increase the mortality rate from 40% to 70%. Diabetes is a chronic disease that manifests as an elevation in blood glucose. Patients with diabetes are more susceptible to, and at increasing risk of developing, infections and subsequently sepsis.

Activation of the NF-κB pathway plays a crucial role in the pathophysiology of sepsis-associated cardiac dysfunction and diabetic cardiomyopathy. The effect of diabetes on outcomes in patients with sepsis is highly controversial and it is still unclear whether pre-existing T2DM augments the cardiac dysfunction associated with sepsis and whether activation of NF-κB drives the cardiac dysfunction in T2DM/sepsis patients.

In this thesis, I have first developed two models of high fat diet (HFD)-induced diabetes and diabetic cardiomyopathy in mice. Then, I developed two models of sepsis associated cardiac dysfunction using lipopolysaccharide (LPS) or caecum-ligation and puncture (CLP) in diabetic mice. I have demonstrated that mice with pre-existing T2DM exhibit a significantly greater cardiac (organ) dysfunction after challenge with either (low dose) LPS or mild CLP surgery. The exacerbated cardiac dysfunction was accompanied by an increase in NF-κB activation and reduction in Akt phosphorylation in the heart and an increase in the serum levels of proinflammatory cytokines. The increase in cardiac dysfunction, as well as the increase in the activation of NF-κB, caused by sepsis in animals with T2DM was

largely attenuated by treatment with a selective IκB kinase inhibitor (IKK-16) or a DPP-4 inhibitor (linagliptin).

Thus, excessive activation of NF-κB in animals with diabetes/sepsis drives the observed excessive cardiac dysfunction, and that inhibition of NF-κB may be a useful target to treat the excessive inflammation and sepsis associated cardiac (organ) dysfunction in patients with T2DM and sepsis.

ACKNOWLEDGEMENTS

All thanks and praise be to God Almighty for giving me the strength and capability to complete this thesis. Without his mercy, this work would not have been done.

I would like to express my great gratitude and appreciation to my supervisor; Prof. Chris Thiemermann, for his invaluable and continuous support, assistance and guidance in both academic and personal levels through the past three years. I consider myself lucky to work under his supervision and I hope this work continuous in the future.

Special thanks go to my role model, mentor and best friend, my mother; Eng. Suad Al-Shihab, for her unconditional love, care, concern and support. Thank you for being with me every day to listen to my stories and giving me advices. All what I have done, I have done to make you proud.

I would like also to thank my siblings; Dr. Tariq, Eng. Sondos, Dr. Muath, Dr. Lubna and Dr. Zaha for their encouragement. A special appreciation is to Dr. Jianmin, who has been a great colleague and friend, for teaching me echocardiography and CLP techniques, helping in the CLP surgeries and making me feel better whenever I had a problem. Great gratitude goes to Prof. Massimo Collino and his team for hosting me in their lab in Turin to learn the western blot technique and for helping me with the signalling analysis.

Finally, I would like to thank my sponsor (Al-Balqa' Applied University) for its financial support through my studies at Queen Mary University of London. Additionally, my appreciation goes to the entire QMUL staff.

LIST OF PUBLISHED PAPERS

Lukas Martin, Matthias Derwall, **Sura Al Zoubi**, Elisabeth, Daniel A. Reuter, Chris Thiemermann, Tobias Schuerholz (2018). THE SEPTIC HEART, Current Understanding of Molecular Mechanisms and Clinical Implications. *Chest*, under revision.

Sura Al Zoubi, Jianmin Chen, Catherine Murphy, Lukas Martin, Fausto Chiazza, Debora Collotta, Massimo Collino, Christoph Thiemermann (2018). Inhibition of NF-κB pathway attenuates cardiac dysfunction caused by sepsis in mice with pre-existing type 2 diabetes mellitus. *Frontiers in Immunology*, under revision.

LIST OF PUBLISHED ABSTRACTS

Sura Al Zoubi, Jianmin Chen, Lukas Martin, Catherine Murphy, Gareth Purvis, Fausto Chiazza, Debora Collotta, Massimo Collino, Christoph Thiemermann. Inhibition of NF-κB Pathway with IKK-16 or Linagliptin Attenuates the Cardiac Dysfunction Associated with Polymicrobial Sepsis in Mice with Pre-existing Type 2 Diabetes Mellitus (T2DM). American Diabetes Association, 78th scientific session, 22nd-26th June 2018, Orlando, USA (Poster presentation).

Sura Al Zoubi, Jianmin Chen, Lukas Martin, Catherine Murphy, Fausto Chiazza, Debora Collotta, Massimo Collino, Christoph Thiemermann. Inhibition of NF-κB pathway attenuates the multiple organ dysfunction associated with polymicrobial sepsis in mice with pre-existing type 2 diabetes mellitus (T2DM). The International Translational and Regenerative Medicine Conference, 25th-27th April 2018, Rome, Italy (Oral presentation).

Sura Al Zoubi, Jianmin Chen, Lukas Martin, Catherine Murphy, Fausto Chiazza, Debora Collotta, Massimo Collino, Christoph Thiemermann. The effect of IKK inhibition on the cardiac dysfunction associated with CLP sepsis in mice with pre-existing type 2 diabetes mellitus. Willium Harvey Research Institute, PhD Symposium, 24th January 2018, London, UK (Oral presentation).

Sura Al Zoubi, Jianmin Chen, Lukas Martin, Catherine Murphy, Fausto Chiazza, Debora Collotta, Massimo Collino, Christoph Thiemermann. Effect of ikk inhibition on organ dysfunction associated with sepsis in mice with pre-existing diabetes. British Pharmacological Society, Pharmacology 2017, 11th-13th December 2017, London, UK (Oral presentation).

Sura Al Zoubi, Jianmin Chen, Lukas Martin, Catherine Murphy, Gareth Purvis, Fausto Chiazza, Debora Collotta, Massimo Collino, Christoph Thiemermann. Inhibition of IκB kinase (IKK) attenuates the multiple organ dysfunction associated with polymicrobial sepsis in mice with pre-existing type 2 diabetes mellitus (T2DM). 17th Congress of European Shock Society, 13th-15th September 2017, Paris, France (Oral presentation). **Travel award winner, Young investigator award finalist**.

Elisabeth Zechendorf, **Sura Al Zoubi**, Caroline O'Riordan, Martin Simons, Gernot Marx, Tobias Schuerholz, Christoph Thiemermann, Lukas Martin. The potential of Ribonuclease A as a new therapeutic strategy in trauma/sepsis-associated cardiomyopathy. 17th Congress of European Shock Society, 13th-15th September 2017, Paris, France (Poster presentation).

Sura Al Zoubi, Jianmin Chen, Lukas Martin, Gareth Purvis, Fausto Chiazza, Debora Collotta, Massimo Collino, Christoph Thiemermann. Inhibition of IκB Kinase attenuates cardiac dysfunction caused by sepsis in mice with pre-existing type 2 diabetes mellitus. 13th World Congress of Inflammation, 8th-12th July 2017, London, UK (Oral presentation).

ABBREVIATIONS

ACCP	American Collage of Chest Physicians
ACR	albumin to creatinine ratio
AD	After Christ
ADBP	adenosine deaminase binding protein
ADP	adenosine di-phosphate
AGEs	advanced glycation end products
AKI	acute kidney injury
AKIN	Acute Kidney Injury Network
ALT	alanine transaminase
AMP	adenosine mono-phosphate
AMPK	adenosine monophosphate-activated protein kinase
ANOVA	analysis of variance
AP-1	activated protein 1
APCs	antigen presenting cells
ATP	adenosine tri-phosphate
ATS	American Thoracic Society
AUC	area under the curve
BC	Before Christ
BMI	body mass index
Ca2+	calcium ion
cAMP	cyclic adenosine mono-phosphate
CAP	community acquired pneumonia
CD26	cluster of differentiation
CKD	chronic kidney disease
CLP	caecal ligation and puncture

CLRs	C-type lectin receptors
CrCl	creatinine clearance
DAMPs	damage associated molecular pattern
DNA	deoxyribonucleic acid
DPP-4	dipeptidyl peptidase 4
Echo	echocardiography
EDTA	ethylenediaminetetraacetic acid
EF	ejection fraction
eNOS	endothelial nitric oxide synthase
ER	endoplasmic reticulum
ESICM	European Society of Intensive Care Medicine
FAC	fractional area change
FPG	fasting plasma glucose
FS	fractional shortening
GIP	glucose-dependant insulinotropic peptide
GIT	gastrointestinal tract
GLP-1	glucagon like peptide-1
GSK-3β	glycogen synthase kinase-3 beta
HbA1c	haemoglobin A1c
HCs	hepatocytes
HDL	high density lipoprotein
HFD	high fat diet
HMGB1	high mobility group box 1
HUVECs	human umbilical vein endothelial cells
i.p.	intraperitoneal
i.v.	intravenous

ICAM-1	intracellular adhesion molecule-1
ICU	intensive care unit
IFN	interferon
IKK	IκB-α kinase
IL-10	interleukin 10
IL-1β	interleukin-1 beta
IL-6	interleukin 6
iNOS	inducible nitric oxide synthase
IRF-3	interferon regulatory factor 3,
ITT	insulin tolerance test
IVS	intraventricular septum
IκB-α	inhibitor of κB-α
JAMA	Journal of the American Medical Association
KC	keratinocyte chemoattractant
KCs	kupffer cells
LDL	low density lipoprotein
LPS	lipopolysachride
LV	left ventricle
LVID	left ventricle internal dimension
LVPW	left ventricle posterior wall thickness
MAP	main arterial pressure
MCP-1	monocyte chemoattractant protein-1
MD2	myeloid differentiation factor 2
mmHG	millimetre of mercury
MODS	multiple organ dysfunction syndrome
MPO	myeloperoxidase

MyD88	myeloid differentiation Marker 88
NAG	N-acetyl-β-D-glucosaminidase
NF-κB	nuclear factor- kappa B
nNOS	neuronal nitric oxide synthase
NO	nitric oxide
NOD	nucleotide-binding oligomerisation domain
NOS	nitric oxide synthase
OGTT	oral glucose tolerance test
PAD-4	peptidylarginine deiminase 4
PAMPs	pathogen associated molecular pattern
PCO2	partial pressure of carbon dioxide
PepG	peptidoglycan
PKA	protein kinase A
PKC	protein kinase C
PRRs	pattern recognition receptors
qSOFA	quick SOFA
RAAS	renin-angiotensin-aldosterone system
RAGE	receptor for advanced glycation end products
RBF	renal blood flow
RIFLE	Risk, Injury, Failure, Loss of kidney function, and End-stage kidney disease
RIP-1	receptor-interacting protein 1
RLRs	retinoic acid inducible gene (RIG)-I-like receptors
ROS	reactive oxygen species
SARM	sterile α and HEAT/Armadillo motif
SCCM	Society of Critical Care Medicine
SEM	standard error of the mean

Ser	serine
SERCA	sarco-endoplasmic reticulum calcium-ATPase
SIRS	systematic inflammatory response syndrome
SIRT1	sirtuin-1
SIS	Surgical Infection Society
SOFA	sequential (Sepsis-related) Organ Failure Assessment
SSC	Surviving Sepsis Champagne
T1DM	type 1 diabetes mellitus
T2DM	type 2 diabetes mellitus
T3	triiodothyronine
TAK1	TGF-β-activated kinase 1
TC	total cholesterol
TG	triglyceride
TGF-β	transforming growth factor-Beta
TIR	toll IL-1 receptor
TIRAP/Mal	TIR domain-containing adapter protein
TLRs	toll like receptors
TNF-α	tumour necrosis factor-α
TRAM	TRIF-related adapter molecule
TRIF	TIR-domain-containing adapter-inducing interferon-β
UTI	urinary tract infection
WBCs	white blood cells
WHO	World Health Organisation

MEASUREMENTS AND UNITS

%	percentage
°C	degrees Celsius
dl	decilitre
fL	femtoliter
g	grams
h	hour
HR	heart rate
Kcal	kilocalories
Kg	kilogram
L	litre
M	mole
mg	milligram
min	minute
ml	millilitre
mm	millimetre
ng	Nano gram
pg	Pico gram
ppm	part per million
U	uunit
µ	micro

TABLE OF CONTENTS

INDEX OF FIGURES

INDEX OF TABLES

CHAPTER 1: GENERAL INTRODUCTION

1.1 Sepsis

1.1.1 Historical background

The medical term 'sepsis' is derived from the Greek word 'σηψις' which means "decomposition of animal or vegetable organic matter" [1]. The term sepsis was first introduced in the medical literature by Hippocrates (ca. 460-370 BC) in the Hippocratic corpus [1,2]. Despite the fact that sepsis is a term related to modern intensive care medicine, the medical concept of sepsis is considered to be old.

In 1862, Mr. Edwin Smith discovered the oldest known report of a case of sepsis secondary to wound infection in Luxor, Egypt, which is now called *'The Edwin Smith Surgical Papyrus* [3]'. The existing scroll, which was written in 1,600 BC [4] is a copy of a previous one from around 3,000 BC [5]. Five of the 48 cases described in the scroll have a reference of fever as a secondary complication of an existing wound [3]. By that, and without knowing the concepts of inflammation and infection, the Egyptian physicians identified clear signs of what was then called *'systemic infection and local suppuration'* [6].

Despite the lack of the microorganism theory, the ancient Greeks were able to observe three key phenomena caused by microorganisms; sepsis (infection), pepsis (fermentation), and infection which was explained by the humeral theory [6]. During this period, Hippocrates contributed the expression *'wound putrefaction',* which is now called septicaemia [7]. Later Ibn Sina (AD 980–1037) observed that fever usually accompanies septicaemia. However, the presence of microorganism or

bacteria was linked to the decay of organic matter only in the 18th century by the French scientist Louis Pasteur (1822 – 1895) [8].

The Hungarian obstetrician Ignaz Semmelweis (1818-1865) identified, for the first time, the mechanisms underlying the transmission of childbed fever (puerperal sepsis) [9]. He also observed the importance of hygienic measures in reducing mortality of women during childbirth [7].

Hugo Schottmüller laid the foundation of the modern definition of sepsis in 1914. He descried that the existence of infection is an essential part of the disease [7]. Lewis Thomas then introduced a new theory which proposed that it is the host's response that is responsible of the clinical responses observed in septic patients [10]. The result of this theory was a large number of clinical and experimental studies, which have changed the focus from the research from the infectious agent to research relating to the host immune response [7].

And finally this theory was transferred into practice after The ACCP/SCCM Consensus Conference Committee American College of Chest Physicians/Society of Critical Care Medicine had been held in 1991. In this conference, it was agreed to define sepsis as a systemic inflammation in the presence of infection [11].

1.1.2 Definitions of sepsis and their evolution

A consensus conference was held in 1991 in Chicago by the American College of Chest Physicians/ Society of Critical Care Medicine with the aim of "agreeing on a set of definitions that could be applied to patient with sepsis and its sequalae" [11]. As a result of this conference, several new definitions were proposed (Systematic Inflammatory Response Syndrome (SIRS), Sepsis, Sever Sepsis, Septic Shock,

Multiple organ Dysfunction Syndrome and Hypotension) (Table 1.1) but other terms were neglected [11].

Table 1.1 Definitions of the ACCP/SCCM consensus conference

This table shows the definitions provided by the ACCP/SCCM consensus conference in 1991. Table adopted from Bone et al. 1992 [11].

Term	Concept
Colonization	Refers to the presence of microorganism in given site, but no harm to the host.
Infection	Presence of a given agent causing harm to the host (the presence of a host inflammatory response to the organism).
Bacteraemia	Presence of viable bacteria in the blood, which may be transient; by extension, viremia, fungemia and parasitemia can be characterized.
Systemic inflammatory response syndrome (SIRS)	Characterized as non-specific body response to a series of conditions causing inflammation including infection, burns, acute pancreatitis, trauma and others. At least 2 of the following conditions are required to meet the definition of SIRS: • Temperature > 38.0 °C or < 36.0 °C • Heart rate > 90 Beat/min • Respiratory rate > 20 breath/min or $PaCO_2$* < 32 mmHg • White blood cell count > 12,000/mm^3 or < 4,000/mm^3 or > 10% of immature bands
Sepsis	SIRS triggered by bacterial, viral, fungal or parasitic infection.
Severe sepsis	Sepsis associated with organ dysfunction, tissue hypoperfusion or arterial hypotension.
Septic shock	Hypotension (not ascribed to another cause) with tissue hypoperfusion caused by sepsis.
Multiple organ dysfunction syndrome (MODS)	Functional organ changes in a severely ill patient, so that homeostasis cannot be maintained without therapeutic intervention.

* PaCO2: partial pressure of carbon dioxide.

It was hoped that these definitions would enable the attending physician to detect the disease earlier and consequently enable early treatment for patients with sepsis, allow the use and development of potential standard protocols of research, and make better use of the data extracted from the clinical studies [11].

According to the above table, it is clear that sepsis is a reaction of the host to an infectious agent. However, a similar reaction can be seen in the absence of infection. So the term systemic inflammatory response syndrome (SIRS) was proposed to describe a systemic inflammatory response regardless of the cause (Figure1.1).

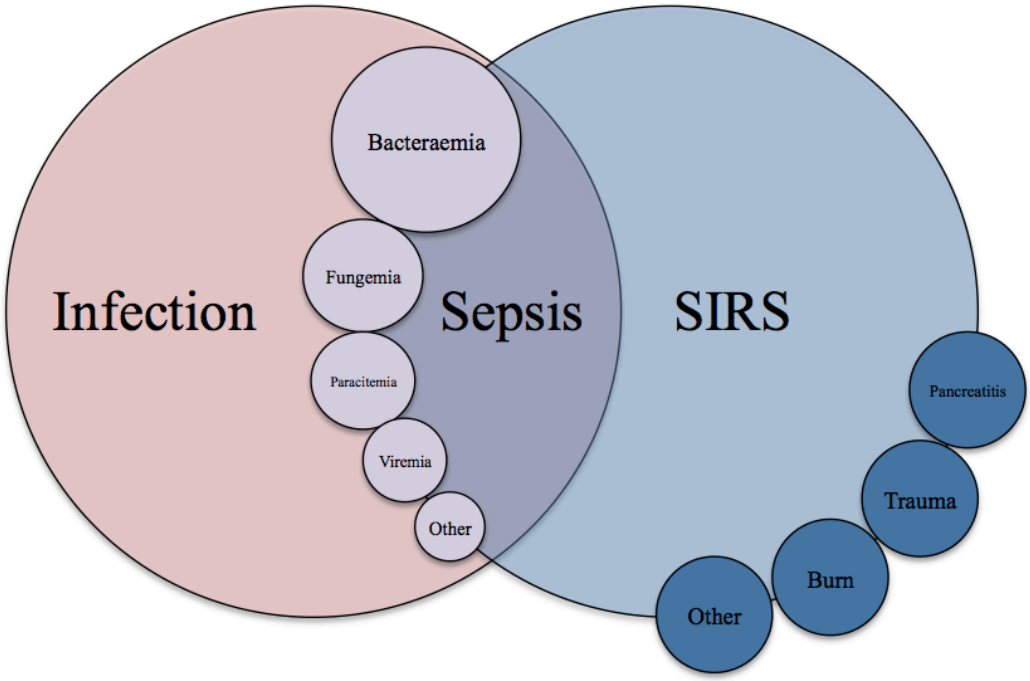

Figure 1.1 Mutual relations through systemic inflammatory response syndrome (SIRS), sepsis, and infection. Figure modified from Bone et al. 1992 [11].

In 2001, the SCCM/ESICM/ACCP/ATS/SIS International Sepsis Definitions Conference was held in Washington D.C. with the aim of amending the first definitions after the introduction of new insights into the pathophysiology of sepsis [12]. The most important outcomes of the conference were the following: It was recommended not to alter the definitions of sepsis, the use of SIRS for the diagnosis of sepsis was regarded as being too unspecific and further more specific clinical markers were recommended to support the diagnosis (Table 1.2).

Table 1.2 Diagnostic criteria of sepsis
The table provide the diagnostic criteria of sepsis that were provided during the second consensus conference in 2001. Table adopted from Levy et al. 2003 [13].

General variables
Temperature > 38.3 °C or < 36.0 °C, Heart rate > 90 beat/min, Tachypnea (respiratory rate > 20 breath/min in adults), Altered mental status.
Inflammatory response variables
White blood count > 12,000 cell/μL, < 4,000 cell/μL, or with > 10% immature form, Plasma C-reactive protein > 2 standard deviations above the normal value
Hemodynamic variables
Systolic blood pressure < 90 mmHg or mean arterial pressure < 70 mmHg, Mixed venous oxygen saturation > 70%, Cardiac index > 3.5 L/min/m^2.
Organ dysfunction variables
PaO_2/FiO_2* < 300, Urine output < 0.5 mL/kg/hr or creatinine increase > 0.5 mg/dL, International normalization ratio > 1.5 or active partial thrompoplastin time > 60 sec, Platelet count < 10,000 cell/μL, Plasma total bilirubin > 4 mg/dL.
Tissue perfusion variables
Hyperlactatemia > 1 mmol/L, Decreased capillary refill or mottling.

* PaO_2/FiO_2: The ratio of partial pressure arterial oxygen and fraction of inspired oxygen.

Finally, in February 2016, The Third International Consensus Definitions for Sepsis and Septic Shock (Sepsis-3) was published by the Journal of the American Medical Association (JAMA). The *European Society of Intensive Care Medicine* and the *Society of Intensive Care Medicine* invited a group of 19 experts in sepsis epidemiology, pathobiology, and clinical trials with the aim of assessing the definitions of sepsis and septic shock and to update them if needed [14]. The panel felt that the definitions of sepsis is highly dependent on the presence of systemic inflammation and that the term severe sepsis is a redundant term, as septic shock develops from sepsis (without a phase of severe sepsis). The panel concluded that sepsis should be defined as *"life-threatening organ dysfunction caused by a*

dysregulated host response to infection", organ dysfunction represent 10 % or more of in-hospital mortality rate and is reflected in two or more points increase in the Sequential (Sepsis-related) Organ Failure Assessment (SOFA) score, and they defined patients with septic shock as subset of patients with sepsis which have intense metabolic, cellular, and circulatory abnormalities resulting in higher mortality rate [14].

1.1.3 Diagnosis

The diagnostic criteria for sepsis and septic shock were first introduced in 1991 and last updated in 2016. According to the latest update by the International Consensus Definitions for Sepsis and Septic Shock (Sepsis-3), septic patients have documented or suspected infection along with sudden change of SOFA score of more than one from the baseline [14].

The task force recommends using of Quick Sofa (qSOFA) (Table 1.3) as bedside criteria for recognising non-ICU patients with sepsis who are likely to have a poor outcome. The qSOFA score combines blood pressure (systolic) of maximum 100 mm Hg, changes in mental status, and respiratory rate of 22 breaths per minute or more. The advantages of using qSOFA over SOFA (Table 1.4), even though less powerful, are the following: The qSOFA score can be done rapidly (and quickly repeated) and does not require any clinical chemistry data. This should help the attending clinician to make a rapid assessment of the degree of organ failure, and allow to start or change a treatment or enable the transfer of the patient to the ICU [14].

Table 1.3 qSOFA (Quick SOFA) Criteria

The table provides qSOFA criteria with the reference values, this scoring system helps physicians doing quick assessment of organ dysfunction in order to change patients' medication or refer to the ICU. Table adopted from Singer et al. 2016 [14].

Criteria	Reference
Respiratory Rate	>= 22 beat/min
Altered mentation	---------
Systolic Blood Pressure	<=100 mm Hg

Table 1.4 SOFA Criteria. Table adopted from Singer et al. 2016 [14].

	SOFA Score				
Organ system	Score 0	Score 1	Score 2	Score 3	Score 4
Respiration PaO_2/FiO_2* (mmHg)	>400	<400	<300	<200	<100
Coagulation Platelet ($10^3/mm^{3)}$	>150	<150	<100	<50	<20
Hepatic Bilirubin (mg/dL)	<1.2	1.2-1.9	2.0-5.9	6.0-11.9	>12.0
Circulatory Hypotension	No hypotension	MAP*<70	Dopamine </=5	Dopamine >5	Dopamine >15
Neurological Glasgow coma scale	15	13-14	10-12	6-9	<6
Renal Creatinine (mg/dL)	<1.2	1.2-1.9	2.0-3.4	3.5-4.9	>5.0

* PaO_2/FiO_2: The ratio of partial pressure arterial oxygen and fraction of inspired oxygen, MAP: mean arterial pressure.

To diagnose septic shock, the patient must present with an abnormal circulation reflected by the need for vasopressor support to keep the mean arterial pressure (MAP) above 65 mm Hg, and with a cellular/metabolic dysregulation resulting in elevated lactate serum levels (more than 2 mmol/L) in the absence of hypovolaemia. This metabolic disorders should be severe enough to cause an increase in mortality (Figure 1.2) [14].

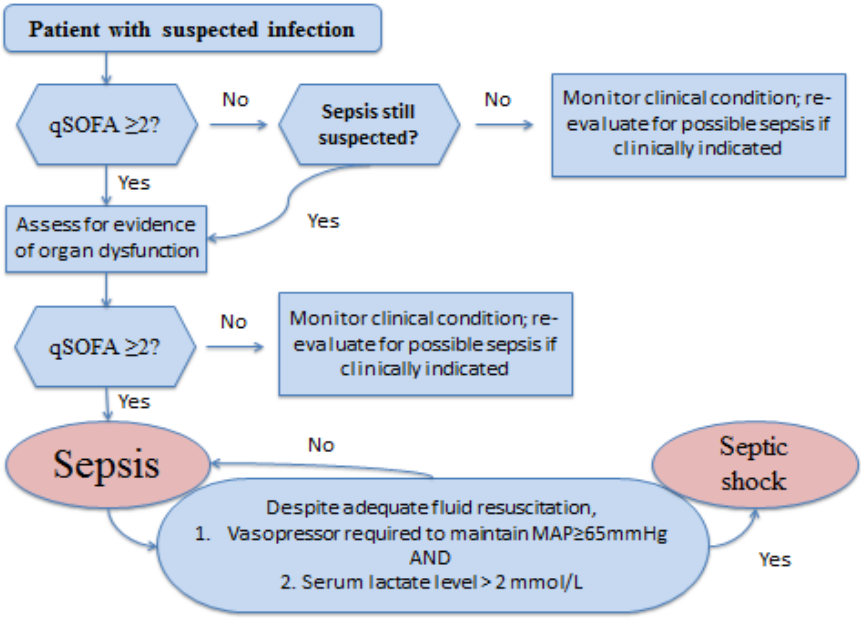

Figure 1.2 Operationalization of Clinical Criteria Identifying Patients with Sepsis and Septic Shock

Baselines SOFA score usually considered to be zero, unless the patient already has chronic or acute change in SOFA (organ failure) before the onset of infection. qSOFA: Quick SOFA, MAP: Main arterial pressure. Figure modified from Singer et al. 2016 [14].

1.1.4 Epidemiology

As the definition of sepsis has been changed recently, all available publications about the epidemiology of sepsis have focussed on cases previously defined as having severe sepsis or septic shock.

Severe sepsis is considered to be the leading cause of death in non-coronary intensive care units (ICU) critically ill patients[15] and the second most common cause of death in this population in high income countries[16]. A study conducted by Angus et al. studying the discharge records in 1995 from seven hospitals in the United States showed that the annual incidence of severe sepsis was 3.0 cases per 1000 of population. Notably, this incidence was much higher in the elderly (26.2

cases per 1000 of population) [17]. About 50% of cases with severe sepsis occur outside the ICU. Twenty-five percent of patients with severe sepsis die because of the disease during hospitalization and this percentage almost doubled in patients with septic shock [15].

Either Gram-positive or Gram-negative bacteria can cause sepsis. However, the incidence of Gram-positive bacterial sepsis has been on the rise for many years, and it is now more common than gram-negative bacterial sepsis [15,16]. The reason for this may be the increase in nosocomial infections and the increasing use of invasive procedures [15].

The type of organism that causes sepsis has a dramatic impact on outcome [15]. Gram-negative bacteria are thought to induce a stronger inflammatory response, are found more frequently in septic shock patients than in patients with sepsis or severe sepsis [18] and sepsis caused by Gram-negative bacteria is associated with a higher mortality rate than those cases caused by Gram-positive bacteria. The most frequent organisms that cause sepsis are: *Staphylococcus aureus* (20.5%), *Pseudomonas species* (19.9%) and *Enterobacteriacae* (mainly E. coli, 16.0%)[19].

Sepsis can start from different sites of infection. The most common site of infection is the respiratory tract (pneumonia), which is also associated with the highest mortality, followed by the genitourinary tract, then abdominal cavity, skin, and implanted devices [15].

The incidence of sepsis has increased recently in the United States. This may be explained due to the aging of the population, increasing burden of chronic health conditions, and increased use of immunosuppressive therapy, transplantation,

chemotherapy, and invasive procedures [15]. However, the mortality rate has declined because of the improvements in supportive care for ICU patients [20].

1.1.5 Treatment

Like other acute illnesses and trauma, early identification and proper management of sepsis are associated with better outcome [21]. The Surviving Sepsis Campaign (SSC) published the first comprehensive guideline for the management of sepsis in 2004. This guideline was then reviewed in 2008 and 2012. In 2015, a committee of 55 experts from 25 different international organizations was assembled and divided into 5 sections (haemodynamic, infection, adjunctive therapy, metabolic and ventilation) to provide an update of the 2012 SSC guideline for the management of sepsis and septic shock. In 2017, the SSC published its latest guideline that provides new recommendations about managing adult patients with sepsis and septic shock aiming to establish best clinical practice (The detailed recommendations are at the end of this thesis in Appendix 1) [21].

In summary, the committee considered sepsis and septic shock as medical emergency that needs immediate intervention. The recommended first step is fluid resuscitation with crystalloid solutions (e.g. normal saline) using at least 30ml/kg, i.v. Additional fluid can then be given depending on the haemodynamic status of the patient. Once sepsis or septic shock is suspected in a patient, microbiological cultures should be obtained (including blood cultures) before the start of antibiotic treatment. Then an empiric broad-spectrum antibiotic should be initiated as soon as possible (the choice of the antibiotic to be used and the dosing regimen are based on the patient's conditions). However, antibiotic treatment for 7-10 days is enough for most patients and most infections. The source of infection should be identified

and controlled as soon as possible. Vasopressor treatment (e.g. norepinephrine) is recommended in patients with septic shock to increase the mean arterial pressure to 65 mmHg. However, the committee did not recommend the use of hydrocortisone in patients with septic shock, if fluid resuscitation and vasopressor therapy were enough to restore haemodynamic stability. Prophylactic strategies for preventing the development of either peptic ulcer (using proton pumps inhibitors or H2 receptors antagonist) or deep vein thrombosis (using unfractionated of low molecular weight heparin) should be considered in high-risk patients.

1.1.6 Pathophysiology

As outlined in the definitions of sepsis, infection is a key element of the disease. Many infectious agents can cause sepsis including fungi, viruses or bacteria [22]. To be able to cause a disease, these pathogens need to pass through the mucosal barriers, spread, and replicate in other organs. They use virulence factors to protect themselves from the host defence [16]. The first line of defence of the host is the innate immune system that recognises the pathogen early and activates the inflammatory response (Figure 1.3) [23].

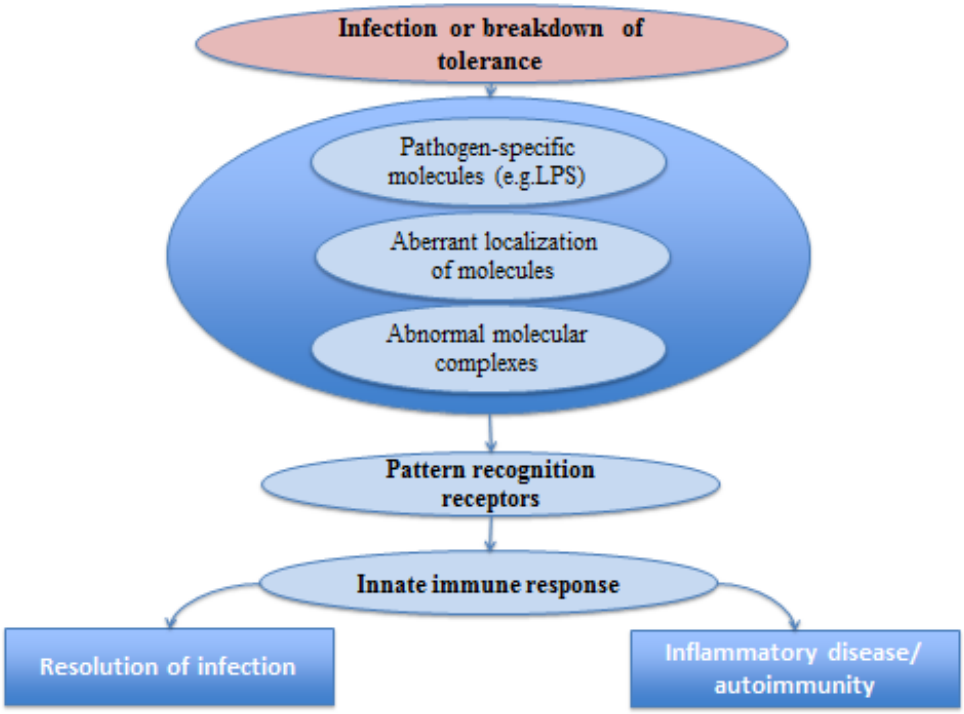

Figure 1.3 Principles in innate immune recognition by PRRs.

During microbial infection or breakdown of tolerance, pathogen-specific molecules, aberrant localization of foreign or self-molecules, or abnormal molecular complexes are recognized by PRRs. This event triggers PRR-mediated signalling and induction of an innate immune response, which ultimately results in resolution of infection but also may cause inflammatory diseases or autoimmunity. Figure adopted from Mogensen 2009 [24].

The presence of microorganisms and pathogens is usually recognised by a group of receptors called Germline-encoded pattern recognition receptors (PRRs) [25]. This happens by recognising a conserved entity within microbes. These entities are called Pathogen Associated Molecular Pattern (PAMPs). However, some of these receptors are also responsible of recognition of endogenous molecules which are released from damaged cells. In this case they are termed Damage Associated Molecular Pattern (DAMPs) [25].

Even though the Toll-Like Receptor (TLR) family is the major and most extensively studied PRR family, three other classes of PRR families have been

identified [24,25]. PRR families can be classified as transmembrane proteins such as Toll Like Receptors (TLRs) and C-type Lectin Receptors (CLRs), or cytoplasmic proteins like Nucleotide-binding Oligomerisation domain (NOD) and the Retinoic Acid Inducible Gene (RIG)-I-Like receptors (RLRs) [25].

Upon recognition of PAMPs, TLRs or other classes of PRRs activate cascades of intracellular signalling that upregulate the gene transcription of antimicrobial proteins, chemokines, type 1 interferon (IFNs), pro-inflammatory cytokines and other proteins [25,26].

Table 1.5 PRRs and their ligands

This table provides the four families of PRRs and their subfamilies, location, ligands, and origin of the ligand. Table is adopted from Takeuchi and Akira 2010 [25].

PRRs	Localization	Ligand	Origin of the ligand
TLR			
TLR1	Plasma membrane	Triacyl lipoprotin	Bacteria
TLR2	Plasma membrane	Lipoprotin	Bacteria, viruses, parasite, self
TLR3	Endolysosome	dsRNA	Virus
TLR4	Plasma membrane	LPS	Bacteria, viruses, self
TLR5	Plasma membrane	Flagellin	Bacteria
TLR6	Plasma membrane	Diacyl lipoprotin	Bacteria, viruses
TLR7(human TLR8)	Endolysosome	ssRNA	Bacteria, viruses, self
TLR9	Endolysosome	CpG-DNA	Bacteria, viruses, protozoa, self
TLR10	Endolysosome	Unknown	Unknown
TLR11	Plasma membrane	Protein-like molecules	Protozoa
RLR			
RIG-1	Cytoplasm	Short dsRNA	RNA viruses, DNA virus
MDAS	Cytoplasm	Long dsRNA	RNA viruses
LGP2	Cytoplasm	Unknown	RNA viruses
NLR			
NOD1	Cytoplasm	iE-DAP	Bacteria
NOD2	Cytoplasm	MDP	Bacteria
CLR			
Dectin-1	Plasma membrane	B-Glucan	Fungi
Dectin-2	Plasma membrane	B-Glucan	Fungi
MINCLE	Plasma membrane	SAP130	Fungi, self

In the following sections, I shall focus on TLRs, as bacteria are their main ligands, and bacteria are the main cause underlying the systemic infections associated with sepsis.

1.1.6.1 TLRs

In humans, 10 TLRs have been identified thus far [24,25] and two more have been discovered solely in mice [25]. Each TLR is able to recognise different PAMPs and DAMPs [25]. TLRs are type 1 integral membrane receptors in which the N-terminal is the ligand binding and recognition domain (leucine-rich repeats); this is followed by a single trans membrane region and then the cytoplasmic C-terminal, which functions as the signalling domain [25,27]. This domain is also called Toll IL-1 receptor (TIR) domain, as it is homologues to the IL-1R family members signalling domains[28].

In the case of sepsis (and for this research project in particular), the most important TLRs are TLR 2 and TLR 4, which recognise peptidoglycan (Pep.G) primarily released from Gram-positive bacteria and lipopolysaccharide (LPS) released from Gram-negative bacteria.

TLR2 can only recognise PAMPs after forming a hetero-dimer either with TLR1 or TLR6. The activation of TLR2 with ligands other than viral components, results in non-type 1 IFNs pro-inflammatory cytokines production such as IFNγ. After binding to LPS and the myeloid differentiation factor 2 (MD2), TLR4 forms a homo-dimer of TLR4-MD2-LPS (Figure 1.4) [25].

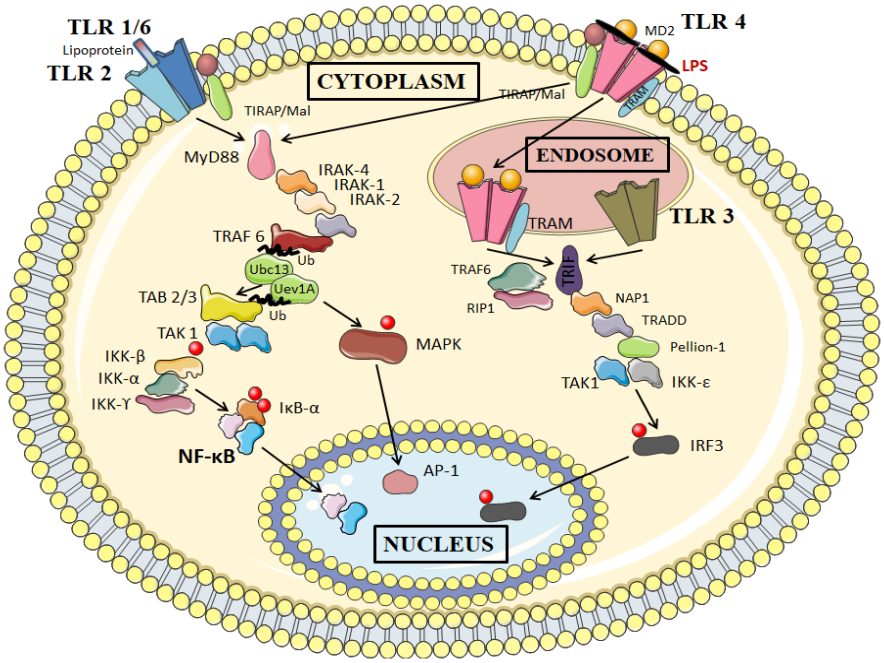

Figure 1.4 Signalling pathways of TLR4 and TLR2.
After being activated by LPS, TLRs activate the MyD88 dependant and independent pathways and lead to activation and translocate of NF-κB to the nucleus. Figure adapted from Takeuchi & Akira 2010 [25].

After binding of ligands to their respective TLRs and the subsequent formation of dimers, a change to their crystal structure occurs, which allows the recruitment of the the suitable Toll/IL-1R- domain-containing adaptor molecule to the TIR domain of the TLR [26]. The following five TIR-domain-containing adaptors have been reported: MyD88, TRIF, TIRAP/Mal, TRAM and SARM [25]. However, signalling of TLR is usually driven by two key pathways, which are either MyD88 or TRIF-dependent.

The MyD88-dependant signalling pathway

With the exception of the TLR3-pathway, MyD88 is a major element in the signalling pathways of all other TLRs [25]. For example, TLR2 and TLR4 need to be bridged with MYD88 using TIRAP/Mal. Then, MyD88 interacts with IL-1R

associated kinase (IRAK)-4, which in turn activates IRAK-1 and IRAK-2 by dissociating them from MyD88. The activated IRAKs then interact with TNF-associated factor 6 (TRAF6). TRAF6, together with E2 ubiquitin-conjugating enzyme complex, catalyses the formation of a lysine 63 (K63)-linked polyubiquitin chain on TRAF6 itself and generates an unconjugated free polyubiquitin chain. This free K63 polyubiquitin chain then activates a complex of TGF-β-activated kinase 1 (TAK1), TAK1-binding protein 1 (TAB1), TAB2, and TAB3. TAK1, TAB1, TAB2, and TAB3 then phosphorylate IKK-β and MAPK kinase 6. Each one of these kinases then activates its effector: IKK-β for example, phosphorylates IκBα and free NF-κB that is then translocates from the cytosol into the nucleus, binds to the respective promoter region and regulates gene transcription. MAPK Kinase 6 activates the transcription factor complex AP-1 resulting in the expression of pro-inflammatory cytokine genes (figure 1.4) [25].

The TRIF-dependant signalling pathway

To activate the TRIF pathway, TLR4 requires TRAM to activate TRIF[25]. Activation of this pathway results in activation of both NF-KB and IRF3 molecule [29]. TRIF recruits both RIP1 and TRAF6 for this activation in 2 different pathways. After that TRIF collectively with RIP1, TRADD, TRAF6, and Pellion-1 forms a multi-protein signalling complex. This signalling complex activates TAK1 that, in turn, phosphorylates and activates MAPK and activates NF-κB by causing IBα phosphorylation[29]. Activation and nuclear translocation of IRF3 occurs when TRIF recruits both IKKi (IKKε) and the non-canonical IKKs (TBK1) to phosphorylate IRF3 at Ser^{396} and Ser^{405}. The result of this activation is the production of type 1 IFN [29].

1.1.7 Cardiovascular dysfunction associated with sepsis

The cardiovascular dysfunction caused by bacteraemia was first described in 1951. Today, we know that most septic patients, and all septic shock patients develop sepsis-related cardiovascular dysfunction [30]. Despite the clear involvement of the immune system [31], the exact cause and mechanism of this cardiovascular dysfunction are still unclear [30,31].

In the past, and before the introduction of pulmonary artery catheters, it was thought that patients with septic shock went through two specific, consecutive phases of shock: a 'warm shock' or hyper-dynamic phase in which, despite of having hypotension, patients have warm extremities and a bounding pulse, and the 'cold shock' or hypo-dynamic phase, in which patients have cold extremities and a weak pulse, which ultimately leads to death [32] [33]. However, after using the pulmonary artery catheter to obtain the accurate measurements of cardiac output (CO) and left ventricular (LV) filling pressure, the hypodynamic phase (cold shock) was revealed to be the result of hypovolaemia due to inadequate fluid resuscitation [33].

1.1.7.1 Characteristics of sepsis related myocardial dysfunction

Using both pulmonary artery catheter and radionuclide cineradiography to measure cardiac function in septic shock patients, Parker and colleagues found that among survivors of sepsis, the ejection fraction was decreased, while the left ventricular end diastolic volume was increased compared to healthy individuals. They also found that these changes were reversible within 10 days. Many recent studies show that decreased ventricular compliance and contractility are the causes of this sepsis

related myocardial dysfunction [30].

1.1.7.2 Aetiology of sepsis related myocardial dysfunction

A complete picture of the aetiology of sepsis related myocardial dysfunction is still needed. The aetiology is multifactorial and it is necessary to gain a better insight into the pathophysiology of this dysfunction in order to develop new drugs to treat septic patients [30]. The following concepts have been introduced to the literature as potential mechanisms.

1.1.7.2.1 Myocardial Ischemia and micro-vascular dysfunction

The tissue hypoperfusion theory postulates that blood perfusion to cardiac cells is reduced in septic patients. Therefore, ischaemic injury of cardiac cells happens due to inadequate O_2 delivery. However, Cunnion et al. disproved this theory by placing thermodilution coronary sinus catheters in 7 septic shock patients to measure both coronary blood flow and cardiac metabolism. They concluded that there were no difference in the coronary blood flow or lactate production between septic patients (with or without cardiac depression) and healthy volunteers [34].

1.1.7.2.2 Myocardial Depressant factors

Parrillo et al. introduced this theory in 1985 by exposing spontaneously beating rat cardiomyocytes to the serum of septic shock patients. A significant reduction in contractility was observed when serum from patients during the acute phase of sepsis was used, while serum from healthy controls or from the same patients during the non-acute phase (either before the shock or after recovery) had no such effect. The authors concluded that the presence of circulating *'myocardial*

depressant substance' is the cause of myocardial dysfunction associated with sepsis [35]. Another study conducted in 1999 confirmed this finding. In this study the authors analysed the ultra-filtrate and found that there are significantly higher concentrations of C3a, IL-8, and IL-1β in septic patients compared to healthy controls [36].

Shortly after that, Pathan et al. partially characterised the physicochemical properties of these substances. These substances are 10-25 KDa in size, proteinaceous, water-soluble and heat stable [37]. Other potential myocardial depressant factors are nitric oxide (NO), prostanoids, and cytokines [30].

Cytokines

It was suggested that TNF-α is responsible for the cardiovascular changes (including the myocardial dysfunction) associated with septic shock [38]. Indeed, TNF-α challenge in canines dose-dependently depresses LV function [39] and after Vincent and colleagues showed an improvement in ventricular function in patients with septic shock treated with murine anti-TNF antibody [40]. However, treatment with murine monoclonal anti TNF-α was not able to improve survival [41]. Interleukin 1 (IL-1) is produced by neutrophils, macrophages and monocytes in response to TNF-α [42]. Because of their short half-lives, TNF-α and IL-1 are responsible only for the early cardiac depression [43] and the prolonged effect of cardiac depression is attributed to an excessive myocardial nitric oxide (NO) synthesis in response to TNF-α and IL-1 [44]. IL-6 is another important cytokine. In the serum of septic patients, IL-6 has higher concentration compared to TNF-α and it also has more prolonged elevation. These two criteria make it a good severity marker in sepsis [45].

Nitric Oxide (NO)

Nitric oxide synthase (NOS) generates NO from the oxidation of L-arginine to form L-citrulline. Three isoforms of NOS have been identified in myocardial cells: neuronal (nNOS), inducible (iNOS), and endothelial (eNOS) [46]. Unlike iNOS, both nNOS and eNOS continuously generate small amounts of NO. iNOS, on the other hand, is expressed in response to inflammation and generates large quantities of NO [47]. In 2010, Bougaki and colleagues suggested that activation of eNOS decreases inflammatory cytokines synthesis and prevents myocardial dysfunction in experimental (CAST) sepsis. Since then, however, it has been suggested that NO formation by eNOS contributes to the early myocardial dysfunction in sepsis [48]. The increased expression of iNOS plays a key role in the late cardiac dysfunction associated with sepsis. Many different mechanisms have been proposed by which an enhanced formation of NO by iNOS contributes to the cardiac dysfunction in sepsis. These include changes in both preload and afterload, down-regulation of β-adrenergic receptors [49], a reduction of the response of cardiac myofilaments to Ca^{2+} [50] and a significant contribution to mitochondrial dysfunction [51] secondary to an increase in mitochondrial permeability as a result of peroxynitrite production (from NO and superoxide anions) [52,53].

1.1.7.2.3 Changes in calcium trafficking

Under normal physiological conditions, extracellular calcium enters the cardiomyocytes via the L-type calcium channels. Once inside the cells, it induces the sarcoplasmic calcium release via the activation of the ryanodine receptors. Intracellular calcium also activates actin-myosin interaction after binging to troponin and inhibiting its inhibitory effect on actin/myosin. After that,

phospholamban is phosphorylated and activated leading to calcium sequestering in the sarcoplasmic reticulum by the sarco-endoplasmic reticulum calcium-ATPase (SERCA) [54]. Under sepsis condition both the calcium current to the cardiomyocytes and the density of L-type calcium channel are reduced [55,56]. Phosphorylation of phospholamban is also impaired in sepsis resulting in impaired calcium sequestering in the endoplasmic reticulum (ER). Ryanodine receptors and myofilaments show reduced responsiveness and sensitivity to calcium during sepsis [57].

1.1.7.2.4 Mitochondrial dysfunction

Cardiomyocytes have a high content of mitochondria that are mainly responsible for energy generation by producing ATP from ADP via oxidative phosphorylation [58]. Mitochondrial dysfunction is (in addition to reduced blood supply) a potential cause of the multiple organs failure, and, hence, a factor influencing prognosis and outcome in patients with sepsis [59]. The mitochondrial dysfunction associated with septic cardiomyopathy comprises a change in mitochondrial architecture (swelling, internal vesicles formation and abnormalities in cristae) [60], damage of mitochondrial DNA [61], elevation in mitochondrial permeability transition [62] and inhibition of the cytochrome C oxidase activity [63]. The drivers of mitochondrial dysfunction in sepsis are multifactorial but include the excessive formation of NO and peroxynitrite, hormonal dysregulation and downregulation of mitochondrial protein gene transcription. Overproduction of NO and peroxynitrite cause mitochondrial protein damage, alter mitochondrial respiration and increase mitochondrial permeability [52,53,64]. Patients with sepsis show altered thyroid hormone levels [65] (low T3 syndrome), which is known to affect both mitochondrial

function and increase mortality in ICU patients [66]. Downregulation of mitochondrial protein gene transcription was observed in healthy volunteers who received bacterial endotoxin [67] and in critically ill patients [68]. As a result of mitochondrial injury, ATP production is reduced and, if low ATP level persists, the pathways leading to cell apoptosis are activated. However, cell death is not the main driver of the cardiac dysfunction associated with sepsis [69]. Cells may compensate the reduction in ATP generation by increasing glycolysis [70], but this alone is not sufficient to deliver the amounts of ATP generated by 'fully functional' mitochondria. Under such circumstances, cells adapt by reducing their metabolic activity and this may be a protective mechanism to prevent cell death similar to the hibernation state (of the heart) triggered by brief episodes of ischemia [71,72].

1.1.8 Acute kidney injury associated with sepsis

The kidney is another vital organ that is affected by sepsis. Acute kidney injury (AKI) occurs in almost 50% of ICU patients [73]. Different aetiologies can lead to the development of AKI in hospitalized patients such as; major cardiac surgery, contrast-induced AKI, severe heart failure and sepsis. Among all causes, sepsis is the most common cause of AKI in critically ill patients with a prevalence of 45-70% [74,75]. The presence of AKI is associated with almost 50% in-hospital mortality [73,76]. After surviving AKI, patients become more susceptible to develop chronic kidneys disease [77].

In 2004, Bellomo and co-workers proposed a classification system for acute kidney failure called RIFLE that depends on the change of serum creatinine from baseline and urine output [73]. However, in 2007, the acute kidney injury network

(AKIN) modified both the definition and the diagnostic criteria for acute kidney failure. In the new definition, a 48-hour time frame was proposed for the serum creatinine to increase a minimum of 0.3 mg/dl or 1.5 times increase from baseline or a decrease in urine output of less than 0.5 ml/kg for at least 6 hours (Table 1.6)[78].

Table 1.6 AKIN definition and staging of AKI

This table provides the three stages of AKI. Table is adopted from Mehtha et al. 2007 [78].

Stage	Serum creatinine criteria	Urine output criteria
1	Increase in serum creatinine of more than or equal to 0.3 mg/dl (≥ 26.4 μmol/l) or increase to more than or equal to 150% to 200% (1.5- to 2-fold) from baseline	Less than 0.5 ml/kg per hour for more than 6 hours
2	Increase in serum creatinine to more than 200% to 300% (> 2- to 3-fold) from baseline	Less than 0.5 ml/kg per hour for more than 12 hours
3	Increase in serum creatinine to more than 300% (> 3-fold) from baseline (or serum creatinine of more than or equal to 4.0 mg/dl [≥ 354 μmol/l] with an acute increase of at least 0.5 mg/dl [44 μmol/l])	Less than 0.3 ml/kg per hour for 24 hours or anuria for 12 hours

The pathophysiology of AKI in sepsis is multi-factorial. Diverse overlapping mechanisms have synergistic effects and result in the development of AKI [77]. In the past, global ischaemia was considered as the cause of AKI in sepsis [79]. However, studies showed that AKI could develop in patients even without a reduction in renal blood flow (RBF) [80,81]. In 2009, Prowle and colleges reviewed the literature for studies that measured RBF in AKI patients. They showed that RBF was not reduced in all critically ill patients with AKI the thing that confirms that renal ischaemia is not the main cause of AKI [82].

The main mechanisms involved in the development of the AKI in septic patients are inflammation, alteration in the microcirculation and adaptive cell response.

Inflammation is a key driver of AKI in sepsis. High cytokines levels (such as IL-6 and IL-10) are associated with the development of AKI [83,84]. Different receptors are activated in response to PAMPs and DAMPs resulting in activation of inflammatory cascades that result eventually in activating leucocytes, epithelial and endothelial cells [25]. Cytokines, PAMPs and DAMPs are filtered in the glomerulus and come into close proximity to endothelial cells in the proximal tubule, where they bind to TLR4 and TLR2 [85–88]. Activated endothelial cells then increase the expression of adhesion molecules, increase the inflammatory cytokines levels and increase leucocytes recruitment to kidneys resulting in further damage to tubular cells. Inhibition of adhesion molecules resulted in complete elimination of AKI development in CLP model of sepsis [89].

Alteration in the microcirculation is another key driver of AKI in sepsis. Both macro- and microcirculation are altered in septic patients as a consequence of a decrease in vascular resistance and a change of blood distribution into tissues and impairment in microcirculatory perfusion, and both result in heterogeneity of blood flow in the body and within organs and these alterations are more profound in severely ill patients with sepsis [90–92]. Even though macro-vascular complication and haemodynamic alterations happen in sepsis, renal blood flow remains normal or even increases. In 2003, Giantomasso and co-workers measured the blood flow to some vital organs including kidneys during E-coli induced sepsis in sheep. They showed a significant increase in renal blood flow in this setting [93]. Microcircular alterations include capillary obstruction, interstitial fluid retention and the

imbalance between vasodilation-vasoconstriction in the endothelial cells [94,95]. All these result in regional ischaemia. This finding is confirmed by the patchy pattern of injury seen in tubular cells [69].

After being exposed to the inflammatory insult and microcircular dysfunction, tubular cells try to adapt to the new environment to prevent apoptosis that may result from the oxidative stress results from sepsis in the kidney [95]. Indeed, tubular cell necrosis is not reported in sepsis-related AKI [69]. The adaptive response is shown as down-regulation of cell metabolism and enhanced cell cycle arrest. In sepsis setting, the tubular cell energy level is decreased because of mitochondrial injury. Tubular cell focuses the energy consumption on cell survival function rather than metabolic function the thing that stops further cell damage [59,96,97]. The low ATP level in AKI stimulates cell-cycle arrest to prevent cell death and allow recovery [98,99].

1.1.9 Liver injury associated with sepsis

To date, the accurate prevalence of liver injury associated with sepsis has not been established. The prevalence ranges from 1-20% depends on the diagnostic criteria used to identify liver injury [100]. For example, Angus and co-workers showed that only 1.3% of 192,980-sepsis cases developed liver failure. They used liver necrosis and liver infarction as the criteria for diagnosing liver failure [17]. In their study, Bakker and colleagues used less restrictive diagnostic criteria for liver injury and reported that almost 20% of 312 patients with septic shock developed liver failure during the study period (72 hours) [101]. Using SOFA scoring, among 541 patients with severe sepsis, 46.6% developed liver dysfunction and 6.3% developed liver failure within 24 hours of ICU admission [102].

The way of diagnosing liver failure is still controversial. Thus far, there is no single standardised diagnostic tool for diagnosing liver failure. However, most available diagnostic criteria require a bilirubin level of ≥ 2 mg/dl and at least duplication in alkaline phosphate or ALT levels for diagnosing liver injury [101]. In the latest consensus definition of sepsis and septic shock (sepsis-3), the panel recommended using the SOFA score to assess organ failure in which bilirubin is used to identify the presence of acute liver injury [14].

Different cell types in the liver are involved in the development of liver injury in septic patients. Kupffer cells (KCs) for example are responsible for scavenging bacteria and endotoxin in sepsis [103]. After exposure to endotoxin, KCs are activated and produce inflammatory cytokines such as TNF-α [104]. TNF-α, in turn, increases neutrophil recruitment leading to enhancement in the inflammatory response. TNF-α also enhances hepatocytes (HCs) to produce NO and IL-6 leading to further activation of the inflammatory response and imbalance in coagulation [105].

1.2 Diabetes Mellitus

1.2.1 Definition and classification

Diabetes is a group of metabolic disorders that manifests as a chronic elevation of blood glucose with abnormal metabolism of fat, carbohydrates and proteins. Elevation in blood glucose in patients with diabetes are due to an either an impairment in insulin secretion from the beta cells of the islets of Langerhans in the pancreas, ineffective use of the secreted insulin secondary to insulin resistance of tissues that use insulin or both [106,107]. This results in sustained hyperglycaemia, which in turn can lead to organ damage, dysfunction and failure. Diabetic patients often do not have symptoms or present with very mild symptoms such as excessive thirst, urination, weight loss and hunger; and many patients usually suffer from prolonged pathological and functional changes in their systems before being diagnosed [108]. However, many other patients may experience severe, acute and life threatening symptoms such as ketoacidosis or non-ketotic hyperosmolar syndrome or long-term complication of diabetes such as retinopathy, nephropathy, peripheral neuropathy and micro- and/or macro-vascular issues including cardiovascular dysfunction, sexual dysfunction, atherosclerosis and cerebrovascular diseases[106,107].

Before developing diabetes and/or its complications, patients usually suffer from an impairment in their oral glucose tolerance test (OGTT). Impairment in OGTT is considered as a transitional state (pre-diabetes) between ‘normal’ and diabetic patients, but is already associated with increased cardiovascular risk. However, not all patients with impairment in OGTT develop diabetes. Diabetes mellitus is

further divided into sub-groups including type-1 diabetes mellitus (T1DM) and type-2 diabetes mellitus (T2DM). T1DM, which is also called insulin-dependent diabetes, is an autoimmune disease characterised by a lack of insulin production. In T1DM, insulin is the cornerstone of treatment and patients cannot survive without it [106–108]. In T2DM, on the other hand, the formation of insulin is normal or slightly impaired, but the effects of insulin (in causing glucose uptake) in tissues are impaired. Many effective ways have been identified to prevent type-two diabetes. Even after developing T1DM or T2DM, tight glycaemic control, exercise and weight loss can prevent both the complications and pre-mature death associated with diabetes [106–108].

1.2.2 Diagnosis

The diagnosis of diabetes and of patients with an impaired OGTT are made by measuring either A1C or plasma glucose (fasting plasma glucose or glucose tolerance test), (Table 1.7) [109,110].

Table 1.7 Criteria for the diagnosis of diabetes. This table provides the tests and the thresholds for diagnosis diabetes mellitus. This table is adopted from the American Diabetes association report 2016 [111].

Criteria for the diagnosis of diabetes
FPG >=126 mg/dL (7.0 mmol/L). Fasting is no caloric intake for at least 8 h. *
OR
2-h PG >=200 mg/dL (11.1 mmol/L) during an OGTT. The test should be performed as described by the WHO, using a glucose load containing the equivalent of 75 g anhydrous glucose dissolved in water. *
OR
A1C >=6.5% (48 mmol/mol). The test should be performed in a laboratory using a method that is NGSP certified and standardized to the DCCT assay. *
OR
In a patient with classic symptoms of hyperglycaemia or hyperglycaemic crisis, a random plasma glucose >=200 mg/dL (11.1 mmol/L).

*In the absence of unequivocal hyperglycaemia, results should be confirmed by repeat testing.

After doing the first diagnostic test and to confirm the diagnosis, a second test is required. It is recommended to repeat the same test directly using a new blood sample. If the two tests give above diagnostic threshold values, the diagnosis is confirmed. The same scenario is applied if different tests give above diagnostic threshold values. However, if a patient gives discordant data of two different tests, the above of diagnostic threshold test should be repeated and the diagnosis is made depending on the new result [110].

The indications and the frequency of screening tests for diabetes depend on many factors such as: age, weight (BMI), risk factors and previous tests results [109].

1.2.3 Epidemiology

The number of patients living with diabetes has quadrupled since the 1980s. The estimated worldwide number of adult patients living with diabetes in 2014 was 422 million. The prevalence of diabetes has recently increased in low and middle income counties more than the increase in the prevalence in high income countries [107].

In the past, T2DM was exclusively seen in adults. However, recently T2DM has also been diagnosed in children. This may be related to an increase in sedentary life style leading to obesity [106,107]. Diabetes was responsible of 3.7 million deaths worldwide in 2012. Almost half of these deaths happen in patients before the age of 70. The hyperglycaemia in diabetic patients increases the risk of pre-mature death associated with cardiovascular dysfunction or failure of other organs [107].

1.2.4 Diabetic cardiomyopathy

Rubler et al. were the first to introduce the concept of diabetic cardiomyopathy as the functional and structural changes in the heart that result from metabolic abnormalities that are associated with diabetes in the absence of other causes, such as hypertension or coronary artery diseases [112]. However, the presence of these co-morbidities can amplify the risk of developing left ventricular hypertrophy, ischaemic injury and heart failure, especially in patients with T2DM [113].

The structural changes in the diabetic heart include: left ventricular hypertrophy [114], increased storage of lipid within myocytes [115], increased oxidative stress [116], increased myocyte necrosis and apoptosis [117] and fibrosis and accumulation of collagen [118]. Metabolic abnormalities include altered substrate utilization [119] and mitochondrial dysfunction [116]. All these structural and metabolic changes lead eventually to functional changes including diastolic dysfunction followed by systolic dysfunction [120].

1.2.4.1 Pathogenesis of diabetic cardiomyopathy

Many hypotheses and mechanisms have been proposed to explain the pathogenesis of diabetic cardiomyopathy. The pathogenesis is clearly multifactorial and the most important mechanisms affecting the contractile dysfunction are: myocardial inflammation, impaired calcium homeostasis, a dysregulated renin-angiotensin system, increased oxidative stress, altered substrate utilization and mitochondrial dysfunction.

1.2.4.1.1 Metabolic abnormalities

Myocardial inflammation

There is good evidence that chronic inflammation in the heart is related to diabetic cardiomyopathy [119,121,122]. This inflammation is usually subclinical and leads to diabetic cardiomyopathy after prolonged periods of time [123]. Different pathological agents and stimulus are able to initiate inflammation and induce secretion of different cytokines (IL-6), chemokines (MCP-1) and adhesion molecules (ICAM-1) in the heart resulting in myocardial infiltration of lymphocytes and monocytes [121,122,124]. Different signalling mechanisms are involved in myocardial inflammation. These mechanisms eventually lead to the activation of the NF-κB pathway, which is considered to be strongly activated in diabetics hearts [123].

Effect of high glucose and fatty acids

High glucose levels in the blood drive increases in cytokine and chemokine expression via activating the Jun NH2-terminal kinase (JNK)/NF-κB pathway [125] and glycogen synthase kinase 3 beta (GSK-3β) [126]. Hyperglycaemia also increases the expression of high-mobility group box 1 (HMGB1) leading to the activation of MAPK and NF-κB pathways and induction of TNF-α and IL-6 secretion [127]. Increased glucose levels dysregulate sirtuin-1 (SIRT1) activity and result in an increase in cardiac inflammation and decreases in SERCA2 expression[128]. Free fatty acids also contribute directly to cardiac inflammation by activating TLR4 and subsequently the NF-κB pathway [129]. Free fatty acids also activate protein kinase C (PKC) and result in MAPK activation and decrease IκB-α [130].

Effect of the Advanced glycation end products (AGEs)

The receptor for advanced glycation end products (RAGE) is a pattern recognition receptor that is upregulated by NF-κB and activated by AGEs. Once activated, it forms a heterodimer with TLR4 leading to the activation of the inflammatory response and pro-inflammatory cytokines production [131].

Effect of DAMPs

Damage associated molecular patterns (DAMPs) are obtained from cells that underwent apoptosis, injured cells or tissues. TLRs can recognise DAMPs leading to its activation and subsequently activating different inflammatory pathways [132]. Diabetes also enhances neutrophil NETosis by upregulating PAD-4 as a result of different stimulations that lead eventually to NF-κB activation. NETosis result in nuclear degradation and the release of digestion product to the extracellular space. These digestion products work as potent DAMPs that activate more leucocytes [133].

Impaired calcium homeostasis

Diabetes alters the homeostasis of calcium and other ions in the diabetic heart [134]. This disturbed homeostasis results from reduced ATPases activity, decreased ability of the sarcoplasmic reticulum to take up Ca^{2+} and reduced activity of both Na^{+}-Ca^{2+} exchangers and Ca^{2+} dependant sarcolemmal ATPases [135].

Dysregulated renin-angiotensin system

The renin-angiotensin system (RAS) is activated in diabetic patients leading to increased oxidative stress, increased apoptosis and necrosis of myocardial and endothelial cells of diabetic hearts and increased fibrosis [117]. Inhibition of RAS

with lisinopril results in protection of cardiac cells from the damage associated with impaired calcium homeostasis and inhibits reactive oxygen species (ROS) production [136].

Increased oxidative stress

In diabetic hearts, ROS production is increased from mitochondrial sources from cells exposed to hyperglycaemia [137] and non-mitochondrial sources as a result of reduced nNOS activity [138]. This increase in ROS production leads to cell death via activating some kinase pathways such as JNK, p38 kinase and Akt [139]. It may also activate protein kinase C isoform, increase production of advanced glycation end-products (AGEs) and increase glucose flux [137,140].

Altered substrate utilisation

Diabetic hearts have enhanced fatty acid metabolism and reduced glucose and lactate metabolism [141]. Even though the metabolism of fatty acids is increased in diabetic patients, lipids accumulate in the heart as a result of lower fatty acid oxidation compared to fatty acid uptake [142]. This results in lipotoxicity and formation of toxic intermediate such as ceramide leading to myocyte apoptosis [143].

Mitochondrial dysfunction

Diabetes causes structural and functional abnormalities in the mitochondria inducing a reduction in oxidative phosphorylation capacity, lower ATP synthesis [144], reduced creatine phosphate activity, lower creatine-stimulated respiration [145] and decrease in mitochondrial uptake of Ca^{2+} [146].

1.2.4.1.2 Structural changes

Cardiac hypertrophy

Diabetic cardiomyopathy manifests as dilated hypertrophic changes in the left ventricle. Although the left ventricle is more commonly affected, hypertrophy can be seen in both right and left ventricles. The increase in LV wall thickness is compensated by increasing in the LV volume [147]. Left ventricle hypertrophy usually develops at late stages of T2DM and the exact mechanism is still not fully understood. However, many factors are known to increase LV mass. Hyperinsulinaemia, for example, showed to increase cardiac mass in rats as insulin is anabolic hormone that works as a growth factor [148,149]. Another study linked the high levels of leptin in obese patients with diabetes and development of left ventricular hypertrophy [150].

Cardiac fibrosis

Biopsies from diabetic patients hearts have showed an increase in collagen deposition in the heart (both interstitial and perivascular fibrosis) [151]. Many factors play role in the development of cardiac fibrosis. For example, collagen production is increased as a result of the activated renin angiotensin aldosterone system [152], collagen degradation is also impaired as a result of decreased degradation by the matrix metalloperoxidase and the decreased susceptibility of collagen to be degraded after cross linking with the AGE [151,153]. This accumulation of collagen results in cardiac stiffness and eventually to development of diastolic dysfunction in the diabetic heart.

1.2.4.1.3 Functional changes

Diastolic dysfunction

Diastolic dysfunction develops early in diabetes and even with patients with impaired glucose tolerance [154,155]. Diastolic function can be measured using Doppler echocardiography to measure mitral valve blood flow, flow velocity and the declaration and the isovolumetric times. Diastolic dysfunction is usually present before systolic dysfunction. In diastolic dysfunction there are impairments in ventricular filling and relaxation and this manifest as an increase in left ventricle end diastolic pressure and a decrease in left ventricle end diastolic volume [156,157].

Systolic dysfunction

Despite the inconsistency about the development of systolic dysfunction in diabetic hearts in the literature, many studies in animal models of diabetes and in diabetic patients showed development of systolic cardiac dysfunction [158,159]. Systolic cardiac dysfunction manifests as decreases in ejection fraction, fractional shortening, fractional area change and cardiac output. Systolic dysfunction usually develops after diastolic dysfunction and is associated with poor prognosis and increased mortality (Figure 1.5) [160].

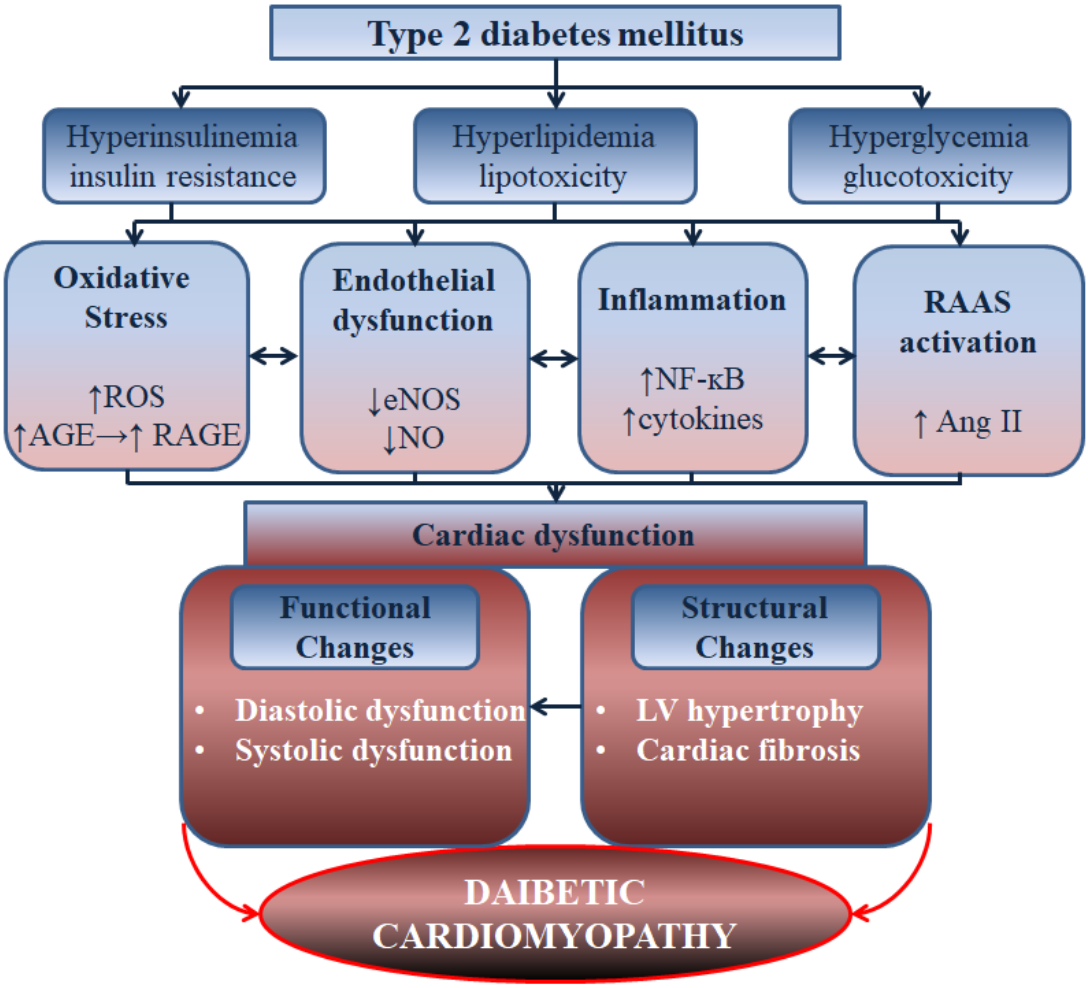

Figure 1.5 Cellular and metabolic factors that result in the development of diabetic cardiomyopathy.

Different cellular and metabolic abnormalities associated with diabetes result in structural and ultimately functional changes in the diabetic hearts. Figure adapted from Reis et al., 2012 [160].

1.2.5 Infection/sepsis in diabetes mellitus

Patients with both T1DM and T2DM are more susceptible to, and at increased risk of, developing infections. This includes both common infections such as lower respiratory tract infections, urinary tract infections and skin and soft tissue infections [161] as well as rare infections, which are almost exclusive to diabetes patients such as invasive external otitis and rhinocerebral mucormycosis [162]. Diabetes can also alter critical elements of the pathophysiology of sepsis and infection. It affects both innate (cellular and humoral) and adaptive immune systems, endothelial function and coagulation [163].

To date, the effects of diabetes on outcome in patients with sepsis are largely controversial: Some studies show that pre-existing diabetes results in increased infection-related mortality, organ dysfunction (marker of bad prognosis) and hospitalization: a study reviewing all medical records of all diabetic patients in Ontario, Canada since 1999 concludes that patients with diabetes are more likely to develop and die from infectious diseases [164]. Other studies show that the mortality among patients with community acquired pneumonia (CAP) and pneumonia in general is higher in the diabetic population and in patients with hyperglycaemia upon hospital admission [165,166]. In the Danish population, diabetes is associated with increased hospitalisation due to pneumonia, urinary tract infection (UTI) and skin infections. In the same population, diabetes was associated with a worse UTI prognosis [167]. Diabetes is also associated with worse prognosis in patients with bacteraemia [168]. In animal models of obesity, diabetes and sepsis, obese mice were more likely to develop sepsis and have higher mortality related to sepsis [169,170].

They also had increased incidence of liver injury, hepatic neutrophil infiltration [169], and hepatic microvasculature damage [171].

Other studies show no influence of diabetes on outcome or mortality related to infection. For instance, hyperglycaemia upon admission to hospital was not associated with poor prognosis in over 2000 patients with CAP [172] and diabetes did not affect outcome in 164 patients with sepsis, who were admitted to the ICU and received standard critical care [173]. The presence of diabetes did not affect the 30-days mortality in patient with community acquired bacteraemia [174] nor the ICU related mortality in insulin-treated diabetics even though they were more ill and more likely to develop renal failure[175].

A protective effect of diabetes was observed in other studies: diabetes reduced the incidence of acute respiratory syndrome in septic patients [176] and lowered the risk of developing acute respiratory distress syndrome in septic shock patients[177]. This protective effect was also seen in animal models of obesity, diabetes and sepsis; obesity decreases airways inflammation in septic animals [171] and the hyperlipidaemia associated with type 1 obesity is thought to improve the innate immune system and increase the survival in these animals [178].

1.3 Dipeptidyl Peptidase 4

Dipeptidyl peptidase 4 (DPP-4), or also called cluster of differentiation 26 (CD26) or adenosine deaminase binding protein (ADBP), is a serine protease enzyme from the S9B family. More than 30% of all proteolytic enzymes known so far are serine proteases. All known proteolytic enzymes can be classified using MEROPS database that was founded by Barrett and colleagues in 1996 [179]. In this database enzymes are grouped according to their structure, the similarities in their amino acids sequence and their activities, according to this system, serine proteases are divided into 13 clans depending on their catalytic activity and 40 families depending on their common structure and ancestry [180]. Serine proteases are also divided into endoproteases and exoproteases depending on the site of the peptide bond being hydrolysed in the polypeptide chain by the enzyme: endoproteases catalyse the hydrolysis of bonds located in the middle of proteins, while exoproteases catalyse the hydrolysis of bonds at the terminal part of the target protein. Serine proteases are distributed widely and found in both eukaryotic and prokaryotic cells [181].

The serine protease S9 family is the most studied among all serine proteases [182] and S9 proteases are responsible for peptide hormone degradation and processing, making it a target for drug design/development. For example, DPP-4 is involved in T2DM and also responsible for the processing of chemokines [183]. DPP-4 is expressed in different tissues in humans. It is mostly found in the gastrointestinal (GI) track (in the small intestine and duodenum), but also highly expressed in the prostate, placenta and kidney and to a lower extent in the heart and liver in its

membrane bound form [184]. A soluble isoform can also be found in the plasma, seminal fluid, cerebrospinal fluid and urine [185,186].

1.3.1 The structure of DPP-4

DPP-4 is a type II integral membrane glycoprotein. It is usually a dimer of 2 identical monomers. Each monomer has a short cytoplasmic portion (N-terminal) consisting of 6 amino acids (AA 1-6), a 22 amino acid transmembrane part (AA 7-29) followed by an extracellular domain consisting of two parts: an 8 blade β-propeller domain and a large catalytic α/β-hydrolase domain [187,188]. The catalytic activity of DPP-4 depends on nucleophilic attack of the substrate peptide bond (carbonyl atom) by the catalytic triad. The catalytic triad is a group of amino acids [serine (Ser), aspartate (Asp) and histidine (His)] in the catalytic site of DPP-4 (Figure 1.6) [189]. Although the homodimer is the most catalytically active form, DPP-4 is also found as monomer and homotetramer on the cell surface [190].

Soluble form of DPP-4 is in the homodimer form and it lacks the cytoplasmic and transmembrane domains. However it still has the catalytic domain, therefore, the enzymatic activity is preserved in this form [191].

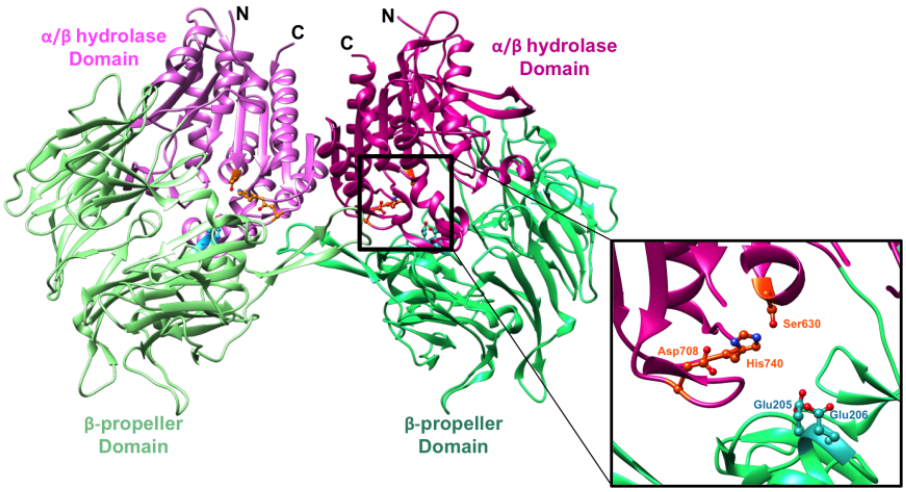

Figure 1.6 Structure of the extracellular part of the symmetric DPP-4 homodimer
Coloured in pink is the α/β hydrolase domain and the β-propeller domain (coloured in green) in each monomer. In the box is a close up of the DPP-4 active site catalytic triad (Ser^{630}, His^{740} and Asp^{708}). Figure adapted from Aertgeerts et al. 2004 [192].

1.3.2 The function of DPP-4

When it is in the active form, DPP-4 performs either catalytic or non-catalytic functions. Catalytic function is the most studied one and DPP-4 works as an exoprotease that cleaves the dipeptide from the N-terminal of the peptide chain if the second to last residue of the polypeptide is alanine, proline, hydroxyproline or dehydroproline [186]. DPP-4 controls glucose metabolism and homeostasis through regulation of incretins [193]. However, recently investigations into the potential importance of the non-catalytic effects of DPP-4 are on the rise. In the non-catalytic pathway, many proteins such as adenosine deaminase, CD45, collagen and others activate DPP-4. Interaction with these molecules leads to co-stimulation of T cells and activation of different pro-inflammatory pathways [186,193].

1.3.2.1 Catalytic activity of DPP-4

Ingestion of food stimulates the secretion of many gastrointestinal hormones. Some of these hormones are responsible for regulating gastric motility and gastric acid secretion. Other hormones such as glucagon like peptide-1 (GLP-1) and glucose-dependant insulinotropic peptide (GIP) help to lower glucose by increasing insulin secretion [194]. GLP-1 is secreted from the L cells in the colon and the ilium and GIP is secreted from the K cells in the jejunum and duodenum. The plasma levels of GLP-1 and GIP elevate within minutes of food intake. However, their levels decrease rapidly due to the enzymatic inactivation by DPP-4 and excretion via the renal system [195]. GLP-1 and GIP exert their effect after binding to G protein coupled receptors on the pancreatic β cells, adipocytes and the central nervous system for GIP and on the pancreatic α and β cells, heart, kidney, lung and gastrointestinal track for GLP-1[194]. Activation of the islet β cells by incretin leads to increase in cAMP level and intracellular calcium hence insulin secretion [196]. Both incretins promote islet β cells proliferation and inhibit apoptosis. However, only GLP-1 is able to slow gastric emptying, decrease food intake and glucagon secretion (Figure 1.7) [197].

Therefore, inhibition of DPP-4 results in an anti-hyperglycemic effect by preserving GLP-1 and GIP and prolonging their half-life [191].

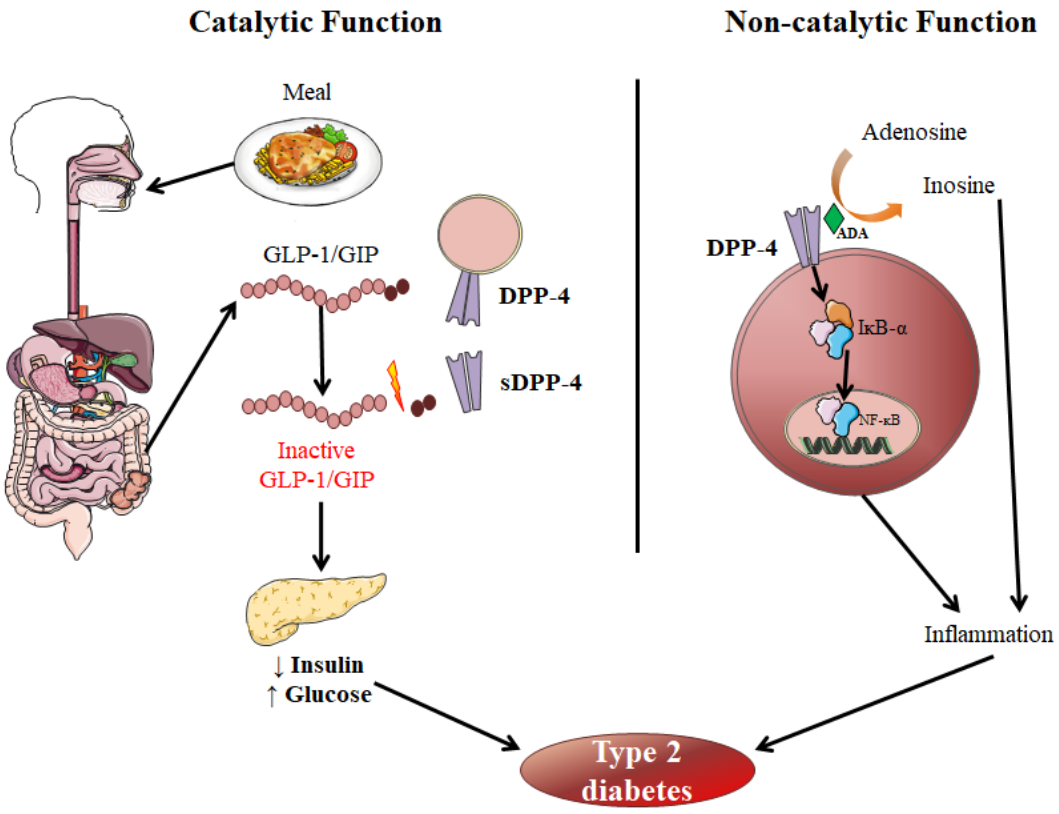

Figure 1.7 Catalytic and non-catalytic function of DPP-4. Figure modified from Zhong, et al. 2015 [198].

1.3.2.2 Non-catalytic activity of DPP-4

In addition to regulating the incretin system, DPP-4 has non-catalytic co-stimulatory function. DPP-4 from T cells binds to adenosine deaminase (ADA) leading to the activation of intracellular inflammatory pathways [199]. ADA is a polymorphic enzyme that regulates intracellular and extracellular adenosine levels by deaminating adenosine irreversibly to inosin [200]. When ADA binds to DPP-4 it potentiates T cell activation, NF-κB translocation and increases pro-inflammatory cytokines production (Figure 1.7) [201].

Binding of the DPP-4 (from the T cells) with the exposed caveolin-1 (from the antigen presenting cells, APC) leads to IRAK-1/Tollip liberation from the caveolin complex in the APC. IRAK-1 is then phosphorylated leading to NF-κB activation and CD86 upregulation and subsequently T cell co-stimulation [202,203]. Within the T cells, the interaction between caveolin-1 and DPP-4 results in the recruitment of a molecular complex of CARMA1-Bcl10MALT1-IKK in lipid rafts leading to strong NF-κB activation [202] (Figure 1.8). This mechanism is suggested to be the drive of some inflammatory diseases [204].

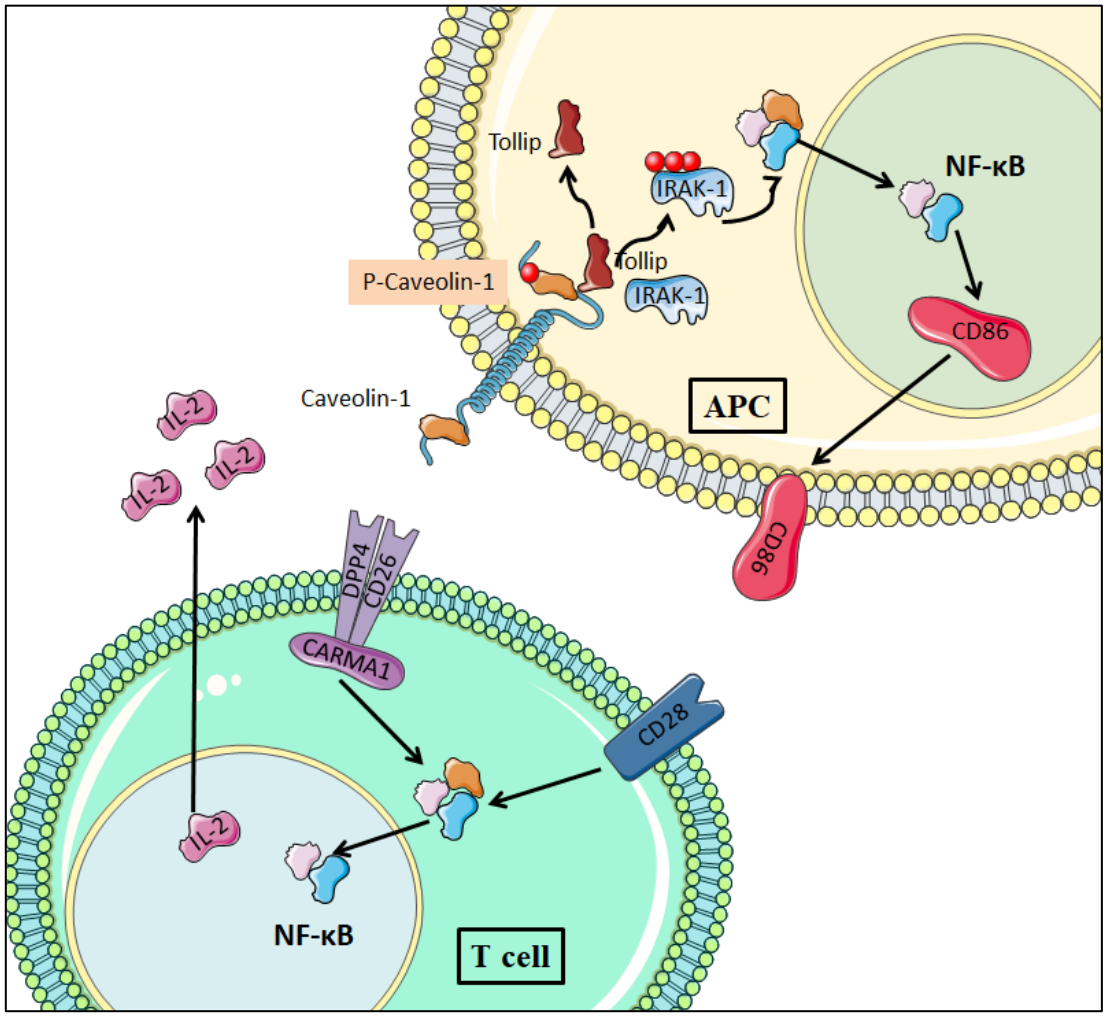

Figure 1.8 Interaction between DPP-4 and caveolin-1 and co-stimulation of T cells. Figure adopted from Klemann et al., 2016 [203].

1.3.3 DPP-4 activity and expression in diabetes mellitus

The serum levels of DPP-4 are increased in diabetic patients with or without metabolic syndrome compared to healthy individuals. This results in decreased GLP-1 levels in diabetic patients [205]. It has recently been suggested that DPP-4 is an adipokine [206] expressed in both subcutaneous and visceral adipocytes and this expression is positively correlated with body mass index. The levels of DPP-4 are also correlated with adipocytes size, HbA1c level and inflammatory status [207]. For example, TNF-α increases DPP-4 release from the differentiated adipocytes. The released DPP-4 then exhibits paracrine activity on insulin sensitivity in skeletal muscle and adipocytes [206]. Peripheral T cell expression of DPP-4 increases in the blood of patients with diabetes and poor glycaemic control [208]. Liver of patients suffering from non-alcoholic fatty liver disease shows increase in DPP-4 activity and this increase is correlated with the degree of insulin resistance and results in impaired glucose metabolism in the liver [209].

1.3.4 DPP-4 inhibitors

DPP-4 inhibitors [approved by the Food and Drug Administration (FDA) and the European Medicine Agency (EMA)] are divided into two groups depending on their structure: dipeptidomimitics (sitagliptin, vildagliptin and saxagliptin) and non-peptidomimetics (linagliptin and alogliptin) [191] (Table 1.8).

Table 1.8 Approved DPP-4 inhibitors classified according to their structure.

Class	Drug	Approved	Base	Structure
Dipeptidomimetics	Sitagliptin	2006	β-amino acid	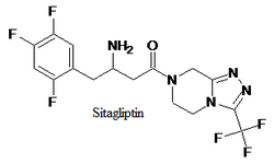
	Vildagliptin	2007	Nitrile	
	Saxagliptin	2009	Nitrile	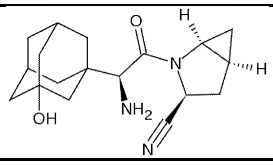
Non-peptidomimetics	Linagliptin	2011	Xanthine	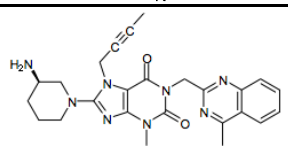
	Alogliptin	2013	Pyrimidinedione	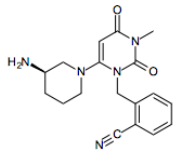

These drugs show moderate efficacy in lowering blood glucose and HbA1c compared to other classes of anti-hyperglycaemic drugs such as sulfonylureas, thiazolidinediones and insulin. However, they provide a good alternative or adjunct therapy to traditional anti-diabetic drugs such as metformin [210]. Gliptins result in less than 1% reduction in HbA1c. This reduction depends on baseline HbA1c and concomitant drugs use [211]. Common side effects related to gliptin use are headache, upper respiratory tract and urinary tract infections. Hypoglycaemia is not common with gliptins use alone. However, incidence of hypoglycaemia increases with the concomitant use of sulfonylurea or insulin [210]. Unlike other gliptins, linagliptin does not need dose adjustment in renal impairment patients [212].

1.3.4.1 Anti-inflammatory effect of DPP-4 inhibitors

DPP-4 inhibitors have been used as anti-diabetic drugs. However, recent evidence indicates that DPP-4 inhibitors also have anti-inflammatory effects.

1.3.4.1.1 DPP-4 effect on vascular inflammation

Endothelial cell apoptosis and vascular dysfunction occur in many diseases including diabetes, atherosclerosis and sepsis. DPP-4 is expressed in endothelial cells and DPP-4 activity plays a role in vascular dysfunction related to these diseases, while inhibition of DPP-4 using different inhibitors results in improved vascular function.

Pretreatment of animals with DPP-4 inhibitors prior to LPS challenge resulted in an increase in survival and an improvement in endothelial cell function. Mice and rats treated with linagliptin prophylactically prior to high dose of LPS showed an increase in survival rate. In contrast, pre-treatment with sitagliptin had no effect on survival in endotoxaemic animals [213,214]. Both drugs attenuated the hypotension [214] and vascular dysfunction [213,214] caused by LPS and corrected the inflammatory status by supressing mRNA expression of some pro-inflammatory cytokines, ROS formation and whole blood nitrosyl-iron haemoglobin [213,214]. These beneficial effects were abolished in AMP-activated kinase (α1) knockout mice suggesting that AMPK mediated NF-κB activation may be the target of these drugs [214]. This hypothesis was confirmed after measuring AMPK activity in diabetic rats aorta after treatment with sitagliptin[215] and in isolated human umbilical vein endothelial cell (HUVECs) incubated with high glucose and treated with sitagliptin [216].

Oral administration of linagliptin in rats for 7 days before LPS challenge reduced inflammatory cell filtration in the aorta and ROS formation in the heart, vesicles and blood [217]. Linagliptin also suppressed the LPS-stimulated adhesion of isolated activated human neutrophils to HUVECs [217], increased the activity of both PKA and PKC, inhibited LPS induced AP-1 nuclear translocation and PKB phosphorylation [218], reduced IL-6 production, translocation of NF-κB to the nucleus and p38 MAPK phosphorylation [219]. These results demonstrate that these beneficial effects of linagliptin are GLP-1 independent, as the effects of linaglipitin were studied in HUVECs which do not secrete GLP-1 [219].

1.3.4.1.2 DPP-4 effect on cardiac function

Long-term linagliptin treatment of mice fed a high fat diet prevented structural (hypertrophy and fibrosis) and functional (contractile dysfunction) abnormalities in the heart by inhibiting TRAF3IP2 expression resulting in reduced NF-κB, AP-1 and p38 MAPK activation [220]. Sitagliptin treatment for 8 weeks in rats fed with high salt diet resulted in attenuation of diastolic dysfunction and improved survival by decreasing collagen deposition in the heart, reducing myocardial oxidative stress, pro-inflammatory cytokines levels and myocardial stiffness [221]. Treatment of cardiac fibroblast incubated with aldosterone with linagliptin reduced TRAF3IP2 expression, inflammatory cytokines and collagen induction [220]. Cardiomyoblast stimulated with LPS showed increase in TNF-α, IL-6, IL-1β, cyclooxygenase-2 and iNOS expression and NF-κB nuclear translocation. All of these effects were dose dependently supressed by sitagliptin [222].

1.4 Hypotheses and Aims of the Thesis

Sepsis is associated with a high mortality rate among ICU patients. The development of cardiac dysfunction results in further increase in the in-hospital mortality among patients with sepsis and septic shock. Both the incidence and the mortality rate of sepsis and septic shock increase with age mainly due to the presence of co-morbidities in this age group (e.g. diabetes). Further investigations are still needed to understand the pathophysiology of sepsis-associated cardiac dysfunction and the effect of pre-existing conditions such as diabetes in the pathophysiology and the severity of the cardiac dysfunction associated with sepsis.

This thesis aims to investigate the following hypotheses:

1. Feeding mice with a HFD results in a T2DM phenotype and diabetic cardiomyopathy.
2. Pre-existing T2DM augments the cardiac dysfunction associated with endotoxaemia or CLP-sepsis in mice.
3. Activation of the NF-κB pathway is the key driver of sepsis-associated cardiac dysfunction in mice with pre-existing T2DM, and
4. Inhibition of the NF-κB pathway with a selective IKK inhibitor (IKK-16) or a DPP-4 inhibitor (linagliptin) attenuates the cardiac dysfunction in mice with sepsis and diabetes.

Based on the above hypotheses, this thesis had the overall aims to:

1. Establish a mouse model of HFD-induced T2DM and diabetic cardiomyopathy,
2. Investigate the effect of pre-existing T2DM on cardiac dysfunction associated with endotoxaemia or CLP-sepsis,
3. Elucidate the signalling mechanism that resulted in the aggravation of cardiac dysfunction in mice with T2DM/sepsis, and
4. Examine the effect of IKK-16 or linagliptin treatment on the cardiac dysfunction associated with sepsis in mice with pre-existing T2DM.

CHAPTER 2: ESTABLISHING A MOUSE MODEL OF TYPE 2 DIABETES AND DIABETIC CARDIOMYOPATHY

2.1 Introduction

Diabetes mellitus is a complex metabolic disorder that develops secondary to impairment in insulin secretion as a result of pancreatic beta cell destruction, reduced sensitivity to insulin in different tissues or a combination of both. Diabetes results in an impairment in glucose homeostasis and manifests as a chronic elevation of blood glucose (hyperglycaemia) [106,223]. The persistent hyperglycaemia can drive the development of different organs dysfunction, damage and failure [108]. Hyperglycaemia is also linked to the increased incidence of premature death associated with different organs dysfunction [223].

The most common types of diabetes are type 1 diabetes mellitus (T1DM), also called insulin-dependent diabetes and type 2 diabetes mellitus (T2DM), also called insulin-independent diabetes [106,108,223]. In T1DM, hyperglycaemia develops secondary to insulin depletion as a result of β cells destruction in the pancreatic islets of Langerhans and it is believed to be a result of an autoimmune disorder that can be triggered by different environmental factors [224,225]. In T2DM, on the other hand, hyperglycaemia develops secondary to insulin resistance or, in more severe cases of T2DM, beta cell failure. The cause of insulin resistance in T2DM is multifactorial and not fully understood and the key trigger for the early insulin

resistance is still unknown. However, studies suggest the involvement of complex genetic and environmental triggers [226].

Around 422 million adults lived with diabetes in 2014, among them almost 90% suffered from T2DM [223]. This number is expected to increase to 592 million by 2035 [227]. The prevalence of T2DM has been increasing steadily for the past few decades and the incidence is increasing in all age groups including children [106]. This makes T2DM a global issue with high economic cost in all countries. Therefore, If we can find effective ways to prevent this disease and manage its complications we can guarantee a better quality of life and reduce its economic burden [227].

For a better understanding of this disease and its complications, different animal models have been introduced in the literature to study diabetes. This enables us to get a better insight of the pathophysiology of the disease, test the efficacy of potential therapies and insulin formulas, and study diabetes complications [228]. Modelling T2DM in animals can be done either by genetic manipulation of single or multiple genes or environmental changes by introducing high fat diet (HFD) to animals to induce obesity and ultimately T2DM. Unfortunately, none of the existing models of T2DM can completely reflect the complex human disease. Different animal models provide different levels of severity of the disease measured as varying degrees of insulin resistance, beta cell dysfunction and diabetic complications.

Genetically induced T2DM is subdivided into monogenic and polygenic models. The most common monogenic models of T2DM depend on the disturbance of leptin signalling. A single mutation in leptin (ob/ob mice) or leptin receptor genes

(db/db mice) results in excessive food consumption and obesity [228]. These two models are frequently used to study potential therapeutic interventions [229–231]. Polygenic models of T2DM are also available. Although they are more clinically relevant than monogenic models, they still can't exactly model the disease seen in man, because more than 50 genes have been identified to play a role in the pathophysiology of human diabetes, and the respective genes are not all affected in these polygenic models [232,233]. Therefore, using gene-dependant models of T2DM to model diabetes may not be the most appropriate approach even though they are well standardised and characterised.

As the increase in the sedentary lifestyle and western diet consumption are the main causes of type 2 diabetes to date [106,223], the administration of a HFD is considered to be the most appropriate strategy for inducing experimental T2DM especially when aiming to study cardiovascular alterations and diabetic cardiomyopathy [234]. Thus far, no single standard protocol of HFD-induced diabetes has been established. Since its introduction in 1988 by Surwit and co-workers [235], different protocols (and compositions) of HFD have been reported in the literature. Protocols described in the recent publications used different i) mouse strains, ii) formulation of HFD (with fat fractions ranging from 20% to more than 60%) [236], iii) duration of feeding (ranging from few weeks up to more than a year) and iv) age of mice at the introduction of the HFD [237]. Even with a similar percentage of fat, various compositions lead to very different biological responses. For example, with increasing amounts of saturated fatty acids and with the introduction of longer fatty acid chains, the diet becomes more obesogenic [238]. Different origins of the fat in the HFD also affect outcome with animal-derived fat (such as lard) being more obesogenic than plant-derived oils (such as sunflower oil) [239].

Like human T2DM, animal models of HFD-induced diabetes affect different tissues and organ systems and resulting in diabetes complications. In adipose tissues, for example, adipocytes change metabolism and morphology in mice fed with HFD. Both number and size of adipocytes increase after the introduction of HFD [240,241]. Adipocytes also secrete adipocytokines as a result of HFD feeding [242]. Visceral white fat is the most pathogenic, as it secretes large quantities of adiponectin, TNFα and IL-6 [243]. HFD also negatively affects the liver [244,245] by causing hepatic steatosis [246]. Liver injury starts with fat accumulation in the liver (steatosis) that then results in inflammation and develops into non-alcoholic steatohepatitis (NASH), fibrosis, cirrhosis and untimely hepatocellular carcinoma with continuous HFD feeding [237]. Unlike adipose tissue and the liver, the effects of HFD on cardiac tissue and function are less clear. Many studies show that HFD results in diabetic cardiomyopathy [247–250] while other studies show no cardiac dysfunction even after longer periods of HFD [234,251]. Although the presence of variable protocols of HFD models of T2DM can be an advantage as it provides high flexibility, it makes finding the best protocol (diet composition and duration of feeding) quite challenging.

In this chapter, I aimed to establish and standardise a mouse model of HFD-induced T2DM with small degrees of diabetic complications (diabetic cardiomyopathy, liver injury and kidney injury) in order to use this model in later studies to investigate the effect of pre-existing T2DM on the cardiac and, indeed, the multiple organ dysfunction associated with sepsis in mice.

2.2 Scientific Hypothesis and Aims

This study is driven by the hypothesis that:

- Feeding mice with a HFD results in type 2 diabetes mellitus phenotype and diabetic cardiomyopathy.

This study aims to:

- Establish a mouse model of HFD-induced type 2 diabetes mellitus and diabetic cardiomyopathy that can be used later as a first hit in the coming experiments to study the effect of diabetes on cardiac dysfunction in sepsis,
- Test an alternative HFD for developing diabetes and diabetic cardiomyopathy to be used instead of the first diet after having some issues with the supply of the first diet,
- Intensify the study about the new diet to make sure that is results in similar diabetes complication to the first diet.

2.3 Methods and Materials

The animal protocols followed in this study were approved by the local Animal Use and Care Committee in accordance with the derivatives of both, the Home Office Guidance in the Operation of Animals (Scientific Procedure Act 1986) published by Her Majesty's Stationary Office, and the Guide for the Care and Use of Laboratory Animals of the National Research Council.

2.3.1 Animals

The studies in this chapter were conducted on 56 ten-week old male C57BL/6 mice (Charles River, Kent, UK) weighing 25-30 g, receiving a standard diet and water *ad libitum* (before starting the experiments). Mice were housed 5 per cage in a temperature-controlled room with a 12-hour light/dark cycle. Sixteen mice were used in the first study to establish the first mouse model of T2DM and diabetic cardiomyopathy and 40 mice were used to establish the second model of T2DM and diabetes complications and the follow-up study.

2.3.2 Measuring body weight and feeding behaviour

The body weight and food and calorie intake of mice were measured weekly to ensure good health and monitor their eating habits. The body weight of all animals was measured at the same time at the beginning of each week using the same balance for the whole experiment. New fresh food (150 gram/cage) was supplied to mice at the beginning of each week and observed every few days during the week for colour or consistency changes. Diet weight was measured at the end of

each week before being changed to measure food intake and calculate weekly calories intake for each cage using the following equations:

$$\text{Food intake} = \frac{Diet\ weight\ (begining\ of\ the\ week) - Diet\ weight\ (end\ of\ the\ week)}{(Number\ of\ mice\ in\ the\ cage \times Number\ of\ days)}$$

Equation 1: Food intake (grams/mouse/day) is calculated using 4 measurements a) diet wait at the start of the week (grams), b) diet weight at the end of the week (grams), c) number of mice in each cage and d) number of days.

$$\text{Calories intake} = \text{Food intake} \times [(\text{Protein}, \% \times 4) + (\text{Fat}, \% \times 9) + (\text{Carb}, \% \times 4)]$$

Equation 2: Calories intake (Kcal/mouse/day) is calculated using 4 measurements a) food intake (grams/mouse/day), the percentage of b) protein, c) fat and d) carbohydrates.

2.3.3 Oral Glucose Tolerance Test (OGTT)

Mice were fasted for 6 h (8 am-2 pm) by being moved to clean cages with no food supply, but with free access to water. At the end of the 6 h fasting, the body weight was measured for each mouse, then a small cut to the side of the tail was made to obtain blood. Fasting blood glucose was measured and mice then received a bolus dose of glucose (2 g/kg, dissolved in drinking water) via oral gavage using an 18 G stainless steel feeding tube. Blood glucose levels were then measured at 15, 30, 45, 60, 90 and 120 min post glucose administration using blood glucose meter Accu-Chek® (Accu-Chek Compact System; Roche Diagnostics, Basel, Switzerland).

2.3.4 Insulin Tolerance Test (ITT)

Mice were fasted for 4 h (10 am-2 pm) by being moved to clean cages with no food supply but with free access to water. At the end of the 4 h fasting, the body weight was measured for each mouse then a small cut to the side of the tail was made to obtain blood. Fasting blood glucose was measured and mice then received a dose of insulin aspart (NovoRapid®) (0.75 U/kg, i.p.). Blood glucose level was then measured at 15, 30, 45, 60, 90 and 120 min post insulin administration using blood glucose meter Accu-Chek® (Accu-Chek Compact System; Roche Diagnostics, Basel, Switzerland).

2.3.5 Measuring fasting insulin level

Mice were fasted for 6 h (8 am-2 pm) by being moved to clean cages with no food supply but with free access to water. Blood samples were obtained from the tail vein and serum samples were then obtained. Serum insulin was measured using a human insulin ELISA kit following manufacturer instructions (Abcam®, Cambridge, UK).

2.3.6 Assessment of Cardiac Function *in Vivo* (Echocardiography)

Echocardiography was conducted *in vivo* at baseline then at week 6 and 12 (and at week 16 in the first study) to measure cardiac function for the development of diabetic cardiomyopathy using a 30 MHz RMV707B scan head and a Vevo-770 imaging system (VisualSonics, Toronto, Ontario, Canada).

Animals were anaesthetized using 3% isoflurane delivered with 0.4 L/min oxygen in the anaesthesia chamber. After being sedated, mice were then transferred to the

echo table and taped from the limbs in a supine position onto the metal ECG leads on the Echo platform. Anaesthesia was maintained during the whole imaging process using 2% isoflurane delivered with 0.4 L/min oxygen via nosecone under spontaneous breathing. The handling platform was warmed to 40 °C in order to keep the core body temperature of the mice. After being placed on the platform, the fur on the chest was then removed carefully using Veet® hair removing cream. A pre-warmed echo gel is then applied to the chest to start the measurement. At least 10 min were left for the animals to stabilise before any measurement was taken. The body temperature was monitored using a rectal probe and the heart rate was obtained from ECG tracing during the whole procedure.

Measurements from both two-dimensional (brightness mode, B-mode) (Figure 2.1) and one-dimensional (motion mode, M-mode) were obtained (Figure 2.2). Measurements of the left ventricle internal dimension (LVID) in both systole (LVID; s) and diastole (LVID; d) from the M-mode at the level of the papillary muscles were used to calculate the percentage ejection fraction (% EF), fractional shortening (% FS) and the measurements of LV end-systolic and end-diastolic areas from the B-mode were used to calculate the percentage functional area change (% FAC) using the following equations:

$$\%\ \mathrm{EF}\ = \frac{(\mathrm{LVID;d}^3 - \mathrm{LVID;s}^3)}{\mathrm{LVID;d}^3} \times 100$$

Equation 3: Ejection fraction (%) is calculated using 2 measurements a) left ventricle internal dimension during diastole (mm) and b) left ventricle internal dimension during systole (mm).

$$\% \text{ FS } = \frac{(\text{LVID; d} - \text{LVID; s})}{\text{LVID; d}} \times 100$$

Equation 4: Fractional shortening (%) is calculated using 2 measurements a) left ventricle internal dimension during diastole (mm) and b) left ventricle internal dimension during systole (mm).

$$\% \text{ FAC } = \frac{(\text{LV area; d} - \text{LV area; s})}{\text{LV area; d}} \times 100$$

Equation 5: Fractional area change (%) is calculated using 2 measurements a) left ventricle end-diastolic area (mm^2) and b) left ventricle end-systolic area (mm^2).

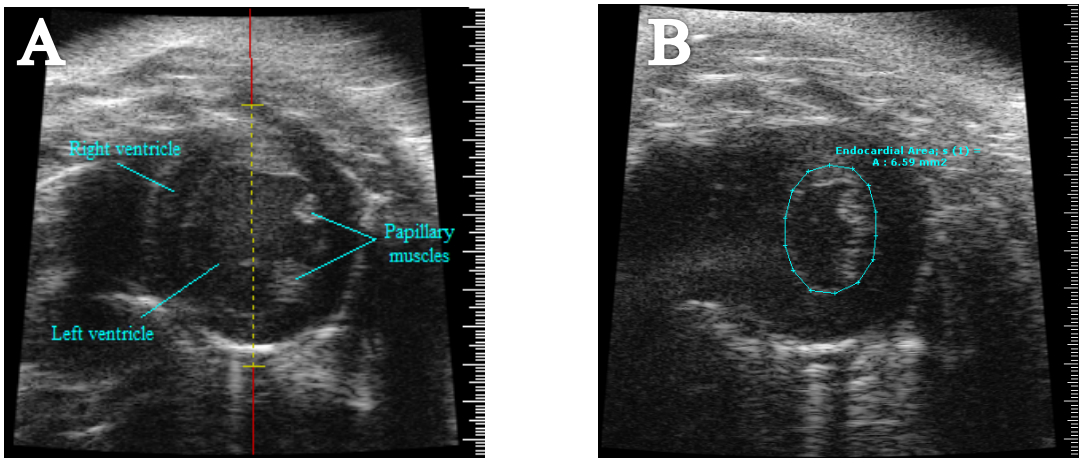

Figure 2.1 Two dimensional (B-mode) murine echocardiography
Representative brightness mode echocardiogram image of **(A)** a mouse heart in a parasternal short axis view at the papillary muscles level and **(B)** a measurement of the left ventricular endocardial area during systole to calculate the percentage fractional area change (FAC %).

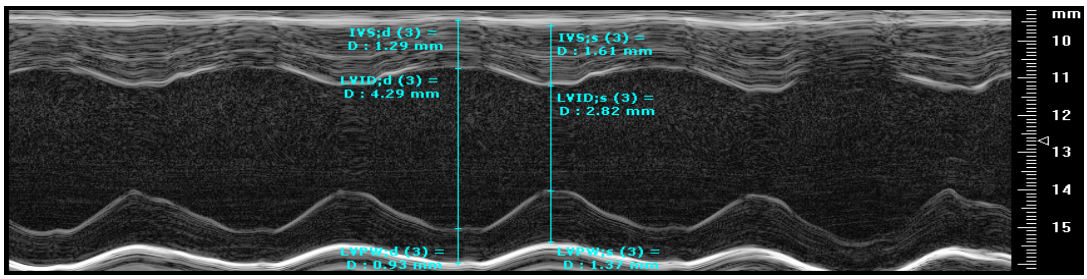

Figure 2.2 One dimensional (M-mode) murine echocardiography

Motion mode is used to measure the left ventricle internal dimensions (LVID) during systole and diastole in order to calculate the percentage ejection fraction (EF %) and fractional shortening (FS %).
IVS: Intraventricular septum, LVPW: left ventricular posterior wall, s: systole, d: diastole.

2.3.7 Assessment of kidney function

During the last week of the experiment, mice were housed in the metabolic cages to collect urine. They were housed (one mouse per cage) for 24 h with free access to food and water. Urine biochemistry (creatinine and sodium levels) was assessed blindly by IDEXX the commercial veterinary testing laboratory (IDEXX Ltd; West Sussex, UK). Urine albumin was measured using a mouse albumin ELISA kit following manufacturer instructions (Cambridge Bioscience®, Cambridge, UK). Then creatinine clearance (CrCl) and urine albumin to creatinine ratio (ACR) were calculated to measure glomerular and tubular functions using the following equations:

$$\mathrm{CrCl} = \frac{\text{Urine Creatinine}}{\text{Serum Creatinine}} \times \frac{\text{Urine Volume}}{\text{Time}}$$

Equation 6: Creatinine clearance (ml/min) is calculated using 4 measurements a) urine creatinine (µmol/L), b) serum creatinine (µmol/L), c) urine volume (ml) and d) time (minutes).

$$\mathrm{ACR} = \frac{\text{Urine Albumin}}{\text{Urine Creatinine}}$$

Equation 7: Urine albumin to creatinine ratio is calculated using 2 measurements a) urine albumin (µg/L) and b) urine creatinine (mg/L).

2.3.8 Blood and organ collection

At the end of the last cardiac function assessment, mice were anesthetised with high dose isoflurane then blood samples were collected by cardiac puncture and then mice were sacrificed to terminate the experiment. Blood samples were immediately transferred into EDTA tubes for immediate whole blood analysis

and/or gel tubes (for serum separation). Serum samples were obtained by centrifugation of the blood at 9000 RPM for 3 min and then snap frozen in liquid nitrogen and then kept in -80 °C freezer. Vital organs were collected and snap frozen in liquid nitrogen or frozen in cold 2-methyl butane and kept later in -80°C freezer for long-term storage or fixed in 10% neutral buffered formaldehyde for 48 h then transferred into 70% ethanol for long-term storage and further analysis.

2.3.9 Blood Analysis

Serum biochemical markers (creatinine, urea, ALT, total cholesterol, triglycerides, LDL, HDL, glucose and sodium) were measured blindly by the commercial veterinary testing laboratories IDEXX (West Sussex, UK) and MRC Harwell institute (Oxford, UK).

Whole blood analysis (complete blood count and WBC differential count) was conducted using IDEXX ProCyte Dx® haematology analyser (IDEXX BioResearch, Ludwigsburg, Germany)

2.3.10 Histological analysis

For collagen visualization, formalin-fixed liver samples were embedded in paraffin and cut into 4 μm sections. For staining, sections were deparaffinised using two washes of xylene and rehydrated with decreasing concentrations of ethanol (100%, 95%, 90%, 80% and finally 70%) and washed with distilled water. Hydrated sections were adequately covered with Picro-Sirius Red stain (Abcam ®, Cambridge, UK) and incubated in the dark for 1 hour then rinsed twice with 0.5% acetic acid solution. Sections then were dehydrated in absolute alcohol (100%

ethanol), cleared with d-limonene (national diagnostic®, Nottingham, UK) and coverslipped using distyrene, plasticizer and xylene (DPX) mountant.

For fat visualization, frozen liver samples (using 2-methyl butane) were embedded in optimal cutting temperature compound (OCT compound) and cut into 10 µm sections. Frozen sections were left at room temperature for 10 min and fixed in 10% neutral buffered formaldehyde for 5 min then rinsed thoroughly with running tap water. Sections then were adequately covered with Oil Red-O stain (1% Oil Red-O in 60% isopropyl alcohol) and incubated for 15 min, differentiated twice with 60% isopropyl alcohol solution and rinsed with water. Sections were counterstained with Mayer's haematoxylin for 2 min, blue in running tap water and coverslipped using aqueous Dako glycergel mounting medium (Dako, Cambridge, UK).

Slides from both protocols were then scanned using a NanoZoomer Digital Pathology Scanner (Hamamatsu Photonics K.K. Japan) and high-resolution images were obtained for analysis. Form each image, 10 fields were selected randomly at magnification (40x) to quantify collagen or lipid. Percentages of Oil Red-O or Sirius Red positive staining were calculated using ImageJ software.

2.3.11 Statistical analysis

Data was analysed using GraphPad Prism 7.0 (GraphPad Software, San Diego, California, USA). Values stated in the text and figures are presented as a mean ± standard error of the mean (SEM) of n observations, where n is the number of animals used. Data was tested for normality using D'Agostino-Pearon normality test and then assessed using Two-way or One-way ANOVA test followed by

Bonferroni's post hoc test or unpaired Student t-test where appropriate. *P* values of less than 0.05 were considered to be statically significant.

2.3.12 Materials

Unless otherwise stated, all materials, reagents and solutions were purchased from Sigma-Aldrich Ltd (Poole, Dorset, UK).

2.4 Experimental Designs and Studies Groups

2.4.1 First Model of T2DM Using HFD (58R3: Red diet):

10 weeks old mice were randomised to receive HFD or chow diet as following

Table 2.1 Experimental groups used to establish a mouse model of high fat diet induced T2DM and diabetic cardiomyopathy.

Group name	Diet	Intervention	Number
Chow	Normal chow diet	None	8
HFD*	High fat diet	None	8

* Diet compositions and nutritional profile are provided in Table 2.4. Chow diet was purchased from TestDiet® (St. Louis, Missouri, USA) and the high fat diet (58R3: red diet) was purchased from LabDiet® (St. Louis, Missouri, USA).

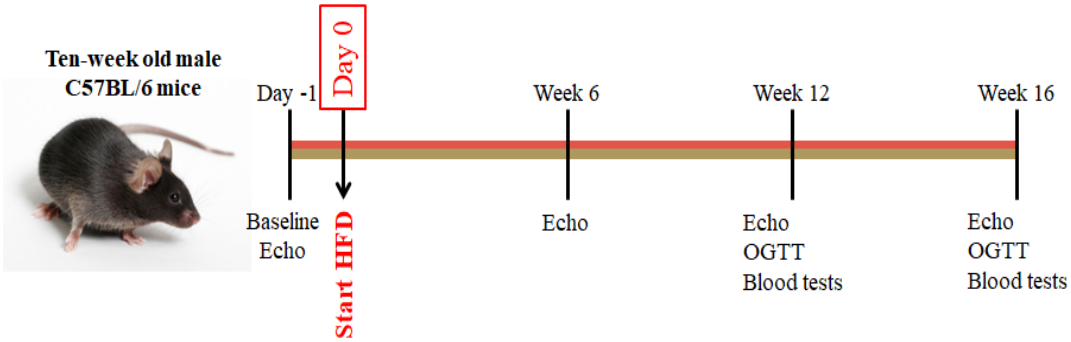

Figure 2.3 Summary of the experimental procedures and the follow-up plan used to study the first mouse model of high fat diet induced T2DM and diabetic cardiomyopathy.
Mice were randomised to receive chow or high fat diet for 16 weeks. Body weight, food and calorie intakes were measured weekly. At 0, 6, 12 and 16 weeks, cardiac function was measured using *in vivo* echocardiography. At 12 and 16 weeks blood samples were collected to measure kidney and liver function. Mice were also challenged with bolus oral glucose to measure the degree of impaired glucose tolerance at 12 and 16 weeks.

2.4.2 Second Model of T2DM Using HFD (58Y1: Blue diet):

Table 2.2 Experimental groups used to establish a second mouse model of high fat diet induced T2DM and diabetic cardiomyopathy.

Group name	Diet	Intervention	Number
Chow	Normal chow diet	None	10
HFD*	High fat diet	None	10

* Diet compositions and nutritional profile are provided in Table 2.4. Chow diet was purchased from TestDiet® (St. Louis, Missouri, USA) and the high-fat diets (58Y1: blue diet) was purchased from LabDiet® (St. Louis, Missouri, USA).

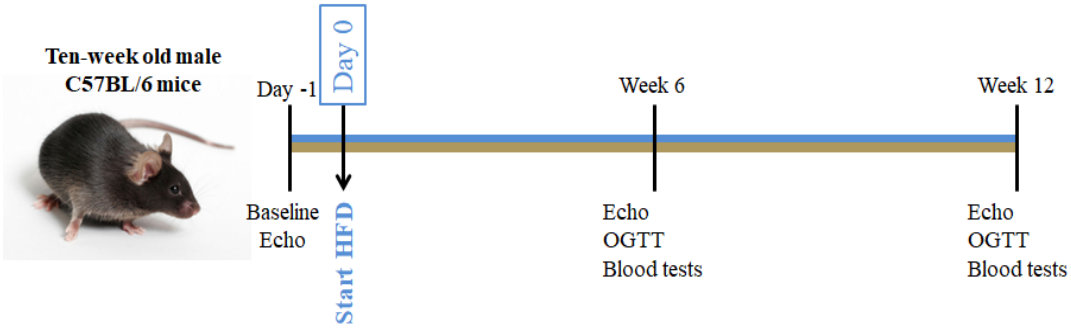

Figure 2.4 Summary of the experimental procedures and the follow-up plan used to study the second mouse model of high fat diet induced T2DM and diabetic cardiomyopathy.
Mice were randomised to receive chow or high fat diet for 12 weeks. Body weight, food and calorie intakes were measured weekly. At 0, 6 and 12 weeks, cardiac function was measured using *in vivo* echocardiography. At 6 and 12 weeks blood samples were collected to measure kidney and liver function. Mice were also challenged with bolus oral glucose to measure the degree of impaired glucose tolerance at 6 and 12 weeks.

2.4.3 Follow up Study to Measure the Diabetes Complications that Result from the Second Model of T2DM Using HFD (58Y1: Blue diet):

Table 2.3 Experimental groups used to study the diabetes complications in the second mouse model of high fat diet induced T2DM and diabetic cardiomyopathy.

Group name	Diet	Intervention	Number
Chow	Normal chow diet	None	10
HFD*	High-fat diet	None	10

* Diet compositions and nutritional profile are provided in Table 2.4. Chow diet was purchased from TestDiet® (St. Louis, Missouri, USA) and the high-fat diets (58Y1: blue diet) was purchased from LabDiet® (St. Louis, Missouri, USA).

Figure 2.5 Summary of the experimental procedure used to study the diabetes complications in the second mouse model of HFD induced T2DM and diabetic cardiomyopathy.
Mice were randomised to receive chow or high-fat diet for 12 weeks. Body weight, food and calorie intakes were measured weekly. At weeks, mice were challenged with insulin to measure insulin resistance, blood samples were collected to measure serum insulin, glucose, lipids' profile and haematology markers. Urine samples were collected to measure CrCl and ACR. Vital organs were collected for later analysis.

Table 2.4 Diet compositions and nutritional profile for the test diets used in chapter 2.

		Diet		
		Chow	**Red**	**Blue**
				
Energy (Kcal/g) [2]	Protein, %	24.5	14.9	18.1
	Fat, %	13.1	59.4	61.6
	Carbohydrate, %	62.4	25.7	20.3
Fat composition	Cholesterol, ppm	142	0.0	301
	Linoleic Acid, %	2.14	1.28	4.7
	Linolenic Acid, %	0.27	0.19	0.39
	Arachidonic Acid, %	<0.01	0.0	0.06
	Omega-3 Fatty Acids, %	0.44	0.19	0.39
	Total Saturated Fatty Acids, %	0.78	31.55	13.68
	Total Monounsaturated Fatty Acids, %	0.97	0.62	14.0
	Polyunsaturated Fatty Acids, %	0.0	1.47	0.0
Fat Origin	Animal (Lard) vs. plant (Coconut oil)	Plant	Plant	Animal

2.5 Results

2.5.1 First Model of T2DM Using the HFD (58R3: Red Diet)

1. Effect of high-fat diet on eating habits and body weight in a model of HFD-induced T2DM

When compared to chow-fed mice, food intake in mice fed the HFD was significantly lower during the whole experiment ($P<0.05$, Figure 2.6 A). However, there was no significant difference in calorie intake between the two groups ($P>0.05$, Figure 2.6 B). When compared to mice on a chow diet, mice fed the HFD showed a significant increase in body weight starting from week 3 (after the commencement of the diet) until the end of the experiment ($P<0.05$, Figure 2.6 C). At the end of week 16, HFD-fed mice showed a significant net weight gain compared to chow-fed mice ($P<0.05$, Figure 2.6 D).

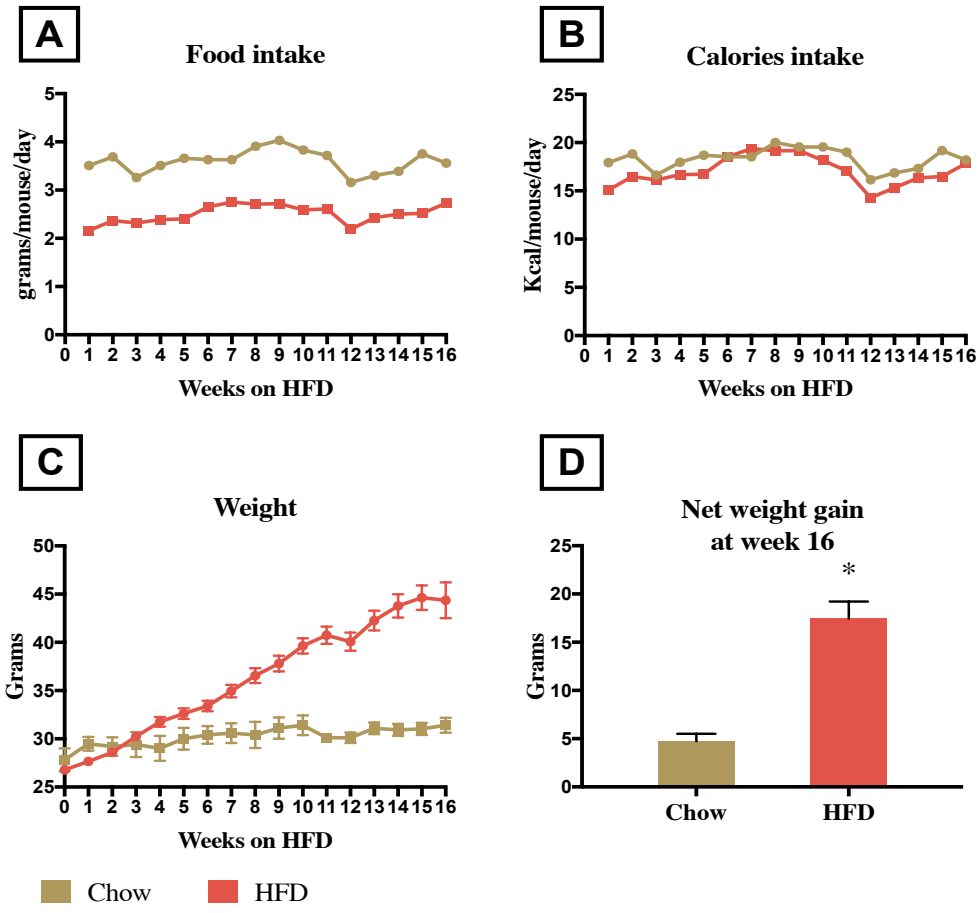

Figure 2.6 Food intakes, calories intake and weight data.
Summary of weekly change in **(A)** food intake, **(B)** calories intake and **(C)** body weight for 16 weeks in both chow and HFD fed groups and the **(D)** net weight gain at the end of the experiment in both groups. Data was analysed using unpaired t-test and presented as mean ± SEM, **P*< 0.05 when compared to chow mice (n=8 per group).

2. Effect of high-fat diet on diabetic parameters in a model of HFD-induced T2DM

When compared to age-matched mice on a chow diet, mice fed the HFD for 12 or 16 weeks and challenged with an oral dose of glucose showed significant impairment of glucose tolerance (*P*<0.05, Figure 2.7). When compared to mice on HFD for 12 weeks, mice on HFD for 16 weeks showed no significant changes in glucose tolerance after being challenged with an oral dose of glucose (*P*>0.05, Figure 2.7).

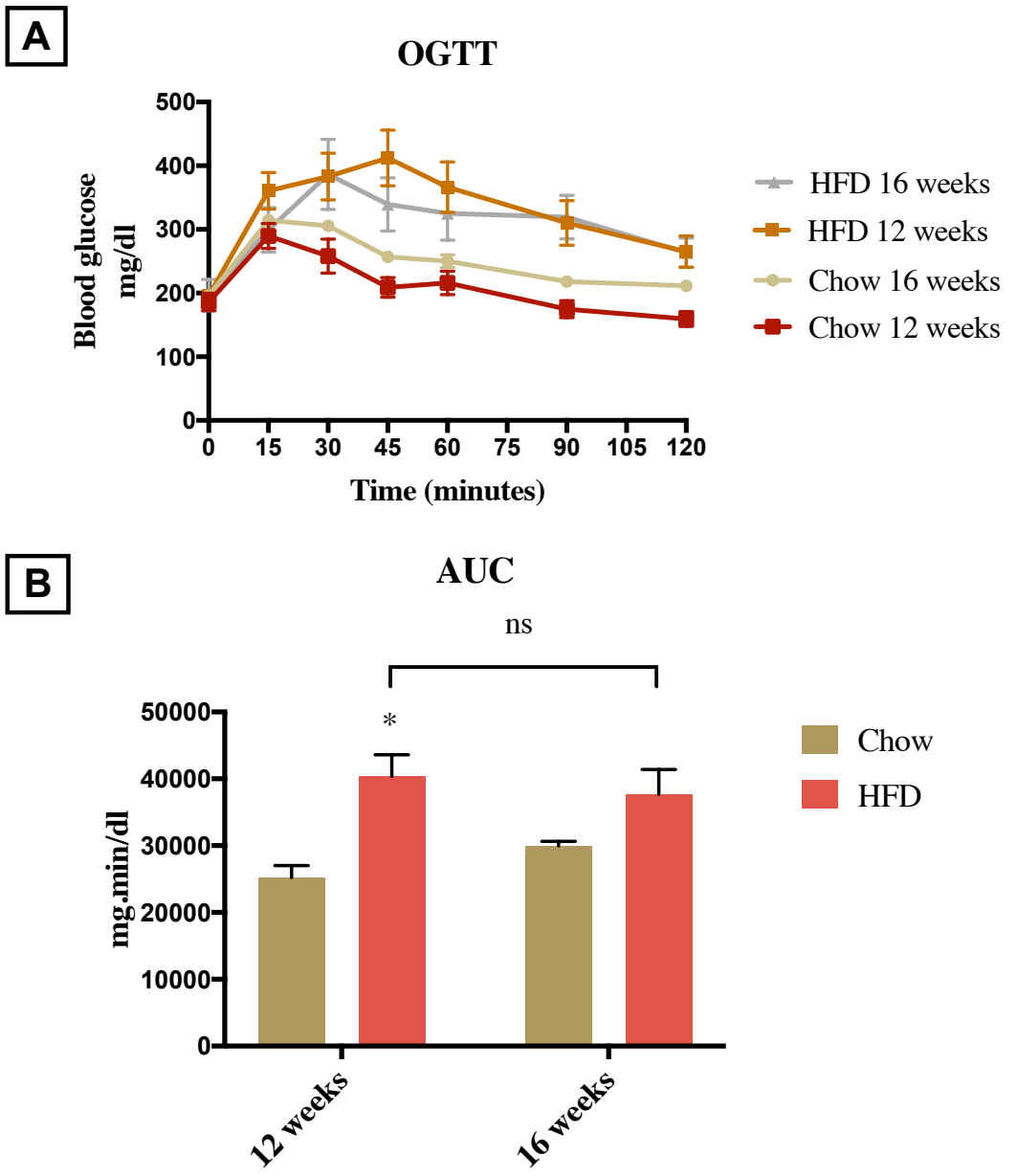

Figure 2.7 Comparison of oral glucose tolerance test (OGTT) between chow and HFD fed mice at different time points.
After 6 hours of fasting, mice were given bolus oral dose of glucose (2 g/kg). We measured **(A)** blood glucose level at 0, 15, 30, 45, 60, 90 and 120 min and **(B)** area under the curve. Data was analysed using two-way ANOVA followed by Bonferroni's post hoc test and expressed as mean ± SEM. **P*<0.05 compared to age-matched mice on chow diet (n=8 per group).

3. Effect of high-fat diet on cardiac function in a model of HFD-induced T2DM

When compared to baseline (time 0), mice fed chow for 6, 12 and 16 weeks showed no significant change in systolic cardiac function (%EF, %FS or %FAC) (P>0.05, Figure 2.8 B-D). When compared to baseline (time 0), mice fed a HFD for 6 weeks showed no significant change in the systolic function (P>0.05, Figure 2.8 A-D). However, mice fed a HFD for 12 weeks showed a small, but significant, reduction in %EF, %FS and %FAC when compared to baseline and mice fed a HFD for 6 weeks (P<0.05, Figure 2.8 A-D). In mice fed a HFD for 16 weeks, there was no further significant reduction in %EF, %FS and %FAC compared to mice fed a HFD for 12 weeks (P>0.05, Figure 2.8 A-D).

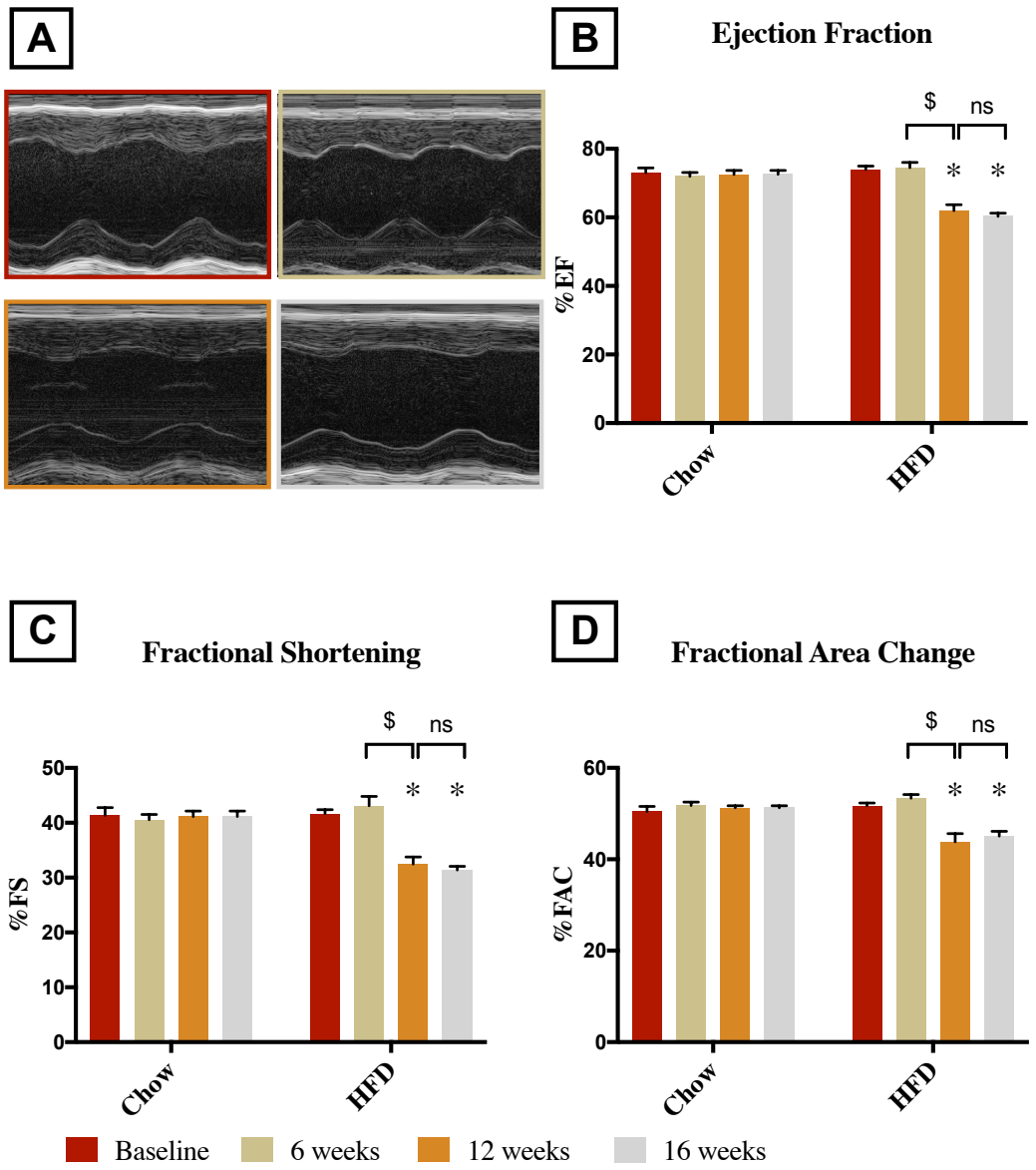

Figure 2.8 Effect of prolonged administration of HFD on cardiac function in C57BL/6 mice

Cardiac function was assessed at baseline, 6, 12 and 16 weeks. **(A)** Representative M-mode echocardiograms of HFD mice at different time points; percentage % **(B)** EF, **(C)** FS and **(D)** FAC. Data was analysed using two-way ANOVA followed by Bonferroni's post hoc test and expressed as mean ± SEM. **P*<0.05 compared to age-matched mice on chow diet, $ *P*<0.05 (n=8 per group).

4. Effect of high-fat diet on kidney and liver function in a model of HFD-induced T2DM

In mice fed either a chow or a HFD, there were no significant changes in serum urea, creatinine, and ALT at 16 weeks when compared to 12 weeks data ($P>0.05$, Figure 2.9 A). When compared to chow-fed mice at week 12, HFD fed mice for 12 weeks showed no significant differences in serum urea or ALT levels ($P>0.05$, Figure 2.9 A, C). However, when compared to age-matched mice fed a chow diet, feeding mice a HFD for 12 weeks resulted in a significant reduction in serum creatinine ($P<0.05$, Figure 2.9 B).

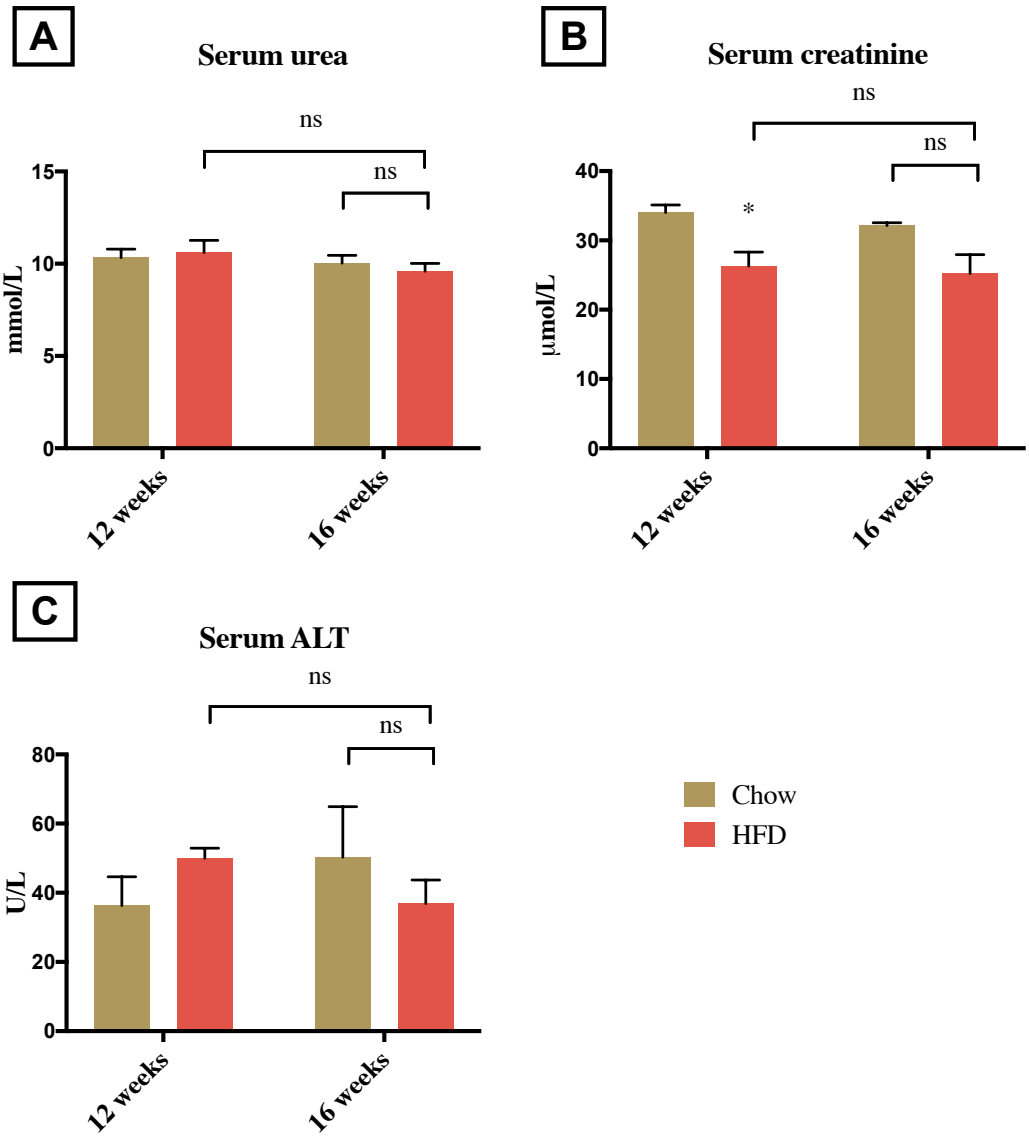

Figure 2.9 Effect of prolonged administration of HFD on kidney and liver function inC57BL/6 mice.
Kidney and liver dysfunction parameters were measured at 12 and 16 weeks. Serum **(A)** urea, **(B)** creatinine and **(C)** ALT. Data was analysed using two-way ANOVA followed by Bonferroni's post hoc test and expressed as mean ± SEM. **P*<0.05 compared to age-matched mice on chow diet, (n=8 per group).

2.5.2 Second Model of T2DM Using the HFD (58Y1: Blue Diet)

1. Effect of high-fat diet on eating habits and body weight in a model of HFD-induced T2DM

When compared to chow-fed mice, food intake in mice fed the HFD was significantly lower during the whole experiment (P<0.05, Figure 2.10 A). However, calorie intake was significantly higher in the HFD group compared to the chow group (P<0.05, Figure 2.10 B). When compared to mice on a chow diet, mice fed the HFD showed a significant increase in body weight starting from the first week of commencement of the diet until the end of the experiment (P<0.05, Figure 2.10 C). At the end of week 12, mice on HFD showed a significant gain in weight compared to mice on chow diet (P<0.05, Figure 2.10 D).

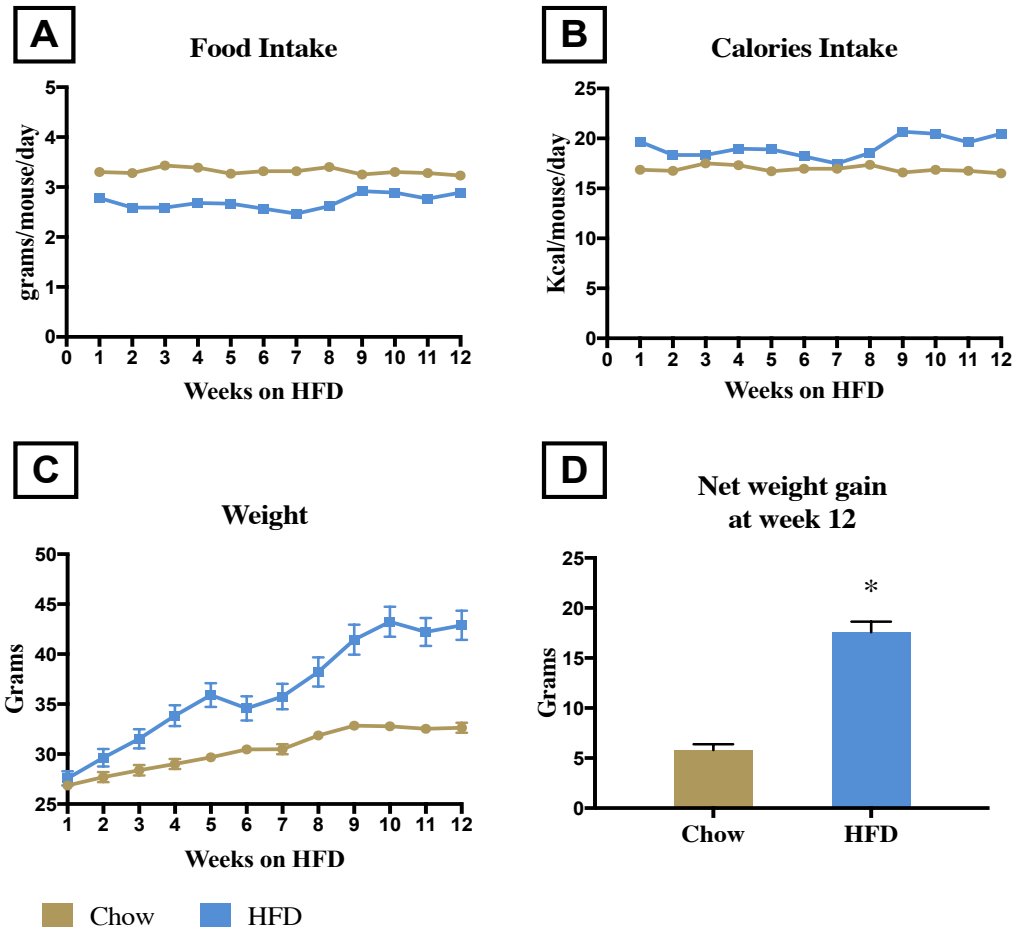

Figure 2.10 Food intakes, calories intake and weight data.
Summary of weekly change in **(A)** food intake, **(B)** calories intake and **(C)** body weight for 12 weeks in both chow and HFD fed groups and the **(D)** net weight gain at the end of the experiment in both groups. Data was analysed using unpaired t-test and presented as mean ± SEM, **P*<0.05 when compared to chow group (n=10 per group).

2. Effect of high-fat diet on diabetic parameters in a model of HFD-induced T2DM

When compared to age-matched mice on a chow diet, mice fed the HFD for 6 or 12 weeks and challenged with an oral dose of glucose showed significant impairment of glucose tolerance (*P*<0.05, Figure 2.11). When compared to mice on HFD for 6 weeks, mice on HFD for 12 weeks showed a further significant increase in the degree of glucose intolerance after being challenged with an oral dose of glucose (*P*<0.05, Figure 2.11).

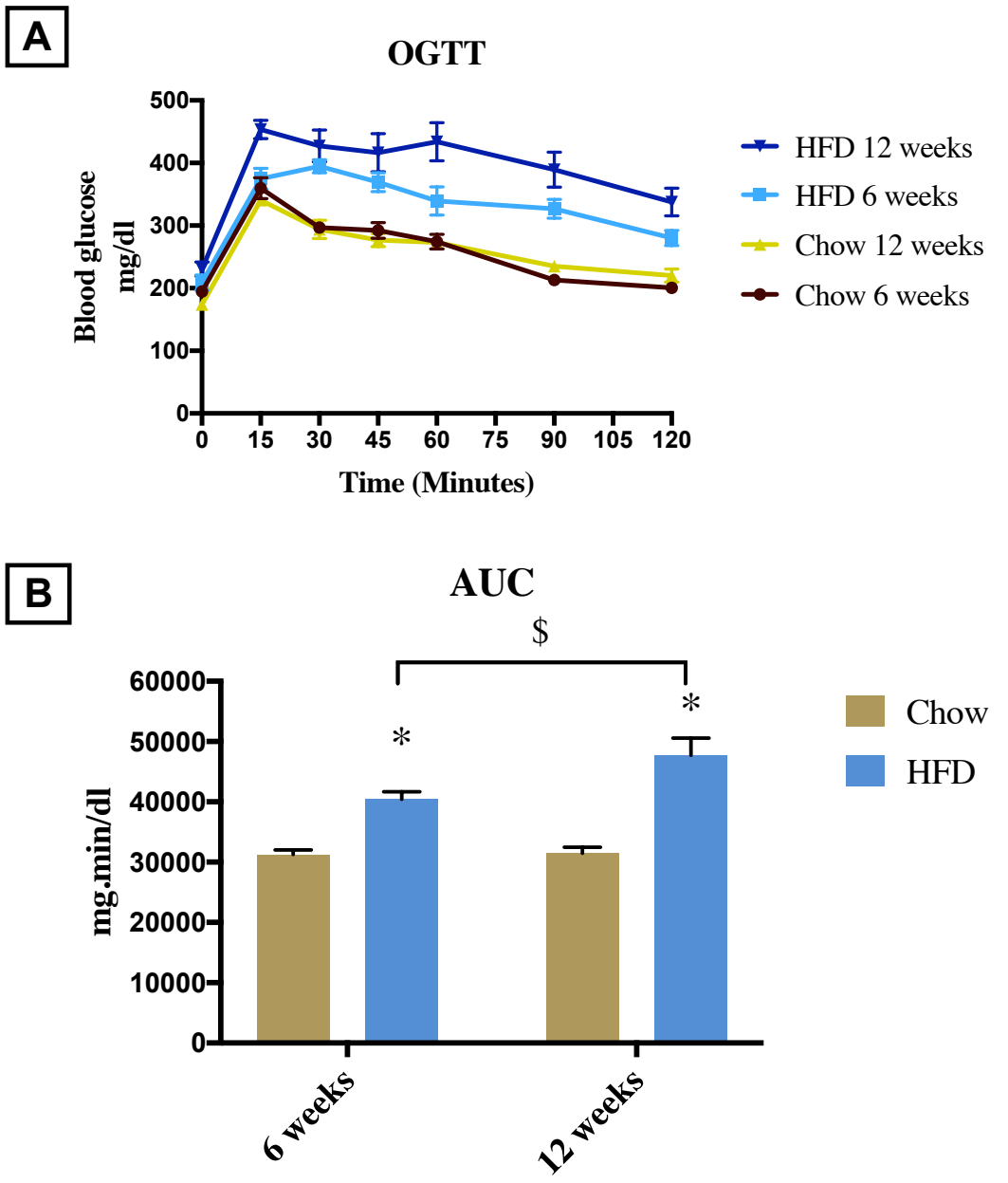

Figure 2.11 Comparison of oral glucose tolerance test (OGTT) between chow and HFD fed mice at different time points.
After 6 hours of fasting, mice were given bolus oral dose of glucose (2 g/kg). We measured **(A)** blood glucose level at 0, 15, 30, 45, 60, 90 and 120 minutes and **(B)** area under the curve. Data was analysed using two-way ANOVA followed by Bonferroni's post hoc test and expressed as mean ± SEM. **P*<0.05 compared to age-matched mice on chow diet, $ *P*<0.05 (n=10 per group).

3. Effect of high-fat diet on cardiac function in a model of HFD-induced T2DM

When compared to baseline (time 0), mice fed chow for 6 and 12 weeks showed no significant change in systolic cardiac function (%EF, %FS or %FAC) (P>0.05, Figure 2.12 B-D). When compared to baseline (time 0), mice fed a HFD for 6 showed a small, but significant, reduction in %EF, %FS and %FAC (P<0.05, Figure 2.12 A-D). In mice fed a HFD for 12 weeks, there was no further significant reduction in %EF, %FS and %FAC compared to mice fed a HFD for 6 weeks (P>0.05, Figure 2.12 A-D).

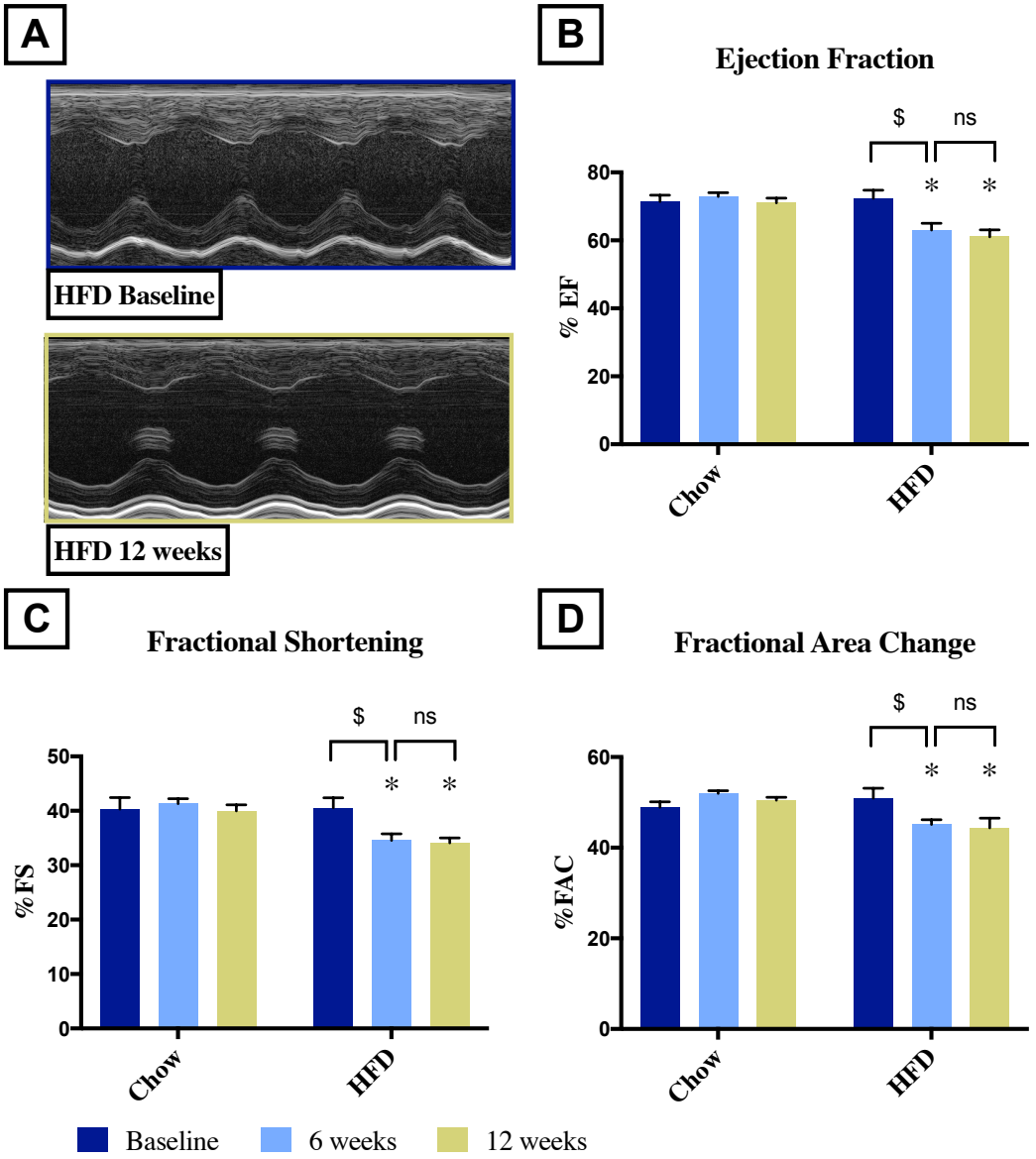

Figure 2.12 Effect of prolonged administration of HFD on cardiac function in C57BL/6 mice

Cardiac function was assessed at baseline, 6 and 12 weeks. **(A)** Representatives M-mode echocardiograms of HFD mice at baseline and at 12 weeks. Percentage % **(B)** EF, **(C)** FS and **(D)** FAC. Data was analysed using two-way ANOVA followed by Bonferroni's post hoc test and expressed as mean ± SEM. **P*<0.05 compared to age-matched mice on chow diet, $*P*<0.05 (n=10 per group).

4. Effect of high-fat diet on kidney function and liver injury in a model of HFD-induced T2DM

When compared to age-matched mice on a chow diet, feeding mice a HFD for 6 weeks showed no significant changes in serum urea, creatinine or ALT levels (P>0.05, Figure 2.13 A-C). In mice fed either chow or a HFD, there were no significant changes in serum urea or creatinine at 12 weeks when compared to 6 weeks data (P>0.05, Figure 2.13 A-B). When compared to mice fed a chow diet for 12 weeks, feeding mice HFD for 12 weeks resulted in significant increase in serum ALT (P<0.05, Figure 2.13 C).

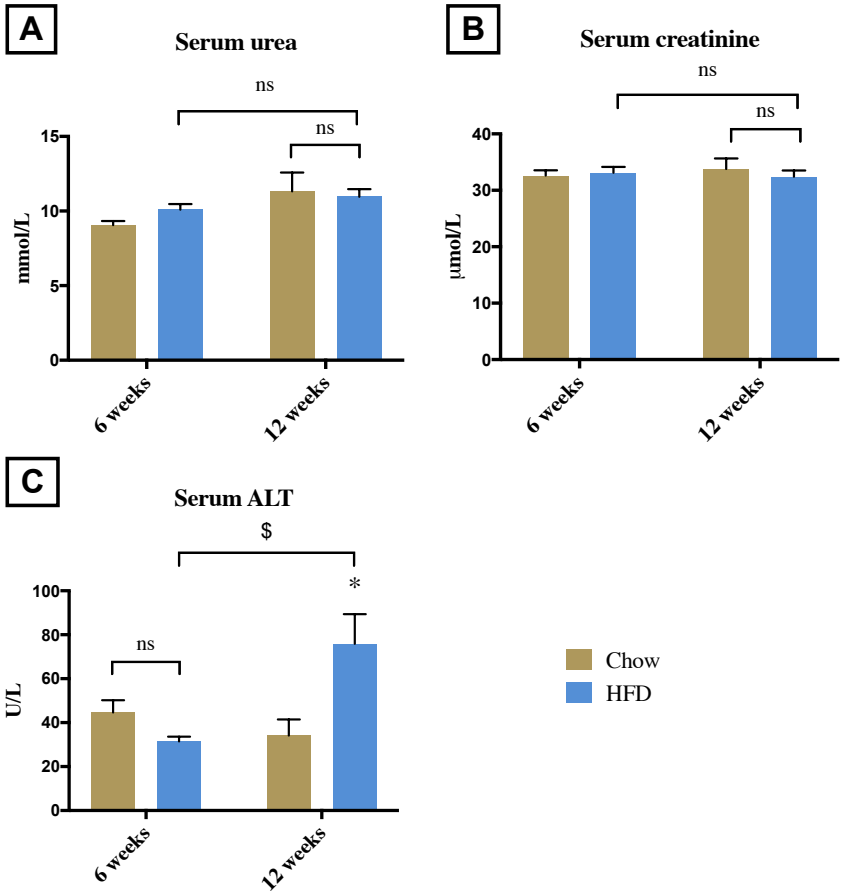

Figure 2.13 Effect of prolonged administration of HFD on kidney and liver function in C57BL/6 mice. Kidney and liver dysfunction parameters were measured at 6 and 12 weeks. Serum **(A)** urea, **(B)** creatinine and **(C)** ALT. Data was analysed using two-way ANOVA followed by Bonferroni's post hoc test and expressed as mean ± SEM. *P<0.05 compared to age-matched mice on chow diet, \$$P$<0.05 (n=10 per group).

2.5.3 Follow up Study to Measure Diabetes Complications that Result from Modeling T2DM Using the HFD (58Y1: Blue diet)

1. Effect of HFD on insulin resistance

When compared to chow-fed mice, mice fed with HFD for 12 weeks showed significantly higher levels of glucose when challenged with insulin. There was a significant increase in AUC after the HFD (P<0.05, Figure 2.14 A-B). Mice fed with HFD showed significant increases in fasting blood glucose and fasting serum insulin when compared to chow-fed mice (P<0.05, Table 2.14 C-D).

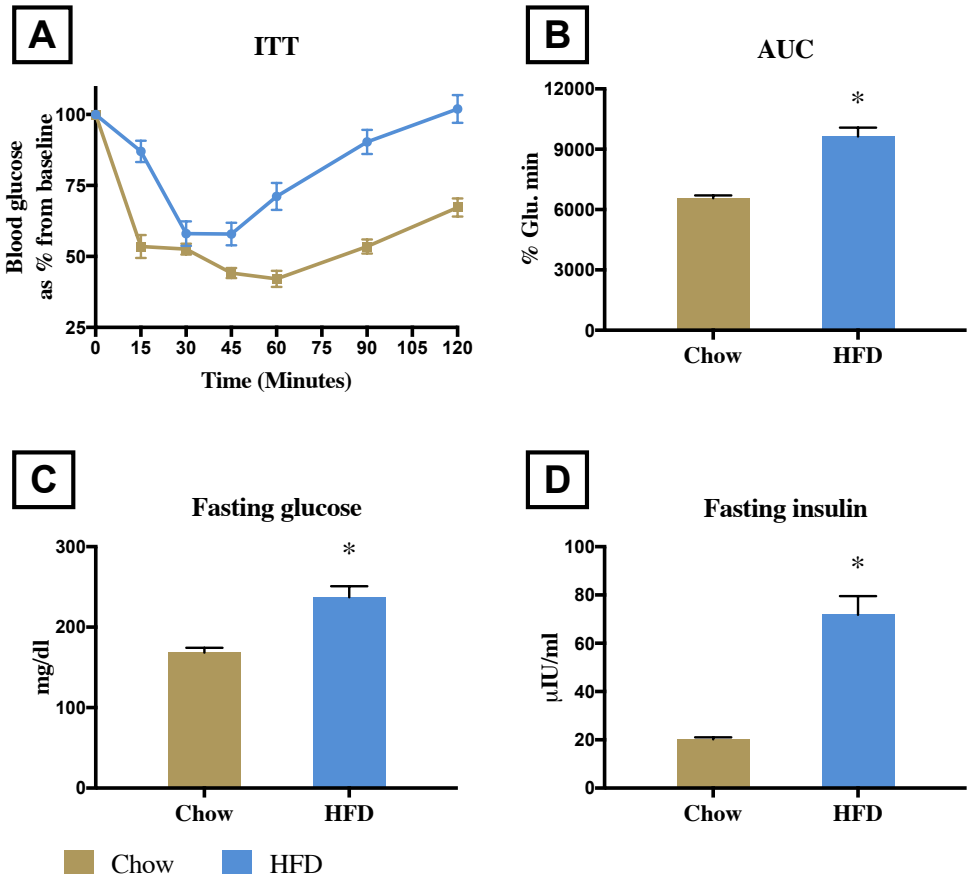

Figure 2.14 Effect of HFD administrations on insulin resistance markers. After 6 hours of fasting, mice were given a dose of insulin (0.75U/kg, i.p.). We measured **(A)** blood glucose level at 0, 15, 30, 45, 60, 90 and 120 minutes, **(B)** area under the curve **(C)** fasting blood glucose and **(D)** fasting insulin level. Data was analysed using unpaired t-test and expressed as mean ± SEM. *P<0.05 when compared to chow group (n=10 per group).

2. Effect of HFD on kidney function

When compared to mice fed with chow diet, mice on HFD showed a significant reduction in creatinine clearance (P<0.05, Figure 2.15 A). They also showed a significant increase in urine albumin to creatinine ratio (P<0.05, Figure 2.15 B).

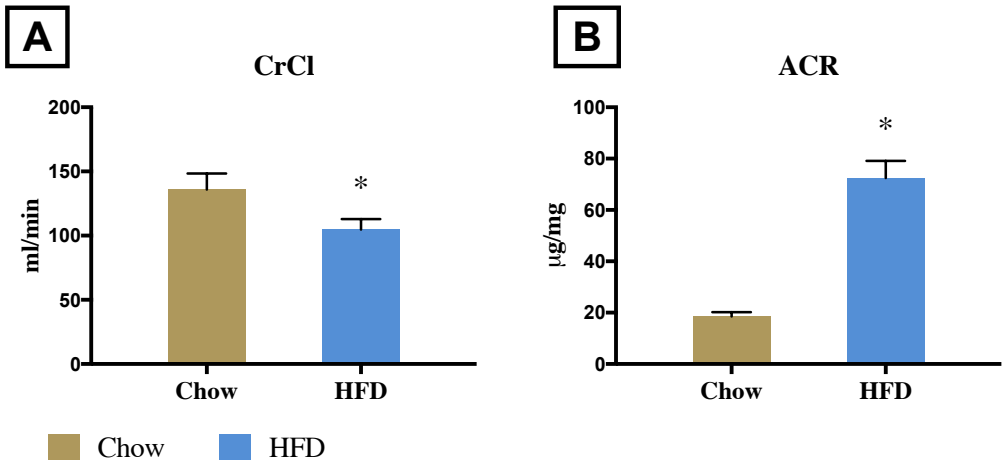

Figure 2.15 Effect of HFD on kidney function
Mice were housed in metabolic cages for 24 hours. **(A)** Creatinine clearance and **(B)** albumin to creatinine ratio were calculated. Data was analysed using unpaired t-test and expressed as mean ± SEM. *P<0.05 when compared to chow group (n=10 per group).

3. Effect of HFD on liver histology

Histological analysis of liver biopsies showed that when compared to mice fed with chow diet for 12 weeks, feeding mice a HFD resulted in a significant perivascular accumulation of collagen in the liver (P<0.05, Figure 2.16 A-B). Feeding mice with HFD for 12 weeks also resulted in a significant increase in fat in the liver when compared to mice fed with chow diet (P<0.05, Figure 2.16 C-D). Livers obtained from mice fed with HFD looked significantly enlarged when compared to livers obtained from mice on chow diet (Figure 2.16 E) and they were significantly heavier (P<0.05, Figure 2.16 F).

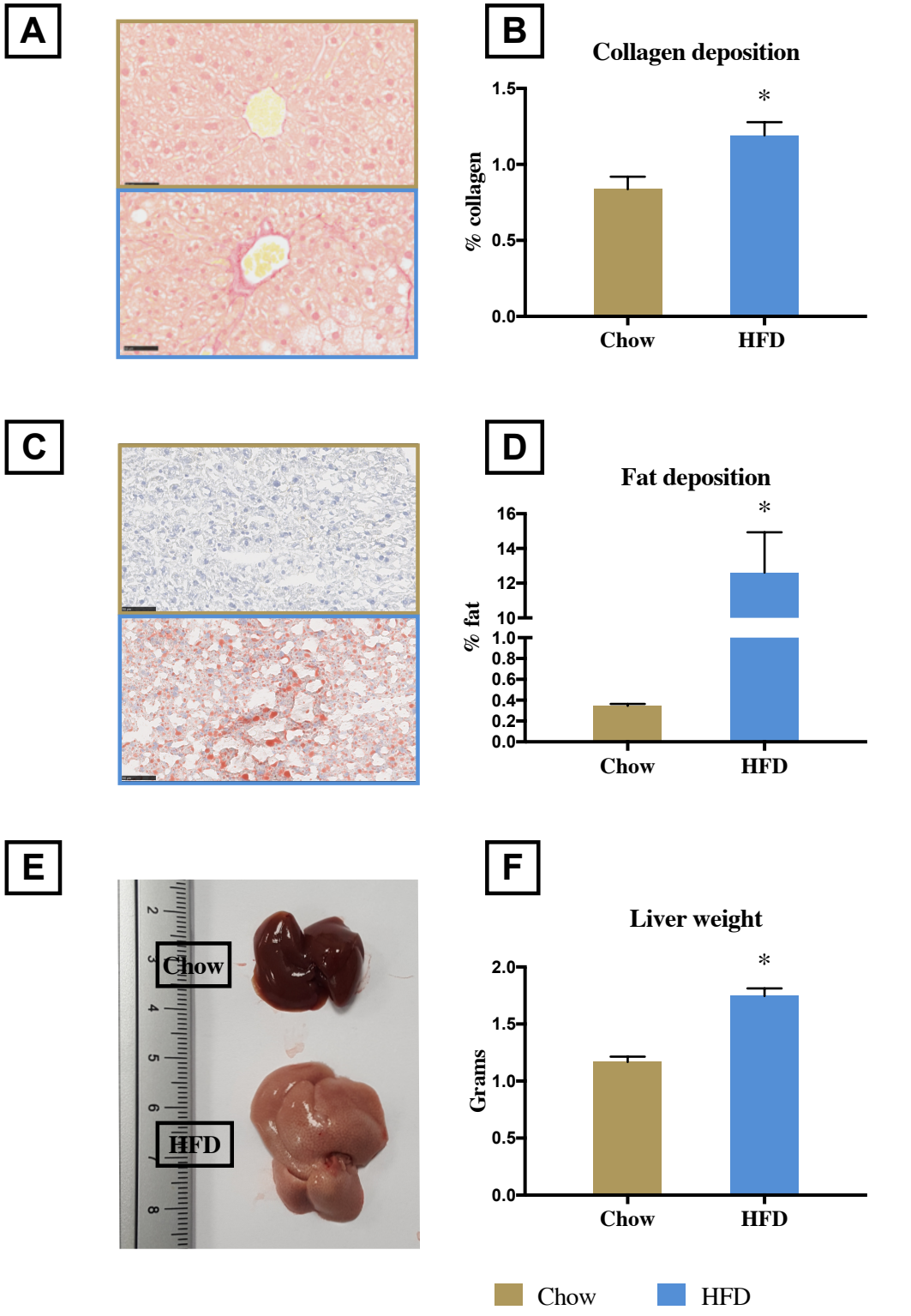

Figure 2.16 Effect of HFD on liver histology after 12 weeks
Liver sections were stained with **(A)** Picro-Sirius Red and **(B)** % collagen was calculated. Liver sections also stained with **(C)** Oil red-O and **(D)** % fat was calculated. **(E)** Liver appearance and **(F)** liver weight were compared. Data was analysed using unpaired t-test and expressed as mean ± SEM. **P*<0.05 when compared to chow group (n=10 per group).

4. Effect of HFD on lipids' profile and blood haematology markers

When compared to mice on chow diet, feeding the mice a HFD for 12 weeks resulted in significant impairment in the lipid profile with detection of significant increases in total cholesterol, LDL and HDL (P<0.05, Table 2.5).

Table 2.5 Effect of HFD on serum lipid profile and blood haematology after 12 weeks.

	Parameter	Chow	HFD
Lipid profile	Total cholesterol (TC)	100.20±13.79	200.10±4.2*
	Low-density lipoprotein (LDL)	25.23±3.34	57.84±1.12*
	Triglyceride (TG)	114.50±9.17	116.70±10.11
	High-density lipoprotein (HDL)	72.31±7.54	132.20±3.18*
Haematology	Red blood cells count (RBC)	10.25±0.29	10.32±0.57
	Haemoglobin (HGB)	14.37±0.39	14.59±0.78
	Haematocrit (HCT)	47.40±1.34	49.59±2.7
	Mean cell volume (MCV)	46.24±0.09	48.11±0.46*
	Mean cell haemoglobin (MCH)	14.02±0.06	14.15±0.09
	Mean cell haemoglobin concentration (MCHC)	30.30±0.1	29.43±0.29*
	RBC distribution width (RDW-SD)	31.92±0.52	35.38±1.29*
	Reticulocytes (RET) count	465.7±19.76	528.80±61.17
	Reticulocytes %	4.58±0.25	5.46±1.04
	Platelet (PLT) count	651.7±33.57	684±59.18
	PLT distribution width (PDW)	7.16±0.08	7.61±0.07*
	Mean platelet volume (MPV)	5.52±0.07	5.96±0.05*
	White blood cells (WBC)	5.42±0.75	9.91±1.39*
	Neutrophils count	0.51±0.07	0.65±0.13
	Lymphocytes count	4.60±0.70	7.90±1.03*
	Monocytes count	0.15±0.02	0.28±0.03*
	Eosinophils count	0.15±0.03	0.34±0.14
	Basophils count	0.00±0.001	0.02±0.01
	Neutrophils %	9.77±1.22	8.07±1.54
	Lymphocytes %	84.42±1.68	81.67±4.76
	Monocytes %	2.86±0.27	3.16±0.58
	Eosinophils %	2.93±0.51	2.07±0.19
	Basophils %	0.02±0.02	0.13±0.18*

Mice fed a HFD were compared to age-matched mice fed a chow diet. Data is presented as mean ± SEM for n number of observations. Data was analysed using unpaired t-test. *P<0.05 versus chow group (n=7-10 per group).

2.6 Discussion

In this chapter, I have developed a clinically relevant model of T2DM with diabetic cardiomyopathy by feeding mice with a **HFD (58R3: Red diet)** for 12 weeks. Exposure to HFD for 12 weeks resulted in a progressive increase in body weight. This continuous increase in body weight is consistent with a previous study that showed a continuous increase in the body weight after the introduction of HFD for 52 weeks (as two phases of rapid and slow weight gain before and after 12 weeks of the HFD intervention) in C57BL/6 mice [252].

I also report a significant impairment in oral glucose tolerance at week 12 in mice fed with the HFD and this impairment was stable until week 16. Similarly, others have reported that introduction of HFD results in an impairment in glucose tolerance as early as 1 week after dietary manipulation [253], while previous studies of our group show that feeding the same **HFD (58R3: Red diet)** to C57BL/6 mice resulted in an impairment in glucose tolerance after 10 or 14 weeks of dietary manipulation [254,255].

Exposure to **HFD (58R3: Red diet)** for 10-14 weeks has been used by our group to study diabetes, diabetic nephropathy and liver steatosis in C57BL/6 mice [254,255]. However, diabetic cardiomyopathy has not been investigated in this model. Here, I report for the first time a reduction in systolic cardiac function (as a small drop in %EF) after 12 weeks of dietary manipulation with the **HFD (58R3: Red diet)**. This small degree of cardiac dysfunction was stable with no further increase in cardiac dysfunction (reduction in %EF) seen after 16 weeks of HFD. This result is supported by other studies showing the development of systolic cardiac

dysfunction (as reduction in %FS) after 22 weeks on HFD (47% energy from fat) [256], a decrease in %EF after 10 weeks on high sucrose diet [257] and the development of both systolic and diastolic dysfunction after 16 weeks on high-fat high-sucrose diet (45% energy from fat and 17% energy from sucrose) in C57BL/6 mice [258].

I concluded that giving the **HFD (58R3: Red diet)** for 12 weeks to C57BL/6 mice can be used to model diabetes and diabetic cardiomyopathy as a first hit to study the effect of diabetes on the cardiac (organ) dysfunction associated with sepsis in mice in subsequent studies. However, this protocol was only used in the first study to investigate the effect of pre-existing T2DM on cardiac dysfunction caused by endotoxaemia. After facing a problem with the supply of the **HFD (58R3: Red diet)**, I had to establish and test a new HFD-model of diabetes and diabetes complications using the most similar diet available **HFD (58Y1: Blue diet)** and compare it to first model to be used later in the subsequent study to investigate the effect of pre-existing T2DM on cardiac dysfunction associated with CLP induced sepsis.

Using the second **HFD (58Y1: Blue diet)**, I report a decrease in systolic cardiac function as early as week 6 after initiation of HFD. This decrease in cardiac function was maintained (stable) throughout the remaining experimental period. I also discovered an impaired glucose tolerance at week 6, and this impairment in glucose tolerance worsened after 12 weeks on HFD. This result is consistent with a previous study showing that mice fed with HFD develop glucose intolerance early after initiation of the HFD and then develop more severe alterations in glucose homeostasis after prolonged exposure to this diet [253]. Although mice developed cardiac dysfunction and impaired glucose tolerance after 6 weeks of dietary

manipulation, they only showed a 26% increase in body weight from the baseline at this point. It has been suggested that models of obesity and diabetes should show at least a 33% increase in body weight from baseline [259] which was achieved at week 12 on HFD using the HFD **(58Y1: Blue diet)**. This makes 12 weeks is the optimal duration of HFD in this protocol too.

Using the **HFD (58Y1: Blue diet)** for 12 weeks, I also confirmed the development of insulin resistance. I reported an impairment in insulin tolerance and increases in fasting glucose and insulin levels. Previous studies also showed similar effects of HFD on insulin resistance criteria [260].

Diabetic nephropathy has been reported in mice and patients with T2DM. An increase in ACR is a reliable indicator of the development of microalbuminurea in HFD-induced models of diabetes [261,262] and in patients with T2DM and pre-diabetes [263,264]. A reduction in CrCl has also been reported in diabetic patients [265]. In this chapter, I demonstrate that the **HFD (58Y1: Blue diet)** also resulted in the development of renal dysfunction (higher ACR and lower CrCl) secondary to insulin resistance and hyperglycaemia. Using the first protocol with the **HFD (58R3: Red diet)** for 12 weeks resulted in similar kidney dysfunction as reported in previous studies by our group using the red diet for 10 or 14 weeks [254,255].

The effect of HFD and diabetes on liver injury and steatosis is well characterised in the literature. Studies have shown an increase in lipid accumulation in the liver secondary to insulin resistance [266–268]. Indeed, in this model, liver obtained from mice treated with the **HFD (58Y1: Blue diet)** showed significant lipid accumulation and subsequent increase in serum ALT. Similarly, mice expose to the **HFD (58R3: Red diet)** also exhibit liver steatosis [254,255].

Dyslipidaemia is well identified in both patients with T2DM [269] and in animal models of HFD diabetes (by us and others) [254,255,270,271]. Mice fed the **HFD (58Y1: Blue diet)** also showed significant dyslipidaemia compared to chow-fed mice.

2.7 Conclusion

In this chapter, I concluded that using the **HFD (58R3: Red diet)** for 12 weeks to C57BL/6 male mice resulted in T2DM phenotype and diabetic cardiomyopathy, I also discovered that using the **HFD (58Y1: Blue diet)** for 12 weeks in C57BL/6 mice can be used as an alternative model to the first model after knowing that the long-term supply of the **HFD (58R3: Red diet)** was no longer guaranteed.

CHAPTER 3: THE EFFECT OF PRE-EXISTING TYPE TWO DIABETES MELLITUS ON CARDIAC DYSFUNCTION ASSOCIATED WITH SEPSIS

3.1 Introduction

The cardiovascular system is one of the important systems affected by sepsis. Most septic patients, and all patients with septic shock develop sepsis-related cardiovascular dysfunction [272], which is a key driver of in-hospital mortality in these patients [273]. Both the incidence of sepsis and sepsis-related mortality increase with age due to the presence of significant comorbidities including diabetes and chronic kidney disease in the elderly [17]. The prevalence of diabetes is increasing worldwide [223]. Patients with diabetes are at high risk of developing diabetic cardiomyopathy, left ventricular (LV) hypertrophy, ischaemic cardiac injury and heart failure [112,114,223,274]. Diabetic patients are more susceptible to both common and rare infections and have a higher incidence of sepsis than patients that do not suffer from the disease [162,275]. Activation of NF-κB plays a crucial role in both sepsis-related cardiac dysfunction [276–278] and in diabetic cardiomyopathy [279]. In sepsis, activation of NF-κB is secondary to activation of TLR 2 and 4 by e.g. wall fragments of Gram-negative (e.g. LPS) or Gram-positive bacteria (e.g. PepG) and/or pro-inflammatory cytokines including TNF-α or IL-1. In addition to pro-inflammatory cytokines, the activation of NF-κB in diabetes is also driven by free fatty acids [129] (which activate TLR4) and AGE (which activate RAGE) [131]

The effect of diabetes on outcome in patients with infections is controversial with some studies showing increased hospitalization, organ dysfunction/injury and mortality in diabetic patients with e.g. pneumonia [166,168,280], while other studies report either no effect [175,176,281] or even protective effects of diabetes [172,177–179].

Some of the protective effects of diabetes can be explained by a phenomenon called "obesity paradox". The prevalence of obesity among diabetic patients is high. Almost 90% of patients with T2DM are overweight or obese [282] . While the role of T2DM and obesity in developing chronic cardiovascular diseases is well known [283], the effect these conditions in acute illness (e.g. sepsis-associated cardiac dysfunction) is still not fully established [284]. In 2007, the "obesity paradox" was first described in patients with decompensated heart failure by Fonarow and co-workers [285]. They showed that among 108,927 patients with decompensated heart failure, patients with higher BMI and diabetes had a better prognosis (higher %EF) and lower in-hospital mortality rate [285]. Similar results were reported in two more recent studies showing that patients with higher BMI had better outcomes (than patients with normal BMI) after either an acute coronary event [286] or acute respiratory distress syndrome [287] although they had higher incidence of T2DM.

In two recent meta-analyses, Pepper et al. and Wang et al. studied the obesity paradox in septic patients. They showed that obese and overweight patients have lower adjusted mortality in adult septic patients admitted to the ICU [288] and that overweight septic patients, but not obese septic patients, have lower sepsis-related mortality compared to patients with normal body weight [289]. However, the authors did not investigate the diabetes status among their patients and only reported the

effect of BMI on all-cause mortality with no information about the cardiac performance and cardiac related mortality.

Therefore, the effect of T2DM (and obesity related to T2DM) on cardiac dysfunction associated with sepsis is still not clear and warrants further investigation. In this chapter, I have investigated i) the effects of pre-existing type 2 diabetes mellitus (T2DM) caused by high fat diet (HFD) on cardiac dysfunction in mice with sepsis and ii) the role of NF-κB activation in the cardiac dysfunction in mice with diabetes and sepsis.

3.2 Scientific Hypothesis and Aims

This study is driven by the hypothesis that:

- Pre-existing T2DM augments the cardiac dysfunction associated with LPS induced endotoxaemia and CLP-induced polymicrobial sepsis in mice.

This study aims to:

- Investigate the effect of pre-existing T2DM on cardiac dysfunction associated with low dose LPS induced endotoxaemia or CLP-induced polymicrobial sepsis,
- Understand the signalling mechanism that resulted in the aggravation of cardiac dysfunction in mice with T2DM and sepsis.

3.3 Methods and Materials

3.3.1 Animals

Studies in this chapter were conducted on 76 ten-week-old male C57BL/6 mice (Charles River, Kent, UK) weighing 25-30g, receiving a standard diet and water *ad libitum* (before starting the experiments). Mice were housed 5 per cage in a temperature-controlled room with a 12-hour light/dark cycle. Forty mice were used in the first experiment to study the effect of T2DM on cardiac dysfunction after LPS challenge and 36 mice were used in the second experiment to study the effect of T2DM on cardiac dysfunction after CLP surgery. The ethical statement is provided in section 2.3.

3.3.2 Model of HFD induced T2DM and diabetic cardiomyopathy

In this model of HFD-induced T2DM and diabetic cardiomyopathy, ten-week-old male C57BL/6 mice were randomised to receive HFD (≈ 60% energy from fat) or normal chow diet with free access to water for 12 weeks.

3.3.3 Baseline Measurements for development of T2DM

During the whole 12-week period, body weight and feeding behaviour were measured weekly to ensure healthy feeding behaviour as described in section 2.3.2. During week 12, OGTT was measured in all mice to ensure the development of impairment in glucose tolerance as described in section 2.3.3, baseline echocardiography was conducted in all mice to test the development of diabetic cardiomyopathy as described in section 2.3.6, urine samples were collected from

all mice to measure CrCl as described in section 2.3.7 and blood were collected from all mice from the tail vein to measure baseline urea, creatinine and ALT as described in section 2.3.9.

3.3.4 Model of lipopolysaccharide (LPS) induced endotoxaemia

Mice are considered to be more resistant and tolerant to LPS than other species (e.g. humans or rabbits) [290]. To model sepsis and to cause systemic inflammation which leds to cardiac and organ dysfunction, a high dose LPS is be used (e.g. 9 mg/kg) in young mice without co-morbidities [291]. However, in mice with CKD, a much lower dose of LPS (2 mg/kg) was used to induce the same degree of systemic inflammation and cardiac (organ) dysfunction [292].

In this study, a low dose of LPS was used to induce endotoxaemia in mice after 12 weeks of HFD; mice fed either chow or HFD were randomised to receive LPS (2 mg/kg, i.p.) or vehicle (PBS 5 ml/kg, i.p). At 18 h after the onset of endotoxaemia, mice were anaesthetised for cardiac function assessment in vivo using echocardiography. Then, as a terminal procedure, mice were anaesthetised using high dose isoflurane (3 % delivered in 0.9 L/min O_2) before being sacrificed. Blood samples were collected by cardiac puncture and vital organs were collected and snap frozen using liquid nitrogen then stored for further analysis at -80°C freezer.

3.3.5 Model of caecal ligation and puncture (CLP) induced polymicrobial sepsis

At 12 weeks after starting the HFD, mice fed either chow or HFD were randomised to undergo either sham operation or CLP surgery. Before surgery, mice were anaesthetised using (1.5 ml/kg, i.p.) of 2:1 ketamine (100 mg/ml): xylazine (20 mg/ml) solution. To obtain adequate analgesia, buprenorphine (0.05 mg/kg, i.p.) was administered just before starting the surgery. The fur of the abdomen was removed using Veet® hair removing cream and the area cleaned with 70% ethanol. A 1.5 cm midline incision of the abdomen was made and the caecum was exposed. The caecum then was ligated below the ileocaecal valve and two punctures were made one at each end using an 18-G needle. A small amount of faecal matter was then squeezed from both punctures before the caecum was returned to its anatomical position and the cut in the abdomen was then sutured. Each mouse then received a resuscitation fluid (1 ml 0.9 % NaCl, s.c.). Mice were left on a homeothermic blanket to recover then placed back into fresh clean cages. At 6 and 18 h after surgery, antibiotic (imipenem/cilastatin, 20 mg/kg) dissolved in resuscitation fluid (15 ml/kg 0.9% NaCl, s.c.) was administered along with analgesia (buprenorphine, 0.05 mg/kg, i.p.). At 24 h, mice were anaesthetised for assessment of cardiac function *in vivo*. Then, as a terminal procedure, mice were anaesthetised using high dose isoflurane (3 % delivered in 0.9 L/min O_2) before being sacrificed. Blood samples were collected by cardiac puncture and vital organs were collected and snap frozen using liquid nitrogen then stored for further analysis at -80°C freezer. Mice underwent sham surgery were not subjected to perforation of the cecum, but otherwise treated the same.

3.3.6 Measuring physical activity and vital signs

At 18 h after LPS challenge or 24 h after CLP surgery, mice were observed in their cages to assess the reduction in their physical activity. A scale of 0 to -5 was used to quantify the reduction in physical activity with 0 representing the most physically active (e.g. no reduction in physical activity compared to baseline) before starting the experiment (before starting the HFD).

Body temperature and heart rate were documented directly after the induction of anaesthesia and before starting echocardiography measurements using rectal probe and ECG trace on the Echo platform. Then, they were monitored during the stabilisation phase and during the whole experiment. All the measurements of the cardiac function were conducted after stabilizing the mice to get a heart rate in the range of 450-500 beat/min and a body temperature of 35 °C or higher.

3.3.7 Quantification of organs dysfunction

Cardiac functions was assessed at 18 h after LPS challenge or at 24 h after CLP surgery using a 30 MHz RMV707B scan head and a Vevo-770 imaging system (VisualSonics, Toronto, Ontario, Canada) as described in section 2.3.6. Blood samples and vital organs were collected to measure organs dysfunction as described in section 2.3.8.

3.3.8 Western blot analysis

Immunoblot analyses of the hearts were carried out using a semi-quantitative western blotting. I measured the degree of phosphorylation of IKK, IκBα and Akt, nuclear translocation of p65 NF-κB subunit to the nucleus and iNOS expression.

For samples preparation, a piece weighing 20-30 mg of the heart was taken from the apical site of the samples. A 10-time dilution with homogenisation buffer (HB) was used to homogenize the sample at 4 °C (composition of HB is detailed in Appendix 2, Table A.2.). For cytosolic protein extraction, the homogenate was centrifuged (at 4000 RPM, 5 min, 4 °C). The resulted supernatant contained cytosolic protein and the pellet contained nuclear protein (this pellet was used for nuclear protein extraction later). The supernatant was centrifuged again (at 14000 RPM, 40 min, 4 °C). This time the pellet was discarded and supernatant kept at -80°C freezer for cytosolic protein analysis later. The first pellet was re-suspended in extraction buffer (EB) and kept in ice for 30 min (composition of EB is detailed in Appendix 2, Table A.2.) before being centrifuged (at 14000 RPM, 20 min, 4 °C). The pellet resulted was discarded and supernatant kept at -80°C freezer for nuclear protein analysis later. Both cytosolic and nuclear protein concentrations were measured using bicinchoninic acid (BCA) protein assay following manufacturer's directions (Therma Fisher Scientific, Rockford, IL). Proteins were separated by gel electrophoresis using 8% sodium dodecyl sulphate polyacrylamide (SDS-PAGE) then transferred into a Polyvinylidene difluoride (PVDF) membrane. The membrane then was blocked using 10% milk solution in TBS-tween. Incubation of the membrane was conducted overnight at 4 °C with primary antibody in 5% blocking solution then incubated the next day with the secondary antibody at room temperature for 30 min and then developed using ECL detection system. Bands analysis was performed using densitometry Gel pro analyser 4.5, 2000 software (Media Cybernetics, Silver Spring, MD, USA). Results were normalized using the related sham bands.

3.3.9 Cytokines measurements using multiplex method

Serum cytokines levels (TNF-α, IL-6, KC and IL-10) were measured using a bead-based immunoassay method. Serum samples were prepared and handled following manufacturer instructions (Biolegend®, San Diego, USA). Data was obtained using a LSR Fortessa (Biociences®, Berkshire, UK) and analysed using the Legendplex™ 7.1.0.0 software.

Serum samples were diluted with assay buffer and incubated with the selected set of captures beads for 2 h in the dark under continuous shaking. The samples then centrifuged (at 2500 RPM, 5 min, at room temperature). Supernatants were discarded and the pallet washed and re-suspended with the biotinylated detection antibodies and incubated for 1 h in the dark under continuous shaking to form capture bead-analyte-detection antibody sandwiches. Then the Streptavidin-phycoerythrin (SA-PE) was added and incubated for 30 min in the dark under continuous shaking to bind with the antibodies and form fluorescent signals. The samples then centrifuged (at 2500 RPM, 5 min, at room temperature). Supernatants were discarded and the pallet washed and re-suspended with washing buffer. The intensity of PE signal fluorescence was then quantified using flow cytometry. The concentrations of TNF-α, IL-6, KC and IL-10 were then calculated based on known standards concentrations.

3.3.10 Measuring MPO activity in the lung

MPO was extracted from the tissues according to the methods described by Barone et al. in 1991 [293] with slight modifications to measure neutrophil accumulation in the lungs.

For samples preparation, a piece of lung weighing 30-40 mg was used. A 20-time dilution with 5 mM potassium phosphate buffer was used to homogenize the sample (at 4 °C). For measurements of MPO activity, the homogenate was centrifuged (at 13000 RPM, 30 min, 4 °C). The resulted supernatant was discarded. A 5-time dilution with 0.5% hexadecyltrimethylammonium bromide in 50 mM potassium phosphate buffer was used to re-suspend and homogenize the pellet. The resulted solution was then frozen and thawed 3 times followed by 10 sec sonication at room temperature and then incubated at 4 °C for 30 min then centrifuged (at 12500 RPM, 15 min, 4 °C). MPO activity was measured in the supernatant by mixing 100 µl of the supernatant with 0.167 mg/ml o-dianiside dihydrochloride and 0.0005% hydrogen peroxide in 2.9 ml 50 mM potassium phosphate buffer. UV-visible spectrophotometer was used to measure the change in absorbance at 460 nm for 1.5 min. MPO activity was presented as the quantity of the enzyme degraded 1 µmol of peroxide/min at 25 °C and expressed as µU/gram of the lung tissue.

3.3.11 Measuring N-Acetyl-Beta-D-Glucosaminidase (NAG) activity in the lung

NAG activity was analysed to measure macrophage accumulation in the lung. For samples preparation, a piece of lung weighing 30-40 mg was used. Samples were then diluted with 0.01 M phosphate buffer saline and homogenised (at 4 °C). The resulted solutions were then frozen and thawed 3 times followed by 10 sec sonication at room temperature to break the cells. For measurements of NAG activity, the homogenate was centrifuged (at 5000 RPM, 30 min, 4 °C). The resulted supernatants were then used to measure NAG activity using a NAGase

ELISA kit following manufacturer instructions (Elabscience®, Houston, Texas, USA).

3.3.12 Statistical analysis

Data were analysed using GraphPad Prism 7.0 (GraphPad Software, San Diego, California, USA). Values stated in the text and figures are presented as a mean ± standard error of the mean (SEM) of n observations, where n is the number of animals used. Data was tested for normality using D'Agostino-Pearon normality test and then assessed using Two-way or One-way ANOVA test followed by Bonferroni's post hoc test or unpaired Student t-test where appropriate. *P* values of less than 0.05 were considered to be statically significant.

3.3.13 Materials

Unless otherwise stated, all materials, reagents and solutions were purchased from Sigma-Aldrich Ltd (Poole, Dorset, UK).

3.4 Experimental Designs and Studies Groups

3.4.1 Effect of T2DM on the cardiac dysfunction associated with endotoxaemia

Ten-week old mice were randomised to revive chow diet or HFD. At 12 weeks mice from both groups were challenged with LPS or vehicle as following.

Table 3.1 Experimental groups used to study the effect of low dose LPS on cardiac dysfunction in animals with pre-existing T2DM.

Group name	Diet	Intervention	Number
Chow	Chow	PBS 5ml/kg i.p.	10
Chow+LPS	Chow	LPS 2mg/kg i.p.	10
HFD	High fat diet	PBS 5ml/kg i.p.	10
HFD+LPS	High fat diet	LPS 2mg/kg i.p.	10

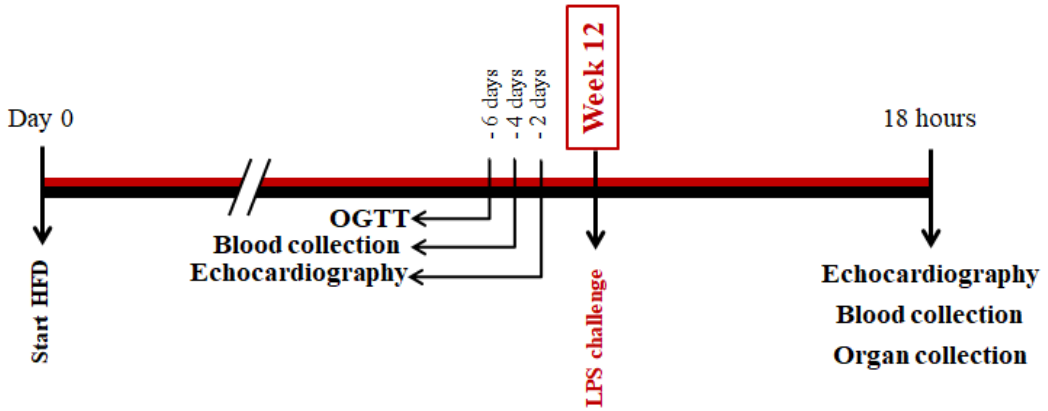

Figure 3.1 Timeline and summary of the protocol used to study the effect of low dose LPS on cardiac dysfunction in animals with pre-existing T2DM.

Mice were randomised to either chow diet or high fat diet (HFD). At 12 weeks, HFD fed mice were tested for development of diabetes phenotype and compared to chow-fed mice. Mice were then challenged with either low dose LPS (2 mg/kg, i.p.) or vehicle (5 ml/kg PBS, i.p.). At 18 h after LPS, cardiac function was assessed using *in vivo* echocardiography.

3.4.2 Effect of T2DM on cardiac dysfunction associated with CLP-induced polymicrobial sepsis

Ten-week old mice were randomised to revive chow diet or HFD. At 12 weeks mice from both groups were subjected to sham or CLP surgery as following.

Table 3.2 Experimental groups used to study the effect of CLP on cardiac dysfunctions in animals with pre-existing T2DM.

Group name	Diet	Intervention	Number
Chow+sham	Chow	Sham surgery	8
Chow+CLP	Chow	CLP surgery	10
HFD+sham	High fat diet	Sham surgery	8
HFD+CLP	High fat diet	CLP surgery	10

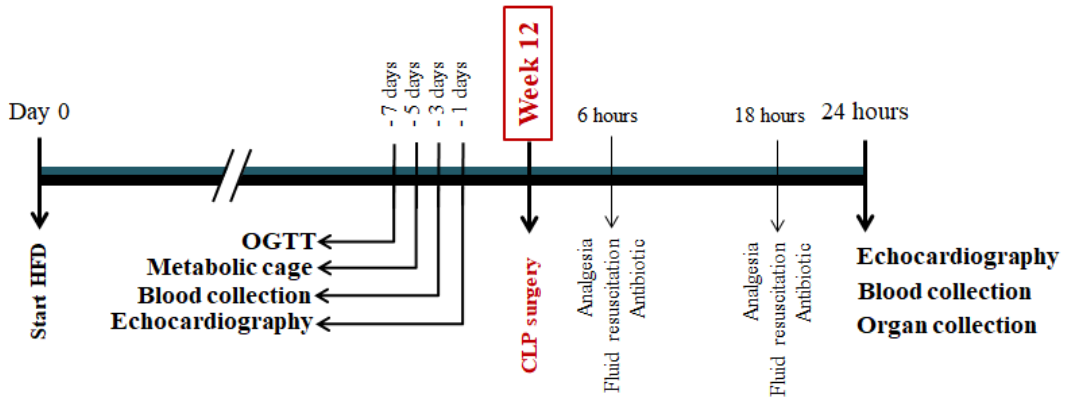

Figure 3.2 Timeline and summary of the protocol used to study the effect of CLP surgery on cardiac dysfunction in animals with pre-existing T2DM.

Mice were randomised to either chow diet or high fat diet (HFD). At 12 weeks, animals on HFD were tested for development of diabetes phenotype and compared to chow-fed mice. Mice were then subjected to either CLP or sham surgery. At 24 h after CLP surgery, cardiac function was assessed using *in vivo* echocardiography.

3.5 Results

3.5.1 Endotoxaemia in mice with pre-existing T2DM

1. Effect of HFD on organ function before LPS challenge

After 12 weeks of dietary manipulation and before sepsis challenge, mice on HFD showed signs of the development of T2DM including a significant increase in body weight and a significant impairment in OGTT when compared to mice on chow diet. When compared to age-matched mice on chow diet, HFD-fed mice also showed significant reduction in systolic cardiac function (%EF) (P<0.05, Table 3.3).

Table 3.3 Baseline data for both chow and HFD groups before interventions (LPS or PBS challenge).

Parameter	Chow	HFD
Net weight gain *(grams)*	5.7 ± 0.39	14.69 ± 1.41*
Food intake$ *(grams/mouse/week)*	3.71 ± 0.07	2.29 ± 0.39*
Calories intake$ *(Kcal/mouse/week)*	18.81 ± 0.27	15.86 ± 0.8*
AUC for OGTT *(mg.min/dl)*	25244 ± 1776	40343 ± 3253*
Fasting blood glucose *(mg/dl)*	186.4 ± 12.1	188.5 ± 7.91
Ejection fraction *(%)*	70.96 ± 1.28	61.88 ± 1.59*
Fractional shortening *(%)*	33.84 ± 1.08	31.98 ± 1.02*
Fractional area change *(%)*	45.35 ± 1.27	41.44 ± 1.28*
Left ventricle mass *(mg)*	119.8 ± 9.55	132.0 ± 7.09
Urea *(mmol/L)*	10.19 ± 0.42	10.2 ± 0.22
Creatinine *(µmol/L)*	34.52 ± 1.05	21.16 ± 2.59*
Alanine aminotransferase *(U/L)*	43.69 ± 11.32	45.8 ± 3.67

Mice fed a HFD were compared to age-matched mice fed a chow diet. Data are presented as mean ± SEM for n number of observations. Data were analysed by unpaired t-test. *P<0.05 versus the chow-fed group (n=8-10 in each group). $: Mean food intake of 10 mice in each group during the study period 12 weeks (n=12).

2. Effect of pre-existing T2DM on physical activity and vital signs after LPS challenge

When compared to mice fed a chow diet, mice fed with HFD showed no significant change in physical activity, heart rate or body temperature ($P>0.05$; Figure 3.3 A-C). When compared to animals on regular chow diet challenged with vehicle, mice on chow diet challenged with low dose LPS (2 mg/kg i.p.) showed no significant decrease in physical activity, heart rate or body temperature ($P>0.05$; Figure 3.3 B-C). However, mice on HFD challenged with low dose LPS exhibited large and significant reductions in physical activity, heart rate and body temperature when compared to mice on HFD challenged with vehicle ($P<0.05$; Figure 3.3 A-C) and exhibited large and significant reduction in physical activity and heart rate when compred to mice on chow diet and challenged with the same dose of LPS (2 mg/kg i.p.) ($P<0.05$; Figure 3.3 A-B). It should be noted that at the beginning of measurements, and after stabilising the animals, there were no significant difference in the core body temperature or the heart rate between the four groups.

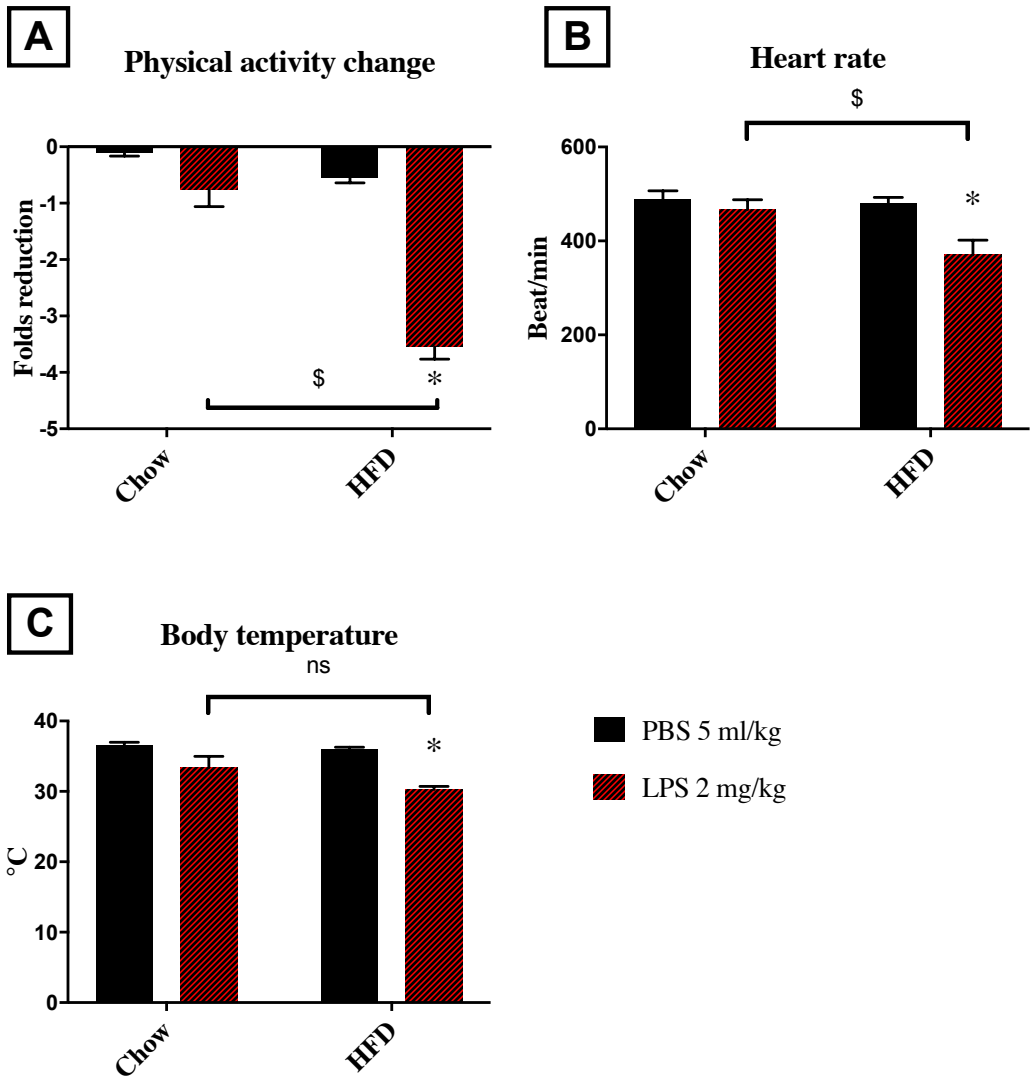

Figure 3.3 Effect of low dose LPS challenge on vital signs and physical activity in mice with T2DM.

Vital signs and physical activity were assessed at 18 h after LPS or vehicle challenge in mice fed a chow diet or a HFD. **(A)** Physical activity change **(B)** heart rate and **(C)** body temperature. Data was analysed using two-way ANOVA followed by Bonferroni's post hoc test and expressed as mean ± SEM. **P*<0.05 compared to respective PBS group, $*P*<0.05. (n=10 per group).

3. Pre-existing T2DM augments the cardiac dysfunction caused by low dose of LPS.

When compared to mice fed with chow diet, mice fed with HFD showed a small, but significant attenuation in cardiac function ($P<0.05$; Figure 3.4 B-D). When compared to animals on regular chow diet challenged with vehicle, mice on chow diet challenged with low dose LPS (2 mg/kg i.p.) showed a small, but significant, reduction in systolic cardiac function (measured as %EF, %FS and %FAC; $P<0.05$; Figure 3.4 B-D). However, animals on HFD challenged with low dose LPS exhibited a large and significant reduction in systolic cardiac function when compared to mice on HFD challenged with vehicle. The reductions in %EF, %FS and %FAC caused by LPS in mice fed a HFD were significantly greater than those caused by LPS in mice fed a normal chow diet ($P<0.05$; Figure 3.4 B-D).

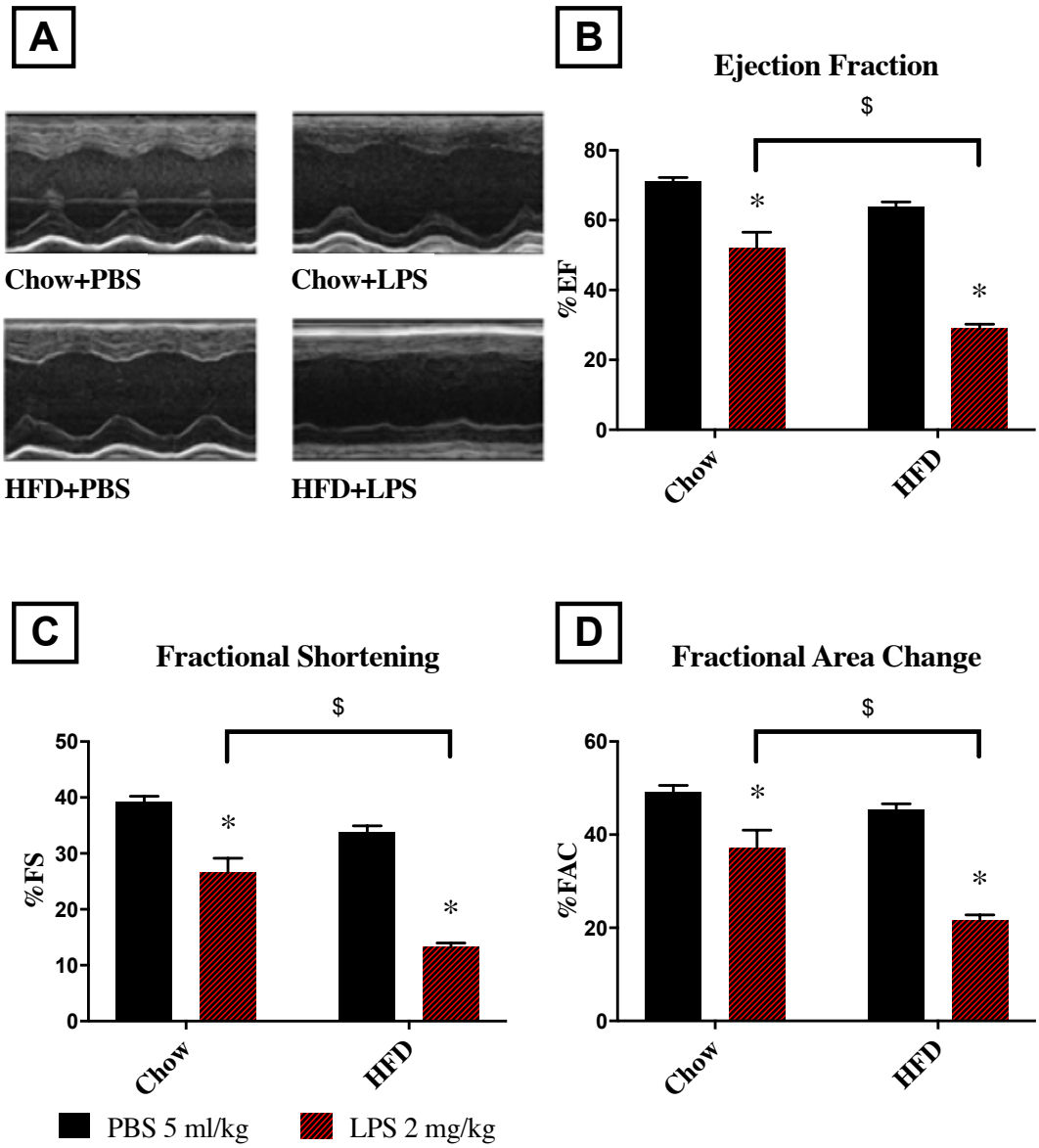

Figure 3.4 Effect of low dose LPS challenge on cardiac function in mice with T2DM.

Cardiac function was assessed at 18 h after LPS or vehicle challenge in mice fed a chow diet or a HFD. **(A)** Representative M-mode echocardiograms; percentage % **(B)** EF, **(C)** FS and **(D)** FAC. Data were analysed using two-way ANOVA followed by Bonferroni's post hoc test and expressed as mean ± SEM. **P*<0.05 compared to respective PBS group, $*P*< 0.05. (n=10 per group).

4. Effect of low dose LPS on NF-κB signalling pathway in mice with pre-existing T2DM

In a separate set of experiments, I investigated the effects of HFD/diabetes on the activation of key signalling pathways including pathways leading to the activation of NF-κB. When compared to cardiac biopsies obtained from chow-fed mice, cardiac tissue obtained from mice fed a HFD exhibited a significant increase in a) the phosphorylation of IKKα/β on $Ser^{178/180}$, b) the phosphorylation of IκBα on $Ser^{32/36}$, c) the translocation of p65 NF-κB to the nucleus, and d) increased expression of iNOS (P<0.05; Figure 3.5 A-D). When compared to cardiac tissue obtained from mice fed on a chow diet challenged with vehicle, cardiac tissue obtained from chow fed diet challenged with LPS showed a significant increase in a) the phosphorylation of IKKα/β on $Ser^{178/180}$, b) the phosphorylation of IκBα on $Ser^{32/36}$, c) the translocation of p65 NF-κB into the nucleus, and d) an increased expression of iNOS (P<0.05; Figure 3.5 A-D). When compared to mice fed a HFD and challenged with vehicle, mice on HFD challenged with LPS did not have a significant effect on the phosphorylation of IKKα/β or IκBα (P>0.05; Figure 3.5 A-B). When compared to mice fed a HFD and subjected to vehicle, challenging mice on HFD with LPS did, however, result in significant increases in a) the translocation of p65 NF-κB to the nucleus and b) iNOS expression (P<0.05; Figure 3.5 C-D). It should be noted that the degree of phosphorylation of IKKα/β and IκBα in cardiac tissue obtained from mice fed a HFD challenged with vehicle was a) significantly greater than that in cardiac tissue of mice fed a chow diet challenged with vehicle (P<0.05; Figure 3.5 A-B), and b) not significantly different from that of cardiac tissue of mice fed a chow-fed diet and challenged

with LPS (*P*>0.05; Figure 3.5 A-B).

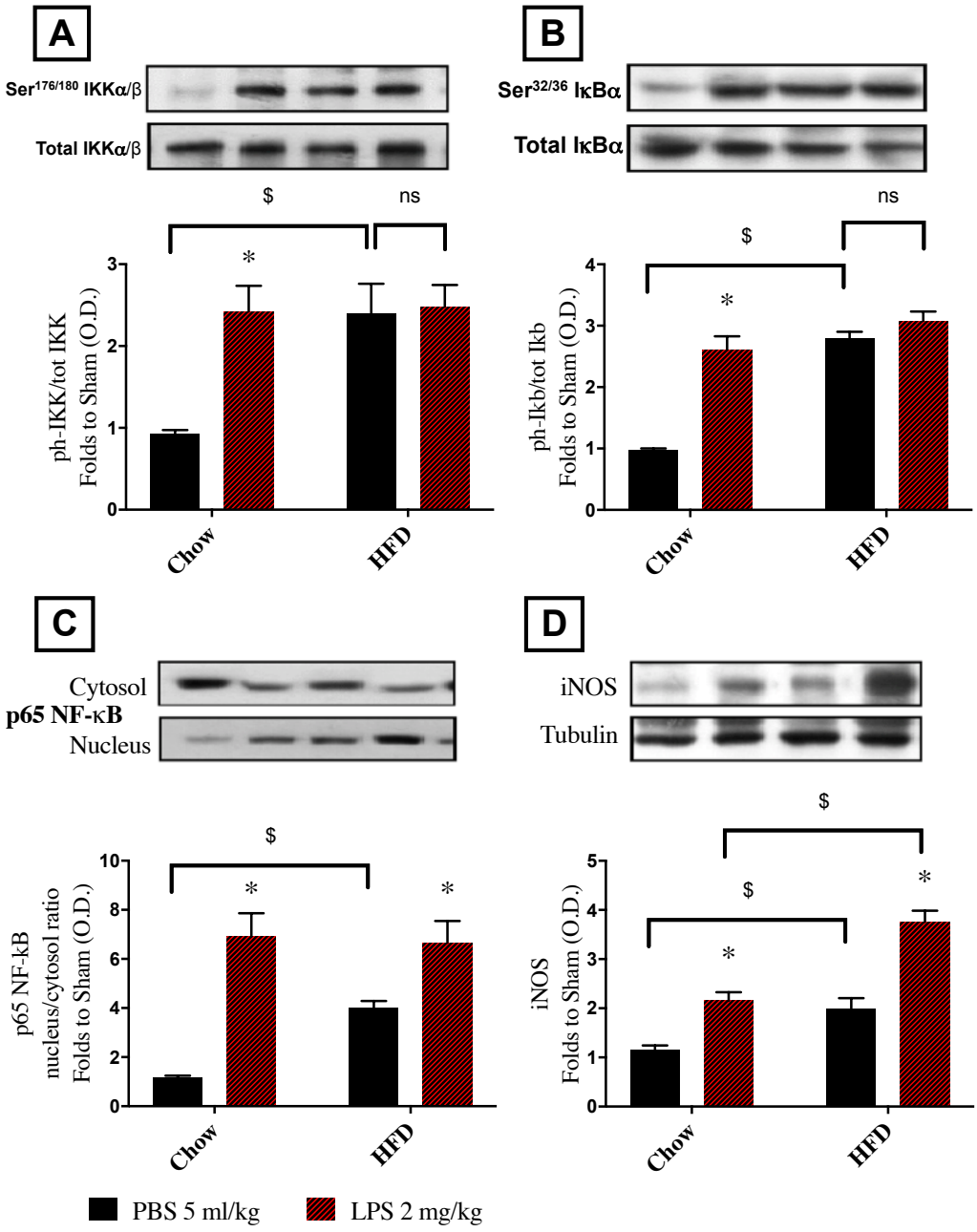

Figure 3.5 Effect of pre-existing T2DM in NF-κB signalling pathway in the heart of mice challenged with low dose LPS (2mg/kg).
Mice on chow and high fat diet were subjected to low dose LPS (2 mg/kg i.p.) or PBS (5 ml/kg i.p.). At 18 h, heart samples were collected and signalling events were assessed. Densitometry analysis of the bands is expressed as relative optical density (O.D.) of **(A)** IKKα/β phosphorylation on $Ser^{178/180}$ corrected to the corresponding total IKKα/β content and normalized using the related sham band; **(B)** IκBα phosphorylation on $Ser^{32/36}$ corrected to the corresponding total IκBα content and normalized using the related sham band; **(C)** NF-κB p65 subunit levels in both, cytosolic and nuclear fractions expressed as a nucleus/cytosol ratio normalized using the related sham bands; **(D)** Inducible nitric oxide synthase (iNOS) expression corrected for the corresponding tubulin band. Data were analysed using two-way ANOVA followed by Bonferroni's post hoc test and expressed as mean ± SEM. **P*<0.05 compared to respective PBS group, $*P*<0.05 (n=3-5 per group).

5. Effect of low dose LPS on the phosphorylation of Akt in mice with pre-existing T2DM

When compared to cardiac biopsies obtained from chow-fed mice, cardiac tissue obtained from mice fed a HFD exhibited a significant decrease in Akt phosphorylation on Ser^{473}. When compared to mice fed a chow diet and challenged with vehicle, challenge with mice on chow diet with LPS did result in a significant reduction in Akt phosphorylation (P<0.05; Figure 3.6). When compared to mice fed a HFD and challenged with vehicle, challenge with mice on HFD with LPS did not, however, result in a significant change in Akt phosphorylation (P>0.05; Figure 3.6).

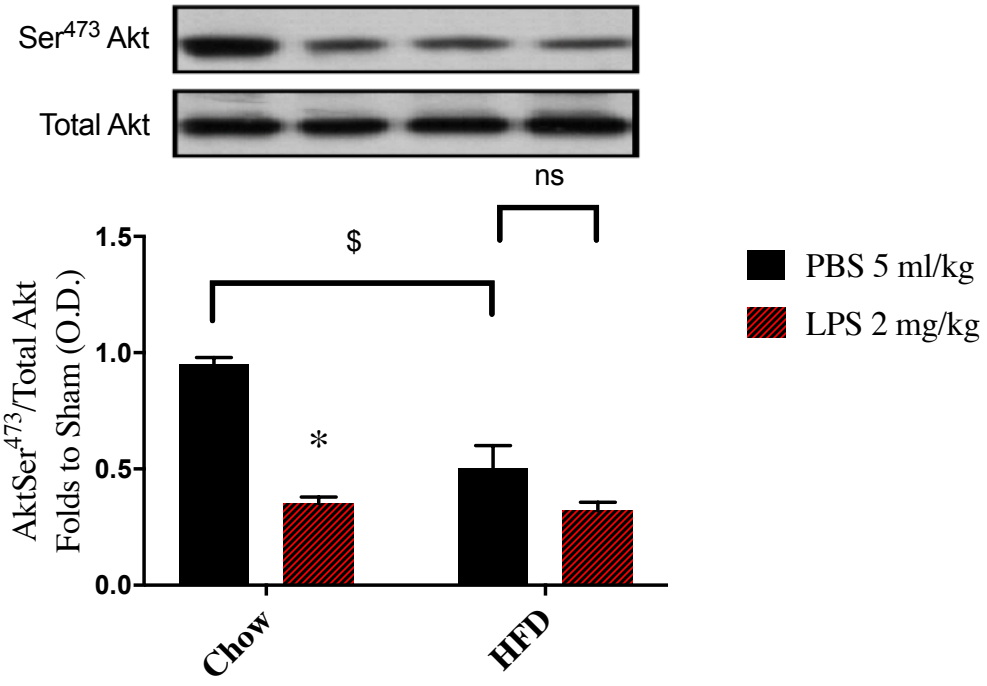

Figure 3.6 Effect of pre-existing T2DM in Akt phosphorylation in the heart of mice challenged with low dose LPS (2mg/kg).
Mice on chow and high fat diet were subjected to low dose LPS (2 mg/kg i.p.) or PBS (5 ml/kg i.p.). At 18 h, heart samples were collected and signalling events were assessed. Densitometry analysis of the bands is expressed as relative optical density (O.D.) of phosphorylated Akt on Ser^{473} corrected for the corresponding total Akt content and normalized using the related sham band. Data were analysed using two-way ANOVA followed by Bonferroni's post hoc test and expressed as mean ± SEM for n number of observations. *P<0.05 compared to respective PBS group. $$P$<0.05 (n=3-5 per group).

6. Effect of low dose LPS on the severity of renal dysfunction and hepatocellular injury in mice with pre-existing T2DM

When compared to mice on chow diet, mice on HFD showed no significant changes in serum urea, creatinine or ALT ($P>0.05$; Figure 3.7 A-C). When compared to mice on regular chow diet challenged with the vehicle, mice on chow diet challenged with low dose LPS (2 mg/kg i.p.) did not show significant changes in the serum levels of creatinine or ALT ($P>0.05$; Figure 3.7 B, C). When compared to animals on regular chow diet challenged with the vehicle, mice on chow diet challenged with low dose LPS did, however, show an increase in serum urea ($P<0.05$; Figure 3.7 A). Animals on HFD challenged with low dose LPS exhibited a large and significant increase in serum urea, creatinine, and ALT when compared to mice on HFD challenged with the vehicle. The increase in serum urea, creatinine, and ALT caused by LPS in mice fed a HFD were significantly greater than those caused by LPS in mice fed a normal chow diet ($P<0.05$; Figure 3.7 A-C).

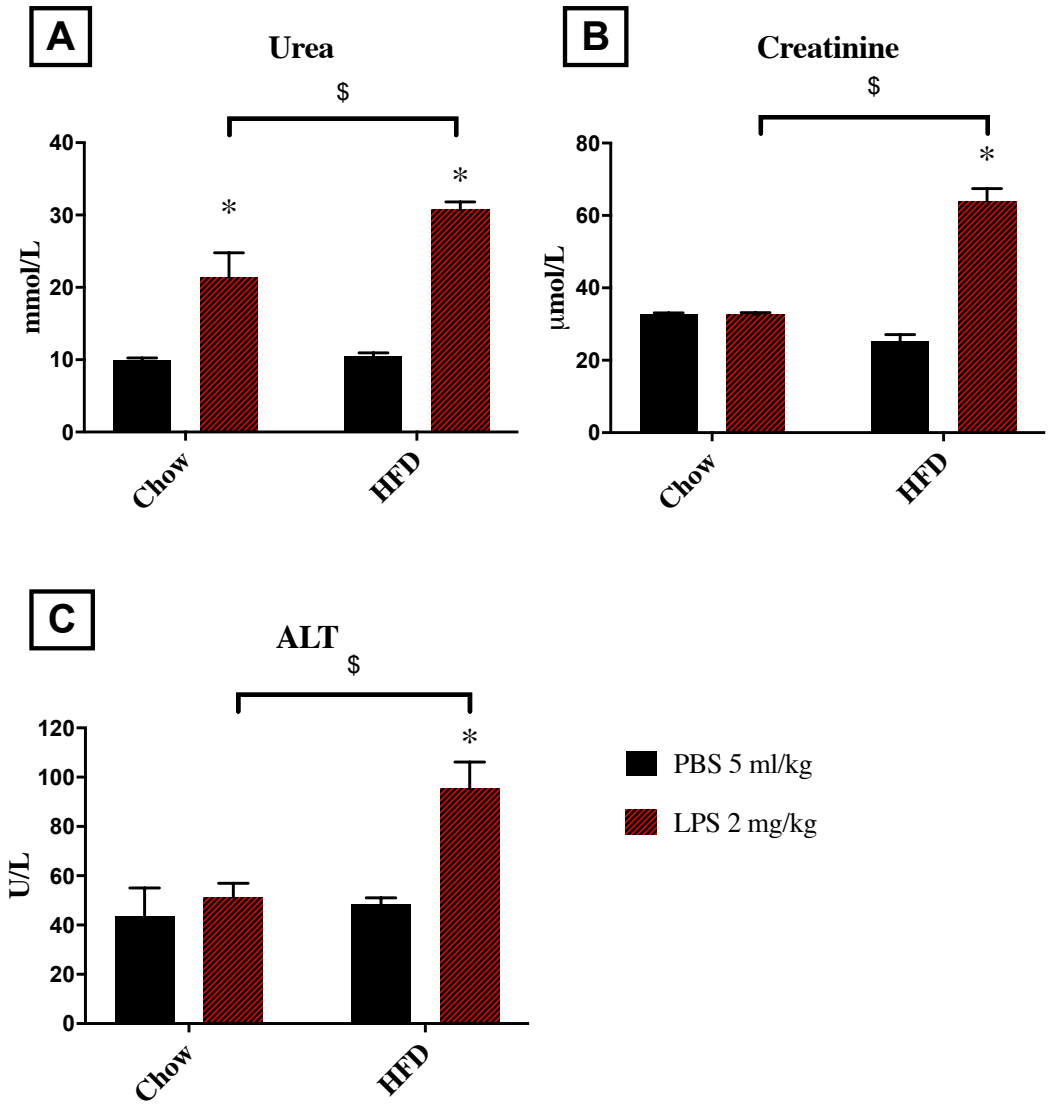

Figure 3.7 Effect of low dose LPS challenge on kidney function and liver injury in mice with T2DM.
Kidney function and liver injury were assessed at 18 h after LPS or vehicle challenge in mice fed a chow diet or a HFD. Serum **(A)** urea, **(B)** creatinine and **(C)** ALT levels were measured. Data were analysed using two-way ANOVA followed by Bonferroni's post hoc test and expressed as mean ± SEM. **P*<0.05 compared respective PBS group, $*P*<0.05 (n=10 per group).

7. Pre-existing T2DM increases neutrophil and macrophage accumulation in the lung after LPS challenge

When compared to mice on chow diet, mice on HFD showed no significant changes in MPO or NAG activities in the lung (P>0.05; Figure 3.8 A-B). When compared to mice on regular chow diet challenged with vehicle, mice on chow diet challenged with low dose LPS (2 mg/kg i.p.) showed significant increases in MPO and NAG activities in the lung (P<0.05; Figure 3.8 A-B). Challenge of mice on HFD with LPS resulted in big increases in both MPO and NAG activities when compred to mice on HFD challenged with vehicle and mice on chow diet challenged with the same dose of LPS (P<0.05; Figure 3.8 A-B).

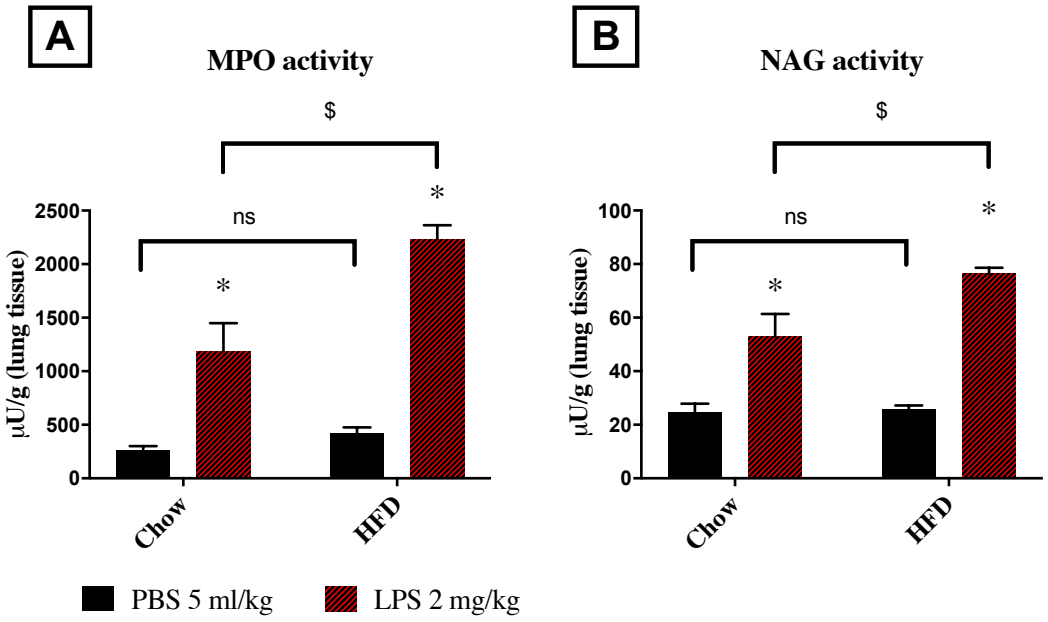

Figure 3.8 Effect of pre-existing T2DM on neutrophil/macrophage infiltration (lung) in mice challenged with low dose LPS (2mg/kg).
Mice on chow and high fat diet were subjected to low dose LPS (2 mg/kg i.p.) or PBS (5 ml/kg i.p.). At 18 h, lung samples were collected and neutrophil and macrophages infiltration were measured as (A) MPO and (B) NAGase activities. Data were analysed using two-way ANOVA followed by Bonferroni's post hoc test and expressed as mean ± SEM for n number of observations. *P<0.05 compared to respective PBS group. $$P$<0.05 (n= 6 per group).

8. Effect of pre-existing T2DM on serum cytokine levels after LPS challenge

When compared to mice on chow diet, mice on HFD showed no significant changes in cytokines levels ($P>0.05$; Figure 3.9 A-D). When compared to mice on regular chow diet challenged with vehicle, mice on chow diet challenged with low dose LPS (2 mg/kg i.p.) showed significant increases in IL-6 and KC concentrations in the serum ($P<0.05$; Figure 3.9 B-C). However, they did not show any significant changes in TNF-α or IL-10 when compred to mice on chow diet and challenged with vehicle ($P<0.05$; Figure 3.9 A, D). Challengin mice on HFD with LPS resulted in huge increases in all cytokines levels when compred to mice on HFD challenged with vehicle and mice on chow diet challenged with the same dose of LPS ($P<0.05$; Figure 3.9 A-D).

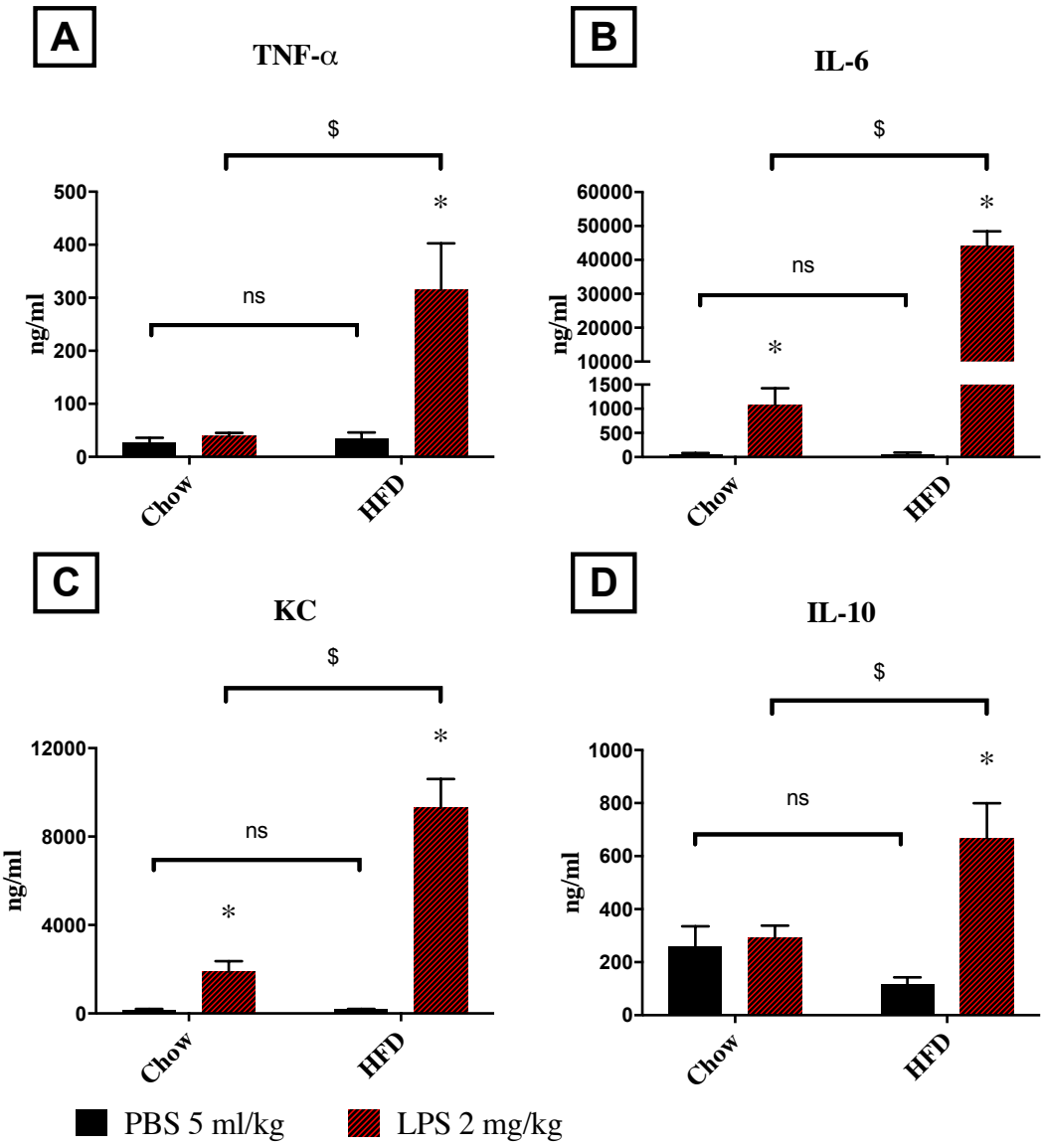

Figure 3.9 Effect of pre-existing T2DM on serum cytokines in mice challenged with low dose LPS (2 mg/kg).

Mice on chow and high fat diet were subjected to low dose LPS (2 mg/kg i.p.) or PBS (5 ml/kg i.p.). At 18 h, blood samples were collected and inflammatory cytokines concentrations were measured in the serum. **(A)** TNF-α, **(B)** IL-6, **(C)** KC and **(D)** IL-10. Data were analysed using two-way ANOVA followed by Bonferroni's post hoc test and expressed as mean ± SEM for n number of observations. **P*<0.05 compared to respective PBS group. $*P*<0.05 (n=4 per vehicle group and n=6-8 per LPS group).

3.5.2 CLP model of polymicrobial sepsis in mice with pre-existing T2DM

1. Effect of HFD on organ function before CLP/sham surgeries

After 12 weeks of dietary manipulation and before sepsis challenge, mice on HFD showed signs of development of T2DM including significant increases in body weight, fasting blood glucose and a significant impairment in OGTT when compared to mice on chow diet. When compared to age matched mice on chow diet, HFD-fed mice showed significant reduction in systolic cardiac function (%EF) and creatinine clearance and significant increases in ALT and total cholesterol levels ($P<0.05$, Table 3.4).

Table 3.4 Baseline data for both chow and HFD groups before interventions (CLP or sham surgeries).

Parameter	Chow	HFD
Net weight gain *(grams)*	5.34 ± 0.47	15.92 ± 1.19*
Food intake$ *(grams/mouse/week)*	3.38 ± 0.02	2.82 ± 0.03*
Calories intake$ *(Kcal/mouse/week)*	17.29 ± 0.12	20.0 ± 0.24*
AUC for OGTT *(mg.min/dl)*	29646 ± 547.5	47727 ± 2958*
Fasting blood glucose *(mg/dl)*	183.9 ± 4.68	294.9 ± 13.9*
Ejection fraction *(%)*	71.92 ± 0.81	64.26 ± 0.95*
Fractional shortening *(%)*	40.73 ± 0.67	34.73 ± 0.68*
Fractional area change *(%)*	51.37 ± 0.41	45.8 ± 1.14*
Left ventricle mass *(mg)*	127.2 ± 2.92	131.6 ± 4.04
Urea *(mmol/L)*	9.47 ± 0.32	9.45 ± 0.24
Creatinine *(µmol/L)*	28.49 ± 1.71	32 ± 1.25
Alanine aminotransferase *(U/L)*	32.9 ± 4.05	68.26 ± 9.54*
Creatinine Clearance£ *(ml/min)*	154.1 ± 17.56	96.55 ± 8.79*
Triglyceride *(mg/dl)*	183.6 ± 9.65	175.4 ± 8.53
Total cholesterol *(mg/dl)*	147.3 ± 2.24	183.7 ± 3.56*

Mice fed a HFD were compared to age-matched mice fed a chow diet. Data are presented as mean ± SEM for n number of observations. Data were analysed by unpaired t-test. *P<0.05 versus the chow-fed group (n=18 per group). $: mean food intake of 18 mice in each group during the study period 12 weeks (n=12). £: Creatinine clearance was calculated using (urine creatinine/serum creatinine) x (urine output/time in min).

2. Effect of pre-existing T2DM on vital signs and physical activity after CLP-sepsis

When compared to mice fed with chow diet, mice fed with HFD for 12 weeks showed no significant change in physical activity, heart rate or body temperature (P>0.05; Figure 3.10 A-C). When compared to animals on regular chow diet subjected to sham surgery, mice on chow diet subjected to CLP surgery showed no significant decrease in physical activity, heart rate or body temperature (P>0.05; Figure 3.10 B-C). However, mice on HFD subjected to CLP surgery exhibited large and significant reduction in physical activity, heart rate and body temperature when compared to mice on HFD subjected to sham surgery (P<0.05; Figure 3.10 A-C) and exhibited large and significant reduction in physical activity and heart rate when compred to mice on chow diet and subjected to the same CLP surgery (P<0.05; Figure 3.10 A-B). It should be noted that at the beginning of measurements, and after stabilising the animals, there were no significant difference in the core body temperature or the heart rate between the four groups.

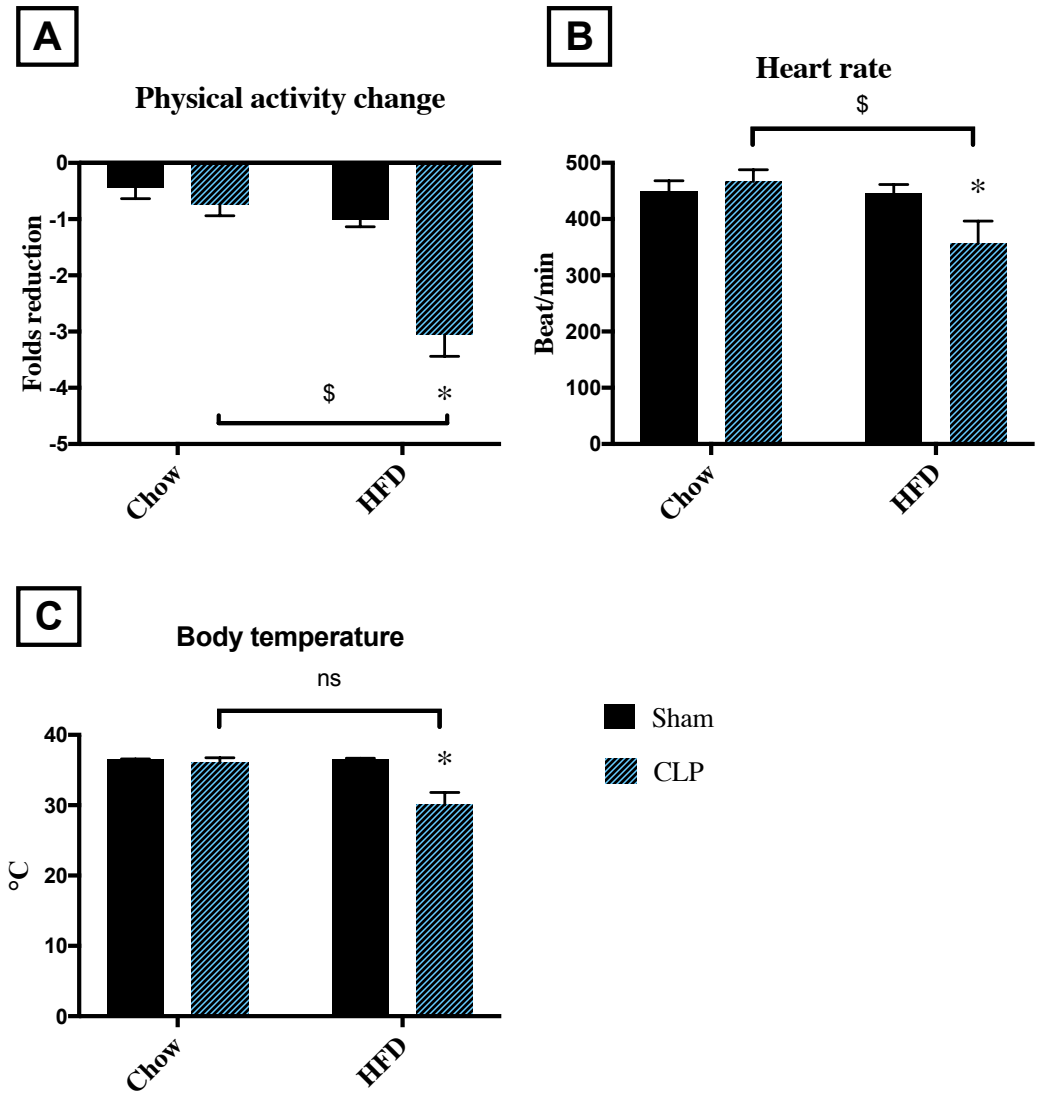

Figure 3.10 Effect of CLP-sepsis on vital signs and physical activity in mice with T2DM.

Physical activity and vital signs were assessed at 24 h after CLP or sham surgeries in mice fed a chow diet or a HFD. **(A)** Physical activity change **(B)** heart rate and **(C)** body temperature. Data were analysed using two-way ANOVA followed by Bonferroni's post hoc test and expressed as mean ± SEM. **P*< 0.05 compared to respective PBS group, $*P*< 0.05. (n=8 per sham surgery group and 10 per CLP surgery group).

3. Pre-existing T2DM augments the cardiac dysfunction associated with poly-microbial sepsis caused by CLP.

When compared to mice fed with chow diet and subjected to sham surgery, mice fed with HFD and subjected to sham surgery showed no significant change in cardiac function ($P>0.05$; Figure 3.11 B-D). When compared to animals on regular chow diet subjected to sham surgery, mice on chow diet subjected to CLP surgery showed no significant reduction in systolic cardiac function (measured as EF, FS and FAC; $P>0.05$; Figure 3.11 B-D). However, animals on HFD subjected to CLP surgery exhibited a large and significant reduction in systolic cardiac function when compared to mice on HFD subjected to sham surgery. The reductions in EF, FS and FAC caused by CLP surgery in mice fed a HFD were significantly greater than those caused by CLP surgery in mice fed a normal chow diet ($P<0.05$; Figure 3.11 B-D).

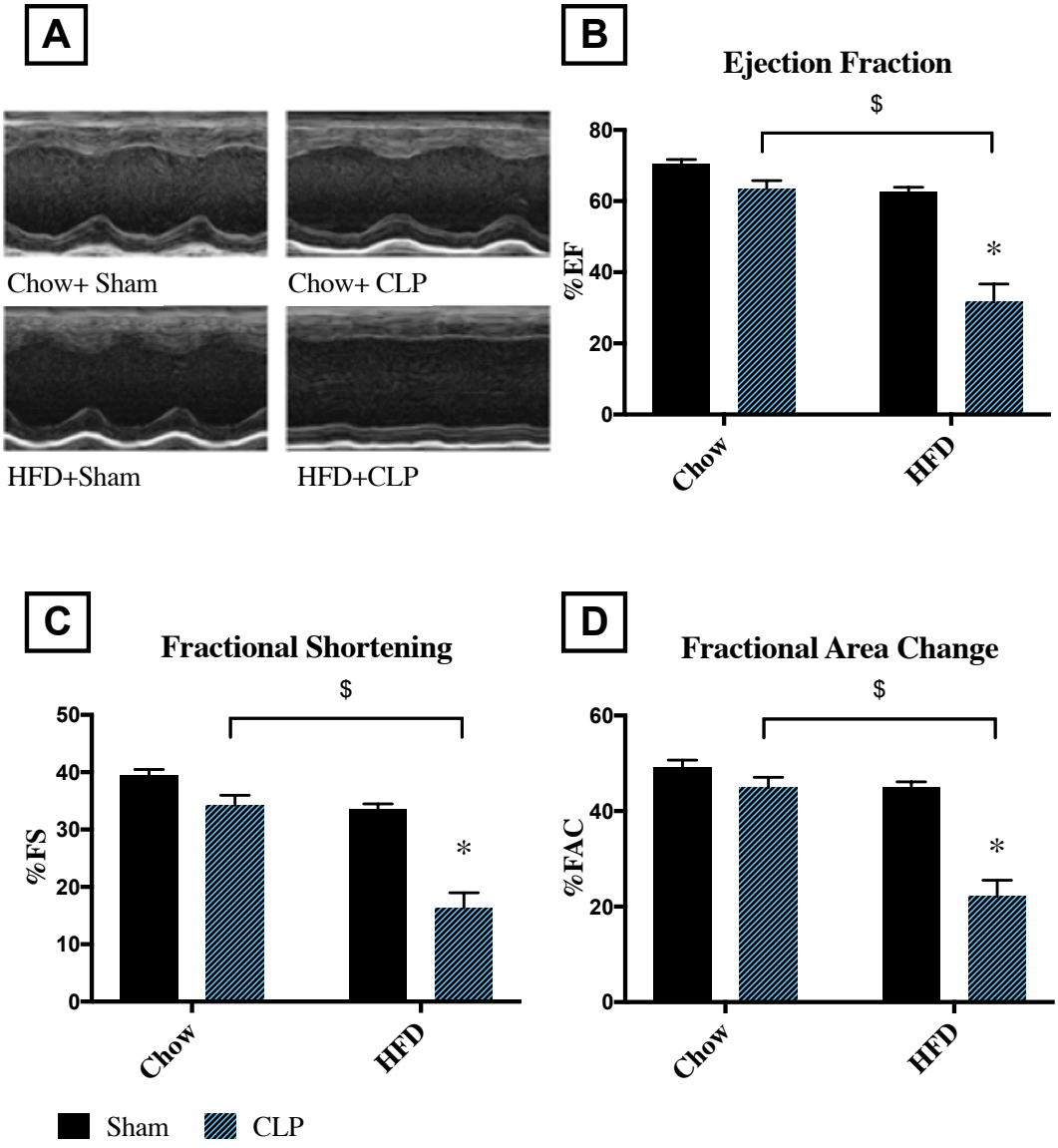

Figure 3.11 Effect of CLP-induced poly-microbial sepsis on cardiac function in mice with pre-existing T2DM.

Cardiac function was assessed at 24 h after CLP or sham surgery in mice fed a chow diet or a HFD. **(A)** Representative M-mode echocardiograms, percentage % **(B)** EF, **(C)** FS and **(D)** FAC. Data were analysed using two-way ANOVA followed by Bonferroni's post hoc test and expressed as mean ± SEM. **P*<0.05 compared respective sham surgery group, $*P*< 0.05. (n=8 for sham surgery group, n=10 for CLP surgery group).

4. Effect of CLP-sepsis on NF-κB signalling in mice with pre-existing T2DM

In a separate set of experiments, I investigated the effects of HFD/diabetes on the activation of key signalling pathways of inflammation and cell survival including pathways leading to the activation of NF-κB. When compared to cardiac biopsies obtained from chow-fed mice, cardiac tissue obtained from mice fed a HFD exhibited a significant increase in a) the phosphorylation of IKKα/β on $Ser^{178/180}$, b) the phosphorylation of IκBα on $Ser^{32/36}$, c) the translocation of p65 NF-κB to the nucleus, and d) increased expression of iNOS (P<0.05; Figure 3.12 A-D). When compared to cardiac tissue obtained from mice fed on a chow diet subjected to sham surgery, cardiac tissue obtained from chow-fed mice subjected to CLP/sepsis showed a significant increase in a) the phosphorylation of IKKα/β on $Ser^{178/180}$, b) the phosphorylation of IκBα on $Ser^{32/36}$, c) the translocation of p65 NF-κB to the nucleus, and d) increased expression of iNOS. When compared to mice fed a HFD and subjected to sham surgery, induction of polymicrobial sepsis in mice on HFD after CLP/sepsis resulted in a further significant increase in a) the phosphorylation of IKKα/β on $Ser^{178/180}$, b) the phosphorylation of IκBα on $Ser^{32/36}$, c) the translocation of p65 NF-κB into the nucleus, and expression of iNOS (P<0.05; Figure 3.12 A-D) The changes in IKKα/β and IκBα phosphorylations, p65 NF-κB translocation, and iNOS expression caused by CLP/sepsis in mice fed a HFD were significantly greater than those caused by CLP/sepsis in mice fed a normal chow diet (P<0.05; Figure 3.12 A-D).

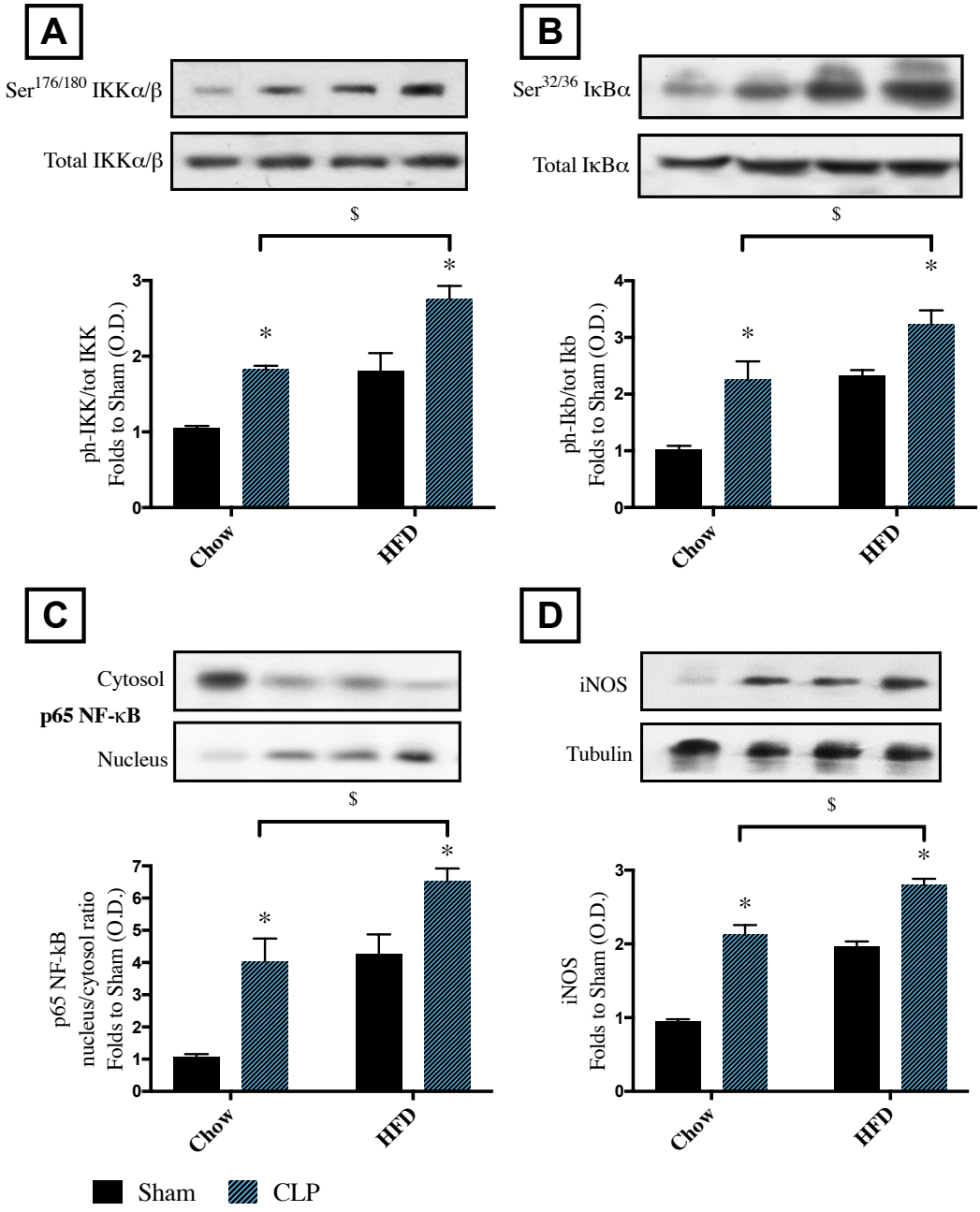

Figure 3.12 Effect of pre-existing T2DM on NF-κB signalling pathway in the heart of mice with CLP/sepsis.

Mice on chow and high fat diet were subjected to CLP or sham surgery. At 24 h, heart samples were collected and signalling events were assessed. Densitometry analysis of the bands is expressed as relative optical density (O.D.) of **(A)** IKKα/β phosphorylation on $Ser^{178/180}$ corrected to the corresponding total IKKα/β content and normalized using the related sham band; **(B)** IκBα phosphorylation on $Ser^{32/36}$ corrected to the corresponding total IκBα content and normalized using the related sham band; **(C)** NF-κB p65 subunit levels in both, cytosolic and nuclear fractions expressed as a nucleus/cytosol ratio normalized using the related sham bands; **(D)** Inducible nitric oxide synthase (iNOS) expression corrected for the corresponding tubulin band. Data were analysed using two-way ANOVA followed by Bonferroni's post hoc test and expressed as mean ± SEM. **P*<0.05 compared to respective sham surgery group, $*P*< 0.05. (n=4-6 per group).

5. Effect of CLP-sepsis on the phosphorylation of Akt in mice with pre-existing T2DM

When compared to cardiac biopsies obtained from chow-fed mice, cardiac tissue obtained from mice fed a HFD exhibited a significant decrease in Akt phosphorylation on Ser^{473}. When compared to mice fed a chow diet and subjected to sham surgery, induction of poly-microbial sepsis by CLP-sepsis in mice on chow diet resulted in a significant reduction in Akt phosphorylation ($P<0.05$; Figure 3.13). When compared to mice fed a HFD and subjected to sham surgery, induction of poly-microbial sepsis by CLP in mice on HFD did not, however, result in a significant change in Akt phosphorylation ($P>0.05$; Figure 3.13). The reductions in Akt phosphorylation caused by CLP in mice fed a HFD was significantly greater than that caused by CLP in mice fed a normal chow diet ($P<0.05$; Figure 3.13 B-D).

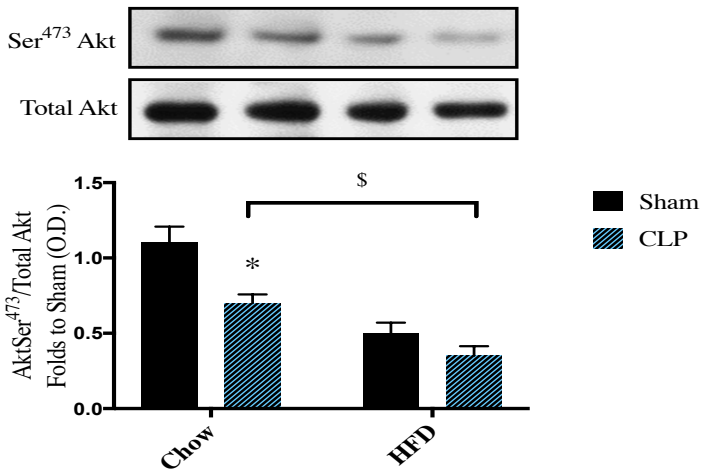

Figure 3.13 Effect of pre-existing T2DM on Akt phosphorylation in the heart of mice subjected to CLP.
Mice on chow and HFD were subjected to CLP or sham surgery. At 24 h, heart samples were collected and signalling events were assessed. Densitometry analysis of the bands is expressed as relative optical density (O.D.) of phosphorylated Akt on Ser^{473} corrected for the corresponding total Akt content and normalized using the related sham band. Data were analysed using two-way ANOVA followed by Bonferroni's post hoc test and expressed as mean ± SEM. *$P<0.05$ compared to respective sham surgery group, $$P<0.05$. (n= 4-6 per group).

6. Effect of CLP-sepsis on the severity of renal dysfunction and hepatocellular injury in mice with pre-existing T2DM

When compared to mice on chow diet subjected to sham surgery, mice on HFD subjected to sham surgery showed no significant changes in serum urea, creatinine or ALT ($P>0.05$; Figure 3.14 A-C). When compared to mice on regular chow diet subjected to sham surgery, mice on chow diet subjected to CLP did not have significant changes in serum urea, creatinine, or ALT levels ($P>0.05$; Figure 3.14 A-C). Animals on HFD subjected to CLP exhibited large and significant increases in serum urea, creatinine, and ALT when compared to mice on HFD subjected to sham surgery. The increases in serum urea, creatinine, and ALT caused by CLP in mice fed a HFD were significantly greater than those caused by CLP in mice fed a normal chow diet ($P<0.05$; Figure 3.14 A-C).

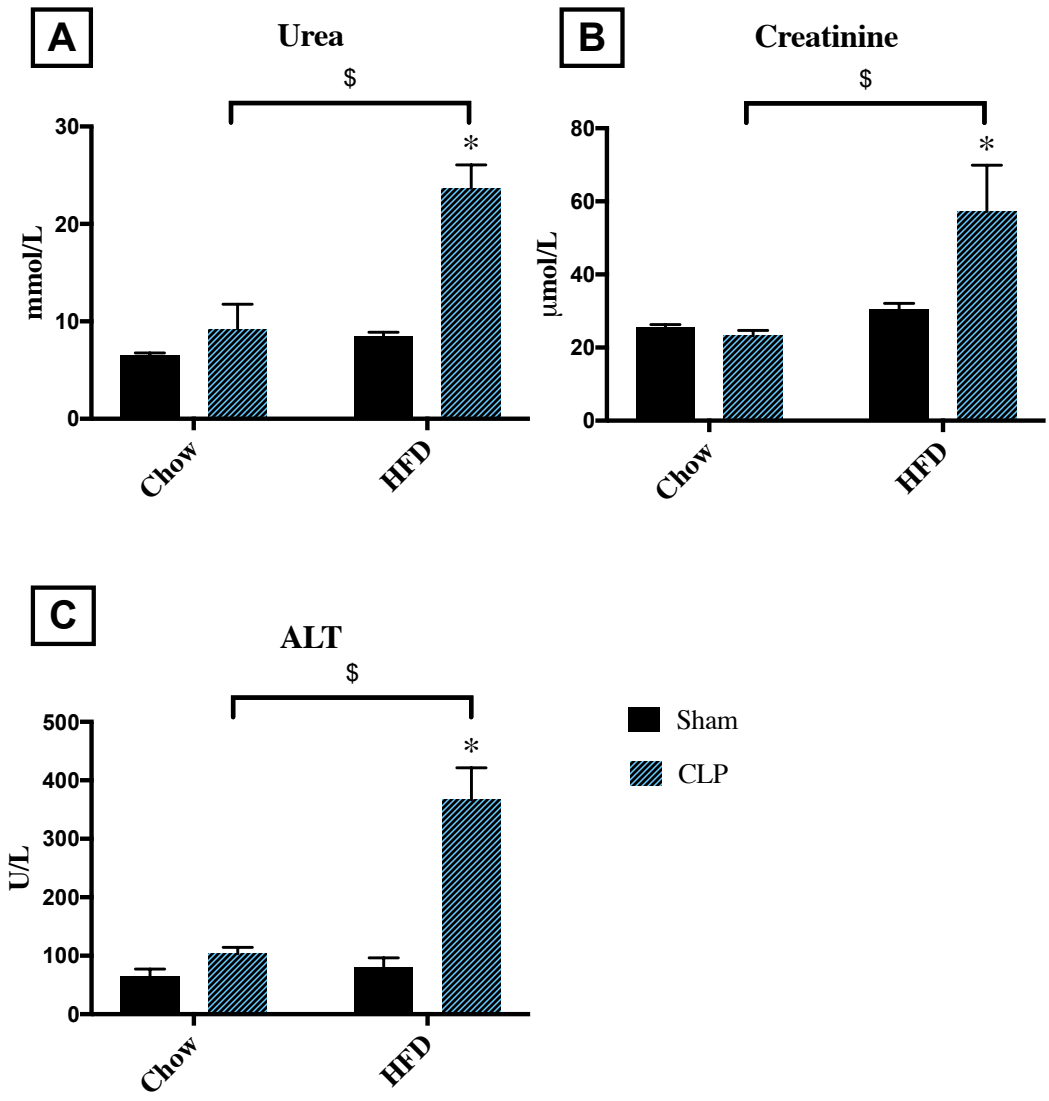

Figure 3.14 Effect of CLP induced poly-microbial sepsis on the severity of renal dysfunction and hepatocellular injury in mice with pre-existing T2DM.

Kidney function and liver injury were assessed at 24 h after CLP or sham surgery in mice fed a chow diet or a HFD. Serum **(A)** urea, **(B)** creatinine and **(C)** ALT levels were measured. Data were analysed using two-way ANOVA followed by Bonferroni's post hoc test and expressed as mean ± SEM. **P*<0.05 compared respective PBS group, $*P*<0.05 (n=8 for sham surgery group, n=10 for CLP surgery group).

7. Pre-existing T2DM increases neutrophil and macrophage accumulation infiltration in the lung after CLP-sepsis

When compared to mice on chow diet, mice on HFD showed no significant changes in MPO or NAG activities in the lungs after sham surgery (P>0.05; Figure 3.15 A-B). When compared to mice on regular chow diet subjected to sham surgery, mice on chow diet subjected to CLP showed a significant increase in NAG activity in the lung (P<0.05; Figure 3.15 B) with no change in MPO activity (P>0.05; Figure 3.8 A). Subjecting mice on HFD to CLP surgery resulted in big increases in both MPO and NAG activities when compred to mice on HFD subjected to sham surgery and mice on chow diet subjected to the same CLP (P<0.05; Figure 3.15 A-B).

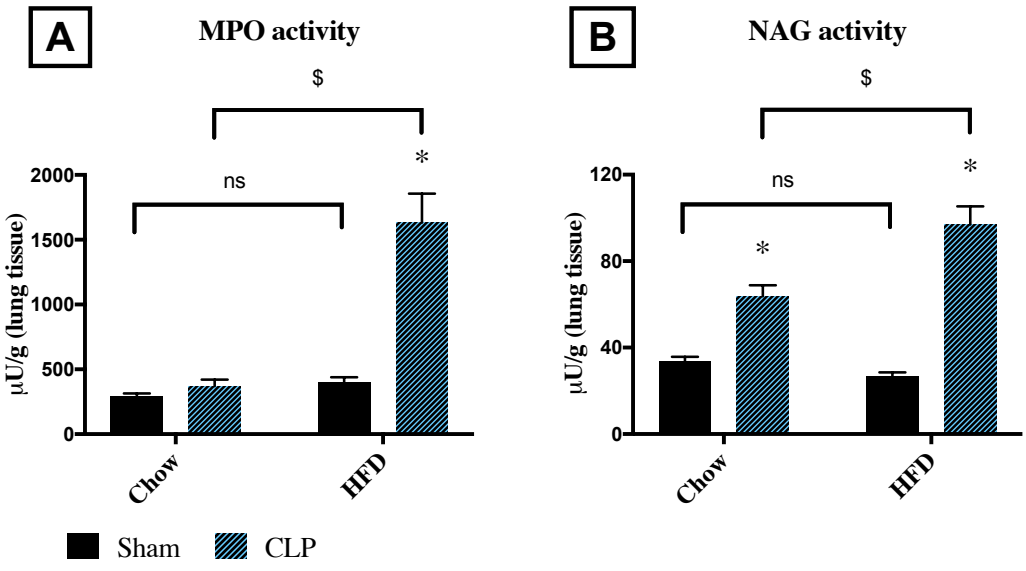

Figure 3.15 Effect of pre-existing T2DM on neutrophil/macrophage infiltration in the lung in mice after CLP-sepsis.

Mice on chow and high fat diet were subjected to sham or CLP surgeries. At 24 h, lung samples were collected and neutrophil and macrophages infiltration were measured as the (A) MPO and (B) NAG activities. Data were analysed using two-way ANOVA followed by Bonferroni's post hoc test and expressed as mean ± SEM for n number of observations. *P<0.05 compared to respective PBS group. \$$P$<0.05 (n=6 per group).

8. Effect of pre-existing T2DM on serum inflammatory cytokines after CLP sepsis.

When compared to mice on chow diet, mice on HFD for 12 weeks showed no significant changes in cytokines levels ($P>0.05$; Figure 3.16 A-D). When compared to mice on regular chow diet subjected to sham surgery, mice on chow diet subjected to CLP surgery showed no significant changes in cytokines levels in the serum ($P>0.05$; Figure 3.16 A-D). Subjecting mice on HFD to CLP resulted in large increases in the serum levels of TNF-α, IL-6, KC and IL-10 when compred to mice on HFD subjected to sham surgery and mice on chow diet subjected to CLP ($P<0.05$; Figure 3.16 A-D).

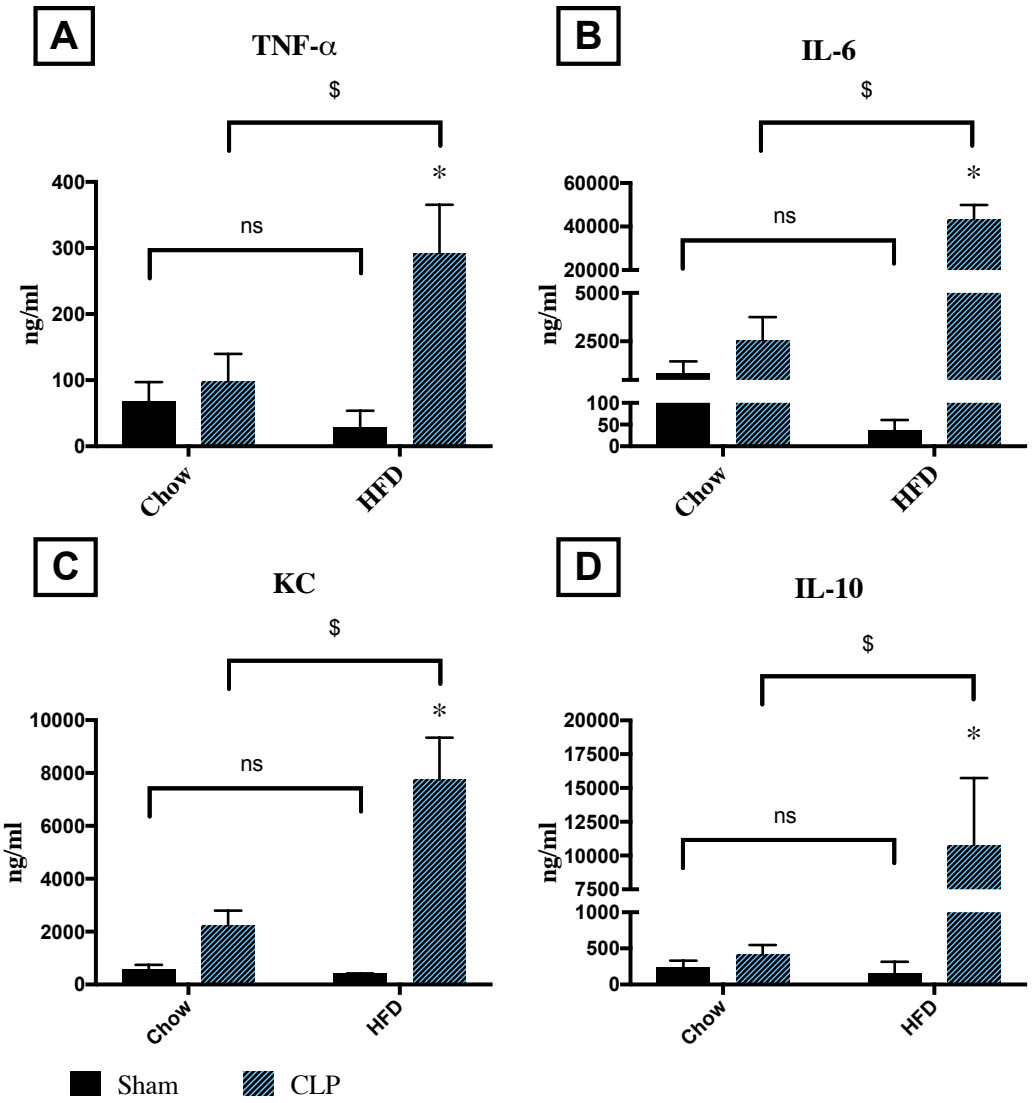

Figure 3.16 Effect of pre-existing T2DM on serum cytokines in mice subjected to CLP-sepsis.

Mice on chow and high fat diet were subjected to sham or CLP. At 24 h, blood samples were collected and inflammatory cytokines concentrations were measured in the serum. **(A)** TNF-α, **(B)** IL-6, **(C)** KC and **(D)** IL-10. Data were analysed using two-way ANOVA followed by Bonferroni's post hoc test and expressed as mean ± SEM for n number of observations. **P*<0.05 compared to respective sham group. $*P*<0.05 (n=4 per sham surgery group and n=6-8 per CLP group).

3.6 Discussion

Among patients with sepsis and septic shock, there is a strong association between the development of cardiac dysfunction and the increased mortality rate [273]. The exact aetiology and pathophysiology of the cardiac dysfunction associated with sepsis (in previously healthy patients or patients with pre-existing conditions) is not fully understood and stills warrants further investigation in order to develop new therapeutic interventions that may reduce the high mortality rate among those patients. Patients with diabetes have a higher risk of developing infections and subsequently sepsis [161]. However, the effect of pre-existing T2DM on outcomes in patients with infections and sepsis is still highly controversial. In this chapter, I designed a two-hit model to investigate (i) the effect of T2DM on cardiac dysfunction, renal dysfunction, liver injury and lung inflammation in sepsis and (ii) to understand the signalling mechanism underlying the cardiac dysfunction in T2DM/sepsis.

In this study, I induced T2DM by feeding mice with a HFD for 12 weeks as the first hit, then expose the mice to a moderate endotoxemia (by injection of low dose LPS) or CLP-sepsis that (in the absence of diabetes) would result only in a moderate degree of systemic inflammation and cardiac dysfunction in young and, previously, healthy mice.

In mice fed with a HFD for 12 weeks, I detected a development of T2DM phenotype as mice showed increased body weight, fasting blood glucose and impaired glucose tolerance. They also developed some diabetes complications such as a development of systolic cardiac dysfunction (measured as a small, but

significant, reduction in ejection fraction (%EF)), hepatocellular injury (measured as an increase in serum ALT) and a mild reduction in renal function (measured as a decrease in creatinine clearance). These results are consistent with results from previous studies showing a reduction in ejection fraction, development of liver injury and kidney disease in patients with T2DM [265,294,295] and in mouse model of HFD-induced type 2 diabetes [296–298]. The baseline cardiac dysfunction developed in this model after 12 weeks on HFD is likely to be a result of the increased NF-κB pathway activation and the subsequent increase in iNOS expression in the heart, as an enhanced formation of NO by iNOS results in a reduction in cardiac myofilament response to calcium, changes both the preload and the afterload and down regulates the β-adrenergic receptors [49,299].

The elevation of ALT is likely to be a result of the fat accumulation in the liver (steatosis) as it is well known that steatosis leads to excessive local inflammation that is associated with liver injury and, hence, high serum ALT levels [300].

I report, here, for the first time that the cardiac dysfunction associated endotoxaemia (caused by low dose LPS) is augmented in mice with T2DM. I also showed that the cardiac dysfunction associated with CLP-sepsis is significantly greater in mice with pre-existing T2DM. The model of CLP-sepsis used here is more clinically relevant than LPS-model as it is a model of local infection and sepsis (rather than hyperinflammation) and the animals are treated with both antibiotics and fluids. Studies have shown that iNOS expression and high IL-6 levels are responsible for the late cardiac dysfunction in sepsis [45]. In my study, mice with diabetes and sepsis (LPS or CLP) showed an augmentation in NF-κB activation and subsequent increase in iNOS expression in the heart and a dramatic

increase in the serum levels of the proinflammatory cytokines TNF-α, IL-6 and KC, both of which may importantly contribute to the development of a significant systolic cardiac dysfunction in T2DM/sepsis. Although there was also a small activation of the NF-κB pathway after low dose LPS and CLP in mice fed with chow diet, it did not result in a large decrease in systolic cardiac function (as the one seen in mice on HFD) suggesting that there is an association between the degree of iNOS expression and cytokines levels and the severity of cardiac dysfunction in sepsis.

I also studied the Akt pro-survival pathway in the heart. In the cardiomyocytes, insulin receptor substrate-1 (IRS-1) is phosphorylated as a result of insulin binding to the insulin receptors on the cell surface. IRS-1 transmits insulin signalling by activating the phosphatidylinositol 3 kinase (PI3K). PI3K activation ultimately leads to Akt phosphorylation and activation [301]. Activated Akt modulates cell survival by regulating apoptosis, chemotaxis and inflammatory responses. It is known that diabetes results in impaired insulin signalling [302]. Indeed, in my study Akt phosphorylation was attenuated in mice after HFD and the subsequent development of insulin resistance. Previous studies have shown that the cardiac dysfunction associated with sepsis was attenuated by Akt activation [277,278,302,303]. In my study, both LPS and CLP models of hyperinflammation/sepsis resulted in a reduction in Akt phosphorylation in chow-fed mice. However, no further decline in Akt phosphorylation in HFD-fed mice after sepsis challenge was observed.

In addition to cardiac dysfunction, both endotoxaemia and sepsis resulted in an augmentation of both liver injury and acute kidney injury in diabetic mice. The liver failure in sepsis is secondary to excessive local inflammation driven by high

TNF-α and IL-6 levels [104,105]. Indeed, the acute kidney injury associated with sepsis also develops as a result of the high IL-6 and IL-10 levels [83,84]. In my study, the development of acute liver and kidney injury may be, at least partially, the result of the high serum cytokines levels (TNF-α, IL-6, IL-10 and KC) after sepsis challenge in diabetic mice. The incidence of liver injury is increased in mouse model of sepsis and T2DM [169], and the PROWESS trial showed that the presence of baseline liver injury is associated with worse outcome in patients with sepsis [304]. In addition, a recent meta-analysis also suggests that the incidence of acute kidney injury associated with sepsis is higher in diabetic patients [305].

In this study, I also reported a development of a small degree of lung inflammation (measured as an increase in neutrophil and macrophage accumulation) in the lung in response to sepsis in previously healthy mice. However, sepsis challenge in diabetic mice resulted in further increase in lung inflammation with recruitment of both neutrophils (increase in MPO activity) and macrophages (increases in NAG activity). This further increase in leukocytes infiltration may be a result of the high inflammatory cytokines levels and the development of AKI, both of which have been reported to be key drivers for the development of lung injury in sepsis [306].

3.7 Conclusion

In this chapter, I have detected an augmentation of cardiac dysfunction associated with sepsis in mice with pre-existing T2DM. After the first hit (T2DM) there was moderate activation of NF-κB (and subsequent iNOS expression) in the heart tissues. However, sepsis as a second hit resulted in dramatic increase in the pro-inflammatory cytokines (in the serum) and further increase in NF-κB activation (and subsequent iNOS expression) in the heart.

CHAPTER 4: INHIBITION OF NF-κB ATTENUATES THE CARDIAC DYSFUNCTION ASSOCIATED WITH SEPSIS IN MICE WITH PRE-EXISTING T2DM

4.1 Introduction

Many potential therapeutic agents showed beneficial effects in different animal models of sepsis. However, a lot of these agents failed to improve outcomes in clinical studies. Both experimental design and animal model limitations contribute to this lack of translation of these agents from pre-clinical to clinical settings [307]. Many elements are usually tightly controlled in order to get consistent results in animal models. For example, young and healthy [with no pre-existing diseases; hypertension, diabetes or chronic kidney disease (CKD)] animals that are from the same gender, genetic background and strain that are housed in a clean environment are used to conduct experiments and to test these potential therapeutic agents, the thing that may decrease its clinical relevance [307,308].

Activation of NF-κB plays a crucial role in both sepsis related cardiac dysfunction [276–278] and in diabetic cardiomyopathy [279]. Different stimuli such as inflammatory cytokines, LPS, PepG, AngII, AGE and FFA activate receptors such as TLR 2, TLR 4 and RAGE leading to NF-κB pathway activation. Under physiological conditions, NF-κB is sequestered in the cytoplasm as inactive complex with IκB-α. For NF-κB to be activated, IKK phosphorylates IκB-α. This phosphorylation results in IκB-α degradation and NF-κB release from the complex. NF-κB then enters the nucleus and starts different gene expression (Figure 4.1) [309].

DPP-4 receptors are also involved in the activation of NF-κB [201–204]. In sepsis, microbial components activate different antigen presenting cells (APCs) after binding to TLR 4 and 2. Exposed caveolin-1 from the activated APC interacts with the DDP-4 receptors in T cells which results in strong NF-κB activation in both the APCs and the T cells [204]. Adenosine deaminase (ADA) is another activator of DPP-4. The activity of ADA in the serum is increased during inflammatory diseases (e.g sepsis) as a results of increased macrophages activity [310] the interaction of ADA with DPP-4 receptors leads to NF-κB activation in T cells [201] (Figure 4.1).

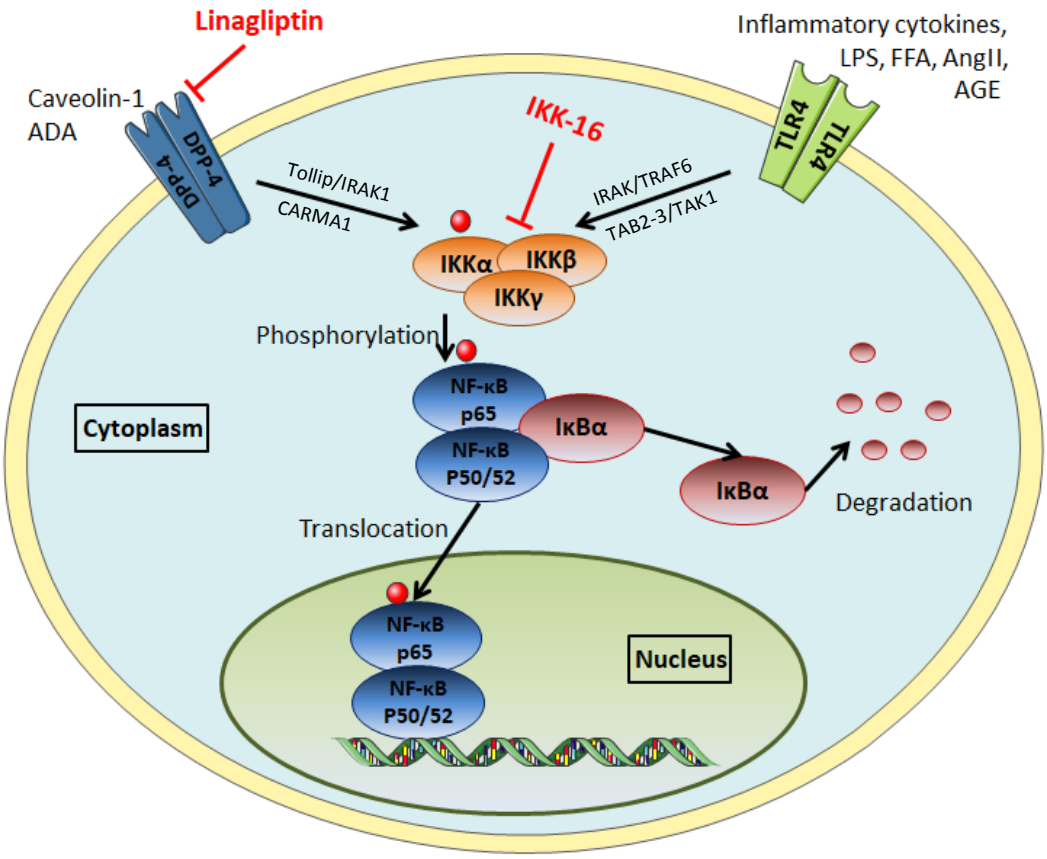

Figure 4.1 An overview of the NF-κB pathway.

Different stimuli such as pro-inflammatory cytokines, bacterial cell wall components, FFAs, AngII result in TLR 4 activation. ADA and exposed caveolin-1 activate DPP-4 receptors. TLR 4 and DPP-4 activations lead to downstream activation of the NF-κB pathway.

Recent studies of our group showed that inhibition of NF-κB with a selective IKK inhibitor (IKK-16) attenuates the multiple organ dysfunction associated with sepsis in mice without co-morbidities [291], and also attenuates the cardiac dysfunction caused by sepsis in mice with pre-existing chronic kidney disease [292]. Other studies suggest that inhibition of DPP-4 receptors by different gliptins (DPP-4 receptor inhibitors) results in less cardiac dysfunction in mice model of HFD-induced fibrosis and inflammation [220] and rat model of heart failure [221] by inhibiting the NF-κB pathway and by reducing the formation of pro-inflammatory cytokines. However, the effect of DPP-4 inhibitors on the cardiac (organ) dysfunction associated with sepsis has not yet been investigated.

Having found that HFD exacerbates the degree of cardiac dysfunction caused by sepsis in mice and augments NF-κB activation, iNOS expression and inflammatory cytokines concentrations, I have investigated the effect of NF-κB inhibition using IKK-16 or linagliptin on cardiac performance in a two-hit model of sepsis/T2DM.

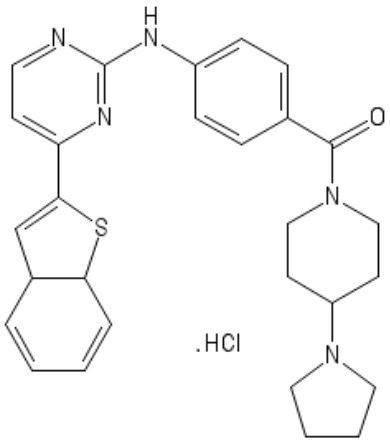

Figure 4.2 The chemical structure of IKK-16.

IKK-16 is a selective IKK inhibitor. The compound name is [N-(4-Pyrrolidin-1-ylpiperidin-1-yl-)-[4-(4-benzo[b]thiophen-2-yl-pyrimidin-2-ylamino)-phenyl]-carbox-amide hydrochloride]. Figure adapted from Waelchli *et al*., 2006.

4.2 Scientific Hypothesis and Aims

This study is driven by the hypothesis that:

- Inhibition of the NF-B pathway attenuates the cardiac dysfunction associated with endotoxaemia and CLP sepsis in mice with pre-existing T2DM

This study aims to:

- Examine the effect of IKK-16 treatment after LPS challenge and CLP surgery on cardiac dysfunction in mice with pre-existing T2DM using *in vivo* echocardiography, and
- Investigate whether pharmacological treatment with Linagliptin (Anti-diabetic and anti-inflammatory drug) is able to reduce CLP-associated cardiac dysfunction in mice with pre-existing T2DM.

4.3 Methods and Materials

4.3.1 Animals

Studies in this chapter were conducted on 68 ten-week-old male C57BL/6 mice (Charles River, Kent, UK) weighing 25-30g, receiving a standard diet and water *ad libitum* (before starting the experiments). Mice were housed 5 per cage in a temperature-controlled room with a 12-hour light/dark cycle. Thirty mice were used in the first experiment to study the effect of IKK-16 treatment on cardiac dysfunction after LPS challenge and 38 mice were used in the second experiment to study the effect of IKK-16 or linagliptin treatments on cardiac dysfunction after CLP surgery. The ethical statement is provided in section 2.3.

4.3.2 Model of HFD induced T2DM and diabetic cardiomyopathy

In this model of HFD induced T2DM and diabetic cardiomyopathy, ten-week-old male C57BL/6 mice were randomised to receive HFD (≈ 60% energy from fat) or normal chow diet with free access to water for 12 weeks.

4.3.3 Baseline Measurements for development of T2DM

During the whole 12-week period, body weight and feeding behaviour were measured weekly to ensure healthy feeding behaviour as described in section 2.3.2. During week 12, OGTT was measured in all mice to ensure the development of impairment in glucose tolerance as described in section 2.3.3, baseline echocardiography was conducted in all mice to test the development of diabetic cardiomyopathy as described in section 2.3.6, urine samples were collected from

all mice to measure CrCl as described in section 2.3.7 and blood were collected from all mice from the tail vein to measure baseline urea, creatinine and ALT as described in section 2.3.9.

4.3.4 Model of lipopolysaccharide (LPS) induced endotoxaemia

At 12 weeks after starting the HFD, mice were randomised to receive low dose LPS (2 mg/kg, i.p.) or vehicle (PBS 5 ml/kg, i.p.). At 1 h after LPS, mice were randomised to receive IKK-16 (1 mg/kg, i.v.) or vehicle (2% DMSO, 3 ml/kg, i.v.). At 18 h after the onset of endotoxaemia, mice were anaesthetised for cardiac function assessment using *in vivo* echocardiography. As a terminal procedure, mice were anaesthetised using high dose isoflurane (3 % delivered in 0.9 L/min O_2) before being sacrificed. Blood samples were collected by cardiac puncture and vital organs were collected and snap frozen using liquid nitrogen then stored for further analysis at -80°C freezer.

4.3.5 Model of caecal ligation and puncture (CLP) induced polymicrobial sepsis

At 12 weeks after starting the HFD, mice were randomised to undergo either sham or CLP surgery. Polymicrobial sepsis was induced by caecal ligation and double puncture using 18 G needle. Mice received analgesia (buprenorphine, 0.05 mg/kg i.p.) and antibiotic (imipenem/cilastatin, 20 mg/kg s.c.) dissolved in the resuscitation fluid (0.09% NaCl, 15 ml/kg s.c.). Detailed surgery is described in section 3.3.5. At 1 h after CLP surgery, mice randomised to receive IKK-16 (1 mg/kg, i.v.), linagliptin (10 mg/kg, i.v.) or vehicle (2% DMSO, 3 ml/kg, i.v.). At 24 h, mice were anaesthetised for assessment of cardiac function *in vivo*. As a

terminal procedure, mice were anaesthetised using high dose isoflurane (3 % delivered in 0.9 L/min O_2) before being sacrificed. Blood samples were collected by cardiac puncture and vital organs were collected and snap frozen using liquid nitrogen then stored for further analysis at -80°C freezer. Mice underwent sham surgery were not subjected to perforation of the cecum, but otherwise treated the same.

4.3.6 Measuring physical activity and vital signs

At 18 h after LPS challenge and 24 h after CLP surgery, physical activity and vital signs were measured as described in section 3.3.6.

4.3.7 Quantification of organs dysfunction

Cardiac functions was assessed at 18 h after LPS challenge and at 24 h after CLP surgery using a 30 MHz RMV707B scan head and a Vevo-770 imaging system (VisualSonics, Toronto, Ontario, Canada) as described in section 2.3.6. Blood samples and vital organs were collected to measure organs dysfunction as described in sections 2.3.8.

4.3.8 Western blot analysis

Immunoblot analyses of heart tissues were carried out using a semi-quantitative western blotting. I measured the degree of phosphorylation of IKK, IκBα and Akt, nuclear translocation of p65 NF-κB subunit to the nucleus and iNOS expression. Detailed procedure is described in section 3.3.8.

4.3.9 Cytokines measurements using multiplex method

Serum cytokines levels (TNF-α, IL-6, KC and IL-10) were measured using a bead-based immunoassay method. Serum samples were prepared and handled following manufacturer instructions (Biolegend®, San Diego, USA). Data was obtained using a LSR Fortessa (Biociences®, Berkshire, UK) and analysed using the Legendplex^{TM} 7.1.0.0 software. Detailed procedure is described in section 3.3.9.

4.3.10 Measuring MPO activity in the lung

MPO was extracted from the lung tissues according to the methods described by Barone et al. in 1991 [293] with slight modifications to measure neutrophil accumulation in the lungs. MPO activity was presented as the quantity of the enzyme that degrades 1 μmol of peroxide/min at 25 °C and expressed as micro-unit/gram of the lung tissue. The detailed protocol is described in section 3.3.10.

4.3.11 Measuring NAG activity in the lung

NAG activity was analysed to measure macrophages accumulation in the lungs using a NAGase ELISA kit following manufacturer instructions (Elabscience®, Houston, Texas, USA). The detailed procedure is descriped in section 3.3.11.

4.3.12 Statistical analysis

Data was analysed using GraphPad Prism 7.0 (GraphPad Software, San Diego, California, USA). Values stated in the text and figures are presented as a mean ± standard error of the mean (SEM) of n observations, where n is the number of animals used. Data was tested for normality using D'Agostino-Pearon normality

test and then assessed using using One-way ANOVA test followed by Bonferroni's post hoc test. *P* values of less than 0.05 were considered to be statically significant.

4.3.13 Materials

Unless otherwise stated, all materials, reagents and solutions were purchased from Sigma-Aldrich Ltd (Poole, Dorset, UK).

4.4 Experimental Designs and Studies Groups

4.4.1 Effect of IKK-16 treatment on cardiac dysfunction associated with endotoxaemia in mice with T2DM

At 12 weeks after dietary manipulation, mice were randomised into 3 groups (Table 4.1) to study the effect of IKK inhibition on the cardiac (organ) dysfunction associated with endotoxaemia.

Table 4.1 Experimental groups used to study the effect of IKK-16 treatment on cardiac dysfunction after a low dose LPS challenge in mice with pre-existing T2DM.

Group name	Diet	Intervention	Treatment	Number
HFD	High fat	PBS 5ml/kg i.p.	2 % DMSO	10
HFD+LPS	High fat	LPS 2mg/kg i.p.	2 % DMSO	10
HFD+LPS+IKK-16	High fat	LPS 2mg/kg i.p.	1 mg/kg IKK-16	10

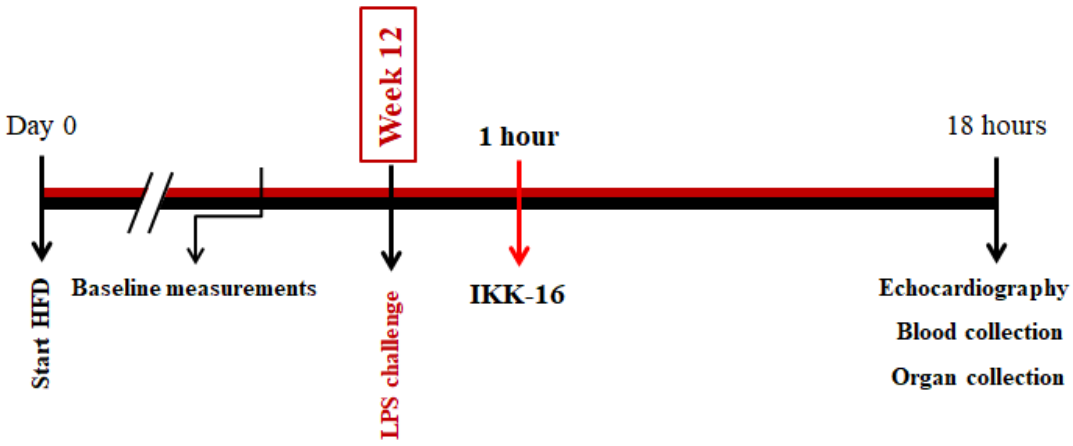

Figure 4.3 Timeline and summary of the protocol used to study the effect of IKK-16 treatment on the cardiac dysfunction after low dose LPS challenge in mice with pre-existing T2DM.

At 12 weeks after dietary manipulation, mice were tested for development of diabetes phenotype. Mice were then challenged with either low dose LPS (2 mg/kg, i.p.) or vehicle (5 ml/kg PBS, i.p.). At 1 h, mice were treated with IKK-16 or vehicle. At 18 h after LPS, cardiac function was assessed using *in vivo* echocardiography.

4.4.2 Effect of IKK-16 or linagliptin treatments on cardiac dysfunction associated with CLP induced polymicrobial sepsis in mice with pre-existing T2DM

At 12 weeks after dietary manipulation, mice were randomised into 4 groups (Table 4.2) to study the effect of NF-κB inhibition on the cardiac (organ) dysfunction associated with CLP-sepsis.

Table 4.2 Experimental groups used to study the effect of IKK-16 or linagliptin treatments on cardiac dysfunction after CLP sepsis in mice with pre-existing T2DM.

Group name	Diet	Intervention	Treatment	Number
HFD+sham	HFD	Sham	2 % DMSO	8
HFD+CLP	HFD	CLP	2 % DMSO	10
HFD+CLP+IKK-16	HFD	CLP	1 mg/kg IKK-16	10
HFD+CLP+linagliptin	HFD	CLP	10 mg/kg linagliptin	10

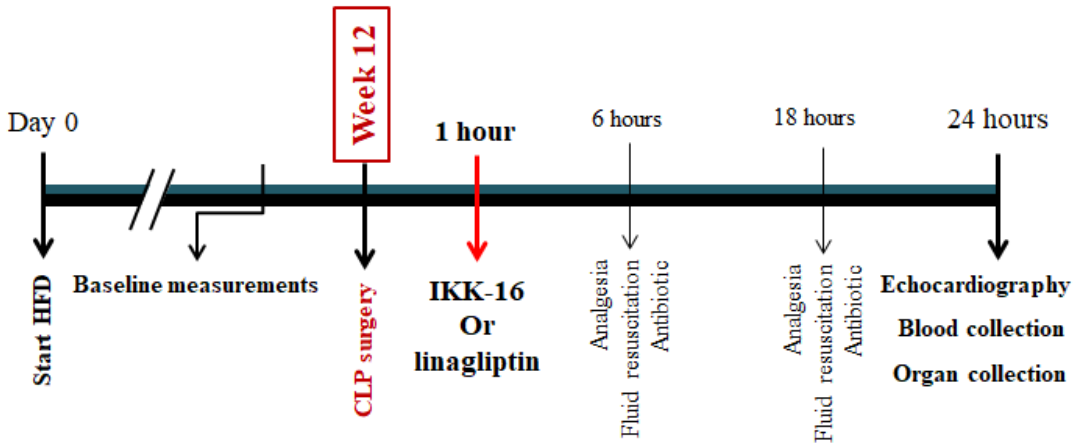

Figure 4.4 Timeline and summary of the protocol used to study the effect of IKK-16 or linagliptin treatment on cardiac dysfunction after CLP surgery in animals with pre-existing T2DM.

At 12 weeks after dietary manipulation, mice were tested for development of diabetes phenotype. Mice were then subjected to either CLP or sham surgery. At 1 h, mice were treated with IKK-16, linagliptin or vehicle. At 6 and 18 h, mice received analgesia, antibiotic and fluid resuscitation. At 24 h after CLP surgery, cardiac function was assessed using *in vivo* echocardiography.

4.5 Results

4.5.1 LPS model of endotoxaemia in mice with pre-existing T2DM

1. IKK-16 improves the physical activity and stabilise heart rate after LPS challenge

When compared to mice on HFD challenged with vehicle, HFD fed mice challenged with LPS showed significant reduction in the core body tempreture, baseline heart rate and physical activity at 18 h after the LPS challenge ($P<0.05$, Figure 4.5). When compred to HFD fed mice challenged with LPS and treated with vehicle, treatment with IKK-16 (at 1 h) significantly increased the physical activity and baseline heart rate at 18 h after the LPS challenge ($P<0.05$, Figure 4.5). However, Treatment with IKK-16 after LPS challenge did not improve the core body temperature when compred to mice challenged with LPS and treated with vehicle ($P>0.05$, Figure 4.5). It should be noted that at the beginning of the measurements, and after stabilising the animals, there was no significant difference in the core body tempreture and heart rate between the three groups.

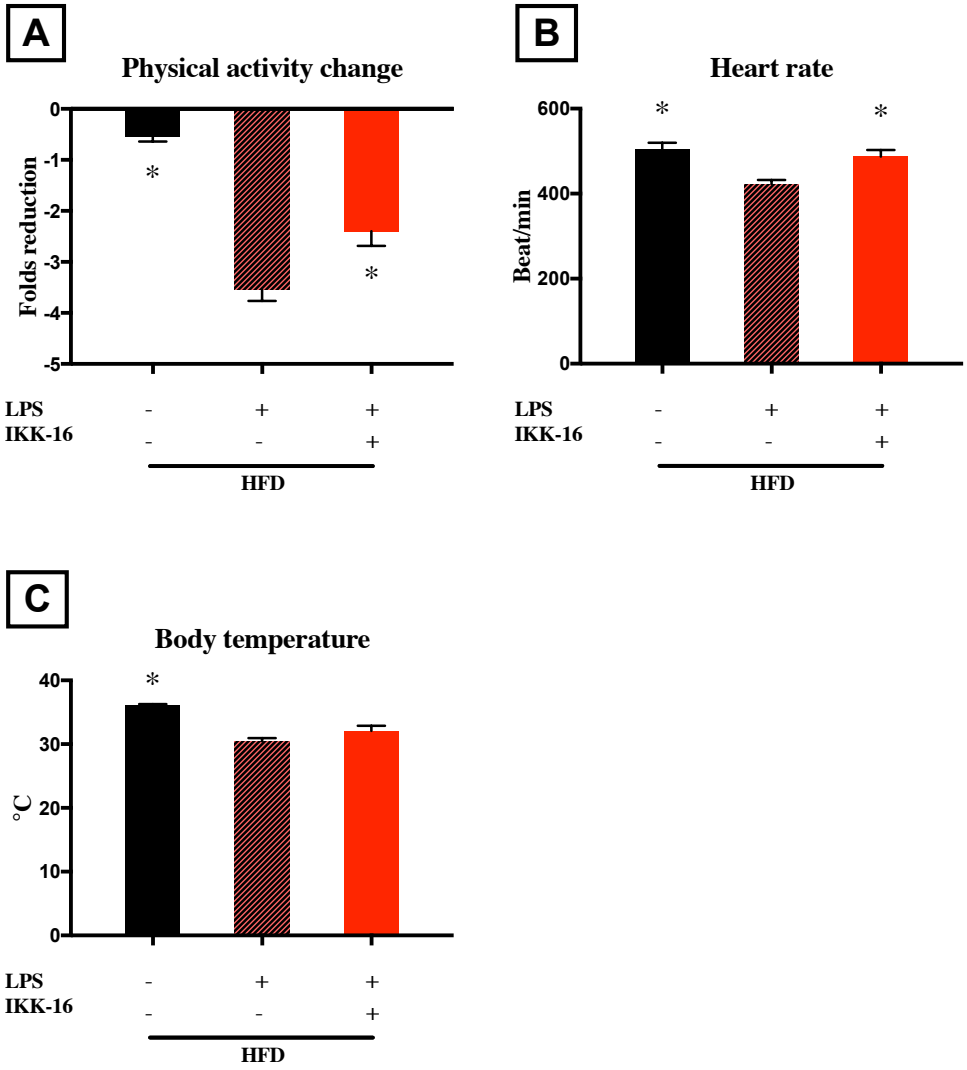

Figure 4.5 Effect of IKK-16 treatment on physical activity and vital signs after low dose LPS challenge in mice with T2DM.
Physical activity and vital signs were assessed at 18 h after LPS challenge. **(A)** Physical activity change **(B)** heart rate and **(C)** body temperature. Data were analysed using one-way ANOVA followed by Bonferroni's post hoc test and expressed as mean ± SEM. **P*< 0.05 compared to LPS+vehicle group (n=10 per group).

2. IKK-16 attenuates cardiac dysfunction associated with endotoxaemia cause by a low dose of LPS in mice with pre-existing T2DM

When compared to mice on HFD challenged with vehicle, mice on HFD challenged with low dose LPS (2 mg/kg i.p.) showed significant reduction in systolic cardiac contractility ($P<0.05$, Figure 4.6 B-D). The degree of cardiac dysfunction was significantly attenuated by treatment of HFD/LPS-mice with IKK-16 (1 h after LPS challenge) ($P<0.05$, Figure 4.6 B-D).

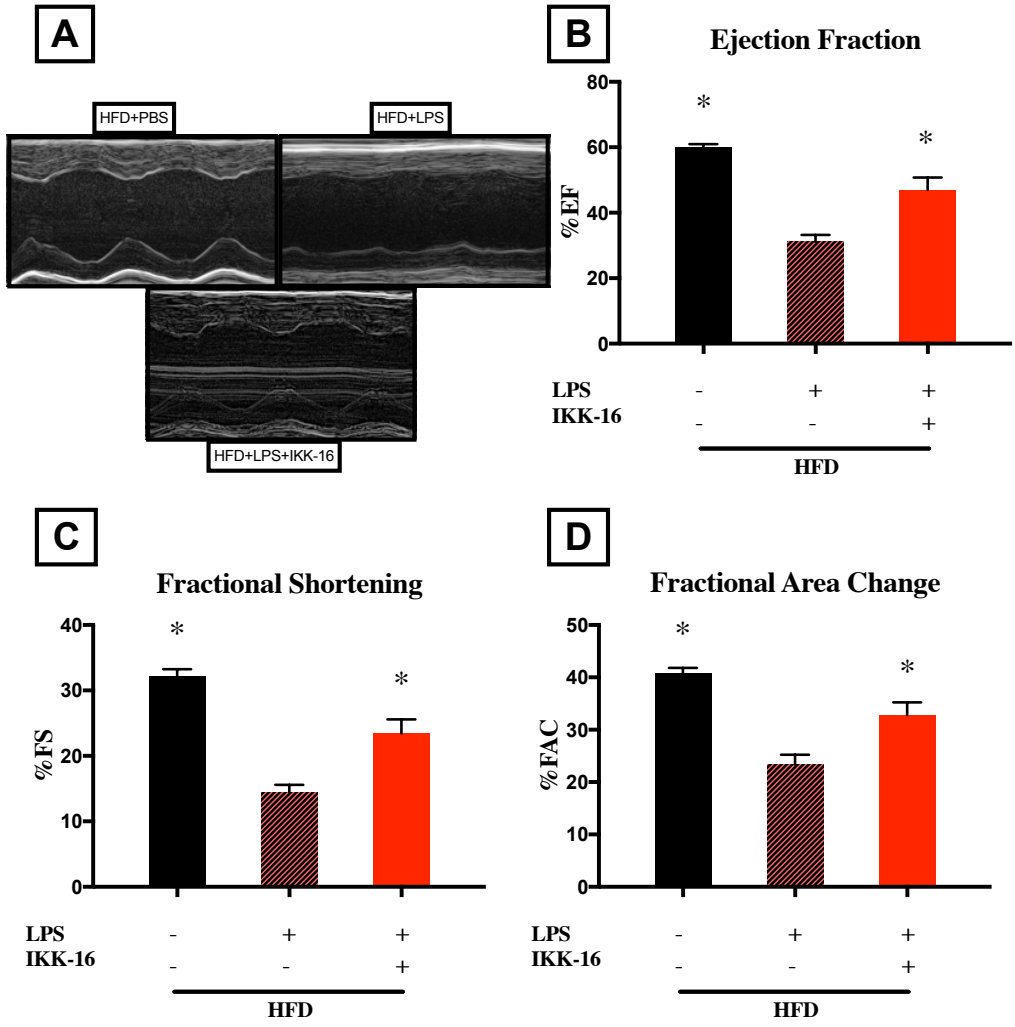

Figure 4.6 Effect of IKK-16 treatment at 1 hour after LPS challenge on cardiac function in mice with pre-existing T2DM.

Mice fed a HFD were challenged with low dose LPS (2 mg/kg i.p.) or PBS (5 ml/kg i.p.). At 1 h, mice challenged with LPS were treated with IKK-16 (1 mg/kg i.v.) or vehicle (2 % DMSO i.v.). Cardiac function was assessed at 18 h. **(A)** Representative M-mode echocardiograms, percentage % **(B)** EF, **(C)** FS and **(D)** FAC. Data was analysed using one-way ANOVA followed by Bonferroni's post hoc test and expressed as mean ± SEM. **P*< 0.05 compared to HFD+LPS group (n=10 per group).

3. Effect of IKK-16 post treatment on NF-κB signalling pathway in mice with pre-existing T2DM challenged with low dose LPS.

In a separate set of experiments, I investigated the effects of IKK-16 on the activity of key signalling pathways including pathways leading to the activation of NF-κB. When compared to cardiac biopsies obtained from mice fed a HFD and challenged with vehicle, challenging the mice on HFD with LPS did not have a significant effect on the phosphorylation of IKKα/β or IκBα ($P>0.05$; Figure 4.7 A-B). When compared to mice fed a HFD and challenged with vehicle, challenge of mice on HFD with LPS did, however, result in significant increases in a) the translocation of p65 NF-κB to the nucleus and b) iNOS expression ($P<0.05$; Figure 4.7 C-D). The degree of a) the IKKα/β phosphorylation, b) IκBα phosphorylation, c) the translocation of p65 NF-κB to the nucleus and d) iNOS expression was significantly attenuated by treatment of HFD/LPS-mice with IKK-16 (1 h after LPS challenge) ($P<0.05$; Figure 4.7 A-D).

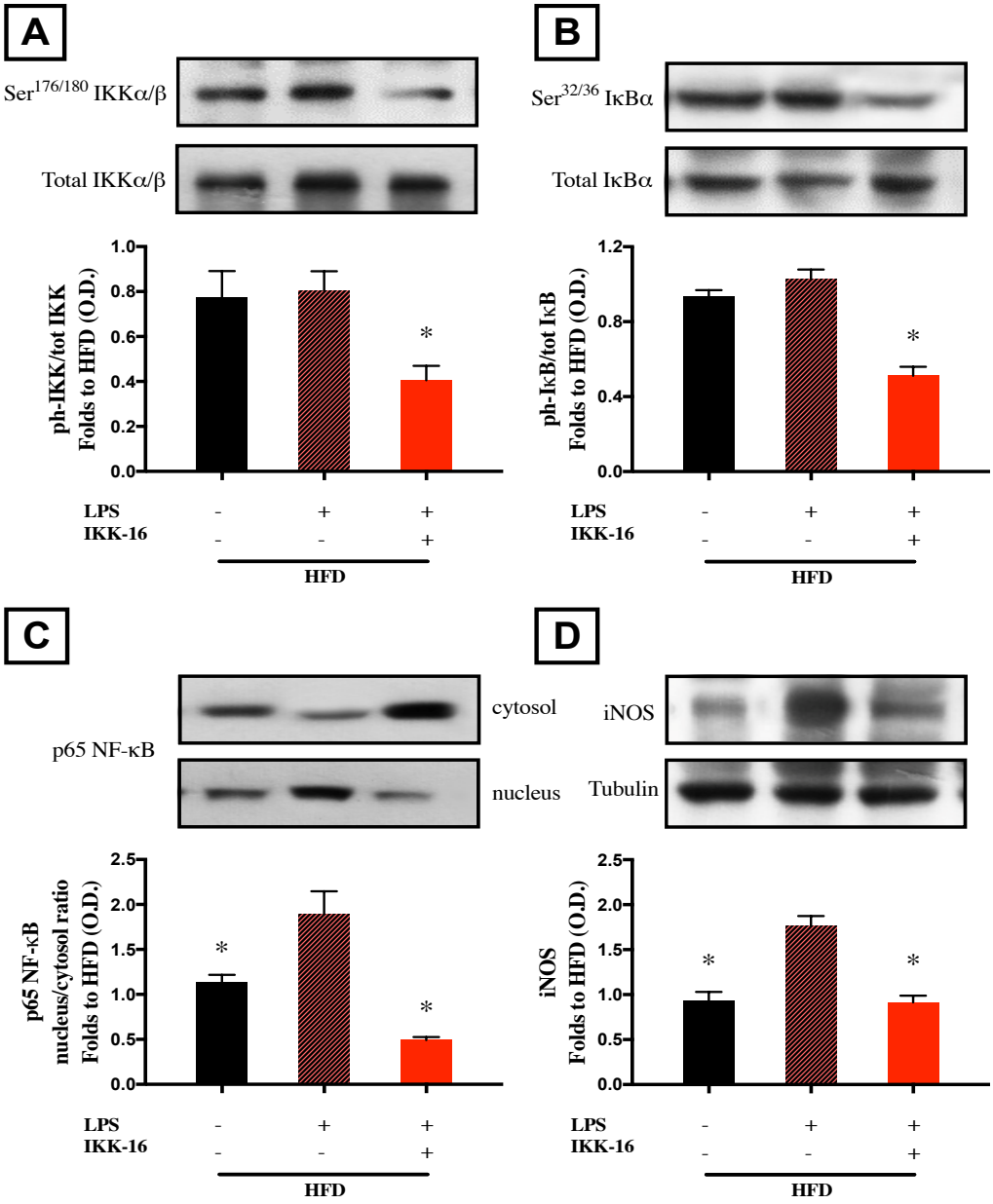

Figure 4.7 Effect of IKK-16 post-treatment on NF-κB signalling pathway in the heart of mice with pre-existing T2DM and challenged with low dose LPS.

Mice fed a HFD were challenged with low dose LPS (2 mg/kg i.p.) or PBS (5 ml/kg i.p.). At 1h, mice challenged with LPS were treated with IKK-16 (1 mg/kg i.v.) or vehicle (2 % DMSO i.v.). At 18 h, heart samples were collected and signalling events were assessed. Densitometry analysis of the bands is expressed as relative optical density (O.D.) of **(A)** IKKα/β phosphorylation on $Ser^{178/180}$ corrected to the corresponding total IKKα/β content; **(B)** IκBα phosphorylation on $Ser^{32/36}$ corrected to the corresponding total IκBα content; **(C)** NF-κB p65 subunit levels in both, cytosolic and nuclear fractions expressed as a nucleus/cytosol ratio; **(D)** Inducible nitric oxide synthase (iNOS) expression corrected for the corresponding tubulin band. All bands were normalised using the related HFD band. Data was analysed using one-way ANOVA followed by Bonferroni's post hoc test and expressed as mean ± SEM. **P*<0.05 compared to HFD+LPS group. (n=3-5 per group).

4. Effect of IKK-16 post treatment on Akt phosphorylation in mice with pre-existing T2DM challenged with low dose LPS.

When compared to cardiac biopsies obtained from HFD-fed mice challenged with vehicle, cardiac tissue obtained from mice fed a HFD and challenge with LPS did not result in a significant change in Akt phosphorylation on Ser^{473} (P>0.05; Figure 4.8). In contrast, the degree of Akt phosphorylation on Ser^{473} was significantly higher (and therefore restored) by treatment of HFD/LPS-mice with IKK-16 (1 h after LPS challenge) (P<0.05; Figure 4.8).

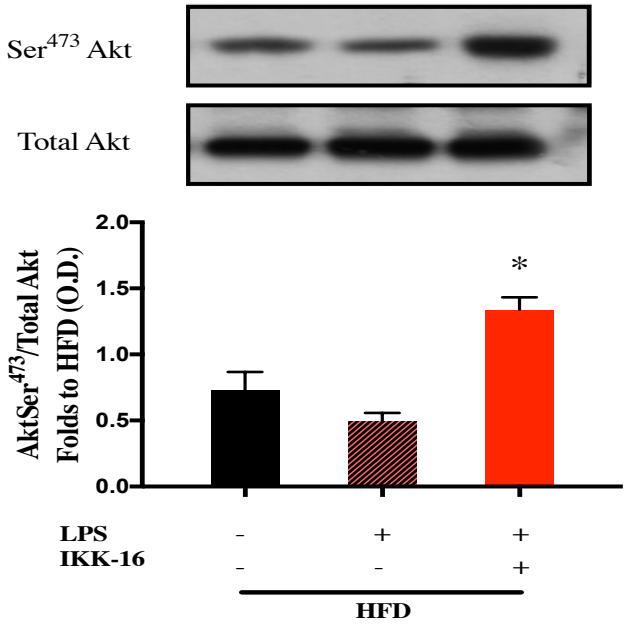

Figure 4.8 Effect of IKK-16 post-treatment on Akt phosphorylation in the heart of mice with pre-existing T2DM and challenged with low dose LPS (2mg/kg).

Mice fed a HFD were challenged with low dose LPS (2 mg/kg i.p.) or PBS (5 ml/kg i.p.). At 1h, mice challenged with LPS were treated with IKK-16 (1 mg/kg i.v.) or vehicle (2 % DMSO i.v.). At 18 h, heart samples were collected and signalling events were assessed. Densitometry analysis of the bands is expressed as relative optical density (O.D.) of phosphorylated Akt on Ser^{473} corrected for the corresponding total Akt content and normalized using the related HFD band. Data was analysed using one-way ANOVA followed by Bonferroni's post hoc test and expressed as mean ± SEM. *P<0.05 compared HFD+LPS group. (n=3-5 per group).

5. Effect of IKK-16 post tretment on the severity of kidney dysfunction and hepatocelleular injury in mice with pre-existing T2DM challenged with low dose LPS

When compared to mice fed a HFD and challenged with vehicle, mice fed a HFD and challenged with low dose LPS exhibited a large and significant increase in serum urea, creatinine, and ALT ($P<0.05$, Figure 4.9 A-C). Post treatment with IKK-16, however, did not result in significant changes in urea, creatinine or ALT levels in the serum compared to mice on HFD challenged with low dose LPS and treated with vehicle ($P>0.05$, Figure 4.9 A-C).

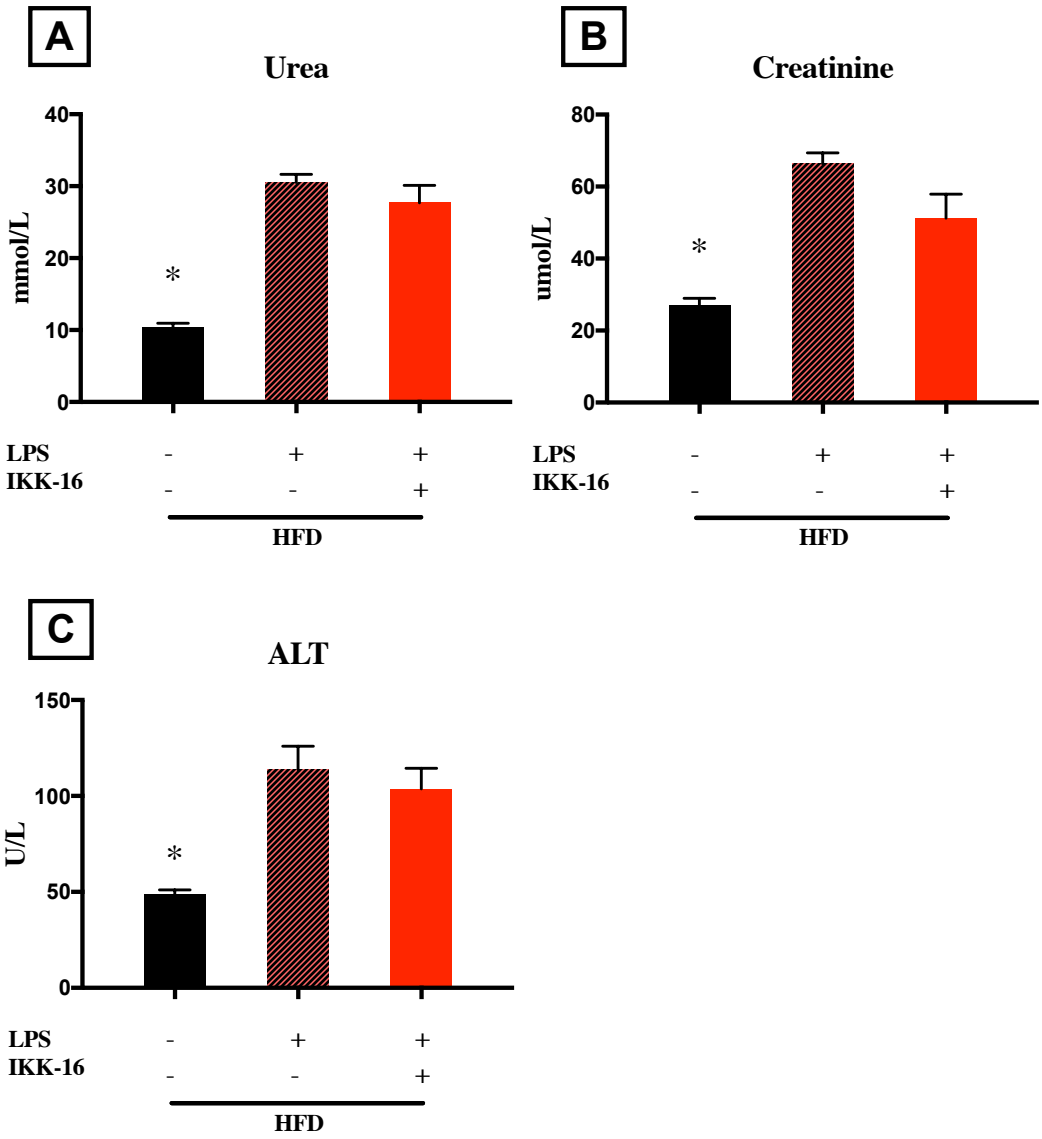

Figure 4.9 Effect of IKK-16 treatment on the severity of renal dysfunction and hepatocelleular injury in mice with pre-existing T2DM challenged with LPS.

Mice fed a HFD were challenged with low dose LPS (2 mg/kg i.p.) or PBS (5 ml/kg i.p.). At 1h, mice challenged with LPS were treated with IKK-16 (1 mg/kg i.v.) or vehicle (2 % DMSO i.v.). At 18 h, blood samples were collected and serum **(A)** urea, **(B)** creatinine and **(C)** ALT levels were measured. Data was analysed using one-way ANOVA followed by Bonferroni's post hoc test and expressed as mean ± SEM. **P*<0.05 compared to HFD+LPS group. (n=10 per group).

6. Effect of IKK-16 post tretment on neutrophils and macrophages infiltration to the lungs in mice with pre-existing T2DM challenged with low dose.

When compared to mice fed a HFD and challenged with vehicle, mice fed a HFD and challenged with low dose LPS exhibited large and significant increases in MPO and NAG activities in the lung (P<0.05, Figure 4.10 A-B). Post treatment with IKK-16, resulted in significant reduction in the MPO and NAG avtivities in the lungs compared to mice on HFD challenged with low dose LPS and treated with vehicle (P<0.05, Figure 4.10 A-B).

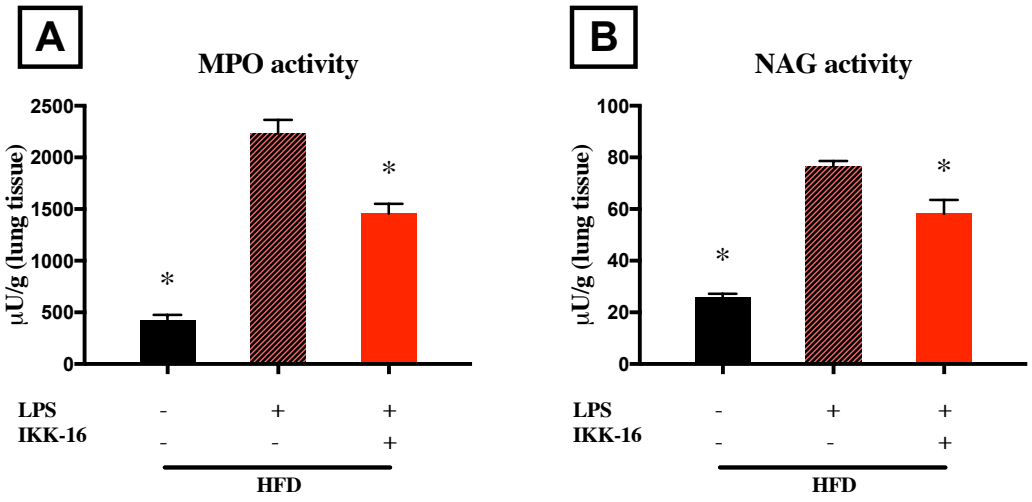

Figure 4.10 Effect of IKK-16 treatment on neutrophil/macrophage infiltration (lung) in mice with pre-existing T2DM challenged with LPS.

Mice fed a HFD were challenged with low dose LPS (2 mg/kg i.p.) or PBS (5 ml/kg i.p.). At 1h, mice challenged with LPS were treated with IKK-16 (1 mg/kg i.v.) or vehicle (2 % DMSO i.v.). At 18 h, lungs were collected and **(A)** MPO and **(B)** NAG activities were measured. Data was analysed using one-way ANOVA followed by Bonferroni's post hoc test and expressed as mean ± SEM. *P<0.05 compared to HFD+LPS group. (n=6 per group).

7. Effect of IKK-16 post tretment on serum inflammatory cytokines in mice with pre-existing T2DM challenged with low dose LPS.

When compared to mice fed a HFD and challenged with vehicle, mice fed a HFD and challenged with low dose LPS exhibited large and significant increases in TNF-α, IL-6, KC and IL-10 concentrations in the serum ($P<0.05$, Figure 4.11 A-D). Post treatment with IKK-16, resulted in significant reduction in the TNF-α, IL-6, KC levels when compared to mice on HFD challenged with low dose LPS and treated with vehicle ($P<0.05$, Figure 4.11 A-C). However, Treatment with IKK-16 did not result in reduction in IL-10 concentration in the serum when compared to vehicle treatement after LPS challenge in diabetic mice ($P>0.05$, Figure 4.11 D).

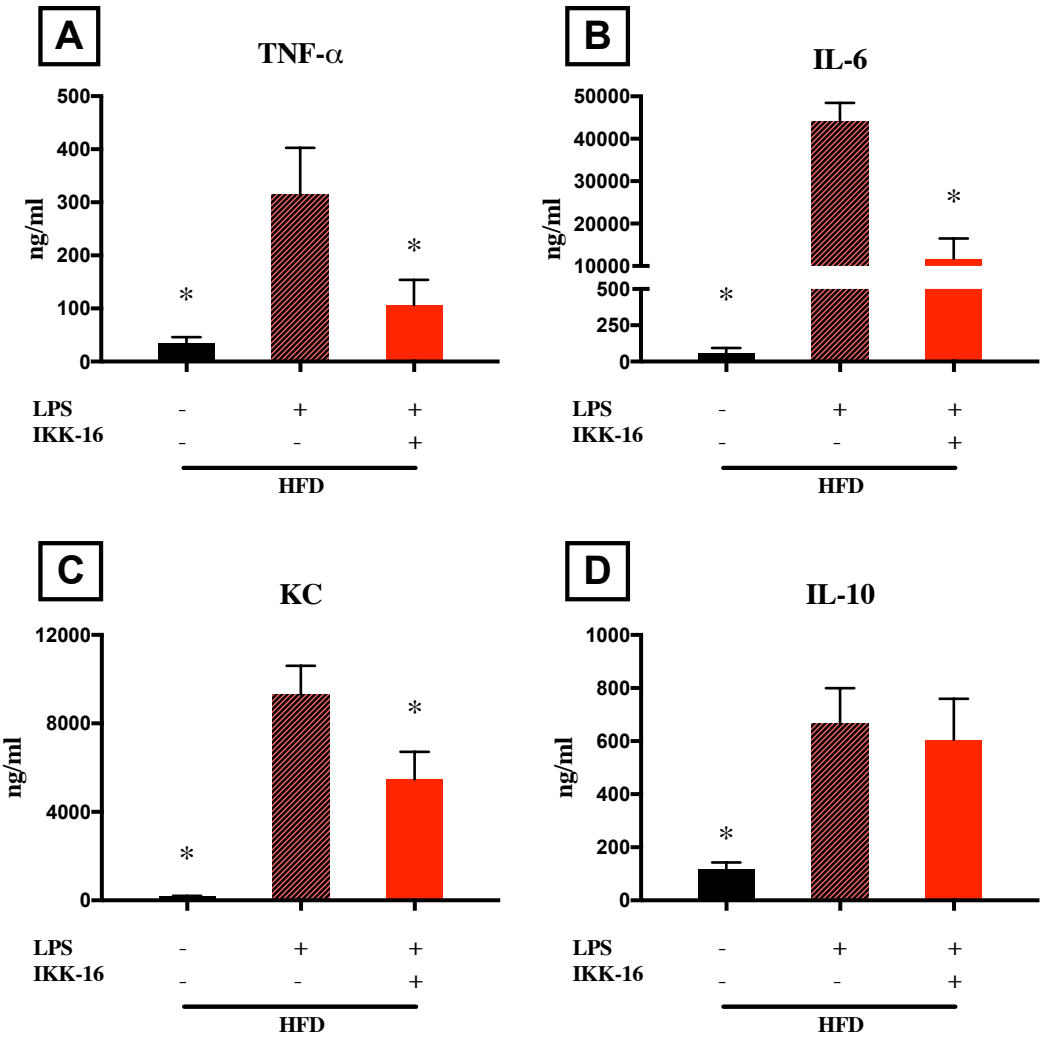

Figure 4.11 Effect of IKK-16 treatment on serum inflammatory cytokines in mice with pre-existing T2DM challenged with LPS.

Mice fed a HFD were challenged with low dose LPS (2 mg/kg i.p.) or PBS (5 ml/kg i.p.). At 1 h, mice challenged with LPS were treated with IKK-16 (1 mg/kg i.v.) or vehicle (2 % DMSO i.v.). At 18 h, blood samples were collected and inflammatory cytokines concentrations were measured in the serum. **(A)** TNF-α, **(B)** IL-6, **(C)** KC and **(D)** IL-10. Data was analysed using one-way ANOVA followed by Bonferroni's post hoc test and expressed as mean ± SEM. **P*<0.05 compared to HFD+LPS. (n=4 per vehicle group and n=6-8 per LPS group).

4.5.2 CLP model of polymicrobial sepsis in mice with pre-existing T2DM

1. Effect of IKK-16 or linagliptin treatments on the physical activity, heart rate and body temperature after CLP sepsis

When compared to mice on HFD subjected to sham surgery, HFD-fed mice subjected to CLP surgery showed significant reduction in the core body tempreture, baseline heart rate and physical activity at 24 h after the surgery (P<0.05, Figure 4.12). When compred to HFD fed mice subjected to CLP and treated with vehicle, treatment with IKK-16 or linagliptin (at 1 h) significantly increased body tempreture, baseline heart rate and physical activity at 24 h after the CLP surgery (P<0.05, Figure 4.12). It should be noted that at the beginning of the measurements, and after stabilising the animals, there was no significant difference in the core body tempreture or heart rate between the four groups.

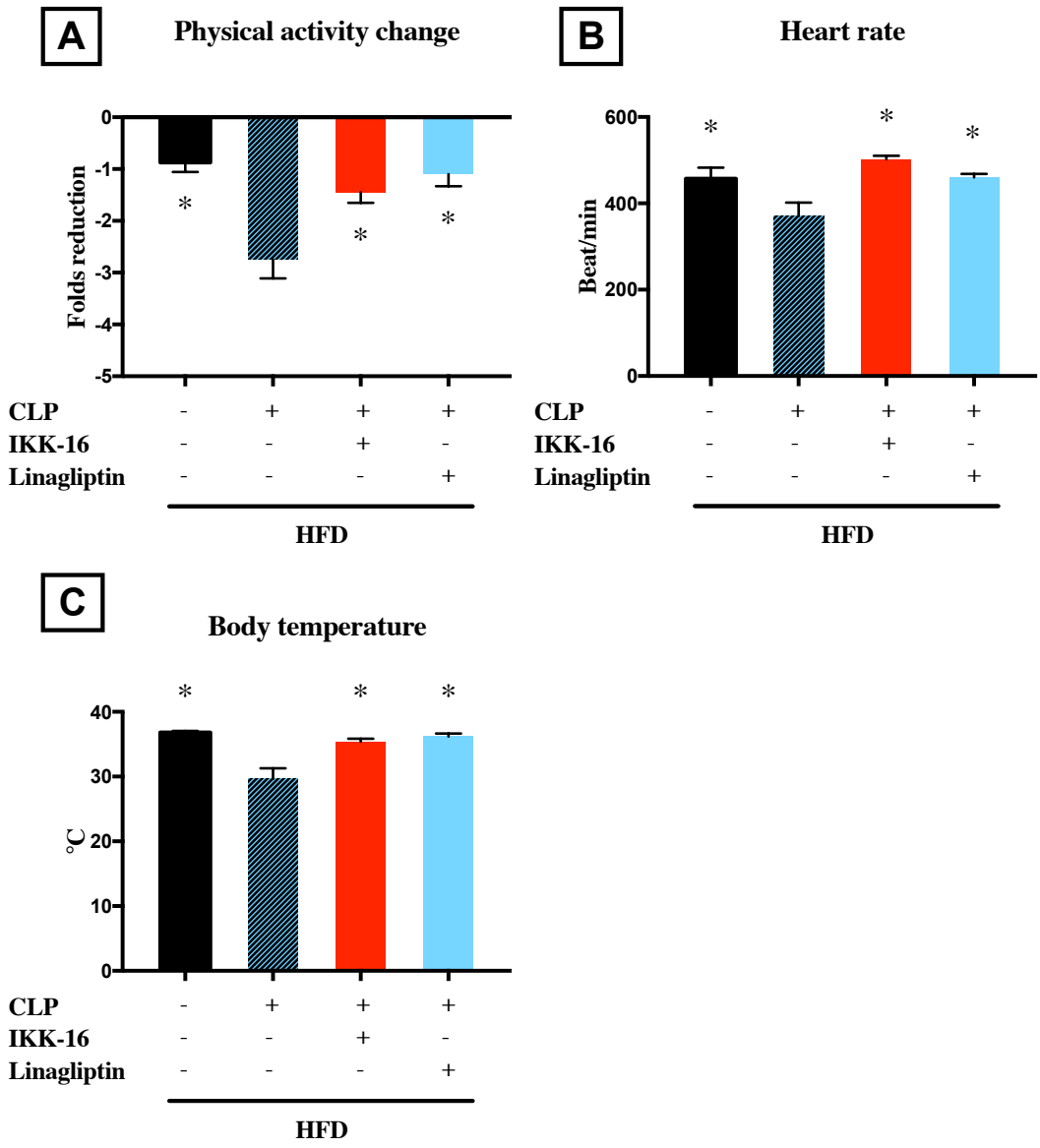

Figure 4.12 Effect of IKK-16 or linagliptin treatments on the physical activity and the vital signs after CLP surgery in mice with T2DM.

Physical activity and vital signs were assessed at 24 h after CLP surgery. **(A)** Physical activity change **(B)** heart rate and **(C)** body temperature. Data were analysed using one-way ANOVA followed by Bonferroni's post hoc test and expressed as mean ± SEM. **P*<0.05 compared to the HFD+CLP group (n=8-10 per group).

2. Treatments with IKK-16 or linagliptin attenuate cardiac dysfunction associated with the polymicrobial sepsis in mice with pre-existing T2DM

When compared to mice on HFD subjected to sham surgery, mice on HFD subjected to CLP surgery showed significant depression in systolic cardiac function ($P<0.05$, Figure 4.13 B-D). The degree of cardiac dysfunction was significantly attenuated by treatment of HFD/CLP-mice with IKK-16 or linagliptin (1 h after CLP surgery) ($P<0.05$, Figure 4.13 B-D).

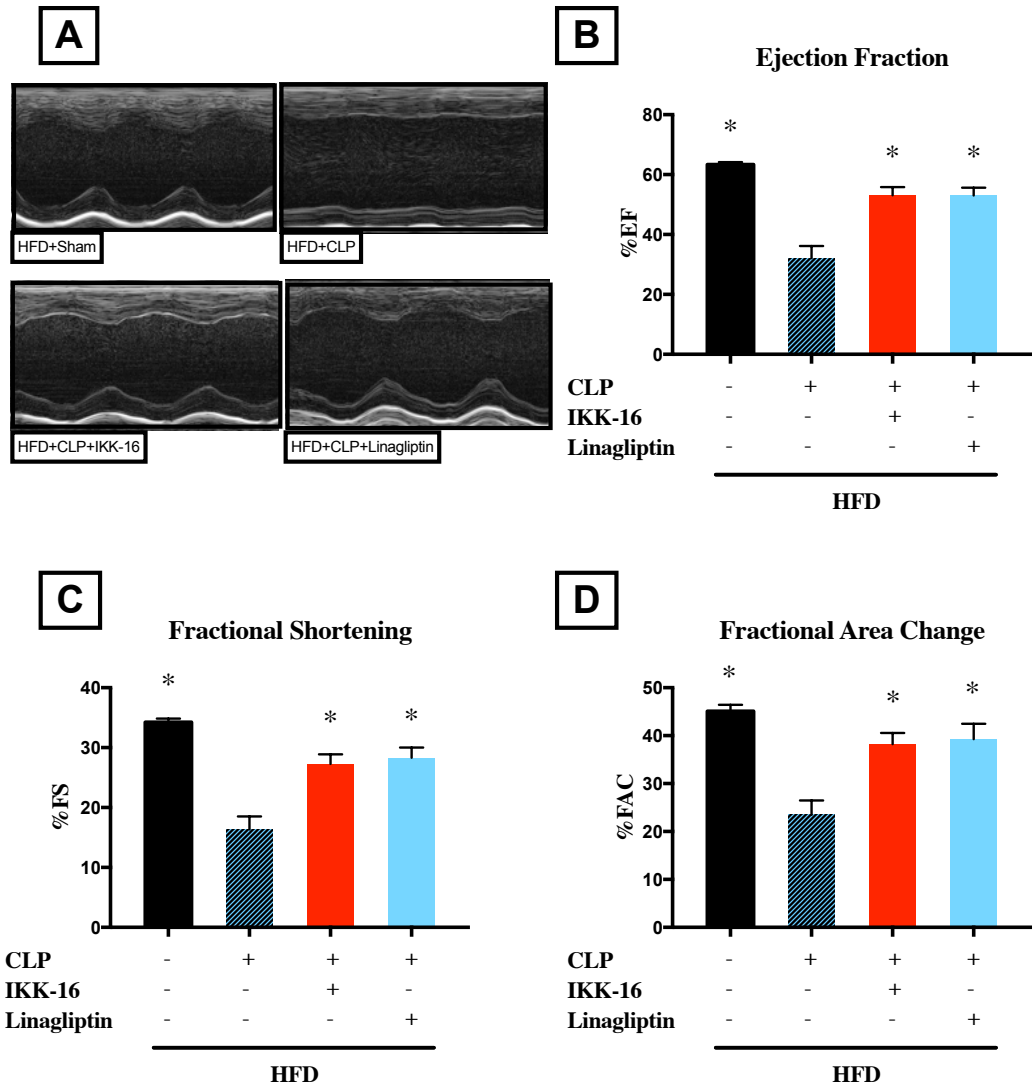

Figure 4.13 Effect of IKK-16 or linagliptin treatments 1 hour after CLP surgery on cardiac function in mice with pre-existing T2DM.

Mice on HFD were subjected to CLP or sham surgery. At 1 h, mice subjected to CLP surgery were treated with IKK-16 (1mg/kg i.v.), linagliptin (10 mg/kg i.v.) or vehicle (2% DMSO i.v.). Cardiac function was assessed at 24 h. **(A)** Representative M-mode echocardiograms, percentage % **(B)** EF, **(C)** FS and **(D)** FAC. Data was analysed using one-way ANOVA followed by Bonferroni's post hoc test and expressed as mean ± SEM. * $P<0.05$ compared to HFD+CLP group. (n=8-10 per group).

3. Effect of IKK-16 or linagliptin post treatment on the NF-κB signalling pathway in mice with pre-existing T2DM underwent CLP surgery.

In a separate set of experiments, I investigated the effects of IKK-16 and linagliptin on the activity of key signalling pathways including pathways leading to the activation of NF-κB. When compared to cardiac biopsies obtained from mice fed a HFD and subjected to sham surgery, subjecting the mice on HFD to CLP surgery resulted in significant increase in a) the phosphorylation of IKKα/β on $Ser^{178/180}$, b) the phosphorylation of IκBα on $Ser^{32/36}$, c) the translocation of p65 NF-κB to the nucleus, and d) increased expression of iNOS ($P<0.05$; Figure 4.14 A-D). The degree of a) the IKKα/β phosphorylation, b) IκBα phosphorylation, c) the translocation of p65 NF-κB to the nucleus and d) iNOS expression were significantly attenuated by treatment of HFD/CLP-mice with IKK-16 or linagliptin (1 h after CLP surgery) ($P<0.05$; Figure 2.23 A-D).

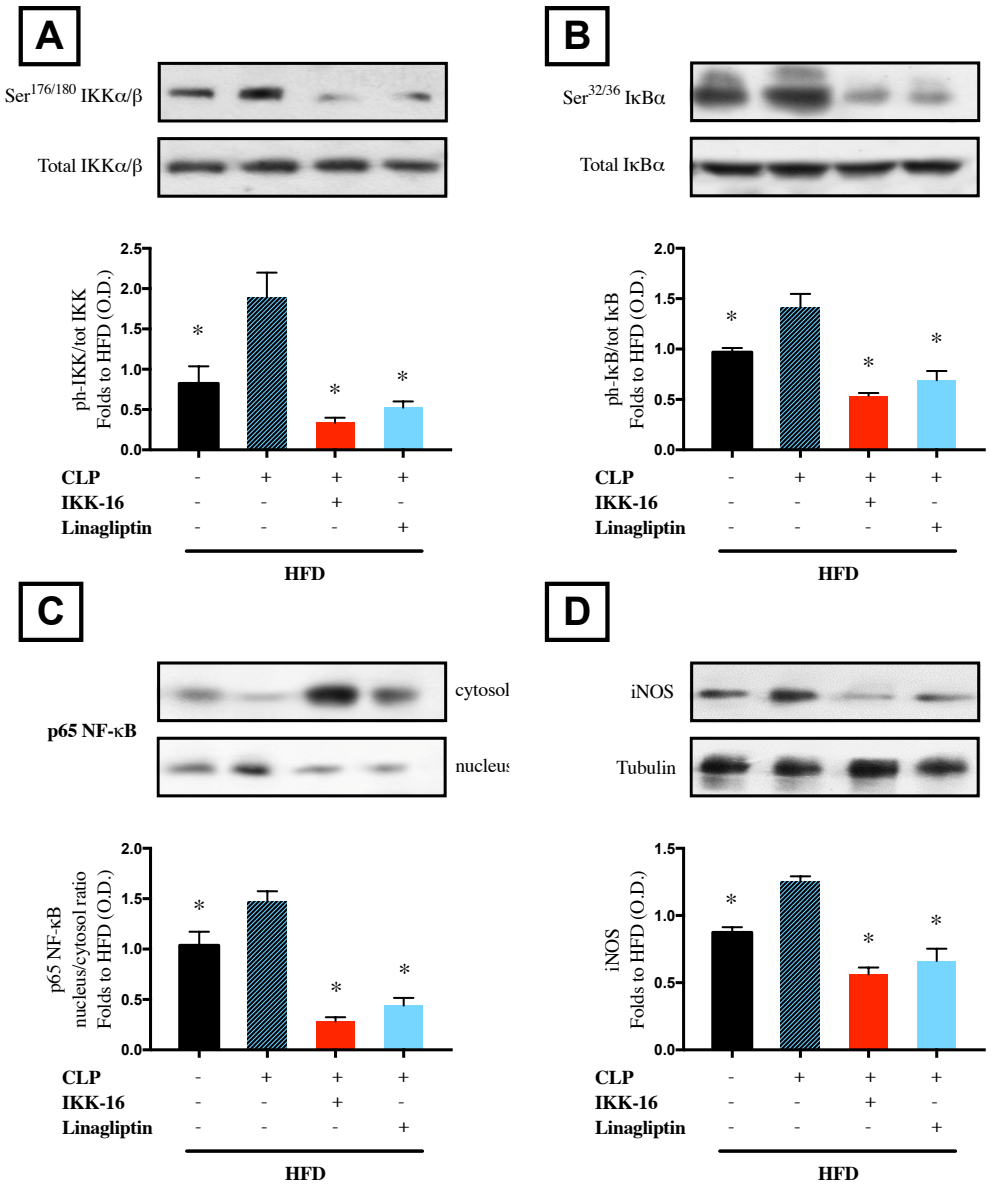

Figure 4.14 Effect of IKK-16 or linagliptin post-treatment on NF-κB signalling pathway in the heart of mice with pre-existing T2DM that were subjected to CLP surgery.

Mice on HFD were subjected to CLP or sham surgery. At 1 h, mice subjected to CLP surgery were treated with IKK-16 (1 mg/kg i.v.), linagliptin (10 mg/kg i.v.) or vehicle (2 % DMSO i.v.). At 24 h, heart samples were collected and signalling events were assessed. Densitometry analysis of the bands is expressed as relative optical density (O.D.) of **(A)** IKKα/β phosphorylation on $Ser^{178/180}$ corrected to the corresponding total IKKα/β content; **(B)** IκBα phosphorylation on $Ser^{32/36}$ corrected to the corresponding total IκBα content and; **(C)** NF-κB p65 subunit levels in both, cytosolic and nuclear fractions expressed as a nucleus/cytosol ratio; **(D)** Inducible nitric oxide synthase (iNOS) expression corrected for the corresponding tubulin band. Bands were normalized using the HFD band. Data was analysed using one-way ANOVA followed by Bonferroni's post hoc test and expressed as mean ± SEM. *P< 0.05 compared to HFD+CLP surgery group. (n=4-6 per group).

4. Effect of IKK-16 or linagliptin post treatment on Akt phosphorylation in mice with pre-existing T2DM subjected to CLP surgery.

When compared to cardiac biopsies obtained from HFD-fed mice subjected to sham surgery, cardiac tissue obtained from mice fed a HFD and subjected to CLP surgery did not result in a significant change in Akt phosphorylation on Ser^{473} (P>0.05; Figure 4.15). In contrast, the degree of Akt phosphorylation on Ser^{473} was significantly higher (and therefore restored) by treatment of HFD/CLP-mice with IKK-16 or linagliptin (1 h after CLP surgery) (P<0.05; Figure 4.15).

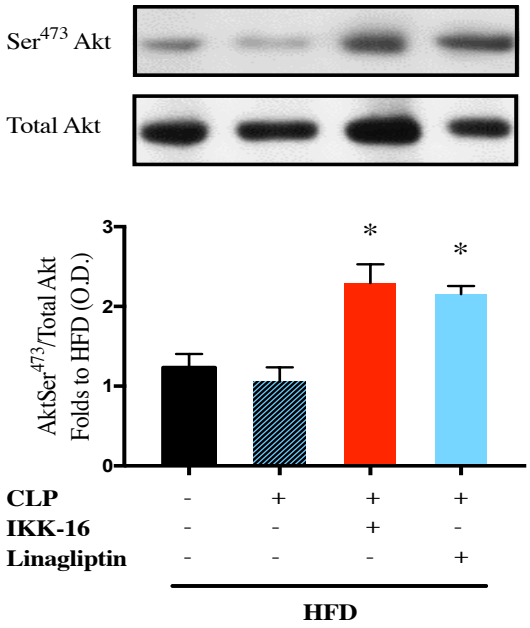

Figure 4.15 Effect of IKK-16 or linagliptin post-treatment on Akt phosphorylation in the heart of mice with pre-existing T2DM subjected to CLP surgery.

Mice on HFD were subjected to CLP or sham surgery. At 1 h, mice subjected to CLP surgery were treated with IKK-16 (1 mg/kg i.v.), linagliptin (10 mg/kg i.v.) or vehicle (2 % DMSO i.v.). At 24 h, heart samples were collected and signalling events were assessed. Densitometry analysis of the bands is expressed as relative optical density (O.D.) of phosphorylated Akt on Ser^{473} corrected for the corresponding total Akt content and normalized using the HFD band. Data was analysed using one-way ANOVA followed by Bonferroni's post hoc test and expressed as mean ± SEM. *P< 0.05 compared HFD+CLP group. (n=4-6 per group).

5. Effect of IKK-16 or linagliptin post treatment on the severity of kidney dysfunction and hepatocellular injury in mice with pre-existing T2DM subjected to CLP surgery

When compared to mice fed with a HFD and subjected to sham surgery, mice fed a HFD and subjected to CLP surgery exhibited a large and significant increases in serum urea, creatinine, and ALT ($P<0.05$, Figure 4.16 A-C). Post-treatment with IKK-16 or linagliptin in mice on HFD subjected to CLP surgery attenauted the CLP-induced rise in serum urea, creatinine and ALT compared to mice on HFD subjected to CLP surgery and treated with vehicle ($P>0.05$, Figure 4.16 A-C).

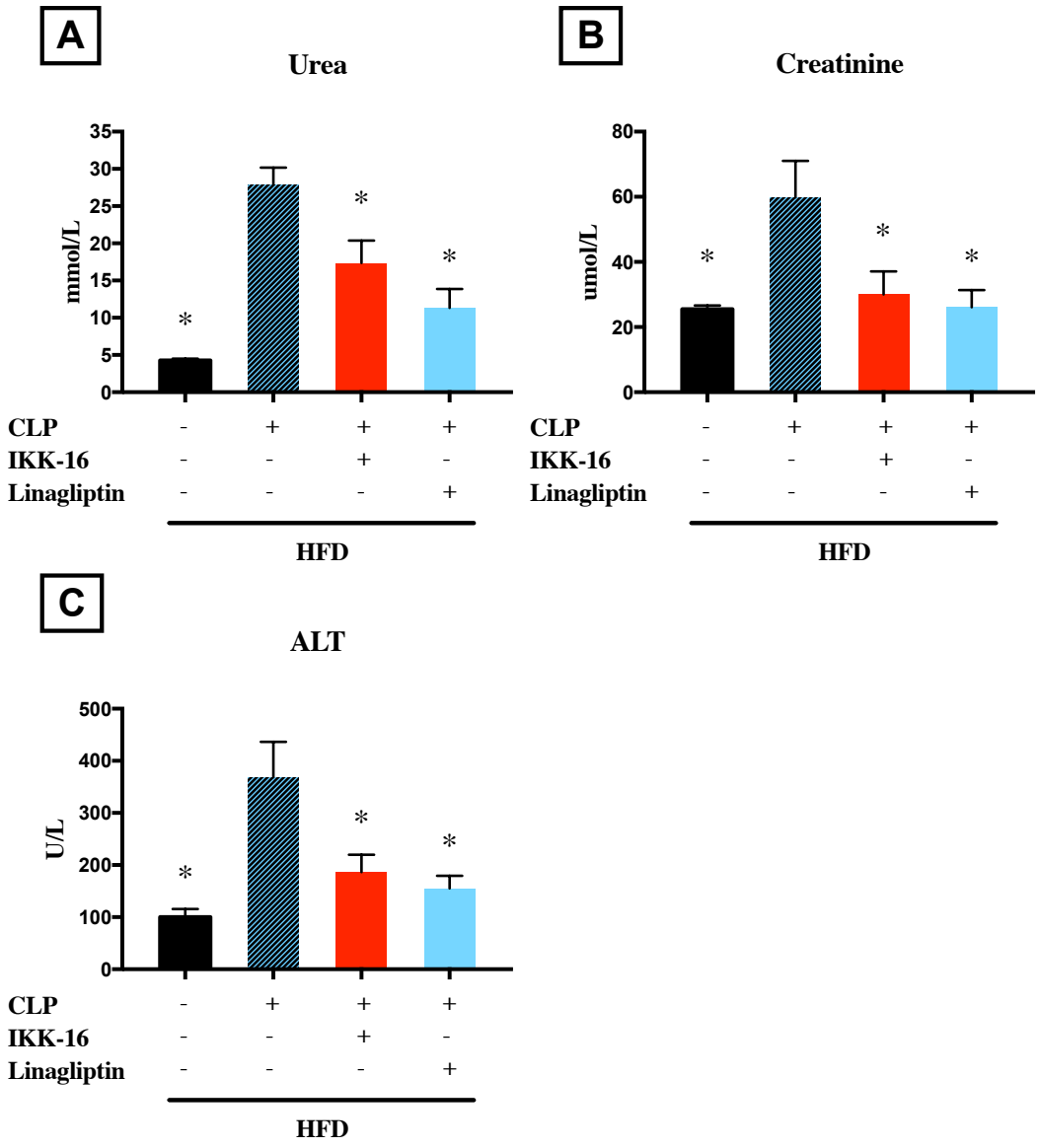

Figure 4.16 Effect of IKK-16 or linagliptin treatments on the severity of renal dysfunction and hepatocelleular injury in mice with pre-existing T2DM underwent CLP surgery.

Mice on HFD were subjected to CLP or sham surgery. At 1 h, mice subjected to CLP surgery were treated with IKK-16 (1 mg/kg i.v.), linagliptin (10 mg/kg i.v.) or vehicle (2 % DMSO i.v.). At 24 h, blood samples were collected and serum **(A)** urea, **(B)** creatinine and **(C)** ALT levels were measured. Data was analysed using one-way ANOVA followed by Bonferroni's post hoc test and expressed as mean ± SEM. **P*<0.05 compared to HFD+CLP group. (n=8-10 per group).

6. Effect of IKK-16 or linagliptin post treatment on neutrophils and macrophages infiltration to the lungs after CLP sepsis in mice with pre-existing T2DM

When compared to mice fed a HFD and subjected to sham surgery, induction of polymicrobial sepsis by CLP in mice on HFD resulted in large and significant increases in the MPO and NAG activities in the lung (P<0.05, Figure 4.17 A-B). Post treatment with IKK-16 or linagliptin, resulted in significant reduction in the MPO and NAG avtivities in the lungs compared to mice on HFD subjected to CLP and treated with vehicle (P<0.05, Figure 4.17 A-B).

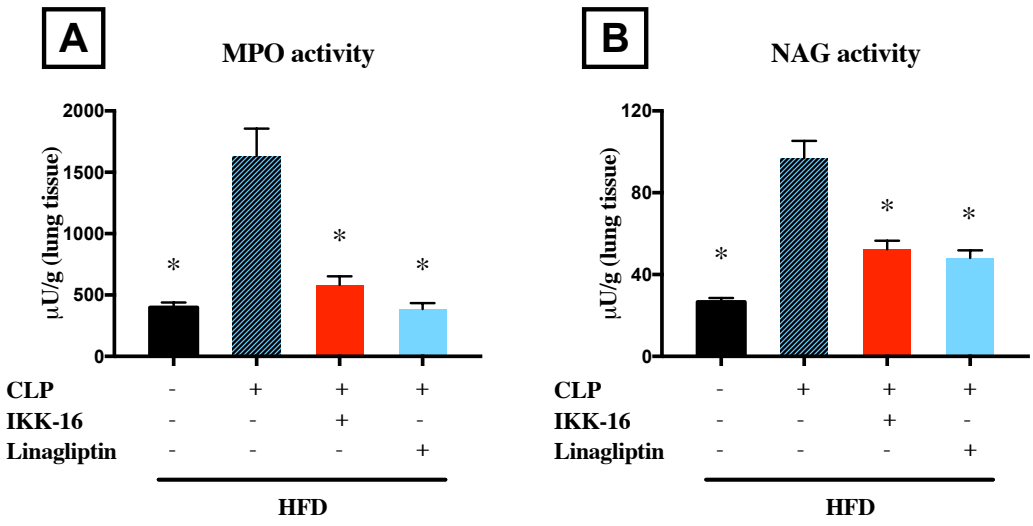

Figure 4.17 Effect of IKK-16 or linagliptin treatments on nuetrophil/macrophage infiltration (lung) in mice with pre-existing T2DM underwent CLP surgery.

Mice on HFD were subjected to CLP or sham surgery. At 1 h, mice subjected to CLP surgery were treated with IKK-16 (1 mg/kg i.v.), linagliptin (10 mg/kg i.v.) or vehicle (2 % DMSO i.v.). At 24 h, lungs were collected and tissue **(A)** MPO and **(B)** NAG activities were measured. Data was analysed using one-way ANOVA followed by Bonferroni's post hoc test and expressed as mean ± SEM. *P<0.05 compared to HFD+CLP group. (n=6 per group).

7. Effect of IKK-16 post tretment on serum inflammatory cytokines in mice with pre-existing T2DM after CLP sepsis.

When compared to mice fed a HFD and subjected to sham surgery, induction of polymicrobial sepsis by CLP in mice on HFD resulted in a large and significant increase in TNF-α, IL-6, KC and IL-10 concentrations in the serum ($P<0.05$, Figure 4.18 A-D). Post-treatment with IKK-16, resulted in significant reduction in the TNF-α, IL-6, KC and IL-10 levels when compared to mice on HFD subjected to CLP sepsis and treated with vehicle ($P<0.05$, Figure 4.18 B-D). Treatment with linagliptin resulted in significant reduction in the IL-6, KC and IL-10 levels ($P<0.05$, Figure 4.18 B-D) and in a reduction in TNF-α that did not, however, reached statistical significancy when compared to mice treated with vehicle ($P=0.06$, Figure 4.18 A).

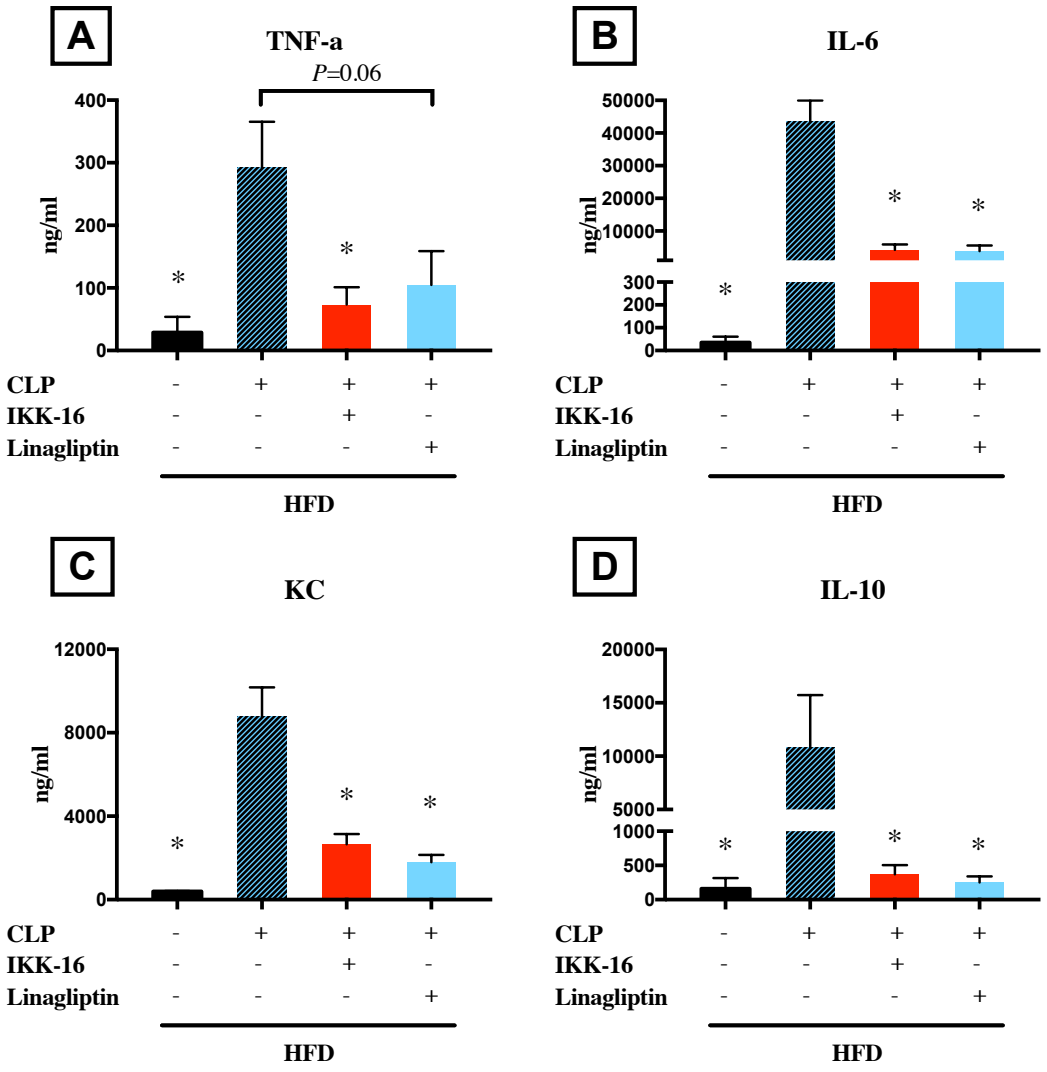

Figure 4.18 Effect of IKK-16 or linagliptin treatments on serum inflammatory cytokines in mice with pre-existing T2DM subjected to CLP surgery.

Mice on HFD were subjected to CLP or sham surgery. At 1 h, mice subjected to CLP surgery were treated with IKK-16 (1 mg/kg i.v.), linagliptin (10 mg/kg i.v.) or vehicle (2 % DMSO i.v.). At 24 h, blood samples were collected and inflammatory cytokines concentrations were measured in the serum. **(A)** TNF-α, **(B)** IL-6, **(C)** IL-1β, **(D)** IL-10 and **(E)** KC. Data was analysed using one-way ANOVA followed by Bonferroni's post hoc test and expressed as mean ± SEM. **P*<0.05 compared to HFD+CLP group. (n=4 per sham group and n=6-8 per CLP group).

4.6 Discussion

Activation of NF-κB is a key driver of the cardiac dysfunction in sepsis [291]. NF-κB activation results in increases in the inflammatory cytokines synthesis and the iNOS expression. By working as myocardial depressant factors, the inflammatory cytokines and the NO contribute to the development of cardiac dysfunction in sepsis [35]. Studies have shown that pharmacological inhibition of NF-κB activation enhanced the cardiac performance and attenuated the cardiac (organ) dysfunction associated with sepsis in previously healthy mice and in mice with CKD [277,291,292,302].

Having found that the cardiac dysfunction and the NF-κB activity are augmented after sepsis challenge in diabetic mice (chapter 3), I have investigated (this chapter) the effect of NF-κB inhibition on the degree of cardiac dysfunction associated with sepsis in mice with T2DM.

I have studied the effect of the selective inhibition of IKK (using IKK-16) on the cardiac (organ) dysfunction in mice with T2DM/sepsis. I demonstrated for the first time that a single dose of IKK-16 (at 1 h after LPS or CLP) preserves the systolic cardiac function after 18 or 24 h of endotoxaemia or polymicrobial sepsis in mice with T2DM respectively. I also reported that treatment with IKK-16 increases the physical activity and stabilises the core body temperature and/or the heart rate in the mice after LPS or CLP. Previous studies of our group showed similar effect of IKK-16 treatment in septic mice [291,292].

Mechanistically, IKK-16 inhibits NF-κB activity by preventing IKKα/β (an upstream regulator of NF-κB) phosphorylation on $Ser^{178/180}$ [311]. Indeed, in this

study treating mice with IKK-16 after LPS or CLP significantly attenuates the IKK phosphorylation and the subsequent IκB-α phosphorylation, NF-κB translocation to the nucleus and iNOS expression in the heart. Furthermore, my results show that treatment with IKK-16 activates the Akt pro-survival pathway in the heart. It is known that Akt phosphorylation and activation enhances cell survival by regulating different biological responses in the cells such as apoptosis and chemotaxis [302]. Similar to the results reported in this chapter, Akt phosphorylation was also restored after IKK-16, erythropoietin or peptide 19-2.5 treatment in murine models of sepsis and this increase in Akt phosphorylation was associated with attenuated cardiac dysfunction [277,291,302]. Thus, the cardioprotective effect of IKK-16 in T2DM/sepsis is, at least partially, a result of NF-κB pathway inhibition and Akt pathway activation.

In addition to reducing the cardiac dysfunction, treatment with IKK-16 in T2DM/sepsis mice reduces the serum inflammatory cytokines levels. This reduction in inflammatory cytokines levels is most likely a result of NF-κB inhibition and the subsequent inhibition of the acute cytokines release after sepsis challenge [312].

After investigating the effect of IKK-16 on cardiac dysfunction, I studied its effect on the dysfunction of other organs. In this chapter, I showed for the first time that (when compared with vehicle) treatment with IKK-16 results in attenuation of the kidney dysfunction and the liver injury associated with CLP-sepsis in mice with T2DM. It is known that high levels of TNF-α, IL-6 and IL-10 contribute to the development of the acute kidney dysfunction and the liver injury in sepsis [83,84,104,105]; therefore, the attenuated kidney dysfunction and liver injury may be, at

least partially, a result of the lower inflammatory cytokine levels after NF-κB inhibition by IKK-16 treatment in mice with T2DM and CLP-sepsis. These results are consistent with a study by Coldeway and co-workers who showed attenuation in kidney dysfunction and liver injury after IKK-16 treatment in mice with sepsis [291]. Although inhibition of NF-κB with IKK-16 in T2DM/CLP-sepsis resulted in attenuation of kidney dysfunction and liver injury, IKK-16 treatment after endotoxaemia in mice with T2DM did not show similar beneficial effects. This could be a result of a lower degree of attenuation of the TNF-α and IL-6 and IL-10 synthesis after IKK-16 treatment in the LPS model compared to the CLP model. This result is consistent with a previous study that showed no reduction in kidney dysfunction or liver injury after IKK-16 treatment in mice with CKD and sepsis [292].

In this study, I also reported less sepsis-induced lung inflammation in response to IKK-16 treatment (at 1 h after sepsis challenges) in mice with T2DM. I detected lower MPO and NAG activities (markers of neutrophil/macrophage infiltration) in the lungs. This result is in line with previous studies that showed attenuated lung inflammation as a result of IKK-16 treatment after sepsis in previously healthy mice and in mice with CKD [291,292].

In parallel with IKK-16 treatment in CLP model of sepsis, I studied the effect of inhibiting NF-κB using a DPP-4 inhibitor (linagliptin) on the cardiac (organ) dysfunction in mice with T2DM/sepsis. I showed here, for the first time, that a single dose of linagliptin (1 h after CLP surgery) ameliorates the cardiac dysfunction associated with CLP-sepsis in mice with T2DM. This attenuation of cardiac dysfunction is a result of the reduction in NF-κB activity and the

subsequent reduction in iNOS expression in the heart. My results also show that the improvement in cardiac function may be a result of the increased activation of the Akt pro-survival pathway in the heart and the reduced formation of proinflammatory cytokines (lower serum inflammatory cytokines levels) after the inhibition of NF-κB with linagliptin. A recent study by Suda and co-workers also reported a protective effect of DPP-4 inhibitors on cardiac function in a model of cardiac ischemia in obese mice [313]. Moreover, Treatment with linagliptin improves the physical activity and stabilise the heart rate and body temperature after CLP in mice with T2DM.

In this study, I reported for the first time that linagliptin attenuates the renal dysfunction and the liver injury in mice with T2DM/sepsis (reductions in serum urea, creatinine and ALT compared to untreated mice). The observed preservation of renal function and liver integrity by linagliptin in sepstic mice are likely to be, at least partially, secondary to the reduced serum TNF-α, IL-6 and IL-10 concentrations after NF-κB inhibition by linagliptin administration. A previous study by Shinjo et al. showed that co-administration of anagliptin with LPS inhibited the NF-κB activation in the liver [313]. Another study by Chen et al. showed that treatment with sitagliptin attenuated the inflammatory reaction in the kidney and preserved the kidney function after ischemia-reperfusion injury by inhibiting the NF-κB activation [314]. In this chapter, I also reported for the first time a reduction in lung inflammation after linagliptin treatment (measured as less MPO and NAG activities in lung tissue) in mice with T2DM/sepsis. This result is in line with a study by Nader et al. showing that treatment with sitagliptin reduced the inflammatory cells accumulation in the lung in a mouse model of asthma [315].

4.7 Conclusion

In this chapter, I have discovered that activation of NF-κB is a key driver of the cardiac dysfunction in T2DM/sepsis. I also showed that inhibiting the NF-κB activation using a selective IKK inhibitor (IKK-16) or a DPP-4 inhibitor (linagliptin) after sepsis challenge revokes the systematic inflammation and the cardiac (organ) dysfunction associated with sepsis in mice with pre-existing T2DM. Therefore, targeting NF-κB activation may be a potential strategy to treat the excessive inflammation and the cardiac (organ) dysfunction in patients with T2DM and sepsis.

CHAPTER 5: GENERAL DISCUSSION, CONCLUSIONS AND RESEARCH LIMITATIONS

Although the mortality rate among septic patients has declined recently due to the improved supportive care for patients in the ICU [20], 25% of patient with sepsis still die from the disease in the ICU. Furthermore, this percentage is almost doubled in patients with septic shock and it can reach 70% in patients with sepsis who develop cardiovascular dysfunction. This makes sepsis the leading cause of death in ICU patients [15].

The incidence of sepsis has increased recently mainly as a result of the aging of the population [15] which is associated with the presence of significant comorbidities such as T2DM [17]. Patients with T2DM are more liable to infections and subsequently sepsis [162,275]. The cardiovascular system is one of the most important systems that are affected by sepsis and the development of cardiovascular dysfunction in sepsis has been linked to several factors including inflammatory cytokines and NO. Many studies targeted these factors showed beneficial effects in pre-clinical models of sepsis. However, clinical studies that targeted these factors failed to improve survival in septic patients.

A possible cause of this lack of translatability from pre-clinical animal studies to clinical setting is that animal models of sepsis do not completely mimic the complex human sepsis. Most of the animals used in the pre-clinical study are young, healthy, adult, male animals with no pre-existing comorbidities. However,

sepsis in the clinical setting develops in patients with different gender, genetic background, age (most frequently in older patients) that frequently have one or more comorbidities including hypertension, diabetes and CKD. Another cause of lack of translatability of animal studies is that treatments are often given before the induction of sepsis or very early in the disease course. However, in the clinical setting, treatment is given after the diagnosis of sepsis was made and this is often at a relatively late stage when complications (e.g. organ dysfunction) have already developed. Therefore, this thesis had the overall aims to a) study the effect of T2DM on the severity of cardiac dysfunction associated with sepsis b) to investigate the pathophysiology of cardiac dysfunction associated with sepsis (in the presence of T2DM) and c) to identify novel therapeutic interventions to attenuate the cardiac dysfunction associated with sepsis/T2DM using a more translatable approach.

So far, there is no single animal model of sepsis or T2DM that reflects all the components of the complex human diseases, but rather a number of complementary models that epitomize individual aspects of the diseases while neglecting others. During my PhD, I have developed two models of T2DM and two models of sepsis to be used to study the effect of T2DM on cardiac dysfunction in sepsis, the pathophysiology of cardiac dysfunction in T2DM/sepsis and to find novel therapeutic interventions for sepsis related cardiac dysfunction in mice with T2DM.

In chapter 2, two clinically relevant models of T2DM caused by prolonged administration of HFD were established using C57BL/6 male mice. In these protocols, two types of HFD with almost similar fractions of fat (≈60%), but with a

different source and compositions of fat, were administered for 12 weeks. As the consumption of the western diet is the main cause of T2DM, this model of prolonged feeding of a HFD recapitulates the main cause of T2DM in human and considered to be the most clinically relevant model of T2DM available. Both models (chapter 2) resulted in the development of a diabetic phenotype (significant weight gain and impaired glucose tolerance) and diabetic cardiomyopathy (reduction in %EF). The development of diabetic cardiomyopathy observed is most probably a result of NF-κB activation in the heart (chapter 3). Although both diets resulted in a similar degree of cardiac dysfunction, there was a difference in the development of liver injury (measured using ALT levels) that only developed after the HFD (58Y1: Blue diet).

In chapter 3, I developed a "two-hit" model of pre-existing T2DM (secondary to HFD administration) followed by low dose LPS injection or mild CLP surgery, aiming to study the effect of pre-existing T2DM on the cardiac dysfunction associated with sepsis and to test novel therapies in order to attenuate cardiac dysfunction in T2DM/sepsis mice (chapter 4). I showed for the first time that pre-existing T2DM augments the cardiac dysfunction associated with sepsis. T2DM alone resulted in a small degree of NF-κB activation and iNOS expression in the heart. However, sepsis (second hit) in diabetic mice resulted in a dramatic increase in the serum concentrations of proinflammatory cytokines and a further increase in both NF-κB activation and iNOS expression in the heart. Diabetes also resulted in reduction in the activation (phosphorylation) of the Akt pro-survival pathway, while sepsis resulted in further reduction Akt phosphorylation in the heart. These two findings suggest that the cardiac dysfunction associated with T2DM/sepsis is most likely a result of NF-κB pro-inflammatory pathway activation (with

subsequent increase in iNOS expression and serum inflammatory cytokines levels) and Akt pro-survival pathway inhibition.

In chapter 4, to confirm the assumptions that the activation of NF-κB pro-inflammatory and the inhibition of Akt pro-survival pathway are the reasons for the cardiac dysfunction in T2DM/sepsis, I studied the effect of NF-κB inhibition and Akt activation on cardiac performance. In this chapter, I used a more translatable approach of treatment. The drug (IKK-16) was administered intravenously at one hour after the induction of sepsis. In my study, I showed for the first time that inhibition of IKK complex with IKK-16 (a selective inhibitor of IKK) at 1 h after sepsis challenge ameliorated the cardiac dysfunction in mice with T2DM/sepsis. This enhanced cardiac function was associated with, or a result of, the decreased NF-κB activation (and iNOS expression) and inflammatory cytokines synthesis and the restored Akt phosphorylation. NF-κB is rapidly activated in sepsis [291]. Many studies showed that pharmacological interventions that inhibit NF-κB reduced the MOD associated with sepsis [291,292,302]. Indeed, in my study a single dose of IKK-16 at 1 h after CLP resulted in attenuation of the multiple organ dysfunction associated with T2DM/sepsis. Although my study showed beneficial effects, further studies are still needed to answer the question how late after the induction of sepsis the IKK-16 can be given to attenuate cardiac (organ) dysfunction and improve survival in mice with T2DM/sepsis. Furthermore, more investigation is still needed to evaluate the efficacy and safety of IKK-16 in large animals before moving to human studies.

To overcome some of the issues related to toxicity and safety that might be encountered during the drug development of IKK-16 to clinical studies and to

make my finding more translational, I repositioned one of the DPP-4 inhibitors that are already in the market from treatment of T2DM to treat the cardiac (organ) dysfunction associated with sepsis in diabetic mice. The non-catalytic effect of DPP-4 inhibitors has recently emerged in the literature as potential new treatment of some inflammatory diseases. Indeed, the results in chapter 4 highlighted, for the first time, that inhibition of DPP-4 using linagliptin attenuates the cardiac dysfunction associated with T2DM/CLP-sepsis. This effect is most likely due to inhibition of NF-κB activation and preservation of Akt pathway activation in the heart. Treatment with linagliptin also resulted in attenuation of the multiple organ dysfunction associated with T2DM/CLP-sepsis. Therefore, inhibiting NF-κB by linagliptin may be a useful and clinically translatable approach to treat cardiac (organ) dysfunction in patients with T2DM and sepsis.

Conclusions

1. Feeding mice with a HFD for 12 weeks results in a T2DM phenotype and small degree of cardiac dysfunction.
2. A pre-existing diabetic phenotype worsens the organ injury/dysfunction associated with sepsis.
3. Activation of the NF-κB pathway is a key, but not the only, driver of the cardiac dysfunction in sepsis.
4. Inhibition of NF-κB with IKK-16 or linagliptin reduces the systemic inflammation and organ injury/dysfunction caused by sepsis in mice with pre-existing T2DM, and
5. Targeting NF-κB activation may be a potential strategy to treat the excessive inflammation and the cardiac (organ) dysfunction in patients with T2DM and sepsis.

Limitations of the study

Many interventions which showed promising results in pre-clinical studies failed to improve outcome in clinical trials. This can be related to limitations in both animal models and experimental design. In this thesis, I have tried to overcome some of these limitations to make my findings more clinically relevant.

To model T2DM, I used a dietary manipulation to induce insulin resistance and diabetes. Although this HFD-model of diabetes is the most clinically relevant, it only models the early stages of diabetes associated with a moderate degree of complications (e.g., cardiac dysfunction and proteinuria) without any impairment in beta-cell function. Therefore, more severe models of diabetes (genetic manipulation or HFD+streptozosin) should be used in future studies to confirm my findings.

To model sepsis, I used two different models of 'sepsis' (administration of bacterial toxin; LPS and alternation of endogenous barrier; CLP). However, none of the established murine models of sepsis can reflect all aspects of the complex human disease. Endotoxaemia is associated with a rapid and large increase in many cytokines, and similar cytokine kinetics are not seen in (all cases) of clinical sepsis. The CLP model on the other hand is a model of systemic infection which, if unchecked (by the use of antibiotics), will cause a high degree of mortality. In addition, the CLP-model is highly variable between animals, which makes it less reproducible.

In my experiments, sepsis challenge was introduced to mice when they were 22-week old. Previous studies in our laboratory used 8-12-week old mice to study

sepsis (as the septic insult was not preceded by a period of HFD). This makes my finding more clinically relevant as sepsis is more prevalent in the elderly. To reproduce my data in 'old' mice, one should ideally repeat these studies in animals that are between 12 and 18 months of age.

To study the effect of interventions, mice then were treated at 1 h after the onset of sepsis. Although I gave drugs after sepsis challenge, 1 h is still very early in the disease process and more studies are needed to see how late after the onset of sepsis the treatment with IKK-16 or linagliptin can be given to attenuate cardiac dysfunction in mice with T2DM/sepsis. This is of particular importance, as most cases of sepsis are diagnosed later in the disease when patients had already developed multiple organ dysfunction.

REFERENCES

1. Geroulanos S, Douka E. Historical perspective of the word “sepsis.” *Intensive Care Med*. 2006;32:2077.

2. Jones W. *Hippocrates*. Vol 1. (Page T, ed.). Harvard University Press; 1923.

3. Breasted J. *Edwin Smith Surgical Papyrus*. 1st ed. (Breasted J, ed.). Chicago, Illinois: The University of Chicago Press; 1980.

4. Allen J. The Art of Medicine in Ancient Egypt. In: Metropolitan Museum of Art/Yale University Press; 2005.

5. Stiefel M, Shaner A, Schaefer S. The Edwin Smith Papyrus: the birth of analytical thinking in medicine and otolaryngology. *Laryngoscope*. 2006;116(2):182-188.

6. Botero JS, Pérez MCF. The History of Sepsis from Ancient Egypt to the XIX Century. In: *Sepsis – An Ongoing and Significant Challenge*. ; 2012:3-32.

7. Rittirsch D, Flierl MA, Ward PA. Harmful molecular mechanisms in sepsis. *Nat Rev Immunol*. 2009;8(10):776-787. doi:10.1038/nri2402.Harmful.

8. Smith KA. Louis Pasteur , the father of immunology. *Front Immunol*. 2012;3(April):1-10. doi:10.3389/fimmu.2012.00068.

9. Noakes TD, Borresen J, Hew-Butler T, Lambert MI, Jordaan E. Semmelweis and the aetiology of puerperal sepsis 160 years on : an historical review. *Epidemiol Infect*. 2008;136:1-9. doi:10.1017/S0950268807008746.

10. Thomas L. Germs. *N Engl J Med*. 1972;287(11):553-555.

11. Bone R, Balk R, Cerra F, et al. accplsccm consensus conference for Sepsis and Organ Failure and. *Chest*. 1992;101:1644-1655.

12. Levy MM, Fink MP, Marshall JC, et al. 2001 SCCM/ESICM/ACCP/ATS/SIS International Sepsis Definitions Conference. *Crit Care Med*. 2003;31(0090-3493 (Print)):1250-1256. doi:10.1097/01.CCM.0000050454.01978.3B.

13. Levy M, Antunes A, Fiette L, Deghmane A, Taha M. Impact of corticosteroids on experimental meningococcal sepsis in mice. *Steroids*. 2015;101:96-102.

14. Singer M, Deutschman CS, Seymour CW, et al. The Third International Consensus Definitions for Sepsis and Septic Shock (Sepsis-3). *JAMA*. 2016;315(8):801-810. doi:10.1001/jama.2016.0287.

15. Mayr FB, Yende S, Angus DC, Mayr FB, Yende S, Angus DC. Epidemiology of severe sepsis Epidemiology of severe sepsis. *Virulence*. 2014;5594:4-11. doi:10.4161/viru.27372.

16. Ramachandran G. Gram-positive and gram-negative bacterial toxins in sepsis A brief review. *Virulence*. 2014;5(1):213-218. doi:10.4161/viru.27024.

17. Angus DC, Linde-Zwirble WT, Lidicker J, Clermont G, Carcillo J, Pinsky MR. Epidemiology of severe sepsis in the United States: analysis of incidence, outcome, and associated costs of care. *Crit Care Med*. 2001;29(7):1303-1310. doi:10.1097/00003246-200107000-00002.

18. Abe R, Oda S, Sadahiro T, Nakamura M, Hirayama Y, Tateishi Y. Gram-negative bacteremia induces greater magnitude of inflammatory response than Gram-positive bacteremia. *Crit care*. 2010;14(R27).

19. Vincent J, Rello J, Marshall J, et al. International study of the prevalence and outcomes of infection in intensive care units. *JAMA*. 2009;302(21):2323-2329.

20. Gavazzi G, Krause K. Ageing and infection. *Lancet Infect Dis*. 2002;2(11):659-666.

21. Rhodes A, Evans LE, Alhazzani W, et al. Surviving Sepsis Campaign: International Guidelines for Management of Sepsis and Septic Shock: 2016. *Inte Care Med*. 2017;43:304-377. doi:10.1007/s00134-017-4683-6.

22. Martin GS, Mannino DM, Eaton S, Moss M. The epidemiology of sepsis in the United States from 1979 through 2000. *N Engl J Med*. 2003;348(16):1546-1554. doi:10.1056/NEJMoa022139.

23. Medzhitov R, Janeway CJ. Innate immune recognition: mechanisms and pathways. *Immunol Rev*. 2000;173:89-97.

24. Mogensen TH. Pathogen Recognition and Inflammatory Signaling in Innate Immune Defenses. *Clin Microbiol Rev*. 2009;22(2):240-273. doi:10.1128/CMR.00046-08.

25. Takeuchi O, Akira S. Pattern Recognition Receptors and Inflammation. *Cell*. 2010;140(6):805-820. doi:10.1016/j.cell.2010.01.022.

26. Akira S, Uematsu S, Takeuchi O. Pathogen Recognition. *Cell*. 2006;3:783-801. doi:10.1016/j.cell.2006.02.015.

27. Bell JK, Botos I, Hall PR, et al. The molecular structure of the Toll-like receptor 3 ligand-binding domain. *PNAS*. 2005;102(31):10976-10980.

28. O'Neill L, Bowie A. The family of five: TIR-domain-containing adaptors in Toll-like receptor signalling. *Nat Rev Immunol*. 2007;7(5):353-364.

29. Kawai T, Akira S. review The role of pattern-recognition receptors in innate

immunity : update on Toll-like receptors. *Nat Publ Gr*. 2010;11(5):373-384. doi:10.1038/ni.1863.

30. Merx MW, Weber C. Cardiovascular Involvement in General Medical Conditions,Sepsis and the heart. *Circulation*. 2007;116(7):793-802 ST - Sepsis and the heart. doi:10.1161/CIRCULATIONAHA.106.678359.

31. Hunter JD, Doddi M, District M, Hospital G, Road V, Sk M. Sepsis and the heart. *Br J Anaesth*. 2010;104(1):3-11. doi:10.1093/bja/aep339.

32. Clowes G, Vucininc M, Weidner M. Circulatory and Metabolic Alterations Associated with Survival or Death in Peritonitis : Clinical Analysis of 25 Cases. *Ann Surg 163*. 1966;163:844-866.

33. Wilson RF, Sarver EJ. Factors Affecting Hemodynamics in Clinical Shock with Sepsis. *Ann Surg*. 1971;174(6):939-943.

34. Cunnion R, Schaer G, Parker M, Natanson C, Parrillo J. The coronary circulation in human septic shock. *Circulation*. 1986;73(4):637-644.

35. Parrillo JE, Burch C, Shelhamer JH, Parker MM, Natanson C, Schuette W. A circulating myocardial depressant substance in humans with septic shock: septic shock patients with a reduced ejection fraction have a circulating factor that depresses in vitro myocardial cell performance. *J Clin Invest*. 1985;76(4):1539-1553.

36. Hoffmann J, Werdan K, Hartl W, Jochum M, Faist E, Inthorn D. Hemofiltrate from patients with severe sepsis and depressed left ventricular contractility contains cardiotoxic compounds. *Shock*. 1999;13:174-180.

37. Pathan N, Sandiford C, Hariding S, Levin M. Characterization of a myocardial depressant factor in meningococcal septicemia. *Crit Care Med*. 2002;30:2191-2198.

38. Natanson C, Eichenholz PW, Danner RL, et al. Endotoxin and tumor necrosis factor challenges in dogs simulate the cardiovascular profile of human septic shock. *J Exp Med*. 1989;169(3):823-832. http://www.ncbi.nlm.nih.gov/pubmed/2647895. Accessed December 5, 2017.

39. Eichenholz PW, Eichacker PQ, Hoffman WD, et al. Tumor necrosis factor challenges in canines: patterns of cardiovascular dysfunction. *Am J Physiol*. 1992;263(3 Pt 2):H668-H675. http://www.ncbi.nlm.nih.gov/pubmed/1415590. Accessed December 5, 2017.

40. Vincent JL, Bakker J, Marécaux G, Schandene L, Kahn RJ, Dupont E. Administration of anti-TNF antibody improves left ventricular function in septic shock patients. Results of a pilot study. *Chest*. 1992;101(3):810-815. http://www.ncbi.nlm.nih.gov/pubmed/1541150. Accessed December 5, 2017.

41. Abraham E, Anzueto A, Gutierrez G, et al. Double-blind randomised controlled trial of monoclonal antibody to human tumour necrosis factor in treatment of septic shock. NORASEPT II Study Group. *Lancet (London, England)*. 1998;351(9107):929-933. http://www.ncbi.nlm.nih.gov/pubmed/9734938. Accessed December 5, 2017.

42. Francis SE, Holden H, Holt CM, Duff GW. Interleukin-1 in Myocardium and Coronary Arteries of Patients with Dilated Cardiomyopathy. *J Mol Cell Cardiol*. 1998;30(2):215-223. doi:10.1006/jmcc.1997.0592.

43. Loppnow H, Werdan K, Reuter G, Flad HD. The interleukin-1 and interleukin-1 converting enzyme families in the cardiovascular system. *Eur Cytokine Netw*. 1998;9(4):675-680. http://www.ncbi.nlm.nih.gov/pubmed/9889413. Accessed December 5, 2017.

44. Finkel MS, Oddis C V, Jacob TD, Watkins SC, Hattler BG, Simmons RL. Negative inotropic effects of cytokines on the heart mediated by nitric oxide. *Science*. 1992;257(5068):387-389. http://www.ncbi.nlm.nih.gov/pubmed/1631560. Accessed December 5, 2017.

45. Damas P, Ledoux D, Nys M, Vrindts Y, Groote DDE. Cytokine Serum Level During Severe Sepsis in Human IL-6 as a Marker of Severity. *Ann Surg*. 1992;215(4):356-362.

46. Schulz R, Rassaf T, Massion PB, Kelm M, Balligand J-L. Recent advances in the understanding of the role of nitric oxide in cardiovascular homeostasis. *Pharmacol Ther*. 2005;108(3):225-256. doi:10.1016/j.pharmthera.2005.04.005.

47. Ziolo MT, Bers DM. The Real Estate of NOS Signaling: Location, Location, Location. *Circ Res*. 2003;92(12):1279-1281. doi:10.1161/01.RES.0000080783.34092.AF.

48. Gorressen S, Stern M, van de Sandt AM, et al. Circulating NOS3 Modulates Left Ventricular Remodeling following Reperfused Myocardial Infarction. Salloum FN, ed. *PLoS One*. 2015;10(4):e0120961. doi:10.1371/journal.pone.0120961.

49. Böhm M, Kirchmayr R, Gierschik P, Erdmann E. Increase of myocardial inhibitory G-proteins in catecholamine-refractory septic shock or in septic multiorgan failure. *Am J Med*. 1995;98(2):183-186. doi:10.1016/S0002-9343(99)80402-1.

50. Shah AM, Spurgeon HA, Sollott SJ, Talo A, Lakatta EG. 8-bromo-cGMP reduces the myofilament response to Ca2+ in intact cardiac myocytes. *Circ Res*. 1994;74(5):970-978. http://www.ncbi.nlm.nih.gov/pubmed/8156644. Accessed December 5, 2017.

51. Zanotti-Cavazzoni SL, Hollenberg SM. Cardiac dysfunction in severe sepsis and septic shock. *Curr Opin Crit Care*. 2009;15(5):392-397. doi:10.1097/MCC.0b013e3283307a4e.

52. Pacher P, Beckman JS, Liaudet L. Nitric Oxide and Peroxynitrite in Health and Disease. *Physiol Rev*. 2007;87(1):315-424. doi:10.1152/physrev.00029.2006.

53. Xu C, Yi C, Wang H, Bruce IC, Xia Q. Mitochondrial Nitric Oxide Synthase Participates in Septic Shock Myocardial Depression by Nitric Oxide Overproduction and Mitochondrial Permeability Transition Pore Opening. *Shock*. 2012;37(1):110-115. doi:10.1097/SHK.0b013e3182391831.

54. Zaky A, Deem S, Bendjelid K, Treggiari MM. Characterization of cardiac dysfunction in sepsis: An ongoing challenge. *Shock*. 2014;41(1):12-24. doi:10.1097/SHK.0000000000000065.

55. Liu S, Schreur KD. G protein-mediated suppression of L-type Ca2+ current by interleukin-1 beta in cultured rat ventricular myocytes. *Am J Physiol Physiol*. 1995;268(2):C339-C349. doi:10.1152/ajpcell.1995.268.2.C339.

56. Zhong J, Hwang TC, Adams HR, Rubin LJ. Reduced L-type calcium current in ventricular myocytes from endotoxemic guinea pigs. *Am J Physiol*. 1997;273(5 Pt 2):H2312-H2324. http://www.ncbi.nlm.nih.gov/pubmed/9374768. Accessed February 19, 2018.

57. Dong LW, Wu LL, Ji Y, Liu MS. Impairment of the ryanodine-sensitive calcium release channels in the cardiac sarcoplasmic reticulum and its underlying mechanism during the hypodynamic phase of sepsis. *Shock*. 2001;16(1):33-39. http://www.ncbi.nlm.nih.gov/pubmed/11442313. Accessed February 19, 2018.

58. Barth E, Stämmler G, Speiser B, Schaper J. Ultrastructural quantitation of mitochondria and myofilaments in cardiac muscle from 10 different animal species including man. *J Mol Cell Cardiol*. 1992;24(7):669-681. http://www.ncbi.nlm.nih.gov/pubmed/1404407. Accessed December 18, 2017.

59. Brealey D, Brand M, Hargreaves I, et al. Association between mitochondrial dysfunction and severity and outcome of septic shock. *Lancet*. 2002;360(9328):219-223. doi:10.1016/S0140-6736(02)09459-X.

60. Vanasco V, Saez T, Magnani ND, et al. Cardiac mitochondrial biogenesis in endotoxemia is not accompanied by mitochondrial function recovery. *Free Radic Biol Med*. 2014;77:1-9. doi:10.1016/j.freeradbiomed.2014.08.009.

61. Suliman HB, Carraway MS, Piantadosi CA. Postlipopolysaccharide Oxidative Damage of Mitochondrial DNA. *Am J Respir Crit Care Med*. 2003;167(4):570-579. doi:10.1164/rccm.200206-518OC.

62. Larche J, Lancel S, Hassoun SM, et al. Inhibition of Mitochondrial Permeability Transition Prevents Sepsis-Induced Myocardial Dysfunction and Mortality. *J Am Coll Cardiol*. 2006;48(2):377-385. doi:10.1016/j.jacc.2006.02.069.

63. Levy RJ, Vijayasarathy C, Raj NR, Avadhani NG, Deutschman CS. Competitive and Noncompetitive Inhibition of Myocardial Cytochrome C Oxidase in Sepsis. *Shock*. 2004;21(2):110-114. doi:10.1097/01.shk.0000108400.56565.ab.

64. Tavener SA, Kubes P. Is There a Role for Cardiomyocyte Toll-Like Receptor 4 in Endotoxemia? *Trends Cardiovasc Med*. 2005;15(5):153-157. doi:10.1016/j.tcm.2005.06.001.

65. Angelousi AG, Karageorgopoulos DE, Kapaskelis AM, Falagas ME. Association between thyroid function tests at baseline and the outcome of patients with sepsis or septic shock: a systematic review. *Eur J Endocrinol*. 2011;164(2):147-155. doi:10.1530/EJE-10-0695.

66. Wang F, Pan W, Wang H, Wang S, Pan S, Ge J. Relationship between thyroid function and ICU mortality: A prospective observation study. *Crit Care*. 2012;16(1):R11. doi:10.1186/cc11151.

67. Calvano SE, Xiao W, Richards DR, et al. A network-based analysis of systemic inflammation in humans. *Nature*. 2005;437(7061):1032-1037. doi:10.1038/nature03985.

68. Carré JE, Orban J-C, Re L, et al. Survival in Critical Illness Is Associated with Early Activation of Mitochondrial Biogenesis. *Am J Respir Crit Care Med*. 2010;182(6):745-751. doi:10.1164/rccm.201003-0326OC.

69. Takasu O, Gaut JP, Watanabe E, et al. Mechanisms of Cardiac and Renal Dysfunction in Patients Dying of Sepsis. *Am J Respir Crit Care Med*. 2013;187(5):509-517. doi:10.1164/rccm.201211-1983OC.

70. Bolaños JP, Almeida A, Moncada S. Glycolysis: a bioenergetic or a survival pathway? *Trends Biochem Sci*. 2010;35(3):145-149. doi:10.1016/j.tibs.2009.10.006.

71. Kakihana Y, Ito T, Nakahara M, Yamaguchi K, Yasuda T. Sepsis-induced myocardial dysfunction: Pathophysiology and management. *J Intensive Care*. 2016;4(1):1-10. doi:10.1186/s40560-016-0148-1.

72. Singer M. The role of mitochondrial dysfunction in sepsis-induced multi-organ failure. *Virulence*. 2014;5(1):66-72. doi:10.4161/viru.26907.

73. Ostermann M, Chang RWS. Acute kidney injury in the intensive care unit according to RIFLE. *Crit Care Med*. 2007;35(8):1837-1843. doi:10.1097/01.CCM.0000277041.13090.0A.

74. Doi K. Role of kidney injury in sepsis. *J Intensive Care*. 2016;4(1):1-6. doi:10.1186/s40560-016-0146-3.

75. Neveu H, Kleinknecht D, Brivet F, Loirat P, Landais P. Prognostic factors in acute renal failure due to sepsis. Results of a prospective multicentre study. The French Study Group on Acute Renal Failure. *Nephrol Dial Transplant*. 1996;11(2):293-299. http://www.ncbi.nlm.nih.gov/pubmed/8700363. Accessed February 19, 2018.

76. Singbartl K, Kellum JA. AKI in the ICU: definition, epidemiology, risk stratification, and outcomes. *Kidney Int*. 2012;81(9):819-825. doi:10.1038/ki.2011.339.

77. Zarbock A, Gomez H, Kellum JA, Care I. Sepsis-induced acute kidney injury revisited: Pathophysiology, prevention and future therapies. *Curr Opin Crit Care*. 2015;20(6):588-595. doi:10.1097/MCC.0000000000000153.Sepsis-induced.

78. Mehta RL, Kellum JA, Shah S V, et al. Acute Kidney Injury Network: report of an initiative to improve outcomes in acute kidney injury. *Crit Care*. 2007;11(2). doi:10.1186/cc5713.

79. Schrier RW, Wang W. Acute Renal Failure and Sepsis. *N Engl J Med*. 2004;3512351:159-169. http://www.nejm.org/doi/pdf/10.1056/NEJMra032401. Accessed February 19, 2018.

80. Gomez H, Ince C, De Backer D, et al. A Unified Theory of Sepsis-Induced Acute Kidney Injury. *Shock*. 2014;41(1):3-11. doi:10.1097/SHK.0000000000000052.

81. Le Dorze M, Legrand M, Payen D, Ince C. The role of the microcirculation in acute kidney injury. *Curr Opin Crit Care*. 2009;15(6):503-508. doi:10.1097/MCC.0b013e328332f6cf.

82. Prowle JR, Ishikawa K, May CN, Bellomo R. Renal Blood Flow during Acute Renal Failure in Man. *Blood Purif*. 2009;28(3):216-225. doi:10.1159/000230813.

83. Murugan R, Karajala-Subramanyam V, Lee M, et al. Acute kidney injury in non-severe pneumonia is associated with an increased immune response and lower survival. *Kidney Int*. 2010;77(6):527-535. doi:10.1038/ki.2009.502.

84. Payen D, Lukaszewicz A-C, Legrand M, et al. A Multicentre Study of Acute Kidney Injury in Severe Sepsis and Septic Shock: Association with Inflammatory Phenotype and HLA Genotype. Burdmann EA, ed. *PLoS One*. 2012;7(6):e35838. doi:10.1371/journal.pone.0035838.

85. Kalakeche R, Hato T, Rhodes G, et al. Endotoxin uptake by S1 proximal tubular segment causes oxidative stress in the downstream S2 segment. *J Am Soc Nephrol*. 2011;22(8):1505-1516. doi:10.1681/ASN.2011020203.

86. Lin M, Yiu WH, Wu HJ, et al. Toll-Like Receptor 4 Promotes Tubular Inflammation in Diabetic Nephropathy. *J Am Soc Nephrol*. 2012;23(1):86-

102. doi:10.1681/ASN.2010111210.

87. Mudaliar H, Pollock C, Komala MG, Chadban S, Wu H, Panchapakesan U. The role of Toll-like receptor proteins (TLR) 2 and 4 in mediating inflammation in proximal tubules. *Am J Physiol Physiol*. 2013;305(2):F143-F154. doi:10.1152/ajprenal.00398.2012.

88. Kruger B, Krick S, Dhillon N, et al. Donor Toll-like receptor 4 contributes to ischemia and reperfusion injury following human kidney transplantation. *Proc Natl Acad Sci*. 2009;106(9):3390-3395. doi:10.1073/pnas.0810169106.

89. Herter JM, Rossaint J, Spieker T, Zarbock A. Adhesion Molecules Involved in Neutrophil Recruitment during Sepsis-Induced Acute Kidney Injury. *J Innate Immun*. 2014;6(5):597-606. doi:10.1159/000358238.

90. De Backer D, Creteur J, Preiser J-C, Dubois M-J, Vincent J-L. Microvascular blood flow is altered in patients with sepsis. *Am J Respir Crit Care Med*. 2002;166(1):98-104. http://www.ncbi.nlm.nih.gov/pubmed/12091178. Accessed February 19, 2018.

91. Donati A, Damiani E, Botticelli L, et al. The aPC treatment improves microcirculation in severe sepsis/septic shock syndrome. *BMC Anesthesiol*. 2013;13(1):25. doi:10.1186/1471-2253-13-25.

92. Spronk PE, Ince C, Gardien MJ, Mathura KR, Oudemans-van Straaten HM, Zandstra DF. Nitroglycerin in septic shock after intravascular volume resuscitation. *Lancet (London, England)*. 2002;360(9343):1395-1396. http://www.ncbi.nlm.nih.gov/pubmed/12423989. Accessed February 19, 2018.

93. Di Giantomasso D, May CN, Bellomo R. Vital organ blood flow during hyperdynamic sepsis. *Chest*. 2003;124(3):1053-1059. http://www.ncbi.nlm.nih.gov/pubmed/12970037. Accessed February 19, 2018.

94. Seely KA, Holthoff JH, Burns ST, et al. Hemodynamic changes in the kidney in a pediatric rat model of sepsis-induced acute kidney injury. *Am J Physiol Physiol*. 2011;301(1):F209-F217. doi:10.1152/ajprenal.00687.2010.

95. Holthoff JH, Wang Z, Seely KA, Gokden N, Mayeux PR. Resveratrol improves renal microcirculation, protects the tubular epithelium, and prolongs survival in a mouse model of sepsis-induced acute kidney injury. *Kidney Int*. 2012;81(4):370-378. doi:10.1038/ki.2011.347.

96. Brealey D, Karyampudi S, Jacques TS, et al. Mitochondrial dysfunction in a long-term rodent model of sepsis and organ failure. *Am J Physiol Integr Comp Physiol*. 2004;286(3):R491-R497. doi:10.1152/ajpregu.00432.2003.

97. Singer M, De Santis V, Vitale D, Jeffcoate W. Multiorgan failure is an adaptive, endocrine-mediated, metabolic response to overwhelming systemic inflammation. *Lancet*. 2004;364(9433):545-548.

doi:10.1016/S0140-6736(04)16815-3.

98. Mandal S, Guptan P, Owusu-Ansah E, Banerjee U. Mitochondrial Regulation of Cell Cycle Progression during Development as Revealed by the tenured Mutation in Drosophila. *Dev Cell*. 2005;9(6):843-854. doi:10.1016/j.devcel.2005.11.006.

99. Aregger F, Uehlinger DE, Witowski J, et al. Identification of IGFBP-7 by urinary proteomics as a novel prognostic marker in early acute kidney injury. *Kidney Int*. 2014;85(4):909-919. doi:10.1038/ki.2013.363.

100. Nesseler N, Launey Y, Aninat C, Morel F, Mallédant Y, Seguin P. Clinical review: The liver in sepsis. *Crit Care*. 2012;16(5):1-8. doi:10.1186/cc11381.

101. Bakker J, Grover R, McLuckie A, et al. Administration of the nitric oxide synthase inhibitor NG-methyl-l-arginine hydrochloride (546C88) by intravenous infusion for up to 72 hours can promote the resolution of shock in patients with severe sepsis: Results of a randomized, double-blind, placebo. *Crit Care Med*. 2004;32(1):1-12. doi:10.1097/01.CCM.0000105118.66983.19.

102. Quenot J-P, Binquet C, Kara F, et al. The epidemiology of septic shock in French intensive care units: the prospective multicenter cohort EPISS study. *Crit Care*. 2013;17(2):R65. doi:10.1186/cc12598.

103. Katz S, Jimenez MA, Lehmkuhler WE, Grosfeld JL. Liver bacterial clearance following hepatic artery ligation and portacaval shunt. *J Surg Res*. 1991;51(3):267-270. http://www.ncbi.nlm.nih.gov/pubmed/1881140. Accessed February 19, 2018.

104. Koo DJ, Chaudry IH, Wang P. Kupffer cells are responsible for producing inflammatory cytokines and hepatocellular dysfunction during early sepsis. *J Surg Res*. 1999;83(2):151-157. doi:10.1006/jsre.1999.5584.

105. Dhainaut JF, Marin N, Mignon A, Vinsonneau C. Hepatic response to sepsis: interaction between coagulation and inflammatory processes. *Crit Care Med*. 2001;29(7 Suppl):S42-S47. http://www.ncbi.nlm.nih.gov/pubmed/11445733. Accessed February 19, 2018.

106. American Diabetes Association. DEFINITION AND DESCRIPTION OF DIABETES OTHER CATEGORIES OF GLUCOSE. *Diabetes Care*. 2010;33(1):s62-s69. doi:10.2337/dc10-S062.

107. World Health Orgaization. *GLOBAL REPORT ON DIABETES*. France; 2016.

108. World Health Orgaization. *Definition, Diagnosis and Classification of Diabetes Mellitus and Its Complication*. Geneva; 1999.

109. Amirican diabetes association. Standards of Medical Care in Diabetes—2016 Abridged for Primary Care Providers. *position statement*. 2016;34:3-

21. doi:10.2337/diaclin.34.1.3.

110. Amirican diabetes association. Classification and Diagnosis of Diabetes. *Diabetes*. 2016;39(January):13-22. doi:10.2337/dc16-S005.

111. American diabetes association. Classification and Diagnosis of Diabetes. *Diabetes*. 2016;39(January):13-22. doi:10.2337/dc16-S005.

112. Rubler S, Dlugash J, Yuceoglu YZ, Kumral T, Branwood, Arthur Whitley Grishman A. New type of cardiomyopathy associated with diabetic glomerulosclerosis. *Am J Cardiol*. 1972;30(6):595-602.

113. Hayat SA, Patel B, Khattar RS, Malik RA, Road O, Manchester M. Diabetic cardiomyopathy : mechanisms , diagnosis and treatment. *Clin Sci*. 2004;107(6):539-557.

114. Rerkpattanapipat P, Agostino RBD, Link KM, et al. Location of Arterial Stif fening Dif fers in Those With. *Diabetes*. 2009;58(946-953). doi:10.2337/db08-1192.

115. Mcgavock JM, Lingvay I, Zib I, et al. Cardiac Steatosis in Diabetes Mellitus A 1 H-Magnetic Resonance Spectroscopy Study. *Circulation*. 2007;116:1170-1175. doi:10.1161/CIRCULATIONAHA.106.645614.

116. Boudina S, Sena S, Theobald H, et al. Mitochondrial Energetics in the Heart in Obesity-Related diabetes: direct evidence for increased uncoupled respiration and activation of uncoupling proteins. *Diabetes*. 2007;56(October):2457-2466. doi:10.2337/db07-0481.Additional.

117. Frustaci A, Kajstura J, Chimenti C, et al. Myocardial Cell Death in Human Diabetes. *Circ Res*. 2000;87:1123-1132.

118. Regan TJ, Lyons MM, Ahmed SS, et al. Evidence for Cardiomyopathy in Familial Diabetes Mellitus. *J Clin Invest*. 1977;60:885-899.

119. Boudina S, Abel ED. Diabetic Cardiomyopathy Revisited. *Circulation*. 2007;115:3213-3223. doi:10.1161/CIRCULATIONAHA.106.679597.

120. Boudina S, Abel ED. Diabetic cardiomyopathy, causes and effects. 2010;11(1):31-39. doi:10.1007/s11154-010-9131-7.Diabetic.

121. Mann DL. Innate immunity and the failing heart: the cytokine hypothesis revisited. *Circ Res*. 2015;116(7):1254-1268.

122. Frieler RA, Mortensen RM. Immune Cell and Other Noncardiomyocyte Regulation of Cardiac Hypertrophy and Remodeling. *Circulation*. 2015;131:1019-1030.

123. Frati G, Schirone L, Chimenti I, et al. An overview of the inflammatory signalling mechanisms in the myocardium underlying the development of diabetic cardiomyopathy. *Cardiovasc reaserch*. 2017;113:378-388. doi:10.1093/cvr/cvx011.

124. Prabhu SD, Frangogiannis NG. The Biological Basis for Cardiac Repair After Myocardial Infarction: From Inflammation to Fibrosis. *Circ Res*. 2016;119:91-112.

125. Pan Y, Wang Y, Zhao Y, et al. Inhibition of JNK Phosphorylation by a Novel Curcumin Analog Prevents High Glucose – Induced In fl ammation and Apoptosis in Cardiomyocytes and the Development of Diabetic Cardiomyopathy. *Diabetes*. 2014;63(October 2013):3497-3511. doi:10.2337/db13-1577.

126. Yuehui W, Wenke F, Wanli X, et al. Inactivation of GSK-3β by Metallothionein Prevents Diabetes-Related Changes in Cardiac Energy Metabolism, Inflammation, Nitrosative Damage, and Remodeling. *Diabetes*. 2009;58(6):1391-1402.

127. H. Christian V, Cathrin S, Danai L, et al. HMGB1: the missing link between diabetes mellitus and heart failure. *Basic Res Cardiol*. 2010;105805–820(6):805-820.

128. Sulaiman M, Matta MJ, Sunderesan NR, Gupta MP, And MP, Gupta M. Resveratrol, an activator of SIRT1, upregulates sarcoplasmic calcium ATPase and improves cardiac function in diabetic cardiomyopathy. *Am J Physiol Hear Circ Physiol*. 2010;298(3):H833-H843.

129. Kim F, Pham M, Luttrell I, et al. Toll-Like Receptor-4 Mediates Vascular Inflammation and Insulin Resistance in Diet-Induced Obesity. *Circ Res*. 2007;100:1589-1596. doi:10.1161/CIRCRESAHA.106.142851.

130. Itani SI, Ruderman NB, Schmieder F, Boden G. Lipid-Induced Insulin Resistance in Human Muscle Is Associated With Changes in Diacylglycerol , Protein Kinase C, and IκB-α. *Diabetes*. 2005;3(17):2005-2011.

131. Yao D, Brownlee M. Hyperglycemia-Induced Reactive Oxygen Species Increase Expression of the Receptor for Advanced Glycation End Products (RAGE) and RAGE Ligands. *Diabetes*. 2010;59:249-255. doi:10.2337/db09-0801.

132. Mann DL. The Emerging Role of Innate Immunity in the Heart and For Whom the Cell Tolls. *Circ Res*. 2011;108:1122-1132. doi:10.1161/CIRCRESAHA.110.226936.

133. Wong SL, Demers M, Martinod K, et al. Diabetes primes neutrophils to undergo NETosis, which impairs wound healing. *Nat Med*. 2015;21:815-819.

134. Cesario D, Brar R, Shivkumar K. Alterations in ion channel physiology in diabetic cardiomyopathy. *Endocrinol Metab Clin North Am*. 2006;35(3):601-610.

135. Lopaschuk G, Tahiliani A, Vadlamudi R, Katz S, McNeill J. Cardiac sarcoplasmic reticulum function in insulin- or carnitine-treated diabetic rats. *Am J Physiol*. 1983;245(6):969-1076.

136. Fiordaliso F, Cuccovillo I, Bianchi R, et al. Cardiovascular oxidative stress is reduced by an ACE inhibitor in a rat model of streptozotocin-induced diabetes. *Life Sci*. 2006;79(2):121-129.

137. Brownlee M. Advanced protein glycosylation in diabetes and aging. *Annu Rev Med*. 1995;46:223-234.

138. Saraiva RM, Minhas KM, Zheng M, et al. Reduced Neuronal Nitric Oxide Synthase Expression Contributes to Cardiac Oxidative Stress and Nitroso-Redox Imbalance in ob/ ob Mice. *Nitric Oxide*. 2009;16(3):331-338. doi:10.1016/j.niox.2006.12.001.Reduced.

139. Kwon S, Pimentel D, Remondino A, Sawyer D, Colucci W. H(2)O(2) regulates cardiac myocyte phenotype via concentration-dependent activation of distinct kinase pathways. *J Mol Cell Cardiol*. 2003;35(6):615-621.

140. Koya D, King G. Protein kinase C activation and the development of diabetic complications. *Diabetes*. 1998;47(6):859-866.

141. Carley A, Severson D. Fatty acid metabolism is enhanced in type 2 diabetic hearts. *Biochim Biophys Acta*. 2005;1734(2):112-126.

142. Sharma S, Adrogue J, Golfman L, et al. Intramyocardial lipid accumulation in the failing human heart resembles the lipotoxic rat heart. *FASEB J*. 2004;18(14):1692-1700. doi:10.1096/fj.04-2263com.

143. Zhou Y, Grayburn P, Karim A, et al. Lipotoxic heart disease in obese rats : Implications for human obesity. *Proc Natl Acad Sci U S A 2000 Feb 15;97(4)1784-9*. 2000;97(4):1784-1789.

144. Pierce G, Dhalla N. Heart mitochondrial function in chronic experimental diabetes in rats. *Can J Cardiol*. 1985;1(1):48-54.

145. Veksler V, Murat I, Ventura-Clapier R. Creatine kinase and mechanical and mitochondrial functions in hereditary and diabetic cardiomyopathies. *Can J Physiol Pharmacol 1991 Jun;69(6)852-8*. 1991;69(6):852-858.

146. Oliveira PJ, Seic R, Coxito PM, Rolo AP, Palmeira CM, Santos MS. Enhanced permeability transition explains the reduced calcium uptake in cardiac mitochondria from streptozotocin-induced diabetic rats. *FEBS Lett*. 2003;554:511-514. doi:10.1016/S0014-5793(03)01233-X.

147. Taegtmeyer H, Overturf ML. Effects of moderate hypertension on cardiac function and metabolism in the rabbit. *Hypertension*. 1988;11(5):416-426. doi:10.1161/01.hyp.11.5.416.

148. Holmäng A, Yoshida N, Jennische E, Waldenström A, Björntorp P. The effects of hyperinsulinaemia on myocardial mass, blood pressure regulation and central haemodynamics in rats. *Eur J Clin Invest*. 1996;26(11):973-978. http://www.ncbi.nlm.nih.gov/pubmed/8957202. Accessed February 19, 2018.

149. Karason K, Sjöström L, Wallentin I, Peltonen M. Impact of blood pressure and insulin on the relationship between body fat and left ventricular structure. *Eur Heart J*. 2003;24(16):1500-1505. http://www.ncbi.nlm.nih.gov/pubmed/12919774. Accessed February 19, 2018.

150. Barouch LA, Berkowitz DE, Harrison RW, O'Donnell CP, Hare JM. Disruption of Leptin Signaling Contributes to Cardiac Hypertrophy Independently of Body Weight in Mice. *Circulation*. 2003;108(6):754-759. doi:10.1161/01.CIR.0000083716.82622.FD.

151. van Heerebeek L, Hamdani N, Handoko ML, et al. Diastolic Stiffness of the Failing Diabetic Heart: Importance of Fibrosis, Advanced Glycation End Products, and Myocyte Resting Tension. *Circulation*. 2008;117(1):43-51. doi:10.1161/CIRCULATIONAHA.107.728550.

152. Fang ZY, Prins JB, Marwick TH. Diabetic Cardiomyopathy: Evidence, Mechanisms, and Therapeutic Implications. *Endocr Rev*. 2004;25(4):543-567. doi:10.1210/er.2003-0012.

153. Aronson D. Cross-linking of glycated collagen in the pathogenesis of arterial and myocardial stiffening of aging and diabetes. *J Hypertens*. 2003;21(1):3-12. doi:10.1097/01.hjh.0000042892.24999.92.

154. Celentano A, Vaccaro O, Tammaro P, et al. Early abnormalities of cardiac function in non-insulin-dependent diabetes mellitus and impaired glucose tolerance. *Am J Cardiol*. 1995;76(16):1173-1176. http://www.ncbi.nlm.nih.gov/pubmed/7484905. Accessed February 19, 2018.

155. Vanninen E, Mustonen J, Vainio P, Länsimies E, Uusitupa M. Left ventricular function and dimensions in newly diagnosed non-insulin-dependent diabetes mellitus. *Am J Cardiol*. 1992;70(3):371-378. http://www.ncbi.nlm.nih.gov/pubmed/1632406. Accessed February 19, 2018.

156. Hamblin M, Friedman DB, Hill S, Caprioli RM, Smith HM, Hill MF. Alterations in the diabetic myocardial proteome coupled with increased myocardial oxidative stress underlies diabetic cardiomyopathy. *J Mol Cell Cardiol*. 2007;42(4):884-895. doi:10.1016/j.yjmcc.2006.12.018.

157. Schannwell CM, Schneppenheim M, Perings S, Plehn G, Strauer BE. Left Ventricular Diastolic Dysfunction as an Early Manifestation of Diabetic Cardiomyopathy. *Cardiology*. 2002;98(1-2):33-39. doi:10.1159/000064682.

158. Mihm MJ, Seifert JL, Coyle CM, Bauer JA. Diabetes related cardiomyopathy Time dependent echocardiographic evaluation in an experimental rat model. *Life Sci*. 2001;69(69):527-542. https://ac.els-cdn.com/S0024320501011419/1-s2.0-S0024320501011419-main.pdf?_tid=bdf33996-157a-11e8-87de-00000aacb362&acdnat=1519047936_97d5c7f974d7c5d71214a879e1a6779

1. Accessed February 19, 2018.

159. Mytas DZ, Stougiannos PN, Zairis MN, Foussas SG, Pyrgakis VN, Kyriazis IA. Diabetic myocardial disease: pathophysiology, early diagnosis and therapeutic options. *J Diabetes Complications*. 2009;23(4):273-282. doi:10.1016/J.JDIACOMP.2007.12.005.

160. Reis F, Nunes S, Soares, Pereira F. The role of inflammation in diabetic cardiomyopathy. *Int J Interf Cytokine Mediat Res*. 2012;Volume 4:59. doi:10.2147/IJICMR.S21679.

161. Muller LMAJ, Gorter KJ, Hak E, et al. Increased Risk of Common Infections in Patients with Type 1 and Type 2 Diabetes Mellitus. *Clin Infect Dis*. 2005;41:281-288.

162. Casqueiro J, Casqueiro J, Alves C. Infections in patients with diabetes mellitus : A review of pathogenesis. *Indian J Endocrinol Metab*. 2012;16:27-36. doi:10.4103/2230-8210.94253.

163. SCHUETZ P, CASTRO P, SHAPIRO NI. Diabetes and Sepsis: Preclinical Findings and Clinical Relevance. *Diabetes Care*. 2011;34:771-778. doi:10.2337/dc10-1185.

164. Shah B, Hux J. Quantifying the risk of infectious diseases for people with diabetes. *Diabetes Care*. 2003;26(2):510-513.

165. Fine M, Smith M, Carson C, et al. Prognosis and outcomes of patients with community-acquired pneumonia. A meta-analysis. *JAMA*. 1996;275(2):134-141.

166. Kornum J, Thomsen R, Riis A, Lervang H, Schønheyder H, Sørensen H. Type 2 diabetes and pneumonia outcomes: a population-based cohort study. *Diabetes Care*. 2007;30(9):2251-2257.

167. Benfield T, Jensen J, Nordestgaard B. Influence of diabetes and hyperglycaemia on infectious disease hospitalisation and outcome. *Diabetologia*. 2007;50(3):549-554.

168. Thomsen RW, Hundborg HH, Lervang H, Johnsen SP, Schønheyder HC, Sørensen HT. Diabetes Mellitus as a Risk and Prognostic Factor for Community-Acquired Bacteremia Due to Enterobacteria : A 10-Year , Population-Based Study among Adults. *Clin Infect Dis*. 2005;40(1):628-631.

169. Kaplan J, Nowell M, Lahni P, Shen H, Shanmukhappa S, Zingarelli B. Obesity enhances sepsis-induced liver inflammation and injury in mice. *Obesity*. 2016;May.

170. Sakai S, Iizuka N, Fujiwara M, et al. Mild obesity reduces survival and adiponectin sensitivity in endotoxemic rats. *J Surg Res*. 2013;185(1):353-363.

171. Khan M, Patrick AL, Fox-robichaud AE. Development of a Murine Model of Early Sepsis in Diet-Induced Obesity. *Biomed Res Int*. 2014;2014. doi:10.1155/2014/719853.

172. McAlister F, Majumdar S, Blitz S, Rowe B, Romney J, TJ M. The relation between hyperglycemia and outcomes in 2,471 patients admitted to the hospital with community-acquired pneumonia. *Diabetes Care*. 2005;28(4):810-815.

173. Stegenga M, Vincent J, Vail G, et al. Diabetes does not alter mortality or hemostatic and inflammatory responses in patients with severe sepsis. *Crit Care Med*. 2010;38(2):539-545.

174. Tsai C, Lee C, Ma M, et al. Impact of diabetes on mortality among patients with community-acquired bacteremia. *J Infect*. 2007;55(1):27-33.

175. Vincent J, Preiser J, Sprung CL, Moreno R, Sakr Y. Insulin-treated diabetes is not associated with increased mortality in critically ill patients. *Crit care*. 2010;14:R12.

176. Esper AM, Moss M, Martin GS. The effect of diabetes mellitus on organ dysfunction with sepsis : an epidemiological study. *Crit care*. 2009;13(1):9-14. doi:10.1186/cc7717.

177. Moss M, Guidot D, Steinberg K, et al. Diabetic patients have a decreased incidence of acute respiratory distress syndrome. *Crit Care Med*. 2000;28(7):2187-2192.

178. Siegl D, Annecke T, Johnson B, et al. Obesity-induced hyperleptinemia improves survival and immune response in a murine model of sepsis. *Anesthesiology*. 2014;121(1):98-114.

179. Rawlings ND, Barrett AJ, Finn R. Twenty years of the MEROPS database of proteolytic enzymes , their substrates and inhibitors. *Nucleic Acids Res*. 2016;44(November 2015):343-350. doi:10.1093/nar/gkv1118.

180. Cera E Di. Serine Proteases. *NIH Public Access*. 2009;61(5):510-515. doi:10.1002/iub.186.Serine.

181. Cera E Di. Serine Proteases. *Int Union Biochem Mol Biol Life*. 2009;61(5):510-515. doi:10.1002/iub.186.Serine.

182. Fulop V, Cskei Z, Polgar L. Prolyl Oligopeptidase : An Unusual - Propeller Domain Regulates Proteolysis. *Cell*. 1998;94:161-170.

183. Polgar L. The prolyl oligopeptidase family. *cell Mol life Sci*. 2002;59(2):349-362.

184. DPP4 dipeptidyl peptidase 4 [Homo sapiens (human)]. Pubmed. https://www.ncbi.nlm.nih.gov/gene/1803. Published 2017.

185. Yaron A, Naider F, Scharpe S. Proline-Dependent Structural and Biological

Properties of Peptides and Proteins. *Critial Rev Biochem Mol Biol*. 1993;23(1).

186. Meester I De, Korom S, Damme J Van, Scharpé S, Cd B. CD26 , let it cut or cut it down. *Immunol Today*. 1999;5699(8):367-375.

187. Weihofen WA, Liu J, Reutter W, Saenger W, Fan H. Crystal Structure of CD26 / Dipeptidyl-peptidase IV in Complex with Adenosine Deaminase Reveals a Highly Amphiphilic Interface. *J Biol Chem*. 2004;279(41):43330-43335. doi:10.1074/jbc.M405001200.

188. Engel M, Hoffmann T, Wagner L, et al. The crystal structure of dipeptidyl peptidase IV (CD26) reveals its functional regulation and enzymatic mechanism. *PNAS*. 2003;100(9):5063-5068.

189. Laskar A, Chatterjee A, Chatterjee S, Rodger EJ. Three-Dimensional Molecular Modeling of a Diverse Range of SC Clan Serine Proteases. *Mol Biol Int*. 2012;2012. doi:10.1155/2012/580965.

190. Mulvihill EE, Drucker DJ, Introduction I, Discovery A. of Dipeptidyl Peptidase-4 Inhibitors. *Endocr Rev*. 2014;35(December):992-1019. doi:10.1210/er.2014-1035.

191. Zhong J, Maiseyeu A, Davis SN, Rajagopalan S. Recent Insights From the Laboratory and Clinical Trials of DPP4 Inhibition. *Circ Res*. 2015;116:1491-1505. doi:10.1161/CIRCRESAHA.116.305665.

192. Aertgeerts K. Crystal structure of human dipeptidyl peptidase IV in complex with a decapeptide reveals details on substrate specificity and tetrahedral intermediate formation. *Protein Sci*. 2004;13(2):412-421. doi:10.1110/ps.03460604.

193. Mortier A, Gouwy M, Damme J Van, Proost P, Struyf S. CD26 / dipeptidylpeptidase IV — chemokine interactions : double-edged regulation of inflammation and tumor biology. *J Leukoc Biol*. 2016;99:1-16. doi:10.1189/jlb.3MR0915-401R.

194. Drucker D, Nauck M. The incretin system: glucagon-like peptide-1 receptor agonists and dipeptidyl peptidase-4 inhibitors in type 2 diabetes. *Lancet*. 2006;386(9548):1696-1705.

195. Orskov C, Wettergren A, Holst JJ. Biological Effects and Metabolic Rates of Glucagonlike Peptide-1 7-36 Amide and Glucagonlike Peptide-1 7-37 in Healthy Subjects Are Indistinguishable. *Diabetes*. 1993;42(5):658-661.

196. Drucker DJ, Philippe J, Mojsov S, William L, Habener JF. Glucagon-like peptide I stimulates insulin gene expression and increases cyclic AMP levels in a rat islet cell line. *PNAS*. 1987;84(May):3434-3438.

197. Drucker DJ. The biology of incretin hormones. *Cell Metab*. 2006;3(March):153-165. doi:10.1016/j.cmet.2006.01.004.

198. Zhong J, Hwang T, Adams HR, et al. Reduced L-type calcium current in ventricular myocytes from endotoxemic guinea pigs. *Am J Physiol*. 1997;273(5 Pt 2):2312-2324.

199. Cordero OJ, Yang C-P, Bell EB. On the role of CD26 in CD4 memory T cells. *Immunobiology*. 2007;212(2):85-94.

200. Brady T, Journal B, Jun 01 1942, 36, (5-6), 478-484; Adenosine deaminase. *Biomed J*. 1942;36:478-484.

201. Jhajharia S, Pradhan T, Ekka A, Das AK. Effect of Dipeptidyl Peptidase-4 Inhibitors on Adenosine Deaminase Ac- tivity in Type-2 Diabetes Mellitus . *Biomed Res*. 2014;25(4):489-493.

202. Ohnuma K, Uchiyama M, Yamochi T, Nishibashi K, Hosono O. Caveolin-1 Triggers T-cell Activation via CD26 in Association. *J Biol Chem*. 2007;282(13):10117-10131. doi:10.1074/jbc.M609157200.

203. Klemann C, Wagner L. Cut to the chase : a review of CD26 / dipeptidyl peptidase-4 ' s (DPP4) entanglement in the immune system. *Clin Exp Immunol*. 2016;185:1-21. doi:10.1111/cei.12781.

204. Ohnuma K, Inoue H, Uchiyama M, Yamochi T, Hosono O, Dang NH. T-cell activation via CD26 and caveolin-1 in rheumatoid synovium. *Mod Rheumatol*. 2006;16:3-13. doi:10.1007/s10165-005-0452-4.

205. Ahmed RH, Huri HZ, Al-hamodi Z, Salem SD. Serum Levels of Soluble CD26 / Dipeptidyl Peptidase-IV in Type 2 Diabetes Mellitus and Its Association with Metabolic Syndrome and Therapy with Antidiabetic Agents in Malaysian Subjects. *PLoS One*. 2015;10(10):1-12. doi:10.1371/journal.pone.0140618.

206. Lamers D, Famulla S, Wronkowitz N, et al. Dipeptidyl Peptidase 4 Is a Novel Adipokine Potentially Linking Obesity to the Metabolic Syndrome. *Diabetes*. 2011;60(July):1917-1925. doi:10.2337/db10-1707.

207. Chlich RAS. Adipose Dipeptidyl Peptidase-4 and Obesity. *Diabetes Care*. 2013;36(February):4083-4090. doi:10.2337/dc13-0496.

208. Kang SH, Park DB, Oh B, Kim J, Heo ST. CD26/DPP4 Levels in Peripheral Blood and T Cells in Patients With Type 2 Diabetes Mellitus. *J Clin Endocrinol Metab*. 2013;98(June):2553-2561. doi:10.1210/jc.2012-4288.

209. Miyazaki M, Kato M, Tanaka K, et al. Increased hepatic expression of dipeptidyl peptidase-4 in non-alcoholic fatty liver disease and its association with insulin resistance and glucose metabolism. *Mol Med Rep*. 2012;5:729-733.

210. Pathak R, Bridgeman MB. Dipeptidyl Peptidase-4 (DPP-4) Inhibitors In the Management of Diabetes. *Drug Cl Rev*. 2010;35(9):509-513.

211. Karagiannis T, Paschos P, Paletas K, Matthews DR, Tsapas A. Dipeptidyl

peptidase-4 inhibitors for treatment of type 2 diabetes mellitus in the clinical setting : systematic review and meta-analysis. *Br Med J*. 2012;1369(March):1-15. doi:10.1136/bmj.e1369.

212. Graefe-Mody U, Friedrich C, Port A, et al. Effect of renal impairment on the pharmacokinetics of the dipeptidyl peptidase-4 inhibitor linagliptin. *Diabetes, Obes Metab*. 2011;13(10):939-946.

213. Stamm P, Hausding M, Kroller-Schon S, et al. Comparison of DPP-4 inhibition versus GLP-1 analogue supplementation on survival and vascular complications in experimental sepsis. *FASEB J*. 2014;28.

214. Sebastian S, Hausding M, Kröller-Schön S, et al. Gliptin and GLP-1 analog treatment improves survival and vascular inflammation/dysfunction in animals with lipopolysaccharide-induced endotoxemia. *Basic Res Cardiol*. 2015;110(2):110-116.

215. Tang S, Zhang Q, Tang H, et al. Effects of glucagon-like peptide-1 on advanced glycation endproduct-induced aortic endothelial dysfunction in streptozotocin-induced diabetic rats: possible roles of Rho kinase- and AMP kinase-mediated nuclear factor κB signaling pathways. *Endocrine*. 2016;53(1):107-116.

216. Wu C, Hu S, Wang N, Tian J. Dipeptidyl peptidase-4 inhibitor sitagliptin prevents high glucose-induced apoptosis via activation of AMP-activated protein kinase in endothelial cells. *Mol Med Rep*. 2017;15(6):434694351.

217. Schuff A, Schell R, Sudowe S, et al. Glucose-independent improvement of vascular dysfunction in experimental sepsis by dipeptidyl peptidase-4 inhibition. *Cardiovasc Res*. 2012;96(1):140-149. doi:10.1093/cvr/cvs246.

218. Nakamura Y, Inagaki M, Tsuji M, et al. Linagliptin Has Wide-Ranging Anti-Inflammatory Points of Action in Human Umbilical Vein Endothelial Cells. *Japanese Clin Med*. 2016;5(7):27-32.

219. Nakamura Y, Hasegawa H, Tsuji M, Oguchi T, Mihara M, Suzuki H. Linagliptin inhibits lipopolysaccharide- stimulated interleukin-6 production , intranuclear p65 expression , and p38 mitogen-activated protein kinase phosphorylation in human umbilical vein endothelial cells. *Ren Replace Ther*. 2016;2(17):1-10. doi:10.1186/s41100-016-0030-6.

220. Aroor AR, Habibi J, Kandikattu HK, et al. Dipeptidyl peptidase - 4 (DPP - 4) inhibition with linagliptin reduces western diet - induced myocardial TRAF3IP2 expression , inflammation and fibrosis in female mice. *Cardiovasc Diabetol*. 2017;16:1-15. doi:10.1186/s12933-017-0544-4.

221. Esposito G, Cappetta D, Russo R, et al. Sitagliptin reduces inflammation, fibrosis and preserves diastolic function in a rat model of heart failure with preserved ejection fraction. *Br J Pharmacol*. 2016;6.

222. Lin CH, Lin CC. Sitagliptin attenuates inflammatory responses in

lipopolysaccharide - stimulated cardiomyocytes via nuclear factor - κ B pathway inhibition. *Exp Ther Med*. 2016;11:2609-2615. doi:10.3892/etm.2016.3255.

223. World Health Orgaization. *Global Report on Diabetes*. France; 2016.

224. Atkinson MA. The Pathogenesis and Natural History of Type 1 Diabetes. *Cold Spring Harb Perspect Med*. 2012;2(11):a007641-a007641. doi:10.1101/cshperspect.a007641.

225. Yoon J-W, Jun H-S. Autoimmune destruction of pancreatic beta cells. *Am J Ther*. 12(6):580-591. http://www.ncbi.nlm.nih.gov/pubmed/16280652. Accessed February 2, 2018.

226. Das SK, Elbein SC. The Genetic Basis of Type 2 Diabetes. *Cellscience*. 2006;2(4):100-131. doi:10.1901/jaba.2006.2-100.

227. Seuring T, Archangelidi O, Suhrcke M. The Economic Costs of Type 2 Diabetes: A Global Systematic Review. *Pharmacoeconomics*. 2015;33(8):811-831. doi:10.1007/s40273-015-0268-9.

228. King AJF. The use of animal models in diabetes research. *Br J Pharmacol*. 2012;166(3):877-894. doi:10.1111/j.1476-5381.2012.01911.x.

229. Park JS, Bae SJ, Choi S-W, et al. A novel 11 -HSD1 inhibitor improves diabesity and osteoblast differentiation. *J Mol Endocrinol*. 2014;52(2):191-202. doi:10.1530/JME-13-0177.

230. Yoshida S, Tanaka H, Oshima H, et al. AS1907417, a novel GPR119 agonist, as an insulinotropic and β-cell preservative agent for the treatment of type 2 diabetes. *Biochem Biophys Res Commun*. 2010;400(4):745-751. doi:10.1016/j.bbrc.2010.08.141.

231. Gault VA, Kerr BD, Harriott P, Flatt PR. Administration of an acylated GLP-1 and GIP preparation provides added beneficial glucose-lowering and insulinotropic actions over single incretins in mice with Type 2 diabetes and obesity. *Clin Sci*. 2011;121(3):107-117. doi:10.1042/CS20110006.

232. McCarthy MI. Genomics, type 2 diabetes, and obesity. *N Engl J Med*. 2010;363(24):2339-2350. doi:10.1056/NEJMra0906948.

233. Bunner AE, Chandrasekera PC, Barnard ND. Knockout mouse models of insulin signaling: Relevance past and future. *World J Diabetes*. 2014;5(2):146-159. doi:10.4239/wjd.v5.i2.146.

234. Calligaris SD, Lecanda M, Solis F, et al. Mice Long-Term High-Fat Diet Feeding Recapitulates Human Cardiovascular Alterations: An Animal Model to Study the Early Phases of Diabetic Cardiomyopathy. Rouet P, ed. *PLoS One*. 2013;8(4):e60931. doi:10.1371/journal.pone.0060931.

235. Surwit RS, Kuhn CM, Cochrane C, McCubbin JA, Feinglos MN. Diet-induced type II diabetes in C57BL/6J mice. *Diabetes*. 1988;37(9):1163-

1167. doi:10.2337/DIAB.37.9.1163.

236. Buettner R, Schölmerich J, Bollheimer LC. High-fat diets: Modeling the metabolic disorders of human obesity in rodents. *Obesity*. 2007;15(4):798-808. doi:10.1038/oby.2007.608.

237. Heydemann A. An Overview of Murine High Fat Diet as a Model for Type 2 Diabetes Mellitus. *J Diabetes Res*. 2016;2016. doi:10.1155/2016/2902351.

238. Hariri N, Gougeon R, Thibault L. A highly saturated fat-rich diet is more obesogenic than diets with lower saturated fat content. *Nutr Res*. 2010;30(9):632-643. doi:10.1016/j.nutres.2010.09.003.

239. Kubant R, Poon AN, Sánchez-Hernández D, et al. A comparison of effects of lard and hydrogenated vegetable shortening on the development of high-fat diet-induced obesity in rats. *Nutr Diabetes*. 2015;5(November):1-6. doi:10.1038/nutd.2015.40.

240. Belzung F, Raclot T, Groscolas R. Fish oil n-3 fatty acids selectively limit the hypertrophy of abdominal fat depots in growing rats fed high-fat diets. *Am J Physiol Integr Comp Physiol*. 1993;264(6):R1111-R1118. doi:10.1152/ajpregu.1993.264.6.R1111.

241. Corbett SW, Stern JS, Keesey RE. Energy expenditure in rats with diet-induced obesity. *Am J Clin Nutr*. 1986;44(2):173-180. http://www.ncbi.nlm.nih.gov/pubmed/3728354. Accessed February 2, 2018.

242. Lee B-C, Lee J. Cellular and molecular players in adipose tissue inflammation in the development of obesity-induced insulin resistance. *Biochim Biophys Acta - Mol Basis Dis*. 2014;1842(3):446-462. doi:10.1016/j.bbadis.2013.05.017.

243. Guo S. Insulin signaling, resistance, and the metabolic syndrome: insights from mouse models into disease mechanisms. *J Endocrinol*. 2014;220(2):T1-T23. doi:10.1530/JOE-13-0327.

244. Kanuri G, Bergheim I. In vitro and in vivo models of non-alcoholic fatty liver disease (NAFLD). *Int J Mol Sci*. 2013;14(6):11963-11980. doi:10.3390/ijms140611963.

245. Nakamura A, Terauchi Y. Lessons from mouse models of high-fat diet-induced NAFLD. *Int J Mol Sci*. 2013;14(11):21240-21257. doi:10.3390/ijms141121240.

246. Yaqoob P, Sherrington EJ, Jeffery NM, et al. Comparison of the effects of a range of dietary lipids upon serum and tissue lipid composition in the rat. *Int J Biochem Cell Biol*. 1995;27(3):297-310. http://www.ncbi.nlm.nih.gov/pubmed/7780834. Accessed February 2, 2018.

247. Abdesselam I, Pepino P, Troalen T, et al. Time course of cardiometabolic alterations in a high fat high sucrose diet mice model and improvement after GLP-1 analog treatment using multimodal cardiovascular magnetic

resonance. *J Cardiovasc Magn Reson*. 2015;17:95. doi:10.1186/s12968-015-0198-x.

248. Carbone S, Mauro AG, Mezzaroma E, et al. A high-sugar and high-fat diet impairs cardiac systolic and diastolic function in mice. *Int J Cardiol*. 2015;198:66-69. doi:10.1016/j.ijcard.2015.06.136.

249. Roberts NW, González-Vega M, Berhanu TK, Mull A, García J, Heydemann A. Successful metabolic adaptations leading to the prevention of high fat diet-induced murine cardiac remodeling. *Cardiovasc Diabetol*. 2015;14(1):127. doi:10.1186/s12933-015-0286-0.

250. Villarroya J, Redondo-Angulo I, Iglesias R, Giralt M, Villarroya F, Planavila A. Sirt1 mediates the effects of a short-term high-fat diet on the heart. *J Nutr Biochem*. 2015;26(11):1328-1337. doi:10.1016/j.jnutbio.2015.07.029.

251. Brainard RE, Watson LJ, DeMartino AM, et al. High Fat Feeding in Mice Is Insufficient to Induce Cardiac Dysfunction and Does Not Exacerbate Heart Failure. Tsai Y-S, ed. *PLoS One*. 2013;8(12):e83174. doi:10.1371/journal.pone.0083174.

252. Winzell MS, Ahre B. The High-Fat Diet–Fed Mouse. *Diabetes*. 2004;53:S215-S219. doi:10.2337/diabetes.53.suppl_3.S215.

253. Mosser RE, Maulis MF, Moullé VS, et al. High-fat diet-induced β-cell proliferation occurs prior to insulin resistance in C57Bl/6J male mice. *Am J Physiol Metab*. 2015;308(7):E573-E582. doi:10.1152/ajpendo.00460.2014.

254. Hull WJ. Treating the changing face of western medicine: pharmacological interventions on the Jak/STAT pathway in diabetic complications and its relationship to ageing. 2017.

255. Purvis G s. d. The role of Annexin-A1 in pathophysiology of diabetes. 2017.

256. Wang H-T, Liu C-F, Tsai T-H, et al. Effect of obesity reduction on preservation of heart function and attenuation of left ventricular remodeling, oxidative stress and inflammation in obese mice. *J Transl Med*. 2012;10:145. doi:10.1186/1479-5876-10-145.

257. Vasanji Z, Cantor EJF, Juric D, Moyen M, Netticadan T. Alterations in cardiac contractile performance and sarcoplasmic reticulum function in sucrose-fed rats is associated with insulin resistance. *Am J Physiol Physiol*. 2006;291(4):C772-C780. doi:10.1152/ajpcell.00086.2005.

258. Pulinilkunnil T, Kienesberger PC, Nagendran J, Sharma N, Young ME, Dyck JRB. Cardiac-specific adipose triglyceride lipase overexpression protects from cardiac steatosis and dilated cardiomyopathy following diet-induced obesity. *Int J Obes*. 2014;38(2):205-215. doi:10.1038/ijo.2013.103.

259. Enriori PJ, Evans AE, Sinnayah P, et al. Diet-Induced Obesity Causes Severe but Reversible Leptin Resistance in Arcuate Melanocortin Neurons.

doi:10.1016/j.cmet.2007.02.004.

260. Fraulob JC, Ogg-Diamantino R, Fernandes-Santos C, Aguila MB, Mandarim-de-Lacerda CA. A Mouse Model of Metabolic Syndrome: Insulin Resistance, Fatty Liver and Non-Alcoholic Fatty Pancreas Disease (NAFPD) in C57BL/6 Mice Fed a High Fat Diet. *J Clin Biochem Nutr*. 2010;46(3):212-223. doi:10.3164/jcbn.09-83.

261. Glastras SJ, Chen H, Teh R, et al. Mouse Models of Diabetes, Obesity and Related Kidney Disease. *PLoS One*. 2016;11(8):e0162131. doi:10.1371/journal.pone.0162131.

262. Idowu AA, Ajose AO, Adedeji AT, Adegoke AO, Jimoh KA. Microalbuminuria, Other Markers of Nephropathy and Biochemical Derangementsin Type 2 Diabetes Mellitus: Relationships and Determinants. *Ghana Med J*. 2017;51(2):56-63. http://www.ncbi.nlm.nih.gov/pubmed/28955101. Accessed February 12, 2018.

263. Li S, Brault A, Sanchez Villavicencio M, Haddad PS. *Rhododendron groenlandicum* (Labrador tea), an antidiabetic plant from the traditional pharmacopoeia of the Canadian Eastern James Bay Cree, improves renal integrity in the diet-induced obese mouse model. *Pharm Biol*. 2016;54(10):1998-2006. doi:10.3109/13880209.2015.1137953.

264. Markus MRP, Ittermann T, Baumeister SE, et al. Prediabetes is associated with microalbuminuria, reduced kidney function and chronic kidney disease in the general population. *Nutr Metab Cardiovasc Dis*. 2017;28(3):234-242. doi:10.1016/j.numecd.2017.12.005.

265. Van Den Hurk K, Smulders YM, Alssema M, et al. Independent associations of glucose status and arterial stiffness with left ventricular diastolic dysfunction: An 8-year follow-up of the Hoorn Study. *Diabetes Care*. 2012;35(6):1258-1264. doi:10.2337/dc11-1336.

266. Chiazza F, Couturier-Maillard A, Benetti E, et al. Targeting the NLRP3 Inflammasome to Reduce Diet-Induced Metabolic Abnormalities in Mice. *Mol Med*. 2015;21(1):1. doi:10.2119/molmed.2015.00104.

267. Cusi K. The Role of Adipose Tissue and Lipotoxicity in the Pathogenesis of Type 2 Diabetes. *Curr Diab Rep*. 2010;10(4):306-315. doi:10.1007/s11892-010-0122-6.

268. Semple RK, Sleigh A, Murgatroyd PR, et al. Postreceptor insulin resistance contributes to human dyslipidemia and hepatic steatosis. *J Clin Invest*. 2009;119(2):315-322. doi:10.1172/JCI37432.

269. Mooradian AD. Dyslipidemia in type 2 diabetes mellitus. *Nat Clin Pract Endocrinol Metab*. 2009;5(3):150-159. doi:10.1038/ncpendmet1066.

270. Vaidya HB, Gangadaran S, Cheema SK. An obesogenic diet enriched with blue mussels protects against weight gain and lowers cholesterol levels in

C57BL/6 mice. *Nutr Res*. 2017;46:31-37. doi:10.1016/j.nutres.2017.07.004.

271. Zhong H, Chen K, Feng M, et al. Genipin alleviates high-fat diet-induced hyperlipidemia and hepatic lipid accumulation in mice via miR-142a-5p/SREBP-1c axis. *FEBS J*. 2018;285(3):501-517. doi:10.1111/febs.14349.

272. Merx MW, Weber CD. Sepsis and the heart. *Circulation*. 2007;116(7):793-802 ST - Sepsis and the heart. doi:10.1161/CIRCULATIONAHA.106.678359.

273. Blanco J, Muriel-Bombín A, Sagredo V, et al. Incidence, organ dysfunction and mortality in severe sepsis: A Spanish multicentre study. *Crit Care*. 2008;12(6):1-14. doi:10.1186/cc7157.

274. American diabetes association. Standards of Medical Care in Diabetes—2016 Abridged for Primary Care Providers. *position statement*. 2016;34:3-21. doi:10.2337/diaclin.34.1.3.

275. Schuetz P, Castro P, Shapiro NI. Diabetes and Sepsis: Preclinical Findings and Clinical Relevance. *Diabetes Care*. 2011;34:771-778. doi:10.2337/dc10-1185.

276. Kapoor A, Shintani Y, Collino M, et al. Protective role of peroxisome proliferator-activated receptor-β/δ in septic shock. *Am J Respir Crit Care Med*. 2010;182(12):1506-1515.

277. Khan A, Coldewey S, Patel N, et al. Erythropoietin attenuates cardiac dysfunction in experimental sepsis in mice via activation of the β-common receptor. *Dis Model Mech*. 2013;6(4):1021-1030.

278. Coldewey SM, Rogazzo M, Collino M, Patel NSA, Thiemermann C. Inhibition of I B kinase reduces the multiple organ dysfunction caused by sepsis in the mouse. *Dis Model Mech*. 2013;6(4):1031-1042. doi:10.1242/dmm.012435.

279. Thomas CM, Yong QC, Rosa RM, et al. Cardiac-specific suppression of NF-κB signaling prevents diabetic cardiomyopathy via inhibition of the renin-angiotensin system. *Am J Physiol Circ Physiol*. 2014;307(7):H1036-H1045. doi:10.1152/ajpheart.00340.2014.

280. Benfield T, Jensen J, Nordestgaard B. Influence of diabetes and hyperglycaemia on infectious disease hospitalisation and outcome. *Diabetol 2007 Mar;50(3)549-54 Epub 2006 Dec 23*. 2007;50(3):549-554.

281. van Vught LA, Holman R, de Jonge E, de Keizer NF, van der Poll T. Diabetes Is Not Associated With Increased 90-Day Mortality Risk in Critically Ill Patients With Sepsis. *Crit Care Med*. 2017;45(10):e1026-e1035. doi:10.1097/CCM.0000000000002590.

282. Daousi C, Casson IF, Gill G V, MacFarlane IA, Wilding JPH, Pinkney JH. Prevalence of obesity in type 2 diabetes in secondary care: association with cardiovascular risk factors. *Postgrad Med J*. 2006;82(966):280-284.

doi:10.1136/pmj.2005.039032.

283. Mozaffarian D, Benjamin EJ, Go AS, et al. *Heart Disease and Stroke Statistics-2015 Update : A Report from the American Heart Association*. Vol 131.; 2015. doi:10.1161/CIR.0000000000000152.

284. Ng PY, Eikermann M. The obesity conundrum in sepsis. *BMC Anesthesiol*. 2017;(10). doi:10.1186/s12871-017-0434-z.

285. Fonarow GC, Srikanthan P, Costanzo MR, Cintron GB, Lopatin M, ADHERE Scientific Advisory Committee and Investigators. An obesity paradox in acute heart failure: Analysis of body mass index and inhospital mortality for 108927 patients in the Acute Decompensated Heart Failure National Registry. *Am Heart J*. 2007;153(1):74-81. doi:10.1016/j.ahj.2006.09.007.

286. Niedziela J, Hudzik B, Niedziela N, et al. The obesity paradox in acute coronary syndrome: a meta-analysis. *Eur J Epidemiol*. 2014;29(11):801-812. doi:10.1007/s10654-014-9961-9.

287. Ni Y-N, Luo J, Yu H, et al. Can body mass index predict clinical outcomes for patients with acute lung injury/acute respiratory distress syndrome? A meta-analysis. *Crit Care*. 2017;21(1):36. doi:10.1186/s13054-017-1615-3.

288. Pepper DJ, Sun J, Welsh J, Cui X, Suffredini AF, Eichacker PQ. Increased body mass index and adjusted mortality in ICU patients with sepsis or septic shock: a systematic review and meta-analysis. *Crit Care*. 2016;20(1):181. doi:10.1186/s13054-016-1360-z.

289. Wang S, Liu X, Chen Q, Liu C, Huang C, Fang X. The role of increased body mass index in outcomes of sepsis: a systematic review and meta-analysis. *BMC Anesthesiol*. 2017;17(1):118. doi:10.1186/s12871-017-0405-4.

290. Munford RS. Murine responses to endotoxin: another dirty little secret? *J Infect Dis*. 2010;201(2):175-177. doi:10.1086/649558.

291. Coldewey S, Rogazzo M, Collino M, Patel N, Thiemermann C. Inhibition of IκB kinase reduces the multiple organ dysfunction caused by sepsis in the mouse. *Dis Model Mech*. 2013;6(4):1031-1042.

292. Chen J, Kieswich JE, Chiazza F, et al. IκB Kinase Inhibitor Attenuates Sepsis-Induced Cardiac Dysfunction in CKD. *J amirican Soc Nephrol*. 2016;May 6.

293. Barone FC, Hillegass LM, Price WJ, et al. Polymorphonuclear Leukocyte Infiltration Into Cerebral Focal Ischemic Tissue: Myeloperoxidase Activity Assay and Histologic Verification. *J Neurosci Res Cell Sci*. 1991;29:336-345.

294. Afkarian M, Zelnick L, Hall Y, et al. Clinical Manifestations of Kidney Disease Among US Adults With Diabetes, 1988-2014. *J amirican Soc*

Nephrol. 2014;4(1):139-148. doi:10.1038/nmeth.2839.A.

295. Harris EH. Elevated Liver Function Tests in Type 2 Diabetes. *Clin Diabetes*. 2005;23(3):115-119. doi:10.2337/diaclin.23.3.115.

296. Glastras SJ, Chen H, Teh R, et al. Mouse models of diabetes, obesity and related kidney disease. *PLoS One*. 2016;11(8):1-15. doi:10.1371/journal.pone.0162131.

297. Fang CX, Dong F, Thomas DP, Ma H, He L, Ren J. Hypertrophic cardiomyopathy in high-fat diet-induced obesity: role of suppression of forkhead transcription factor and atrophy gene transcription. *Am J Physiol Circ Physiol*. 2008;295(3):H1206-H1215. doi:10.1152/ajpheart.00319.2008.

298. Li S, Zeng X-Y, Zhou X, et al. Dietary cholesterol induces hepatic inflammation and blunts mitochondrial function in the liver of high-fat-fed mice. *J Nutr Biochem*. 2016;27:96-103. doi:10.1016/j.jnutbio.2015.08.021.

299. Shah A, MacCarthy P. Paracrine and autocrine effects of nitric oxide on myocardial function. *Pharmacol Ther*. 2000;86(1):49-86.

300. Sanyal D, Mukherjee P, Raychaudhuri M, Ghosh S, Mukherjee S, Chowdhury S. Profile of liver enzymes in non-alcoholic fatty liver disease in patients with impaired glucose tolerance and newly detected untreated type 2 diabetes. *Indian J Endocrinol Metab*. 2015;19(5):597-601. doi:10.4103/2230-8210.163172.

301. Palomer X, Salvadó L, Barroso E, Vázquez-Carrera M. An overview of the crosstalk between inflammatory processes and metabolic dysregulation during diabetic cardiomyopathy. *Int J Cardiol*. 2013;168:3160-3172. doi:10.1016/j.ijcard.2013.07.150.

302. Martin L, Horst K, Chiazza F, et al. The synthetic antimicrobial peptide 19-2.5 attenuates septic cardiomyopathy and prevents down-regulation of SERCA2 in polymicrobial sepsis. *Sci Rep*. 2016;6:37277. doi:10.1038/srep37277.

303. Coldewey SM, Benetti E, Collino M, et al. Elevation of serum sphingosine-1-phosphate attenuates impaired cardiac function in experimental sepsis. *Sci Rep*. 2016;6(1):27594. doi:10.1038/srep27594.

304. Bernard GR, Vincent J-L, Laterre P-F, et al. Efficacy and Safety of Recombinant Human Activated Protein C for Severe Sepsis. *N Engl J Med*. 2001;344(10):699-709. doi:10.1056/NEJM200103083441001.

305. Skube S, Katz S, Chipman J, Tignanelli C. Acute Kidney Injury and Sepsis. *Surg Infect*. 2018;Jan.

306. Doi K. Role of kidney injury in sepsis. *J intensive care*. 2016;4:17. doi:10.1186/s40560-016-0146-3.

307. Marshall J, Deitch E, Moldawer L, Opal S, Redl H, van der Poll T.

Preclinical models of shock and sepsis: what can they tell us? *shock*. 2005;Suppl 1:1-6.

308. Mai S, Khan M, Liaw P, Fox-robichaud A. *Experimental Sepsis Models*. Canada; 2012.

309. Senftleben U, Cao Y, Xiao G, et al. Activation by IKKalpha of a second, evolutionary conserved, NF-kappa B signaling pathway. *Science (80-)*. 2001;293(5534):1495-1499.

310. Conlon BA, Law WR. Macrophages are a source of extracellular adenosine deaminase-2 during inflammatory responses. *Clin Exp Immunol*. 2004;138(1):14-20. doi:10.1111/j.1365-2249.2004.02591.x.

311. Waelchli R, Bollbuck B, Bruns C, et al. Design and preparation of 2-benzamido-pyrimidines as inhibitors of IKK. *Bioorg Med Chem Lett*. 2006;16(1):108-112. doi:10.1016/j.bmcl.2005.09.035.

312. Waelchli R, Bollbuck B, Bruns C, et al. Design and preparation of 2-benzamido-pyrimidines as inhibitors of IKK. *Bioorg Med Chem Lett*. 2006;16(1):108-112. doi:10.1016/j.bmcl.2005.09.035.

313. Suda M, Shimizu I, Yoshida Y, et al. Inhibition of dipeptidyl peptidase-4 ameliorates cardiac ischemia and systolic dysfunction by up-regulating the FGF-2/EGR-1 pathway. Sadoshima J, ed. *PLoS One*. 2017;12(8):e0182422. doi:10.1371/journal.pone.0182422.

314. Chen Y-T, Tsai T-H, Yang C-C, et al. Exendin-4 and sitagliptin protect kidney from ischemia-reperfusion injury through suppressing oxidative stress and inflammatory reaction. *J Transl Med*. 2013;11:270. doi:10.1186/1479-5876-11-270.

315. Shinjo T, Nakatsu Y, Iwashita M, et al. DPP-IV inhibitor anagliptin exerts anti-inflammatory effects on macrophages, adipocytes, and mouse livers by suppressing NF-κB activation. *Am J Physiol Metab*. 2015;309(3):E214-E223. doi:10.1152/ajpendo.00553.2014.

APPENDIX 1

Table A.1. The SSC guideline (2016) recommendations and best practice statements. Table adapted from Rhodes *et al*., 2017 [21].

A. INITIAL RESUSCITATION
1. Sepsis and septic shock are medical emergencies, and we recommend that treatment and resuscitation begin immediately (BPS). 2. We recommend that, in the resuscitation from sepsis-induced hypoperfusion, at least 30 mL/kg of IV crystalloid fluid be given within the first 3 hours (strong recommendation, low quality of evidence). 3. We recommend that, following initial fluid resuscitation, additional fluids be guided by frequent reassessment of hemodynamic status (BPS). Remarks: Reassessment should include a thorough clinical examination and evaluation of available physiologic variables (heart rate, blood pressure, arterial oxygen saturation, respiratory rate, temperature, urine output, and others, as available) as well as other non-invasive or invasive monitoring, as available. 4. We recommend further hemodynamic assessment (such as assessing cardiac function) to determine the type of shock if the clinical examination does not lead to a clear diagnosis (BPS). 5. We suggest that dynamic over static variables be used to predict fluid responsiveness, where available (weak recommendation, low quality of evidence). 6. We recommend an initial target mean arterial pressure of 65 mm Hg in patients with septic shock requiring vasopressors (strong recommendation, moderate quality of evidence). 7. We suggest guiding resuscitation to normalize lactate in patients with elevated lactate levels as a marker of issue hypoperfusion (weak recommendation, low quality of evidence).
B. SCREENING FOR SEPSIS AND PERFORMANCE IMPROVEMENT
1. We recommend that hospitals and hospital systems have a performance improvement program for sepsis, including sepsis screening for acutely ill, high risk patients (BPS).
C. DIAGNOSIS
1. We recommend that appropriate routine microbiologic cultures (including blood) be obtained before starting antimicrobial therapy in patients with suspected sepsis or septic shock if doing so results in no substantial delay in the start of antimicrobials (BPS). Remarks: Appropriate routine microbiologic cultures always include at least two sets of blood cultures (aerobic and anaerobic).
D. ANTIMICROBIAL THERAPY
1. We recommend that administration of IV antimicrobials should be initiated as soon as possible after recognition and within one hour for both sepsis and septic shock (strong recommendation, moderate quality of evidence). 2. We recommend empiric broad-spectrum therapy with one or more antimicrobials for patients presenting with sepsis or septic shock to cover

all likely pathogens (including bacterial and potentially fungal or viral coverage) (strong recommendation, moderate quality of evidence).

3. We recommend that empiric antimicrobial therapy be narrowed once pathogen identification and sensitivity are established and/or adequate clinical improvement is noted (BPS).
4. We recommend against sustained systemic antimicrobial prophylaxis in patients with severe inflammatory states of non-infectious origin (e.g., severe pancreas, burn injury) (BPS).
5. We recommend that dosing strategies of antimicrobials be optimized based on accepted pharmacokinetic/pharmacodynamics principles and specific drug properties in patients with sepsis or septic shock (BPS).
6. We suggest empiric combination therapy (using at least two antibiotics of different antimicrobial classes) aimed at the most likely bacterial pathogen(s) for the initial management of septic shock (weak recommendation, low quality of evidence). Remarks: Readers should review
7. We suggest that combination therapy not be routinely used for ongoing treatment of most other serious infections, including bacteraemia and sepsis without shock (weak recommendation, low quality of evidence). Remarks: This does not preclude the use of multidrug therapy to broaden antimicrobial activity.
8. We recommend against combination therapy for the routine treatment of neutropenic sepsis/bacteraemia (strong recommendation, moderate quality of evidence). Remarks: This does not preclude the use of multidrug therapy to broaden antimicrobial activity.
9. If combination therapy is used for septic shock, we recommend de-escalation with discontinuation of combination therapy within the first few days in response to clinical improvement and/or evidence of infection resolution. This applies to both targeted (for culture-positive infections) and empiric (for culture-negative infections) combination therapy (BPS).
10. We suggest that antimicrobial treatment duration of 7 to 10 days is adequate for most serious infections associated with sepsis and septic shock (weak recommendation, low quality of evidence).
11. We suggest that longer courses are appropriate in patients who have a slow clinical response, undrainable foci of infection, bacteraemia with Staphylococcus aureus, some fungal and viral infections, or immunologic deficiencies, including neutropenia (weak recommendation, low quality of evidence).
12. We suggest that shorter courses are appropriate in some patients, particularly those with rapid clinical resolution following effective source control of intra-abdominal or urinary sepsis and those with anatomically uncomplicated pyelonephritis (weak recommendation, low quality of evidence).
13. We recommend daily assessment for de-escalation of antimicrobial therapy in patients with sepsis and septic shock (BPS).
14. We suggest that measurement of procalcitonin levels can be used to support shortening the duration of antimicrobial therapy in sepsis patients (weak recommendation, low quality of evidence).
15. We suggest that procalcitonin levels can be used to support the disconnection of empiric antibiotics in patients who initially appeared to

have sepsis, but subsequently have limited clinical evidence of infection (weak recommendation, low quality of evidence).

E. SOURSE CONTROL

1. We recommend that a specific anatomic diagnosis of infection requiring emergent source control should be identified or excluded as rapidly as possible in patients with sepsis or septic shock, and that any required source control intervention should be implemented as soon as medically and logistically practical after the diagnosis is made (BPS).
2. We recommend prompt removal of intravascular access devices that are a possible source of sepsis or septic shock after other vascular access has been established (BPS).

F. FLUID THERAPY

1. We recommend that a fluid challenge technique be applied where fluid administration is continued as long as hemodynamic factors continue to improve (BPS).
2. We recommend crystalloids as the fluid of choice for initial resuscitation and subsequent intravascular volume replacement in patients with sepsis and septic shock (strong recommendation, moderate quality of evidence).
3. We suggest using either balanced crystalloids or saline for fluid resuscitation of patients with sepsis or septic shock (weak recommendation, low quality of evidence).
4. We suggest using albumin in addition to crystalloids for initial resuscitation and subsequent intravascular volume replacement in patients with sepsis and septic shock, when patients require substantial amounts of crystalloids (weak recommendation, low quality of evidence).
5. We recommend against using hydroxyethyl starches for intravascular volume replacement in patients with sepsis or septic shock (strong recommendation, high quality of evidence).
6. We suggest using crystalloids over gelatines when resuscitating patients with sepsis or septic shock (weak recommendation, low quality of evidence).

G. VASOACTIVE MEDICATION

1. We recommend norepinephrine as the first-choice vasopressor (strong recommendation, moderate quality of evidence).
2. We suggest adding either vasopressin (up to 0.03 U/min) (weak recommendation, moderate quality of evidence) or epinephrine (weak recommendation, low quality of evidence) to norepinephrine with the intent of raising mean arterial pressure to target, or adding vasopressin (up to 0.03 U/min) (weak recommendation, moderate quality of evidence) to decrease norepinephrine dosage.
3. We suggest using dopamine as an alternative vasopressor agent to norepinephrine only in highly selected patients (e.g., patients with low risk of tachyarrhythmias and absolute or relative bradycardia) (weak recommendation, low quality of evidence).
4. We recommend against using low-dose dopamine for renal protection (strong recommendation, high quality of evidence).
5. We suggest using dobutamine in patients who show evidence of persistent

hypoperfusion despite adequate fluid loading and the use of vasopressor agents (weak recommendation, low quality of evidence). Remarks: If initiated, dosing should be treated to an end point reflecting perfusion, and the agent reduced or discontinued in the face of worsening hypotension or arrhythmias.

6. We suggest that all patients requiring vasopressors have an arterial catheter placed as soon as practical if resources are available (weak recommendation, very low quality of evidence).

H. CORTICOSTEROIDS

1. We suggest against using IV hydrocortisone to treat septic shock patients if adequate fluid resuscitation and vasopressor therapy are able to restore hemodynamic stability. If this is not achievable, we suggest IV hydrocortisone at a dose of 200 mg per day (weak recommendation, low quality of evidence).

I. BLOOD PRODUCTS

1. We recommend that RBC transfusion occur only when haemoglobin concentration decreases to < 7.0 g/dL in adults in the absence of extenuating circumstances, such as myocardial ischemia, severe hypoxemia, or acute haemorrhage (strong recommendation, high quality of evidence).
2. We recommend against the use of erythropoietin for treatment of anaemia associated with sepsis (strong recommendation, moderate quality of evidence).
3. We suggest against the use of fresh frozen plasma to correct clotting abnormalities in the absence of bleeding or planned invasive procedures (weak recommendation, very low quality of evidence).
4. We suggest prophylactic platelet transfusion when counts are <10,000/mm3 (10 × 10 9 /L) in the absence of apparent bleeding and when counts are < 20,000/mm3 (20 × 109 /L) if the patient has a significant risk of bleeding. Higher platelet counts (≥ 50,000/mm3 [50 x 109 /L]) are advised for active bleeding, surgery, or invasive procedures (weak recommendation, very low quality of evidence).

J. IMMUNOLOGY

1. We suggest against the use of IV immunoglobulins in patients with sepsis or septic shock (weak recommendation, low quality of evidence).

K. BLOOD PURIFICATION

1. We make no recommendation regarding the use of blood purification techniques.

L. ANTICOAGULANT

1. We recommend against the use of antithrombin for the treatment of sepsis and septic shock (strong recommendation, moderate quality of evidence).
2. We make no recommendation regarding the use of thrombomodulin or heparin for the treatment of sepsis or septic shock

M. MECHANICAL VENTILATION

1. We recommend using a target dal volume of 6 mL/kg predicted body weight compared with 12 mL/kg in adult patients with sepsis-induced acute respiratory distress syndrome (ARDS) (strong recommendation, high quality of evidence).
2. We recommend using an upper limit goal for plateau pressures of 30 cm H2O over higher plateau pressures in adult patients with sepsis-induced severe ARDS (strong recommendation, moderate quality of evidence).
3. We suggest using higher positive end-expiratory pressure (PEEP) over lower PEEP in adult patients with sepsis-induced moderate to severe ARDS (weak recommendation, moderate quality of evidence).
4. We suggest using recruitment manoeuvres in adult patients with sepsis-induced, severe ARDS (weak recommendation, moderate quality of evidence).
5. We recommend using prone over supine position in adult patients with sepsis-induced ARDS and a PaO2/FIO2 ratio <150 (strong recommendation, moderate quality of evidence).
6. We recommend against using high-frequency oscillatory ventilation in adult patients with sepsis-induced ARDS (strong recommendation, moderate quality of evidence).
7. We make no recommendation regarding the use of non-invasive ventilation for patients with sepsis-induced ARDS.
8. We suggest using neuromuscular blocking agents for ≤ 48 hours in adult patients with sepsis-induced ARDS and a PaO2/FIO2 ratio < 150 mm Hg (weak recommendation, moderate quality of evidence).
9. We recommend a conservative fluid strategy for patients with established sepsis-induced ARDS who do not have evidence of issue hypoperfusion (strong recommendation, moderate quality of evidence).
10. We recommend against the use of ß-2 agonists for the treatment of patients with sepsis-induced ARDS without bronchospasm (strong recommendation, moderate quality of evidence).
11. We recommend against the routine use of the pulmonary artery catheter for patients with sepsis-induced ARDS (strong recommendation, high quality of evidence).
12. We suggest using lower dal volumes over higher dal volumes in adult patients with sepsis-induced respiratory failure without ARDS (weak recommendation, low quality of evidence).
13. We recommend that mechanically ventilated sepsis patients be maintained with the head of the bed elevated between 30 and 45 degrees to limit aspiration risk and to prevent the development of ventilator-associated pneumonia (strong recommendation, low quality of evidence).
14. We recommend using spontaneous breathing trials in mechanically ventilated patients with sepsis who are ready for weaning (strong recommendation, high quality of evidence).
15. We recommend using a weaning protocol in mechanically ventilated patients with sepsis-induced respiratory failure who can tolerate weaning (strong recommendation, moderate quality of evidence).

N. SEDATION AND ANALGESIA

1. We recommend that continuous or intermittent sedation be minimized in mechanically ventilated sepsis patients, targeting specific titration end

points (BPS).

O. GLUCOSE CONTROL

1. We recommend a protocolized approach to blood glucose management in ICU patients with sepsis, commencing insulin dosing when two consecutive blood glucose levels are > 180 mg/dL. This approach should target an upper blood glucose level ≤ 180 mg/dL rather than an upper target blood glucose level ≤ 110 mg/dL (strong recommendation, high quality of evidence).
2. We recommend that blood glucose values be monitored every 1 to 2 hours until glucose values and insulin infusion rates are stable, then every 4 hours thereafter in patients receiving insulin infusions (BPS).
3. We recommend that glucose levels obtained with point-of-care testing of capillary blood be interpreted with caution because such measurements may not accurately estimate arterial blood or plasma glucose values (BPS).
4. We suggest the use of arterial blood rather than capillary blood for point-of-care testing using glucose meters if patients have arterial catheters (weak recommendation, low quality of evidence).

P. RENAL REPLACEMENT THERAPY

1. We suggest that either continuous or intermittent renal replacement therapy (RRT) be used in patients with sepsis and acute kidney injury (weak recommendation, moderate quality of evidence).
2. We suggest using continuous therapies to facilitate management of fluid balance in hemodynamically unstable septic patients (weak recommendation, very low quality of evidence).
3. We suggest against the use of RRT in patients with sepsis and acute kidney injury for increase in creatinine or oliguria without other definitive indications for dialysis (weak recommendation, low quality of evidence).

Q. BICARBONATE THERAPY

1. We suggest against the use of sodium bicarbonate therapy to improve haemodynamics or to reduce vasopressor requirements in patients with hypoperfusion-induced lactic acidemia with pH ≥ 7.15 (weak recommendation, moderate quality of evidence).

R. VENOUS THROMBOEMBOLISM PROPHYLAXIS

1. We recommend pharmacologic prophylaxis (unfractionated heparin [UFH] or low-molecular-weight heparin [LMWH]) against venous thromboembolism (VTE) in the absence of contraindications to the use of these agents (strong recommendation, moderate quality of evidence).
2. We recommend LMWH rather than UFH for VTE prophylaxis in the absence of contraindications to the use of LMWH (strong recommendation, moderate quality of evidence).
3. We suggest combination pharmacologic VTE prophylaxis and mechanical prophylaxis, whenever possible (weak recommendation, low quality of evidence).
4. We suggest mechanical VTE prophylaxis when pharmacologic VTE is contraindicated (weak recommendation, low quality of evidence).

S. STRESS ULCER PROPHYLAXIS

1. We recommend that stress ulcer prophylaxis be given to patients with sepsis or septic shock who have risk factors for gastrointestinal (GI) bleeding (strong recommendation, low quality of evidence).
2. We suggest using either proton pump inhibitors or histamine-2 receptor antagonists when stress ulcer prophylaxis is indicated (weak recommendation, low quality of evidence).
3. We recommend against stress ulcer prophylaxis in patients without risk factors for GI bleeding (BPS).

T. NUTRITION

1. We recommend against the administration of early parenteral nutrition alone or parenteral nutrition in combination with enteral feedings (but rather initiate early enteral nutrition) in critically ill patients with sepsis or septic shock who can be fed enterally (strong recommendation, moderate quality of evidence).
2. We recommend against the administration of parenteral nutrition alone or in combination with enteral feeds (but rather to initiate IV glucose and advance enteral feeds as tolerated) over the first 7 days in critically ill patients with sepsis or septic shock for whom early enteral feeding is not feasible (strong recommendation, moderate quality of evidence).
3. We suggest the early initiation of enteral feeding rather than a complete fast or only IV glucose in critically ill patients with sepsis or septic shock who can be fed enterally (weak recommendation, low quality of evidence).
4. We suggest either early trophic/hypocaloric or early full enteral feeding in critically ill patients with sepsis or septic shock; if trophic/hypocaloric feeding is the initial strategy, then feeds should be advanced according to patient tolerance (weak recommendation, moderate quality of evidence).
5. We recommend against the use of omega-3 fay acids as an immune supplement in critically ill patients with sepsis or septic shock (strong recommendation, low quality of evidence).
6. We suggest against routinely monitoring gastric residual volumes in critically ill patients with sepsis or septic shock (weak recommendation, low quality of evidence). However, we suggest measurement of gastric residuals in patients with feeding intolerance or who are considered to be at high risk of aspiration (weak recommendation, very low quality of evidence). Remarks: This recommendation refers to nonsurgical critically ill patients with sepsis or septic shock.
7. We suggest the use of prokinec agents in critically ill patients with sepsis or septic shock and feeding intolerance (weak recommendation, low quality of evidence).
8. We suggest placement of post-pyloric feeding tubes in critically ill patients with sepsis or septic shock with feeding intolerance or who are considered to be at high risk of aspiration (weak recommendation, low quality of evidence).
9. We recommend against the use of IV selenium to treat sepsis and septic shock (strong recommendation, moderate quality of evidence).
10. We suggest against the use of arginine to treat sepsis and septic shock (weak recommendation, low quality of evidence).
11. We recommend against the use of glutamine to treat sepsis and septic

shock (strong recommendation, moderate quality of evidence).

12. We make no recommendation about the use of carnitine for sepsis and septic shock

U. SETTING GOALS OF CARE

1. We recommend that goals of care and prognosis be discussed with patients and families (BPS).
2. We recommend that goals of care be incorporated into treatment and end-of-life care planning, utilizing palliative care principles where appropriate (strong recommendation, moderate quality of evidence).
3. We suggest that goals of care be addressed as early as feasible, but no later than within 72 hours of ICU admission (weak recommendation, low quality of evidence).

APPENDIX 2

Table A.2. Compositions of the solutions used for protein extraction from cytoplasm and nucleus for western blotting

SOLUTION	COMPONENTS
Homogenisation buffer (HB)	20 mM hepes-KOH pH 7.9 1 mM $MgCl_2$ 0.5 mM EDTA 1 mM EGTA 0.1% Triton X-100 100 ml Distilled H_2O Protease Inhibitors 0.1% Protease inhibitor cocktail (PIC) 0.5 mM PMSF 0.1 mM DL-Dithiethrectol (DTT)
Extraction buffer (EB)	20 mM hepes-KOH pH 7.9 1 mM $MgCl_2$ 0.5 mM EDTA 1 mM EGTA 20% Glycerol 420 mM NaCl 50 ml Distilled H_2O Protease Inhibitors 0.1% Protease inhibitor cocktail (PIC) 0.5 mM PMSF 0.1 mM DL-Dithiethrectol (DTT)